Systematic Implications of Leaf Anatomy and Palynology in the Disinae and Coryciinae (Orchidaceae).

By Pascale Claude Marcelle Henriette Chesselet

A thesis presented for the degree of Master of Science,

University of Cape Town.

Department of Botany.

September 1989.

ABSTRACT

Pollen morphology of 9 species (TEM), 86 species (SEM), and leaf anatomy of 62 species (LM), were surveyed in the Disinae, Coryciinae and, as outgroup taxa, the Orchideae and Satyriinae. Characters extracted from observations made of leaf anatomy and pollen were analysed using cladistic methods, and assessed in relation to the present phylogeny of the group. Leaf anatomy data gave little phylogenetic information. Sclerification associated with vascular bundles was systematically useful. Pollen data served to resolve taxa at the subtribal level. Both data sets provided evidence of relationship for taxonomically problematic taxa. The Coryciinae are palynologically defined by a suite of synapomorphies, including a secondarily tectate exine structure, fasciculate massulae, and elongated tetrads with linear microspore configuration.

Acknowledgements

I wish to thank Peter Linder for his guidance and close supervision of the project, Hubert Kurzweil for help in the field and useful discussion, and Jean Thompson for printing the pollen plates. I am grateful to the staff of the E.M. Unit, Dane Gerneke for teaching me TEM techniques, and Willi Williams for his darkroom assistance. I also thank Barbara Parkinson who introduced me to TEM techniques, and lastly, my family and friends for their encouragement and support.

1.0 INTRODUCTION

The present classification of the orchids rests primarily on studies of floral morphology data i.e. a combination of lip, rostellum, column and petal structures. One might expect, particularly in a group such as the orchids, which shows such extreme specialization to particular pollination mechanisms (Darwin, 1862), that a classification based on floral characters might, to a large extent, reflect pollination syndromes (Clifford and Lavarack, 1974, Linder, 1986). Whether such a classification is an adequate reflection of the phylogeny of the group can only be tested by investigating additional data sets. Since the alpha taxonomy of the Diseae is more or less complete with only few problematic taxa remaining, this Tribe provides an ideal opportunity such testing.

The subtribes Disinae (178 spp.) and Coryciinae (73 spp.) are primarily southern African groups of terrestrial orchids of the subfamily Orchidoideae. The shared possession of root-stem tuberoids, sectile massulae, basitonic anther structure and anomocytic stomata delimit the subfamily (Dressler, 1981, Rasmussen, 1985, Linder, 1986). The Australian Diuridae are problematic in that they may represent a "remnant" group

(Rasmussen, 1985) within which the Orchideae (sensu Rasmussen) may have evolved. According to Rasmussen (1985) the Orchideae (which include the Orchideae and Diseae sensu Dressler, 1981) is one of the most distinct and indisputably monophyletic of all major tribes of Orchidaceae. A cladogram of the subtribes of the Orchidoideae (Linder, 1986) is shown in Figure 1.A.

Past classifications of the Orchidoideae have differed in the interrelationships of suprageneric groups which are based primarily on floral morphology. Historical changes in the major classifications of the Orchidoideae have been summarized by Linder (1986) and are shown in Figure 1.B.

The Diseae are speciose in southern African temperate regions although Disperis and Satyrium have representatives in tropical Asia (Dressler, 1981). The Satyriinae are included in the Diseae and are thought to be the sister group of the Disinae and Coryciinae. The southern African species of Satyrium where recently revised by Hall (1982), and the subtribe Disinae by Linder (1981 a, b, c, d, e, f). According to Linder (1986), although the subtribal classification of the Disinae and Coryciinae is stable, their generic and infra-generic classification is problematic and in need of further investigation. The present classification of the two subtribes is summarized in the cladograms shown in Figures 1.C. and 1.D.

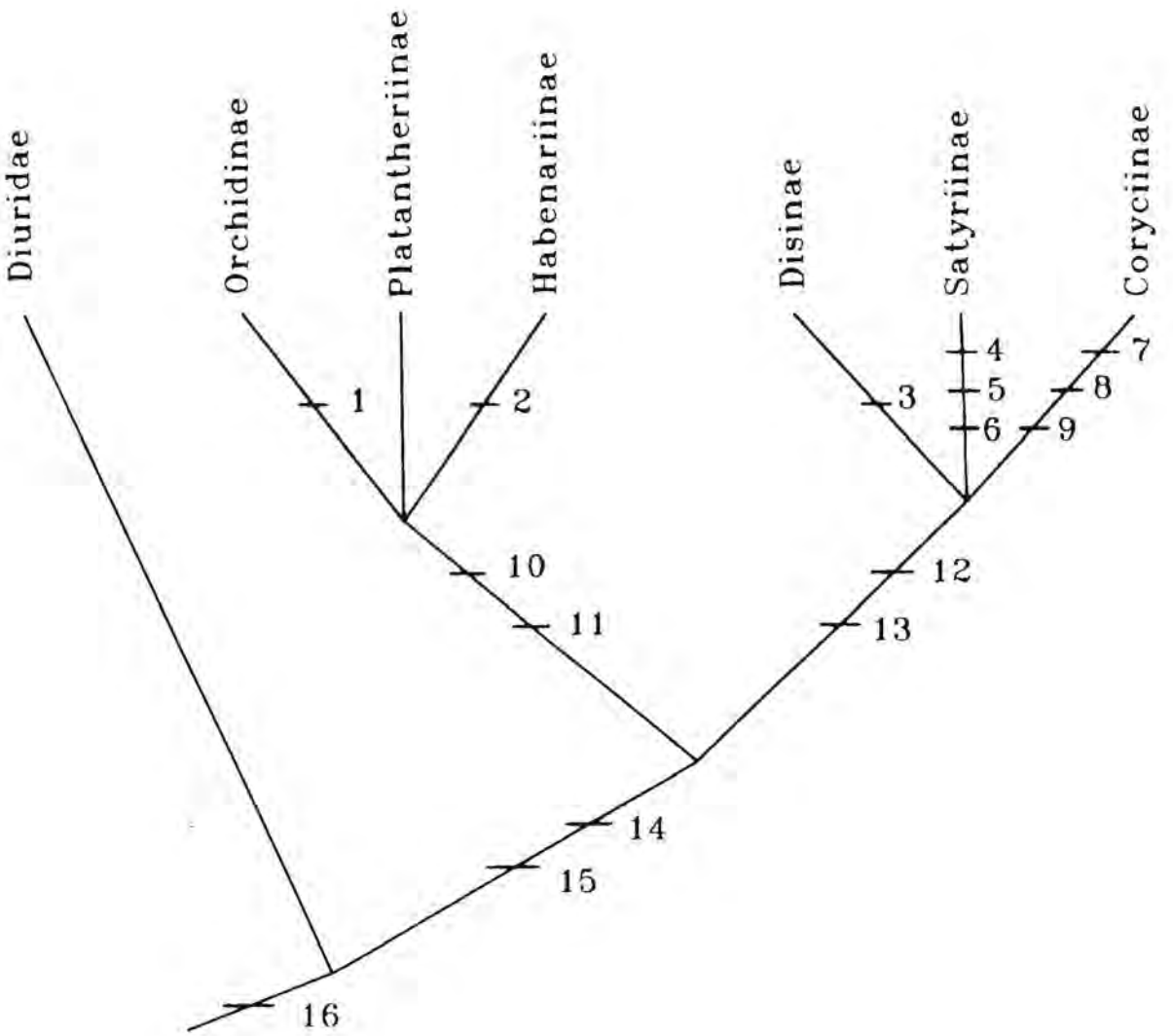

Figure 1.A

Cladogram of the subtribes of the Orchidoideae. Characters used are: 1. viscidia bursiculate; 2. stigmas stipitate; 3. dorsal sepal spurred; 4. column long and slender; 5. anther pendent; 6 flowers non-resupinate; 7. lip-base fused to the column; 8. rostellum lateral lobes well developed; 9. lip usually with an appendage; 10. lip base widened and broadly fused to the column base; 11. lip usually spurred, pollination nototribic; 12. anther usually reflexed, pollination stenotribic; 13. lip simple; 14. anthers basitonic; 15. pollen in massulae; 16 plants with root-stem tuberoids. From Linder (1986).

Figure 1.B.

The major classifications of the Orchidoideae between 1883 and 1981. From Linder (1986).

	Orchidinae	Platantheninae	Huttonaeinae	Androcorythinae	Habenariinae	Satyriinae	Disinae	Coryciinae
Bentham (1883) Ophrydeae	Serapieae			Habenarieae		Diseae		Corycieae
Pfitzer (1889) Ophrydinae	Serapia-deae	Gymnadenieae		Habenarieae		Satyrieae		Corycieae
Schlechter (1926) Ophrydoideae	Platanthereae		Huttonaceae	Androcorydeae	Habenarieae	Satyrieae	Diseae	Disperideae
Senghas (1974) Orchidoideae	Orchidinae	Platantheninae	Huttonaeinae	Androcorythinae	Habenariinae	Satyriinae	Disinae	Disperiinae
	Orchideae					Satyrieae	Diseae	
Dressler (1981) Orchidoideae	Orchidinae		Huttonaeinae	Habenariinae		Satyriinae	Disinae	Coryciinae
	Orchideae					Diseae		

Figure 1.C

Cladogram of genera and sections of the Disinae. The characters used are: 1. stolons present; 2 sterile shoots present; 3. basal sheaths scabrid; 4. leaves basal; 5. leaves linear; 6. leaves less than four; 7. leaves hysteranthous; 8. leaves (a) ribbed (b) rigid; 9. stems nitid; 10. stems flexuose; 11. inflorescences corymbose; 12. inflorescences capitate; 13. floral bracts dry; 14. flowers non-resupinate; 15. flowers less than five per inflorescence; 16. dorsal sepal flat; 17. spur (a) obsolete or (b) twice as long as the sepals; 18. spur (a) ascending (b) pendent; 19. spur massive; 20. petals (a) reflexed or (b) falcate; 21. petals with large basal lobes; 22. petals (a) fused to the galea or (b) fused to the rostellum; 23. lip (a) linear, (b) spathulate, (c) minute, (d) pandurate, (e) ovate, (f) fleshy; 24. lip lacerate; 25. anther (a) erect or (b) pendent; 26. rostellum lateral lobes (a) hornlike or (b) square; 27. rostellum central lobe (a) absent, (b) tall, (c) V-shaped; 28. Rostellum of the Monadenia-type; 29. viscidia fused; 30. caudicles as long as the pollen-mass; 31. tubers absent; 32. petals exserted from the galea; 33. petals villous. From Linder (1986).

Micranthae
Disa
Phlebidia
Hircicornes
Ovalifoliae
Stoloniferae
Austroalpinae
Emarginatae
Coryphaea
Stenocarpa
Amphigena
Disella
Intermedia
Repandra
Aconitoides
Monadenia
Forficaria
Herschelia
Schizodium
Brownleea

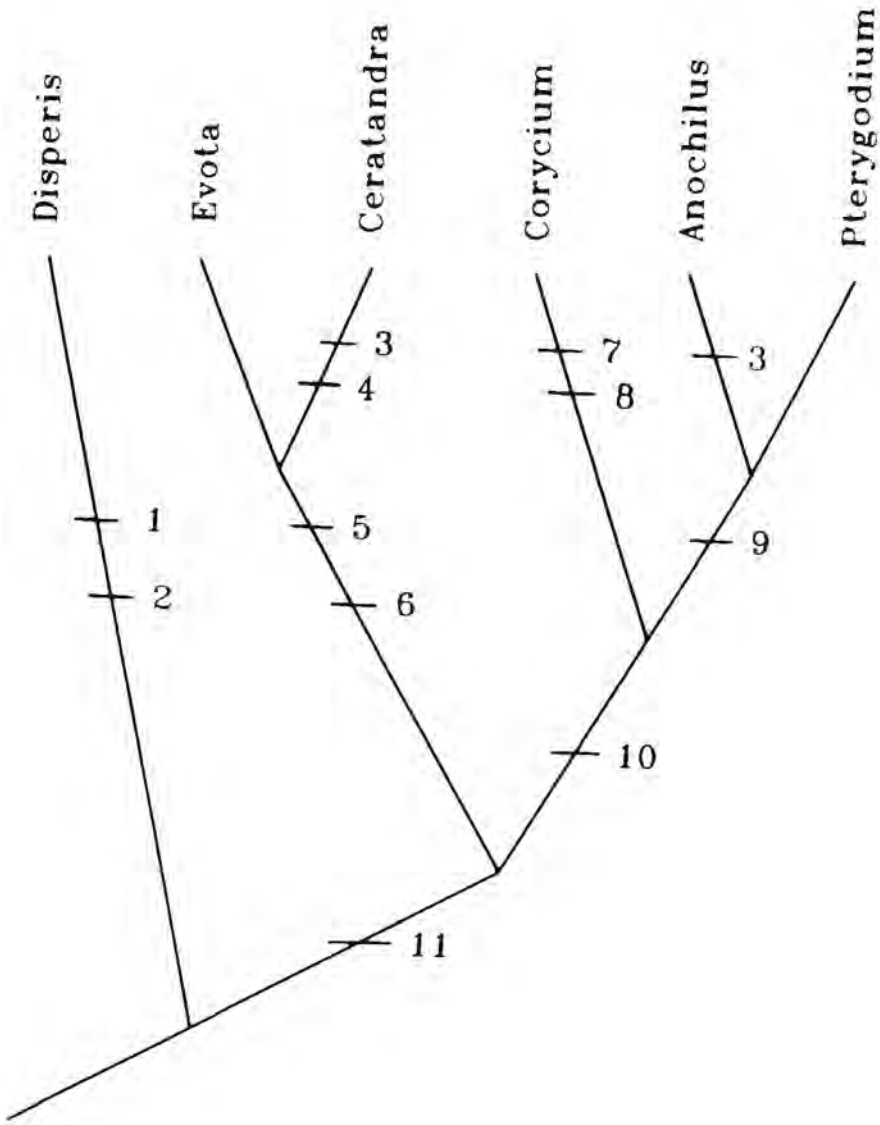

Figure 1.D

Cladogram of the Coryciinae with genera as the terminal groups. The characters used are: 1. lateral sepals saccate to spurred; 2. rostellum lobes covering the anther cells; 3. flowers non-resupinate; 4. lip without an appendage; 5. lip wuth a fleshy callus; 6. root-stem tuberoids cylindrical; 7. galea deep, globose; 8. lip appendage lobes decurved over the anther cells; 9. lip appendage erect; 10. anther cells separated at the base by an elongated split connective; 11. anther cells diverging at least at the apex. From Linder (1986).

The problems relating to the generic and infrageneric classification of the Disinae and Coryciinae were outlined by Linder (1986) and are as follows.

In the Disinae, the genera Monadenia, Schizodium, and Brownleea are by themselves monophyletic. However, in the cladistic analysis, they appear as an unresolved trichotomy with precise phylogenetic relationships unclear. The genus Disa is highly complex, and the relationship between Disa and Herschelianthe is unclear. In a phenetic analysis (Linder, 1986), Herschelianthe was included with sections Stenocarpa and Coryphaea, whereas the cladistic analysis (which relied more on floral characters) kept Herschelianthe as a separate genus. A further systematic problem regarding the Disinae is that of paraphyly. The cohesion of Disa is uncertain in cladistic terms due to the lack of a defining evolutionary novelty for this group. At present the genus is based on the shared retention of a complex of shared plesiomorphic features including the lip, spur and rostellum structures.

In the Coryciinae, resupination of the flower is an important character. The genus Anochilus lacks this resupination. Its removal by Schelpe (1982) from Pterygodium probably leaves Pterygodium as a paraphyletic group (Linder, 1986).

Huttonaea is another problematic genus which is generally placed in its own subtribe (Huttonaeinae) in the Orchideae (Dressler, 1981), and is considered to have no close relatives (Dressler, 1981). Linder (1986) and Kurzweil (1989) suggest that features of the lip, stigma and rostellum structures may indicate affinities with the tribe Diseae, the Coryciinae in particular, as suggested by features of the anther cells and rostellum structures. Kurzweil (1989) points out that ascending, suberect, or erect anthers also occur in all three subtribes of the Diseae. It remains to be shown however, whether the similarities between Huttonaea and the Coryciinae indicate a close relationship, or are the product of convergent evolution.

Linder (1986) has emphasized that data from other character suites would be required to resolve taxa where floral morphology alone has proved inadequate, such as the generic groupings within the Diseae.

The fine structural details of pollen walls as well as detailed sculpturing patterns of the exine surface observable with TEM and SEM techniques can be a source of additional data for systematic studies. Electron microscope investigations of orchid pollen include the works of Williams and Broome (1976), Newton and Williams (1978), Schill and Pfeiffer (1977), Burns-Balogh (1983). Schill and Pfeiffer (1977) found sculpturing to be extremely diverse in the Diseae and

Orchideae. According to Burns-Balogh (1983), the orchid pollinium and its accessory structures has been a source of major characters used in orchid systematics. However, to date most studies have been descriptive, without specific evolutionary goals. Comparative studies of related taxa are necessary to realize the phylogenetic potential of pollen wall morphology (Walker and Doyle, 1976).

An initial survey of the pollen surface ornamentation of the Diseae (Linder, 1986) prompted this more extensive investigation of pollen morphology which is intended to critically assess the systematic value of pollen data, and identify the hierarchic level at which pollen characters are taxonomically useful. Since very little is known of the ultrastructure of the compound massulate pollen of the group, elucidation of modes of cohesion and general morphology are also part of the objectives of the palynological study. In terms of congruence of pollen data with the present classification, it is important to stress that pollen morphology is also related to pollination syndromes.

Classic investigations of orchid anatomy include the works of Holm (1908), Camus (1908), Möbius (1887), Hünecke (1904), and Solereder and Meyer (1930) which are particularly cited (Pridgeon, 1982; Rosso, 1966).

Recent anatomical studies from which phylogenetic inferences have been drawn are those of Rosso (1966), Ayensu and Williams (1972), Pridgeon and Williams (1979), Pridgeon (1981, 1982 a & b), Pridgeon and Stern (1982), and Gasson and Cribb (1986). Pridgeon (1982a) found combinations of anatomical characters to be diagnostic for many genera and species complexes in the Pleurothallidinae, in addition he (Pridgeon 1982 b) demonstrated the utility of statistical procedures in orchid taxonomy and interpretation of phylogeny.

In contrast to the palynological data, leaf anatomical data is unrelated to pollination syndromes. The questions raised are different. Firstly, one might expect that leaves could be fairly plastic, responding to environmental factors, and whether taxonomically useful characters can be extracted from this data base is one of the questions posed in this study. In addition, both anatomical features and morphometric characters were used and tested in the cladistic analyses, the value of quantitative data is assessed. Finally, in the absence of or in addition to phylogenetically linked character combinations, the presence of environmentally determined "adaptive syndromes" were tested using phenetic methods.

2.0 THEORY OF CLADISTIC METHODOLOGY

Cladistic theory was originally formulated by the German entomologist Willi Hennig in the 1930's. It was not until the English translation of his work (Hennig, 1965, 1966) that his ideas received international recognition. Although the theoretical foundations of cladistics have remained more or less unchanged, in the last decade "transformed cladists" (Hull, 1984) have refined the methodology, not without much debate (see Systematic Zoology, Vol. 28 in particular).

Certain restrictive premises have been rejected by the "transformed" school. These are the strictly dichotomous nature of speciation, the disappearance of parental species at speciation, that species must be demonstrably monophyletic, and that sister groups must receive equal ranking (Hull, 1984). The approach of the new school of cladists is one that does not make a priori assumptions about evolutionary processes, but rather attempts to identify patterns of character distribution empirically. Resultant cladograms are then used to make hypotheses relating to phylogeny, evolutionary processes and biogeography, thus avoiding circular argumentation (Linder, 1988)

Cladistic methodology is essentially a procedure of pattern recognition. These patterns may be interpreted to reflect phylogeny, in that they reflect diversity resulting from character modification. The methodology is designed to search for characters that unite taxa by unique common ancestry.
It is necessary to distinguish between cladistics and phylogeny, as cladistics refers only to the cladogenic or branching component of phylogeny (Linder, 1988), and not to evolutionary change within a lineage, the anagenic component.

2.1 CHARACTERS AS TAXONOMIC INDICATORS

The term character, in systematics, is loosely used to cover comparison of homologous conditions. "Homologue" was coined by Owen in 1848 to describe the same parts of different organisms, irrespective of specific differences in form and function, for the purposes of comparative anatomy i.e. with no evolutionary goals.

There is no unequivocal definition of a character. Wiley (1981), in his definition, stresses that a character is the product of the evolutionary process. He defines a character as "a feature of an organism which is the product of an ontogenetic or cytogenetic sequence of previously existing features, or a feature of a previously existing parental organism(s). Such features arise in evolution by modification of a previously existing ontogenetic or cytogenetic or molecular sequence." In a simpler definition, Mayr (1969) defines a character as "any attribute of a member of a taxon by which it differs or may differ from a member of a different taxon." This definition is close to Hennigs' (1966) and Pattersons' (1981), who equate character with synapomorphy. In his treatment of morphological characters and homology Patterson (1982) defines homology as the relation which characterises monophyletic groups. Corollaries to the role of homologies in distinguishing natural groups are that synapomorphy and homology are the same, that every

worthwhile proposal of homology is an hypothesis of a monophyletic (natural) group, that homologies form a hierarchy, and that paraphyletic (unnatural) groups are not characterized by homologies. According to Patterson (1982), his definition of homology in terms of monophyly circumvents the problems of cladistic or evolutionary definitions which are based on common ancestry. Neff (1986) suggests that characters are low level hypotheses of polarity and homology, which can be tested against empirical observations, against ontogeny, and against congruence with other characters on a cladogram. For these reasons the definitions of Patterson (1982) and Neff (1986) are theoretically stronger than that of Wiley (1981), simply in terms of their testability.

Patterson (1982) outlines three types of tests of homology. These are: conjunction (the homologues may not coexist in one organism), similarity (topographic, ontogenetic and compositional) and congruence (with other homologies). Congruence testing is based on the rationale that synapomorphies are the only properties of monophyletic groups and therefore, the test of an hypothesis of homology must be other hypotheses of homology. Testing by congruence is also discussed by Wiley (1975, 1976), Lovtrup (1977), Platnik (1977) and Gaffney (1979).

Congruence testing is the most powerful of the three tests, for it is the only test that descriminates useful comparisons from homoplasy (Patterson, 1982).

Testing is done in relation to phylogenetic relationships founded on other characters. This is the major criterion in the hypothetico-deductive mode implicit in cladistic methodology. Non-homologous similarities are revealed by such tests as the products of convergence or parallelism. Both phenomena are encompassed by the term homoplasy and the difference between these two types of similarity is one of degree of relationship. Generally non-homologous similarity in closely related species is the product of parallel evolution. Homoplasy results if the common ancestor of two or more species did not have the character in question, or if one character was not the precursor of the other (Wiley, 1981). A character which has evolved directly from its preexisting homologue, i.e. the derived state, is described as apomorphic. The character that arose earlier in time, giving rise to the apomorphic state is the plesiomorph. When primitive and derived characters are shared amongst taxa, they are termed symplesiomorphic and synapomorphic characters respectively. In the case of a derived character being in a single taxon only, the state is defined as an autapomorphy relative to that taxon.

At one level of the hierarchy a character may be a synapomorphy

for a taxon or group of taxa, whereas at a lower level a state of a particular character may define a group. In the latter case the character state would be the synapomorphy defining the particular taxon. In character analysis, it is important to bear this in mind as on cannot assess a priori the systematic value of a particular data set or the hierarchical level at which it will operate in the delimitation of taxa. Such levels are termed "levels of universality" by Wiley (1981), and are the root of the equivocality in the strict delimitation of characters and character states. Consequently, Patterson (1982) circumvents this problem and agrees with Bock (1974) who states that "no distinction exists between characters and character states. The latter are simply characteristics which may be homologous with a more restrictive conditional phrase". Patterson (1982) argues further that symplesiomorphies are also synapomorphies that are homologies that circumscribe a group whose generality is wider than, and therefore irrelevant to, the problem under study. He views symplesiomorphy and synapomorphy as terms for homologies which stand in hierarchical relation to one another, and emphasizes that "every worthwhile hypothesis of homology specifies a hierarchy of groups."That a particular feature should be plesiomorphic does not mean that it is irrelevant to the biology of the organism, but essential to the cladistic approach is the need to make precise statements about immediate common ancestry. For this reason synapomorphic characters only are used to test phylogenetic hypotheses. They

are the only characters capable of justifying or rejecting statements of immediate common ancestry i.e. sister group statements. The omission of plesiomorphic characters from cladistic analyses also relates to the principle of overall parsimony which is discussed below.

The criterion of phylogenetic position (Wiley, 1981) is used to determine whether an alternate homologue is apomorphic, this is tested by outgroup comparison.

In the process of character analysis and hypothesis testing diagnostic characters are identified and it becomes clear that all characters do not have the same power of taxonomic resolution. In other words, there are good and bad characters but the value of a character can only be assessed a posteriori, in relation to the most parsimonious cladogram.

Farris' (1969) unit character consistency c(i) is a measure of fit of characters to cladograms. It is defined by the following equation:

$$c(i) = \frac{r(i)}{l(i)}$$

Where r(i) is the range of the character i.e. the smallest value that the patristic unit character length l(i) (for that character) can attain on any tree, or the difference between its numerically least and greatest states. In this study, character consistency is expressed as a percentage.

In practical terms, character identification and analysis involves the observation of a sample of the study group, covering most of the expected range of variation. This is followed by choice and formulation of characters and character states for initial generation of cladograms and subsequent testing of hypotheses. The extent to which the biological and structural properties of characters should be investigated is equivocal. In some cases, a biological understanding of structural features may improve homology postulates, character state definitions and their polarization.

Since the identification of homologous characters and the evolutionary polarization of character states is central to cladistic analysis, these are implicit in the character coding scheme. In non-additive characters any two distinct states are taken to be separated by a single step. In such a character, any state could lead to another and the basal state only, is determined. As a consequence, the coding of a non-additive character is coupled with a loss of evolutionary information. In additive characters, evolutionary polarity postulates follow a linear sequence from the primitive to the more advanced states. Pastristic distances can therefore be established for each apomorphic state.

2.2. CHARACTER WEIGHTING

Mayr (1969) defines weighting as a method for determining the phylogenetic information content of a character. He formulated a classification of weighting criteria which include complexity of structure which would in turn reflect developmental and genetic complexity, joint possession of derived characters, constancy through large groups, correlated suites of characters, characters not associated with an ad hoc specialization, characters not affected by ecological shifts. Empirical methods, however are distinctly lacking for the determination of such criteria.

In numerical taxonomic methods the weighting of characters is a controversial issue. According to Neff (1986) "discrimination between meaningful and meaningless characters is at the heart of what many other taxonomists are addressing by their development of criteria for character weighting." But, as Eldredge and Cracraft (1980) point out, all characters are evolutionary novelties at some level and the problem is finding the characters and recognizing their level of significance in the hierarchy. For this reason, the prevailing view amongst cladists with regard to ad hoc weighting is that it should be avoided by recognizing that all non-convergent i.e. homologous characters are relevant to defining monophyletic groups at some level. Wheeler (1986), however, argues that "not weighting is

one of the most subtle and influencial sources of weighting" (arising from the number of character states and coding methods used), and that some kinds of characters are inherently more informative than others, and that finally it is a problem of definition as delimitation of characters can be problematic.

Relative or differential weighting, on the other hand, is often in accordance to a character's inferred information content. Hecht and Edwards (1976, 1977) assign different values to different kinds of evidence, giving high weight to functional complexes, and higher weight to unique innovations, and no weight to lost characters.

Equivalence weighting (Wheeler, 1986) is based on the assumption that all evidence is equally informative and should have an implicit weight of one. For example, if a character is coded for two or three times it should be deweighted, or if character states are in fact apomorphies, the compound character should be weighted. Wheeler states that "this form of weighting is justified on its objectivity alone and on the knowledge that correctly recognized characters are equally informative".

Wheeler (1986) views ad hoc weighting as applicable to cladistic analyses a posteriori and specifically in response to unresolved homoplasy. Farris'(1988) autoweighting routine is a typical form of a posteriori weighting.

2.3 OUTGROUP COMPARISON

Two methods of determining the evolutionary polarization of character states are widely used. These are the comparative or outgroup method and the ontogenetic method.

The ontogenetic method is based on a combination of Haeckel's Law of recapitulation (Jefferies, 1979), the biogenetic law, and von Baer's Law of generality (Patterson, 1982), whereby the more general state manifests itself in early ontogeny, with the apomorphic change occuring later in the ontogenic sequence. In other words, that ontogeny passes from the simple to the complex, from the general to the particular. Patterson (1982) advocates that ontogeny is the decisive criterion in determining polarity if it depends on von Baer's Law of generality. In such a context he suggests dropping the terms primitive and derived, and that a knowledge of or belief in evolution is clearly unnecessary for the analysis of homologies. However, ontogeny does not always provide unambiguous evidence of character polarity (Kluge, 1985; Blackmore and Crane, 1988)

Outgroup comparison is widely regarded as one of the most reliable and logically justified method of assessing character polarity in cladistic analysis (Eldredge and Cracraft, 1980, Nelson and Platnik, 1981, Wiley, 1981, Watrous and Wheeler, 1981, Maddison et al, 1984).

This method is based on the principle that, for a given character with two or more states within a group, the state occurring in related groups (the outgroup or sister group) is assumed to be the plesiomorphic state (Watrous and Wheeler, 1981). Watrous and Wheeler (1981) qualify their definition by pointing out that if both states of a two state character occur in the taxonomic ingroup and also in the taxonomic outgroup, and if the relative polarities of the two states in the outgroup are unknown, then polarization of character states cannot be immediately resolved by outgroup comparison. Additional problems arise due to lack of resolution of the outgroups to each other. A solution to these problems is to restrict the analysis to only those characters that are uniform throughout the composite outgroup but vary in the ingroup (Cantino, 1982).

Outgroups are selected from clades that originate below the immediate common ancestor of the groups composing the ingroup, preferably immediately below i.e. from the sister group. Outgroup taxa may either be used to construct a single hypothetical ancestor to the study group, or several outgroup species may be specified to root the trees generated in the cladistic analysis. This latter method is in keeping with the suggestion of Donoghue and Cantino (1984) who advocate simultaneous resolution of the outgroups plus the ingroup i.e. the "global parsimony" approach of Maddison et al (1984).

They view this method as most appropriate when one can assume that the plausible outgroups plus the ingroups form a monophyletic group. This method is also in keeping with the HENNIG 86 program, which treats outgroups not as ancestors, but as outgroups which on the basis of character analysis, may eventually be included into the ingroup.

2.4 CLADOGRAMS AND PARSIMONY

Patterson (1982) views the cladogram as a summary of the pattern of homologies, a synapomorphy scheme, or at best, a hierarchical classification. A tree (pattern of descent) is a cladogram modified by eliminating some of the branches, so that taxa lie at or between nodes, and are so designated as ancestors. Sister group relationships, or the relationship between terminal taxa in a cladogram, are specifiable by homology, the homologies characterizing the nodes linking the taxa. The role of homology in phylogeny reconstruction is therefore limited to cladograms.

In cladistic analyses, the choice of characters and their states is critical. Evolutionary polarization of states and hypotheses of homology account for their theoretical content and central role in the generation of cladograms. The low-level hypotheses of homology and evolutionary transformation embodied in the characters are used, subsequently, to test intermediate-level hypotheses or cladograms. Characters are assessed by their corroboration or incongruence with the cladogram. Analysis of character state distribution provides potential tests of the relationships of taxa showing the characters. Characters in the data set that are incongruent with the most parsimonious tree are redefined as cases of convergence or reversal. Farris (1969) distinguishes the unit character consistency from the overall consistency of a set of characters with a tree.

He points out that overall consistency is not, in general, equal to the mean value of the unit character consistencies of the data set with the tree.

The principle of parsimony, as applied to cladograms, is based on the philosophical argument of "Occam's razor" i.e. that the simplest explanation is usually the most plausible. In other words by selecting the shortest possible cladogram it is assumed that, of alternative routes, evolution followed the one that required the fewest reversals and instances of convergence or parallelism, in other words a minimal assumption of evolutionary change.

In computer-based cladistic analyses, which aim at finding branching trees of minimum total length, it is common that large numbers of possible cladograms are generated. If the aim of the study is to eventually reconstruct a possible phylogeny, a single tree must be selected. As there is only one sequence of speciation, for a particular group, there cannot be two or more trees that are correct for a particular group of taxa. According to Wiley (1981), the incompatability of trees stands at the base of phylogenetic testing, and results of character analysis are the major bases for accepting one phylogenetic tree over another.

An alternative solution to the problem of choosing amongst an array of equally parsimonious trees is the use of the consensus tree, originally devised by Adams (1972). It represents only that information that is shared by all of the trees. According to Adams (1972), the consensus is a conservative estimate of a compromise classification, and any information not represented in all the competing trees is not represented in the consensus. If competing cladograms are all quite dissimilar, then the consensus tree will contain very little information, whereas if there is considerable agreement amongst rival trees, this will be reflected in a well structured consensus tree. The advantage of the consensus approach to choosing amongst competing trees is that it yields a unique result.

Recently, the issue of choice among multiple equally parsimonious cladograms has been addressed (Brooks et al, 1986, Carpenter, 1988). Carpenter (1988) points out that, although the consensus tree represents a conservative classification, it has less explanatory power since it is less resolved than any of the competing cladograms from which it is calculated. In his view, any of the competing cladograms would be a better choice as a phylogenetic hypothesis or classification.

Clearly, the choice of methods must be in accordance with the objectives of the study.

2.5 SYSTEMATIC CONGRUENCE

Systematic congruence is a form of testing which may apply either to different classificatory strategies e.g. phenetic as opposed to cladistic approach, or as in this case, to different data sets, analysed by the same method. Congruence refers to the degree to which classifications based on different character sets of the same organisms postulate the same groupings (Mickevich, 1978, 1980), and serves as a measure of the stability of a classification as new sources of information are considered. Hull (1984) has argued that congruence among different data sets is the most rigorous test of classifications or phylogeny hypotheses.

The hypothesis that classifications based on different data sets are congruent is termed the hypothesis of non-specificity (Sokal and Sneath, 1963), and applies largely at higher taxonomic ranks (Sneath, 1971). The hypothesis postulates that different sets of phenotypic characters will represent equivalent samples of the genotype. Stated differently a genotype cannot be partitioned into disjointed classes of loci in such a way that any of those classes of loci affect exclusively a single class of phenotypic characters. Pleiotropy, or the multiple effect of a single gene, is problematic in this context. Farris (1972) points out that there is very little experimental evidence dealing with pleiotropy of the loci of the sort of characters that are used to characterize taxa of rank higher than species.

Farris (1972) further suggests that incongruence between sets of characters as assessed by cladistic techniques, can only occur if homoplasy is present in at least one of the sets of characters.

According to Mickevich and Farris (1981) a stable classification from different sets of characters is sought in order to maximize descriptive power. They stress the importance of congruence studies in the identification of a single historical pattern and in the evaluation of differences in grouping.

Congruence tests may be problematic if one or both cladograms are not fully resolved i.e. if the data set is not effective in resolving taxa at the required level of the taxonomic hierarchy. Also, there is the question of arbitrary versus distinct resolutions. This relates to the degree of confidence one has with regards to the synapomorphies determining branching of the cladogram. Distinction must be made between good and bad characters and trees should only be computed with the uninformative characters left out.

Mickevich and Farris (1981) use a "distortion index" as a measure of congruence. This provides a measure of the degree to which a tree departs from a reference tree. They reject counting the number of informative groups on a consensus tree because consensus trees lack information since they represent information which is consistent with multiple original trees.

The data sets can also be combined to generate a single tree, and test the fit of characters (character consistency index) to the resultant tree. Incongruencies between characters can then be assessed by comparing the fit of characters to individual trees based on separate data sets to that of combined tree. Incongruences should then show up as extra steps for each character.

Since the hierarchic level at which a particular data set will separate taxa cannot be known a priori, the appropriate congruence test cannot be anticipated. In this study patterns at species, sectional and generic levels are assessed. If resolution of taxa analysed using leaf anatomical or palynological characters is inadequate, then congruence between these data sets and the present phylogeny can only be tested in a very broad and loose manner. Eventually when a complete range of data sets is available, these can be combined in a more complete and empirical congruence study.

3.1 LEAF ANATOMY METHODS

3.1.1 MATERIALS AND HISTOLOGY

62 species (43 of the Disinae, 18 of the Coryciinae, two of the Orchideae and a single species of the Satyriinae) were sampled for the leaf anatomical study. Fresh leaf material was mostly collected in the field and some was obtained from the Kirstenbosch National Botanic Gardens (NBG). Leaves were fixed and preserved in FAA (Formalin Acetic Alcohol). The sampling of leaves was standardized to obtain material of comparable parts of the leaves from the same parts of plants to ensure that anatomical observations were carried out on homologous tissues. Due to limited material for certain species as well as the variability in leaf shape and size, absolute comparability was not always possible.

Freehand sections of a selected sample were made for an initial survey of the study group. These were stained in toluidine blue which gives good contrast and shows differentiation of tissues. Temporary sections were mounted in water and the slides were sealed with lacker. Sections for permanent mounts were cut to an approximate thickness of 60-90 um using a Reichert freezing microtome. Safranin (Johansen,

1940) and Alcian Blue 8 GX were used in combination (Tolivia and Tolivia, 1987) to provide differential staining of tissues. Staining was followed by dehydration in an ethanol series to xylene, and sections were mounted in DPX mountant.

Permanent and temporary slides of adaxial and abaxial epidermal scrapes were made according to the method of Cutler (1978) whereby a blade is used to scrape away unwanted leaf material from leaves in the presence of Sodium hypochlorite, leaving behind the upper or lower epidermal layer. In the case of temporary mounts, surface scrapes were stained with toluidine blue, permanent mounts were stained in the same solution as transections through leaves. Specific stains for cuticular preparations were not used, nevertheless staining proved adequate for the objectives of the study.

3.2 CODING OF DATA

In addition to the use of anatomical features, dimensional characters were recorded and coded for use in the cladistic analyses.

Table 3.2.A. Dimensional characters recorded in leaf anatomy study.

Adaxial epidermal cell length
Adaxial epidermal cell width
Adaxial epidermal cell length to width ratio
Adaxial epidermal cell depth**
Abaxial epidermal cell length
Abaxial epidermal cell width
Abaxial epidermal cell length to width ratio
Abaxial epidermal cell depth
Adaxial stomatal length*
Adaxial stomatal width*
Adaxial stomatal length to width ratio*
Abaxial stomatal length*
Abaxial stomatal width*
Abaxial stomatal length to width ratio*
Length of long axis of mesophyll cell
Palisade cell length*
Palisade cell width*
Palisade cell length to width ratio*

* characters excluded from analyses.

** character coded as presence or absence of enlarged adaxial epidermal cell layer.

For each specimen, 10 measurements were taken of each quantitative character. In the anatomical descriptions, only the mean of these readings is reported. For the multivariate analyses, raw measurement data were log-transformed to minimize variance, thereby reducing the effect of size, and used as the basic variables.

Data were divided into subsets by establishing homogeneous groups using the Student-Newman-Keuls test for the Analysis of Variance (SAS ANOVA procedure; SAS Institute 1985). A critical value , alpha = 0.5 was chosen to establish homogeneous or discriminant groups. Homogeneous subset coding (Simon, 1983, Archie, 1985) was used to code the subsets into discrete multistate variables from the (generally) overlapping homogeneous subsets. This was done by ordering the species were ordered log-transformed means for each character. A state of 0 was assigned to the species with the smallest value the variable (or largest dimension). For successive species, the coding value was increased by 0.5 if an homogeneous subset was left or a new one entered.

In order to accommodate the large size of the sample, several coded subsets were grouped together to reduce the number of groups formed for each character. A maximum of ten states are permissible in the HENNIG 86 (Farris, 1988) cladistics program. Loss of information may have resulted from reducing the number of groups obtained by this method. Theoretical papers dealing with the use of measurement data in cladistic analyses (Thiele and Ladiges, 1988; Goldman, 1988; Simon, 1983 and Archie, 1985) mostly use small data sets in their methodological descriptions and no alternative solution for dealing with large data sets could be found in the literature.

3.2 PALYNOLOGY METHODS

3.2.1 TRANSMISSION ELECTRON MICROSCOPY (TEM) OF ULTRATHIN SECTIONS THROUGH POLLEN WALLS

The pollen of Satyrium bracteatum, Disperis capensis, Evota bicolor, Schizodium inflexum, Pterygodium catholicum, Corycium orobanchoides, Disa sagittalis and Disa lineata was used for the TEM study.

Fresh pollinaria were collected in the field and fixed as soon as possible in 4 % glutaraldehyde, over ice. A double fixation procedure was used, and material was post-fixed in 2 % Osmium tetroxide, for two hours. Sorenson's phosphate buffer, buffered at pH 7.2 at 4 ^{0}C, was used as a "physiological buffer system" (Hayat, 1981), serving for the dilution of fixatives and as a rinsing agent between and after double fixation.

All fixing and rinsing of specimens was carried out in the same container to avoid drastic changes in environment or damage through manipulation. Pollinia were left to wash in buffer overnight, after fixation in GLUT, and were rinsed three times prior to postfixation to ensure the removal of any remaining fixative. Following post-fixation, material was rinsed off in three washes prior to dehydration, to minimize any possible reaction between fixative and dehydration agent.

The aim of fixation procedures is to preserve ultrastructural features with minimal alteration and loss of cell constituents. Protection of fine structure against dehydration, sectioning, staining, and exposure to the electron beam necessitates chemical fixation whereby the structure of proteins, lipids and other cell constituents is preserved. Fixation is carried out at low temperatures to decrease the extraction of cell constituents and slow down the rate of autolysis. In living tissue, water plays an important part in the stability of chemical bonds. During fixation, the structural role of these bonds is replaced primarily by the formation of inter- and intra-molecular crosslinks of protein. As a consequence, proteins are denatured, loosing solubility and mobility, and becoming less susceptible to precipitation and crystalization (Hayat, 1981). The rapidity of penetration and ability to fix most proteins without coagulation makes GLUT a widely used prefixative. In contrast, Osmium tetroxide penetrates more slowly, and is used to stabilize lipids and some proteins, and as a heavy metal, it gives density (electron opacity) to the tissues it fixes. Both fixatives are additive, so termed because they chemically become part of the proteins they fix.

Material was dehydrated prior to infiltration and embedding of specimens in a water-insoluble resin. In this process, free water in the tissues is replaced by a suitable organic solvent. Ethanol was used here and the dehydration procedure was carried out as follows:

25% ETOH/H_2O	15 mins.
50%	15 mins.
70%	15 mins.
100%	45 mins.
100% (over molecular sieve)	45 mins.

The choice of resin is largely determined by the type of material and the objective of study. Spurrs' (1969) resin was used primarily because of its good penetration properties (low viscosity), an important attribute in the light of the hard and resistant nature of pollen walls. The trade off in this choice is the brittleness of this resin which may cause problems during sectioning. For this reason, the exact amount of resin components, and catalyst in particular, and careful monitoring of cure timing and temperature are of utmost importance in obtaining a specimen block with the desired cutting properties i.e. homogeneity, hardness, strength and elasticity. In addition to these properties, the resin must withstand the high vacuum of the specimen chamber and be thermostable during electron bombardment.

Problems relating to poor embedding are generally due to the presence of water in the absolute alcohol or resin, inadequate dehydration of specimens prior to infiltration with resins, and high ambient relative humidity at the time of embedding.

Infiltration of specimens is achieved by decreasing the concentration of absolute alcohol, which acts as a solvent for the resin, and proportionately increasing the concentration of resin. Due to the hardness of pollen walls, long infiltration times were allowed. For all dilutions of the resin, specimens were placed in an mechanical shaker for a few hours to ensure even penetration of the resin mixture.

Specimens were infiltrated with diluted solutions of Spurr's resin as follows:

25%	Spurrs'/ETOH	8 hrs.
50%		overnight
75%		8 hrs.
100%		overnight

After this step-wise infiltration of pollina with increasing concentrations of resin, the final embedding mixture was poured into polythene BEEM capsules. These were preferred as their pyramidal tips are shaped to facilitate trimming. Specimen orientation was not crucial in this study due to the easily recognizable massulae through which sections were to be taken. Specimens were simply pushed down to the bottom of the capsule with the aid of a pointed stick. These were allowed to polymerize for 8 hours at 70 C.

The quality of the cutting edge is critical in obtaining good ultrathin sections. Glass knives were used. These have good sectioning qualities provided that they are regularly replaced and that the useful cutting edge is evaluated before use. An LKB Knifemaker was used to fracture triangular glass knives with a 45 diagonal break, termed the knife angle. These were prepared just prior to sectioning to minimize any dust damage or any other damage to the cutting edge. The length of useful edge is assessed using a dissecting microscope. Striations and imperfections scatter light and are easily observed.

Trimming and preparation of the specimen block involves the removal of excess embedding medium around the tissue at the tip of the block. An LKB Pyramitone was used for this purpose. Prior to final trimming, thick sections were cut until the desired area of the specimen was exposed. Semi-thin survey sections of an approximate thickness of 4 um were cut with the pyramitone from the incompletely trimmed specimen blocks. These were placed on glass slides and warmed in drops of water to remove wrinkles as well as for adhesion of sections to the slide. Toluidine Blue in 1% Borax was used for differential staining of the survey sections. These were used to select the part of the specimen to be used for the ultrathin sections.

Final trimming involves shaping the tip of the block into a trapezium to facilitate ribbon formation during sectioning. Compression and distortion of ultrathin sections is minimized provided that the specimen block face is kept fairly small. Blocks were prepared with a trapezium-shaped tip with sides of approximately 0.5 mm.

Ultrathin sections were cut using a Reichert OM U2 Ultramicrotome. Trimmed specimen blocks were mounted into the specimen holder with the long side of the trapezium uppermost, and a plastic boat was mounted onto the knife and sealed with dental wax. The boat was filled with distilled water until the meniscus was more or less flat and reached up to the cutting edge, to provide a floatation fluid for the ribbon. The surface tension forces of water also serve to restore sections to almost their original dimensions after being compressed during cutting. The knife was mounted into the knife holder with its cutting edge inclined at an angle to the face of the specimen block. The clearance angle was set at 4 , preventing the block face from scraping the back of the knife after cutting a section. After mounting the knife and setting the knife angle, adjustments were made to align the knife to the block face. These involve getting the block face and knife edge parallel to each other, moving the knife stage laterally so that the useful part of cutting edge comes in line with the face of the specimen block, and bringing the cutting edge close to the block, so that it almost touches the block face.

The entire process was viewed through a binocular microscope mounted onto the front of the ultramicrotome. The approach of the knife to block face was carefully controlled until the edge produced a single bright image on the block face. At this stage section cutting can begin. Section thickness was controlled by a thermal feed, and estimated by the interference colours of sections as they floated onto the liquid. The colours produced are related to section thickness and the refractive index of the sectioned resin and specimen. Cutting speed and section thickness were varied while cutting to obtain "Gold" sections of approximately 90-150 nm. Throughout the cutting process, the quality of sections was closely watched and the correct meniscus level maintained by adding or removing small amounts of water, using a fine-tipped glass pipette.

Once satisfactory sections were obtained and prior to collecting the ribbons, sections were exposed to the fumes of an organic solvent which acts as a section flattener, eliminating foldings or crumples caused by compression forces. This was done by bringing a small stick dipped in chloroform over the trough, taking care that the applicator stick did not carry too much solvent as this can result in overexpansion and consequent distortion of the specimen. Sections were collected on 300 mesh copper grids. The unpolished sides of the grids were used to lift specimens, from below, off the water. Grids were left to dry on filter paper, and covered to avoid contamination.

In the photomicrographs obtained using the TEM, contrast is achieved through the differential scattering of electrons which arises almost entirely from differences in density and thickness of the specimen. Other factors such as the accelerating voltage (KV) and microscope aperture size also affect contrast; small apertures and low voltages give greater contrast at the expense of resolution. Solutions of heavy metals of high atomic number are effective as electron stains. They provide electron opacity selectively by increasing the mass or density of those sites onto which their ions bind. Lead salts are the most widely used stains for electron microscopy, they have high electron opacity and show affinity for a range of cellular structures (Hayat, 1981). Uranium is the heaviest metal used as an electron stain.

In a double poststaining procedure, sections were stained with millipore-filtered uranyl acetate followed by Reynolds'(1963) lead citrate. Lead citrate is a problematic stain. Upon exposure to CO_2, a lead carbonate precipitate forms and can cause considerable contamination of specimens. For this reason, the distilled water used to make up the solution was boiled, to expell CO_2 and care was taken reduce exposure of the staining solution to atmospheric CO_2. Sodium hydroxide pellets are often used, under a petri dish, for this purpose.

The duration of staining depends on the rate of absorption of metal ions, the formation of precipitates in staining solution, and the possible extraction, by the stain, of cellular material (Hayat, 1981). For these reasons staining time is kept as short as possible. Generally, the thinner the section, the longer the staining duration required. Grids were floated section side down, for four minutes on drops of the staining solutions and rinsed three times in distilled water following each staining treatment. These were left to dry on filter paper, ready for viewing.

Specimens were viewed with a Jeol 200CX Transmission Electron Microscope at an accelerating voltage of 80 KV, and photographed at magnifications ranging from 6200 to 27 000 times. A low accelerating voltage was chosen to maximize contrast (at the expense of resolution). This was in keeping with the objective of this study which was to identify pollen wall stratification and structure.

3.3 SCANNING ELECTRON MICROSCOPY (SEM) OF POLLEN SURFACES

The pollen surface ornamentation of 86 species, representing five genera of the Disinae, six genera of the Coryciinae, two species of Huttonaea (presently classified in the Tribe Orchideae), one species each of the genera Bonatea and Habenaria (Orchideae), and Satyrium (Satyriinae) were examined using scanning electron microscopy (SEM).

Air-dried pollen material was obtained from specimens housed at the Bolus Herbarium (BOL). The pollinia were broken apart and individual massulae were mounted on aluminium stubs using a colloidal-graphite glue (Witcomb, 1985). Stubs were sputter-coated for approximately eight minutes with a gold/palladium alloy.

Pollen was examined using a Cambridge S200 scanning electron microscope at an accelerating voltage of 5 Kev, and photographed at magnifications of 1000 and 5000 times. Higher and lower magnifications were used for certain details such as fractures or entire massulae.

The terminology used to describe surface sculpturing is adapted from that of Kremp (1965) and combined with the definitions of Walker (1976) to encompass both the structural and sculptural aspects of pollen wall morphology.

4.0 ANALYSIS

Temporary sections were used for a rapid assessment of the variability in leaf anatomy in a sample of the study group. On the basis of initial observations of leaf sections and surface scrapes, a preliminary list of characters and character states was drawn up. The data-banking program DELTA (Dullwitz and Paine) implemented on a Bondwell PC 38 was used as a primary data bank, from which draft descriptions were generated using the TONAT routine. In addition, INTKEY and TOPAU were used to extract data for character matrices used in the numerical analyses.

For the cladistic analysis HENNIG 86 (Farris, 1988) was used. Due to the large number of taxa IE* (implicit enumeration) was not practical, and the MHENNIG* was used to find the shortest tree, and to generate the full set of equal length trees. Initially cladograms were rooted using separate hypothetical ancestors for the Disinae and Coryciinae. The construction of such hypothetical taxa proved problematic due to the nature of the variation in leaf anatomical characters. Problems of coding arose when attempting to establish distinct states in continuously variable characters such as shape and size of cells, degrees of lignification of tissues, and degree of arm cell development in the mesophyll. In addition, several characters did not vary in the study group (collateral vascular

bundles, anomocytic stomata and the presence of crystal raphide idioblast cells) and these were not coded. Finally, outgroup taxa differed from each other in potentially useful characters such as cuticular sculpturing and enlarged adaxial epidermal cells so that hypotheses of character evolution could not be made with confidence.

Table 3.4.A. Leaf anatomy characters coded in data matrices for cladistic and phenetic analyses.

0) epidermis ornamentation (0=none, 1=papillae)
1) sculpturing of cuticle (0=psilate, 1=striate, 2=micropapillate, 3=reticulate)
2) anticlinal walls of adaxial epidermal cells undulated (0) or straight (1)
3) anticlinal walls of abaxial epidermis undulated (0=yes, 1=no)
4) stomatal distribution (0=leaves amphistomatic, 1=leaves hypostomatic)
5) bundle sheath of primary vascular bundle (0=absent, 1=parenchymatous, 2= sclerotic)
6) adaxial sclerenchyma caps at pole of primary vascular bundle (0=present, 1=absent)
7) abaxial sclerenchyma caps at pole of primary vascualr bundle (0=present, 1=absent)
8) number of secondary vascular bundles (0=0, 1=2, 2=4, 3=6, 4=8)

9) bundle sheath of secondary vascular bundles (0=absent, 1= parenchymatous, 2=sclerotic)

10) adaxial sclerenchyma cap at pole of secondary vascular bundles (0=present, 1=absent)

11) abaxial sclerenchyma cap at pole of secondary vascular bundles (0=present, 1=absent)

12) number of tertiary vascular bundles (0=1 to 5, 1=6 to 10, 2=11 to 15, 3=16 to 20, 4=21 to 30, 5=31 to 40)

13) bundle sheath of tertiary vascular bundles (0=absent, 1=parenchymatous, 2=sclerotic)

14) adaxial schlerenchyma caps in tertiary vascular bundles (0=present, 1=absent)

15) abaxial schlerenchyma caps in tertiary vascular bundles (0=present, 1=absent)

16) total number of veins (0=1 to 10, 1=11 to 15, 2=16 to 20, 3=21 to 30, 4=31 to 40, 5=41 to 50)

17) expansion cells at midrib (0=present, 1=absent)

18) striate cuticle across anticlinal walls of epidermal cells (0=present, 1=absent)

19) adaxial epidermal cell size reduced at midrib (0=yes, 1=no)

20) adaxial epidermal cell size reduced at secondary veins (0=yes, 1=no)

21) sclereidal leaf margins (0=present, 1=absent)

22) photosynthetic tissue (0=homogeneous, 1=differentiated)

23) seriation of palisade tissue (0=1 tier, 1=2 tiers)

24) degree of arm cell development (0=rounded, 1=less rounded, 2=arm-like, 3=well developed arm cells, 4=extremely well developed arm cells)

For characters 25 to 30 and 32 to 33 numbers correspond to homogeneous subset codes.

25) length of adaxial epidermal cells (0=1, 1=2, 2=3, 3=4, 4=5, 5=6, 6=7, 7=8)

26) width of adaxial epidermal cells (0=1, 1=2, 2=3, 3=4, 4=5, 5=6, 6=7, 7=8, 8=9)

27) length to width ratio of adaxial epidermal cells (0=1, 1=2, 2=3, 3=4, 4=5, 5=6, 6=7, 7=8, 8=9)

28) length of abaxial epidermal cells (0=1, 1=2, 2=3, 3=4, 4=5, 5=6, 6=7)

29) width of abaxial epidermal cells (0=1, 1=2, 2=3, 3=4, 4=5, 5=6, 6=7, 7=8)

30) length to width ratio of abaxial epidermal cells (0=1, 1=2, 2=3, 3=4, 4=5, 5=6, 6=7, 7=8)

31) depth of adaxial epidermal cells (0=presence of adaxial water storage tissue, 1=absence of enlarged adaxial epidermal cells)

32) depth of abaxial epidermal cells (0=1, 1=2, 2=3, 3=4, 4=5, 5=6, 6=7)

33) long axis of spongy mesophyll cells (0=1, 1=2, 2=3, 3=4, 4=5, 5=6, 6=7, 7=8)

34) stalked glands (0=absent, 1=present)

35) unicellular hairs (0=absent, 1=present)

36) leaf ribbed (0=no, 1=yes)

37) midrib with prominent parenchymatous keel (0=no, 1=yes)

Detailed coding for analysis at the subtribal level was not possible due to a high degree of heterobathmy.

In an attempt to reduce "noise" in the data set various characters were excluded during initial analyses. However, in the final cladogram most characters were included. The final cladogram was rooted using specified outgroup species from the Orchideae and Satyriinae.

For the phenetic analysis NTSYS-pc (Rohlf, 1988) was used. The data were standardized (STAND), and the taxonomic distance (DIST option of SIMINT) algorithm was used to determine the dissimilarity coefficients among the OTU's. The OTU's were clustered using UPGMA (in SAHN for SIMINT and SIMQUAL) to produce the phenograms. The goodness-of-fit of the phenogram (produced by SIMQUAL) to the dissimilarity matrix was determined by calculating the cophenetic matrix of the phenogram (COPH), which was then correlated with the original dissimilarity matrix (MXCOMP). To test the hypothesis that the data are scattered, a correlation of the standardized data was calculated (STAND, CORR in SIMINT).

Following both SEM and TEM observations of pollen, a preliminary list of characters was compiled to allow the coding, in a data matrix, of the observed variability in pollen wall morphology of the study group. Initial hypotheses of character homology were tested by observing their congruence with taxonomic groups. Evolutionary polarization of character states was based on the outgroup criterion. In the multistate characters used, the symplesiomorphic state was identified, but various states were not polarized further. Due to the nature of pollen data, many of the character states identified were coded as non-additive, as evolutionary polarization was not possible in a linear sequence without a priori phylogenetic consideration. This may have resulted in some loss of information but was necessary in order to avoid false hypotheses of character evolution, and the circular argumentation of relying on the present phylogeny to assess the direction of pollen character evolution.

Table 3.4.B. Pollen characters coded in data matrices for cladistic analysis.

0) Shape of massulae (non-additive, equivalence weighting 3):

0 - rounded

1 - elongated

2 - fasciculate

1) Tetrad shape:

0 - more or less isodiametric

1 - elongated

2) Basic exine sculpturing category (non-additive, equivalence weighting 3):

0 - semi-tectate reticulate exine (including variations i.e hamulate, ornate)

1 - semi-tectate rugose or verrucose exine

2 - secondarily tectate exine with psilate, striate, rugulate, punctate or foveolate pattern

3) Reticulate sculpturing (non-additive, equivalence weighting 5):

0 - reticulum with muri and inter-mural spaces small and evenly distributed.

1 - reticulum with slight depressions instead of open lumina

2 - reticulate with broken down muri and free baculae.

3 - ornate or loosely reticulate, with large often pilate or baculate lumina

4 - hamulate, with supra-tectal elaborations on the muri

4) Exine sculpturing of semi-tectate, non-reticulate pollen:

0 - rugose

1 - verrucose

5) Exine of secondarily tectate grains (non-additive, equivalence weighting 4):

0 - psilate

1 - striate and perforated by foveolae or punctae

2 - rugulate

3 - granulate

6) Supra-tectal ornamentation:

0 - granulae

1 - fine rugules

7) Pilae, or pilate structural sculpturing elements (columella homologues):

0 - absent

1 - present

8) Baculate structural sculpturing elements (columella homologues):

0 - absent

1 - present

9) Foveolate perforations in tectate grains:

0 - absent

1 - present

10) Punctate perforations in tectate grains:

0 - absent

1 - present

11) Margins of tetrad distinct and slightly raised (non-additive, equivalence weighting 3):

0 - no

1 - yes, in semi-tectate grains

2 - yes, in tectate grains

12) Foveolate perforations in semi-tectate grains (equivalence weighting 3):

0 - absent

1 - present

2 - present such that tectum appears to be broken down, leaving free baculae

13) Punctate perforations in semi-tectate grains:

0 - absent

1 - present

The data matrix was broken up into three smaller matrices since problems arise when a large number of species are analysed on the basis of relatively few characters. Two species level matrices were constructed for the subtribes Disinae and Coryciinae. A third matrix was used to test the value of palynological data at the subtribal level using genera as taxa. In each analysis, several species from the Orchideae and a representative of the Satyriinae were used to root the tree. When analysing species of the Disinae, representatives of the sister group Coryciinae where designated amongst the outgroup taxa, likewise for the Coryciinae where genera of the Disinae were included amongst the outgroup taxa.

For the cladistic analyses the MHENNIG* and BB* options were used in the species level analyses. Implicit enumeration IE* was used for analysis at the generic level.

5.0 RESULTS AND DISCUSSION

5.1 LEAF ANATOMY

5.1.1 OBSERVATIONS AND ANALYSIS OF LEAF ANATOMICAL CHARACTERS

Full descriptions of species are included in Appendix 3, and a sample are illustrated in Figures 5.1.1.A to 5.1.1.P to show the observed variation in the leaf anatomy of the study group.

Stenoglottis fimbriata

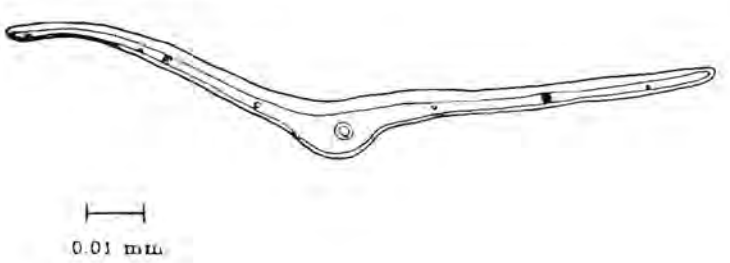

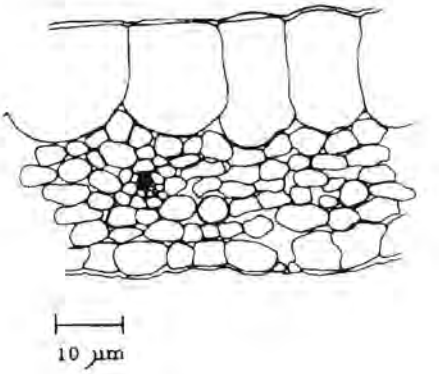

Habenaria laevigata

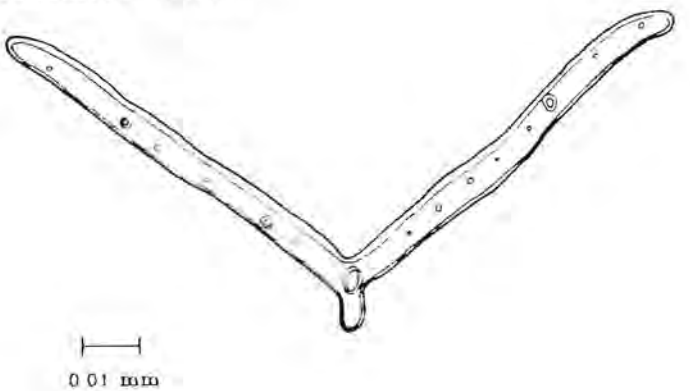

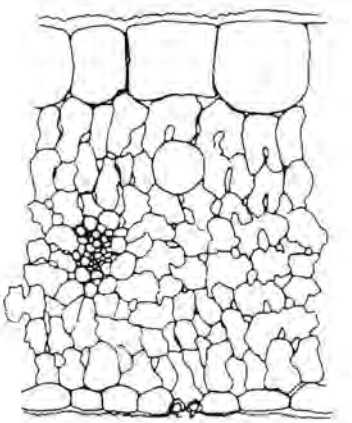

Schizochiles flexuosus

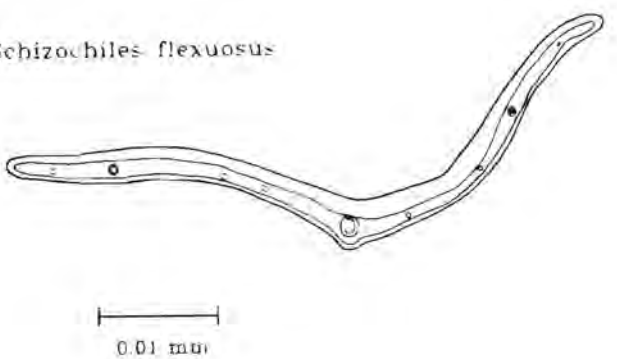

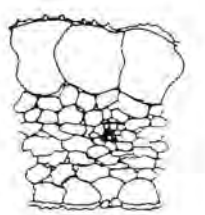

Figure 5.1.1.A

Leaf anatomy in the Orchideae. Plans of leaves and a section throuugh the mesophyll showing abaxial stomata, homogeneous chlorenchyma and a secondary vascular bundle. Note enlarged adaxial epidermal cells which function in water storage. Cuticular sculpturing in the group is micropapillose or reticulate. Cuticular striations occur across anticlinal walls of Habenaria laevigata.

SATYRIINAE

Satyrium erectum

0.01 mm

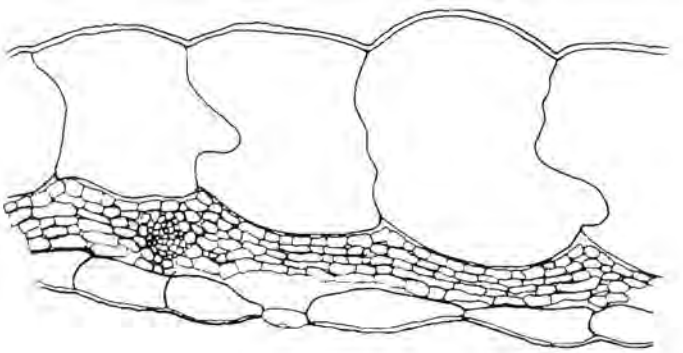

10 µm

Pachites bodkinii

10 µm

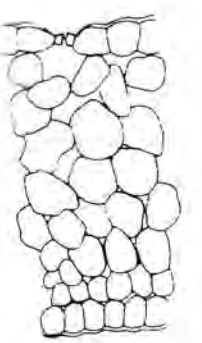

10 µm

Figure 5.1.1.B

Leaf anatomy in the Satyriinae. Satyrium bracteatum has a large flattened leaf with an extremely enlarged adaxial epidermal layer. Stomata are restricted to the lower leaf surface, and photosynthetic tissue is homogeneous. Pachites bodkinii has small crescent-shaped amphistomatic leaves with homogeneous photosynthetic tissue. S. bracteatum has striate cuticular sculpturing, and in P. Bodkinii it is micropapillose.

DISINAE

MONADENIA

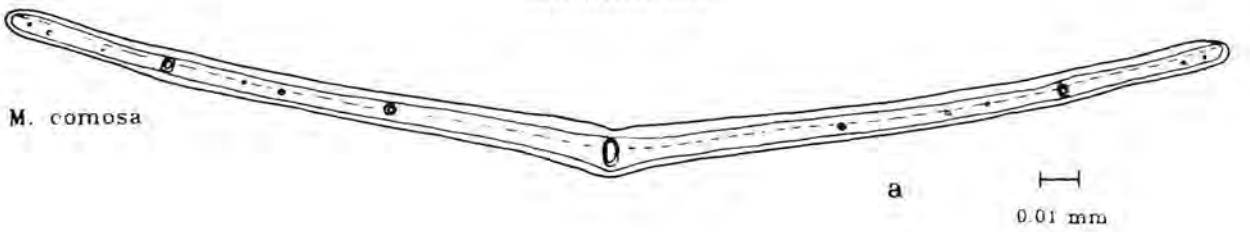

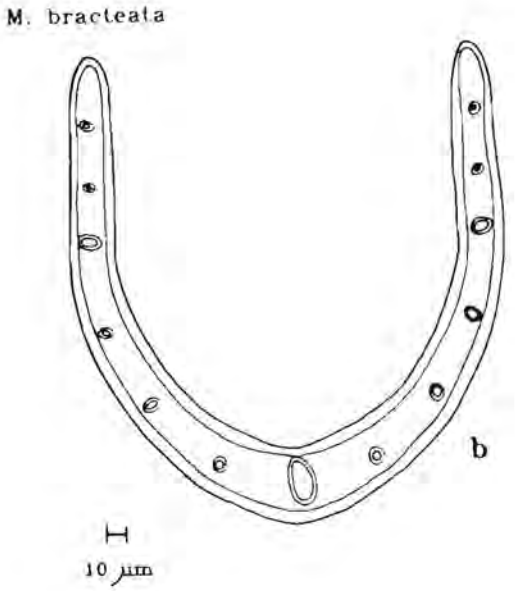

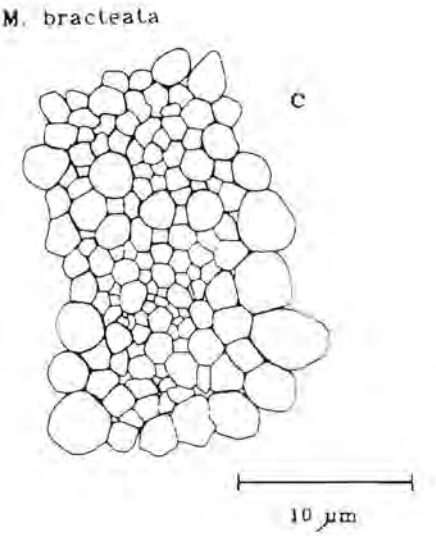

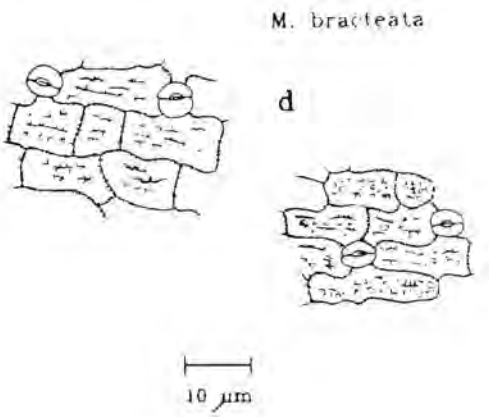

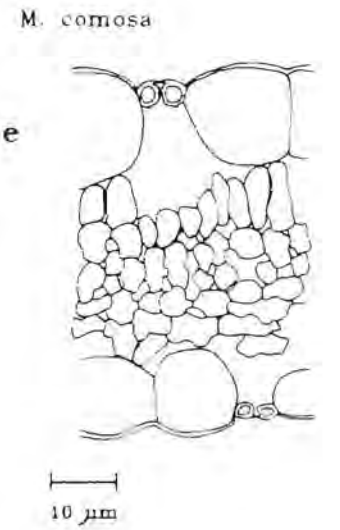

Figure 5.1.1.C

Leaf anatomy in the Disinae: Monadenia. Leaves are mostly with an enlarged adaxial epidermal layer as in M. comosa (a). M. bracteata is the exception, and lacks enlarged adaxial cells. Vascular bundle with parenchyma bundle sheath (c). Photosynthetic tissue is mostly differentiated, and adaxial stomata characteristically pierce the adaxial water storage tissue (e). M. bracteata has a sculptured cuticle with striations across anticlinal walls.

DISINAE

SCHIZODIUM

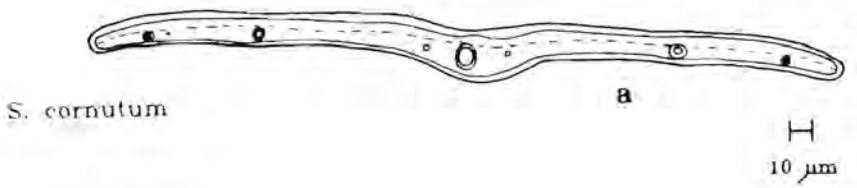

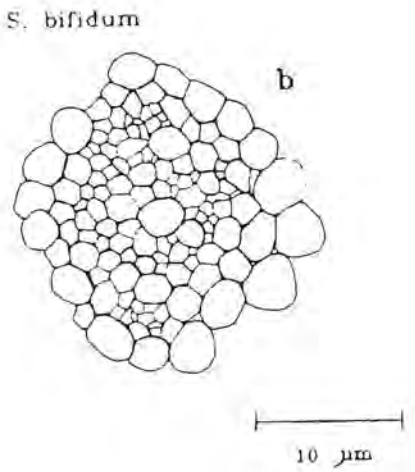

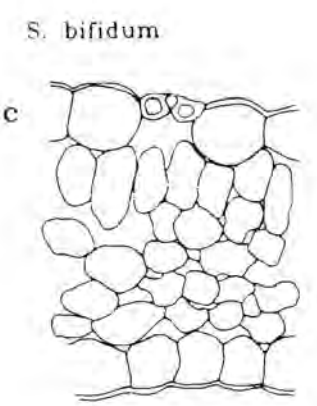

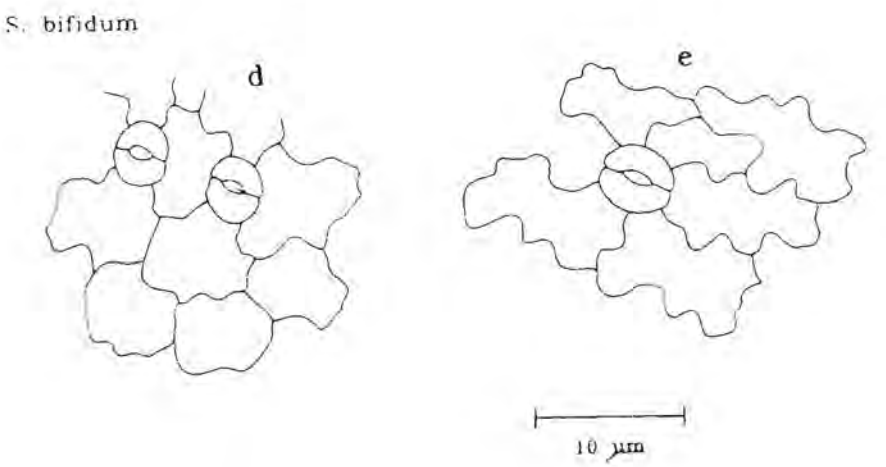

Figure 5.1.1.D

Leaf anatomy in the Disinae: Schizodium. Amphistomatic leaves are differentiated into spongy mesophyll and palisade layer (a, c). Primary vascular bundle with parenchymatous bundle sheath (b). Adaxial (d) and abaxial epidermal cells have undulated anticlinal walls.

DISINAE

BROWNLEEA

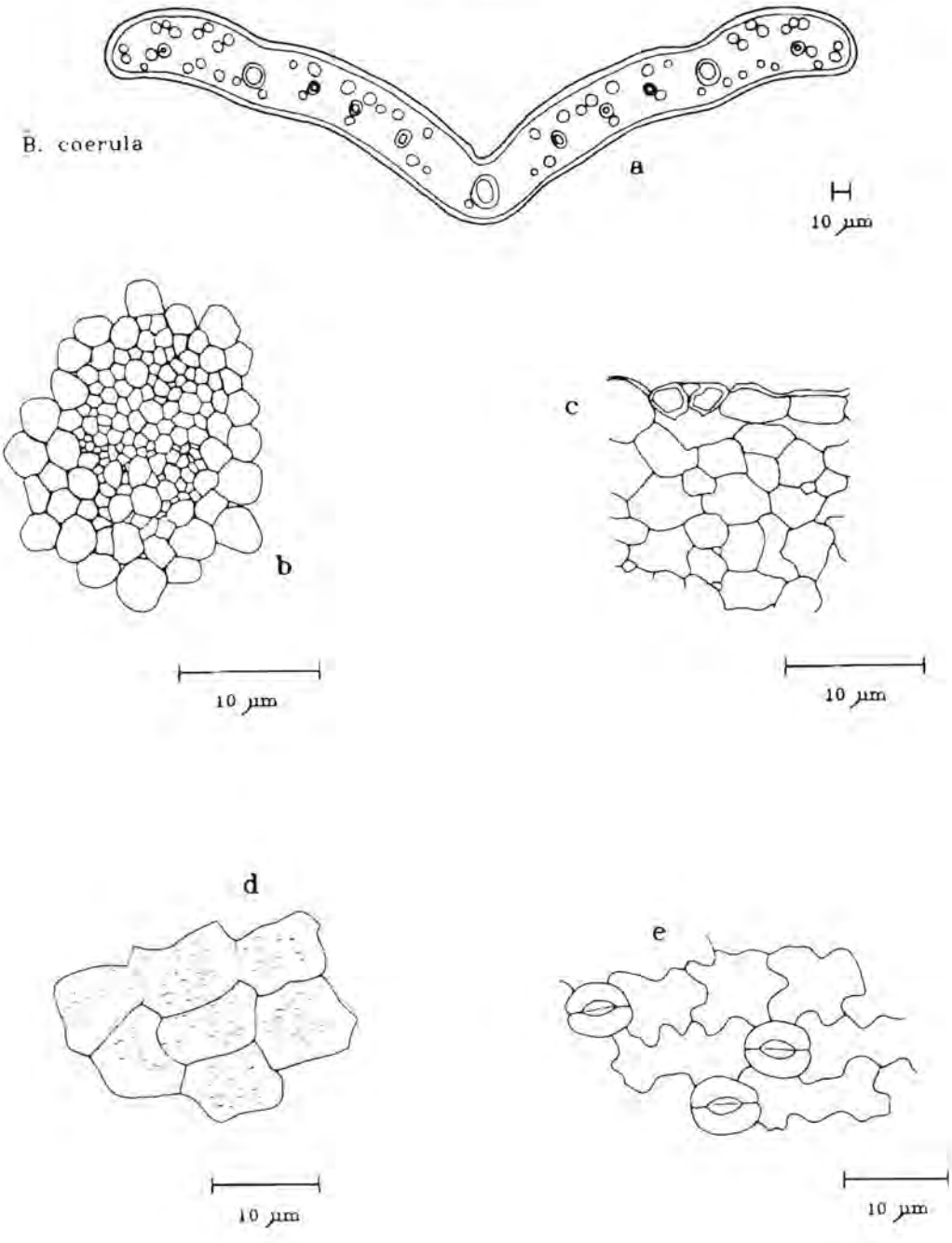

Figure 5.1.1.E

Leaf anatomy in the Disinae: Brownleea. Leaves of Brownleea have numerous idioblast cells, distributed throughout the mesophyll (a). Primary vascular bundle with parenchymatous bundle sheath (b). Anticlinal walls of adaxial cells are straight (d), whilst abaxially they are sinuous.

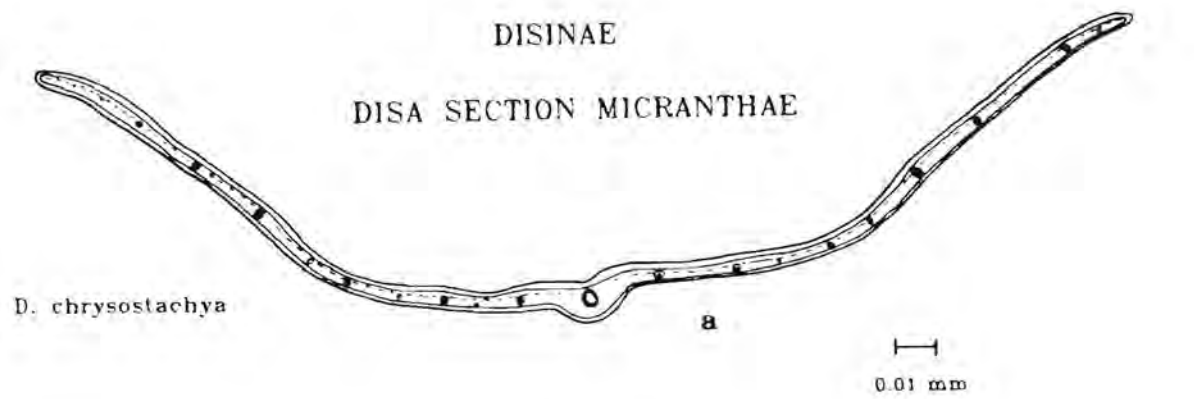

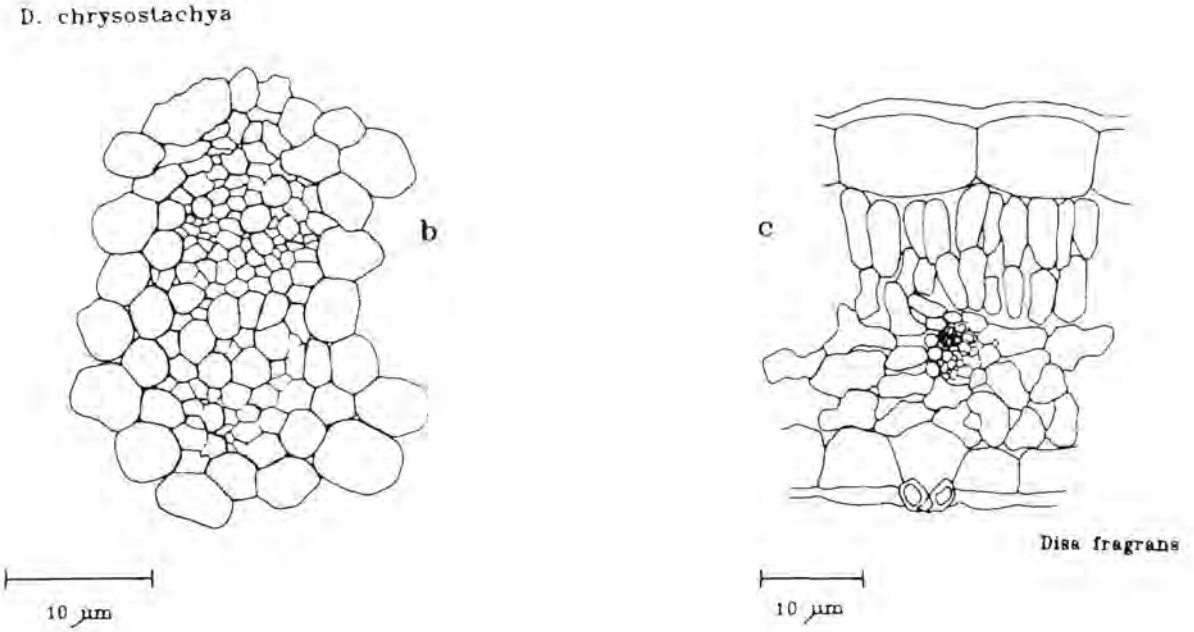

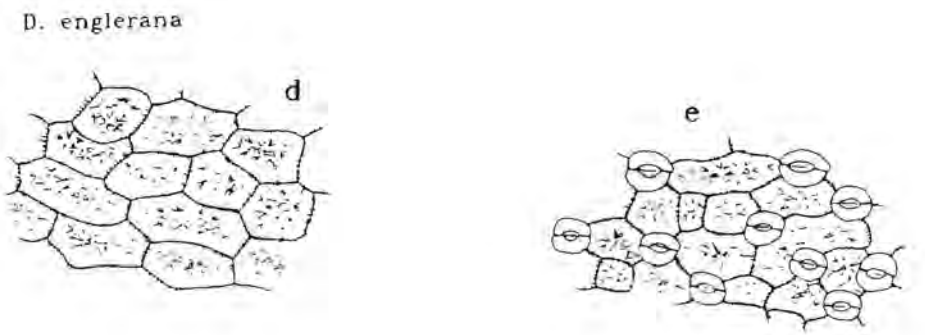

Figure 5.1.1.F

Leaf anatomy in the Disinae: Disa section Micranthae. Leaf anatomy in this section is distinctive. Primary vascular bundle with parenchymatous bundle sheath (b). Photosynthetic tissue is differentiated into one or two palisade layers, stomata occur on the abaxial surface, and cuticles are highly sculpture, usually with a reticulate pattern.

DISA SECTION DISA

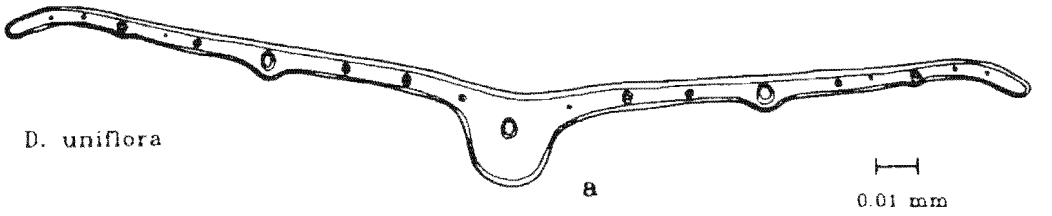

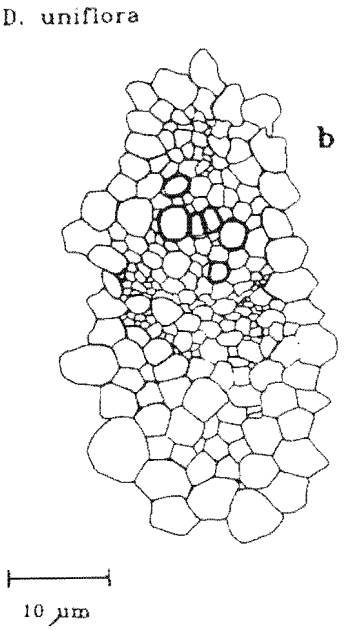

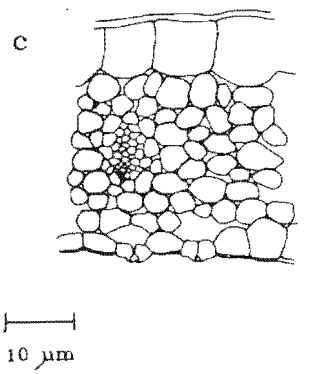

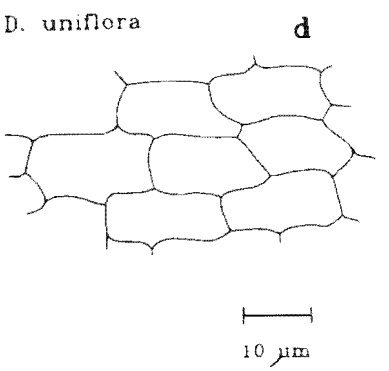

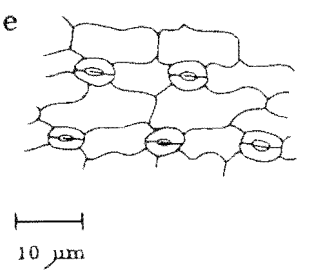

Figure 5.1.1.G

Leaf anatomy in the Disinae: Disa section Disa. Disa uniflora has parenchymatous extentions at the midrib and seconadary ribs (a), primary vascular bundle with parenchymatous bundle sheath (b), Hypostomatic leaf has adaxial water storage and homogeneous chlorenchyma (c), adaxial (d) and abaxial (e) cuticles are psilate.

DISINAE

DISA SECTION PHLEBIDIA

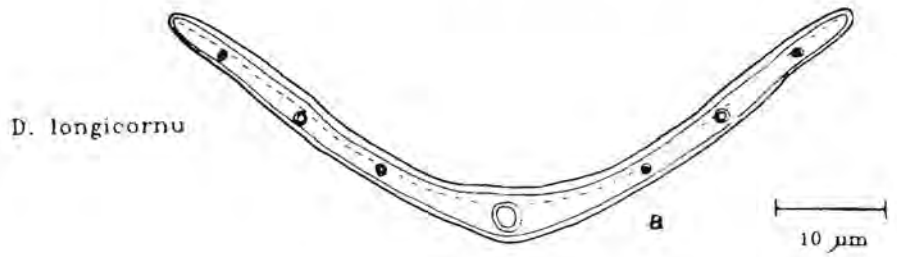

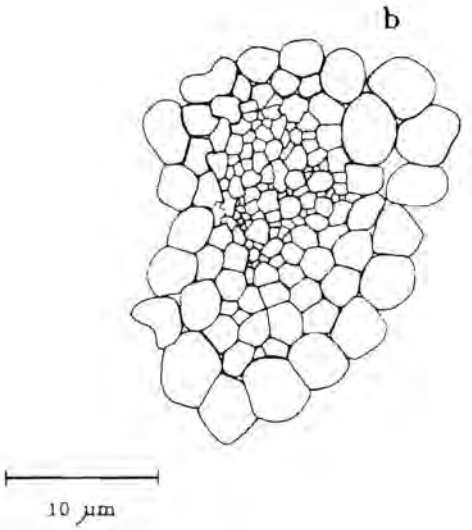

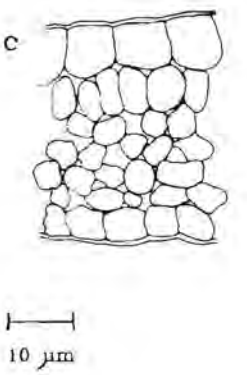

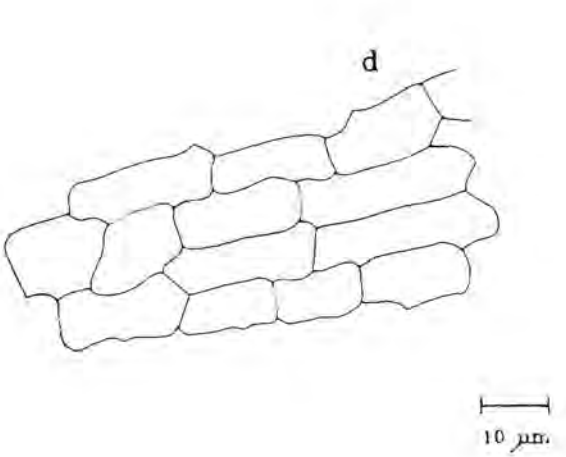

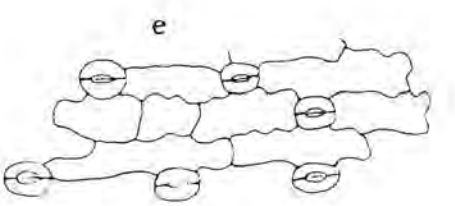

Figure 5.1.1.H

Leaf anatomy in the Disinae: Disa section Phlebidia.
Hypostomatic leaf with adaxial water storage tissue (a, c), primary vascular bundle with parenchymatous bundle sheath (b), adaxial (d) and abaxial (e) cuticles are psilate.

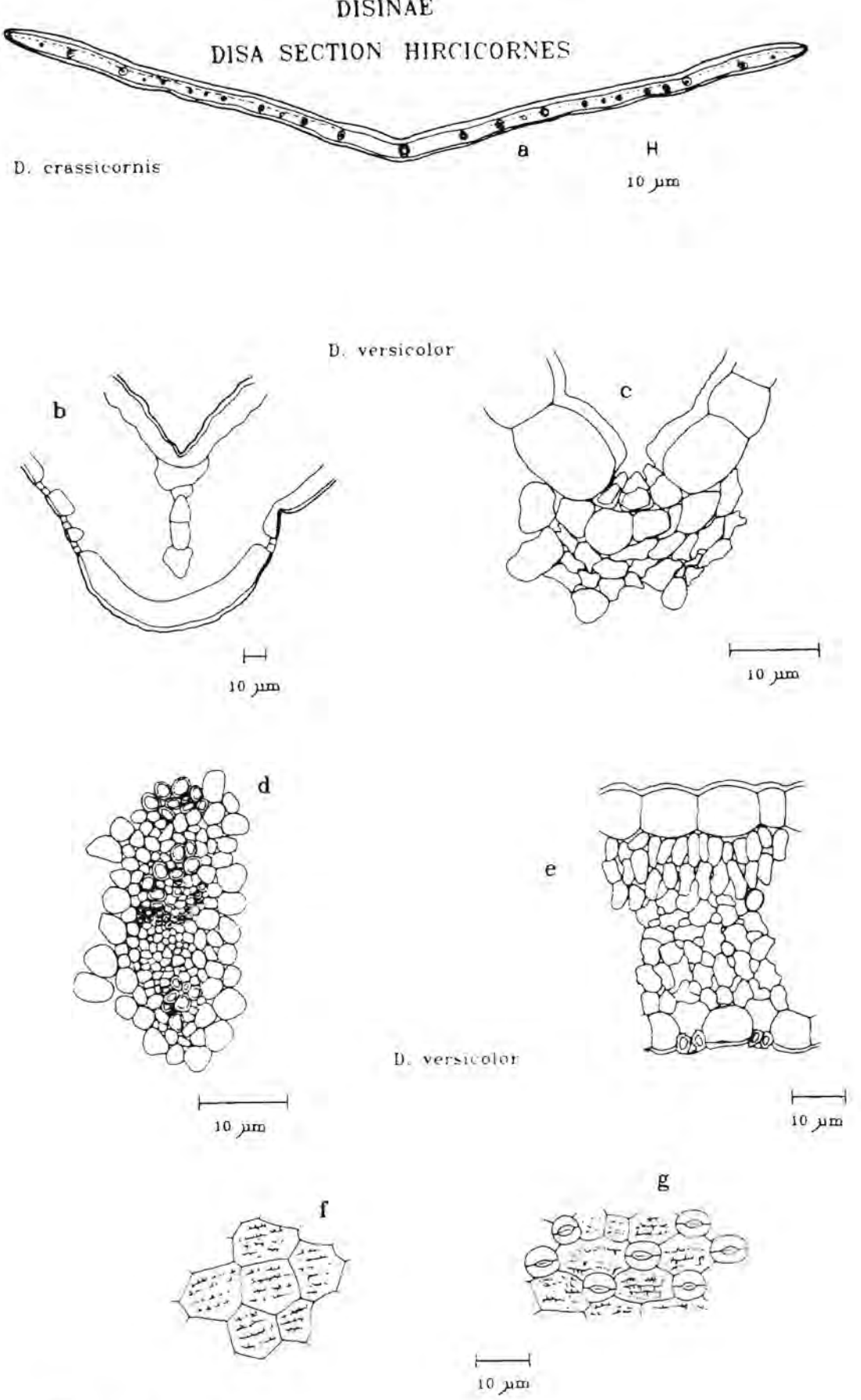

Figure 5.1.1.I

Leaf anatomy in the Disinae: Disa section Hircicornes. Leaves with adaxial water storage tissue and differentiated chlorenchyma (a, e). Epidermal cell size is reduced at midrib, and "expansion cells" are thought to act in leaf articulation, responding to hydration status of the leaf.[b,c] Fibres at the poles of the primary vascular bundle, and some lignification of xylem (d). Reticulate sculpturing of the the cuticle, and stomata reduced to abaxial surface (f, g).

DISINAE

DISA SECTION CORYPHAEA

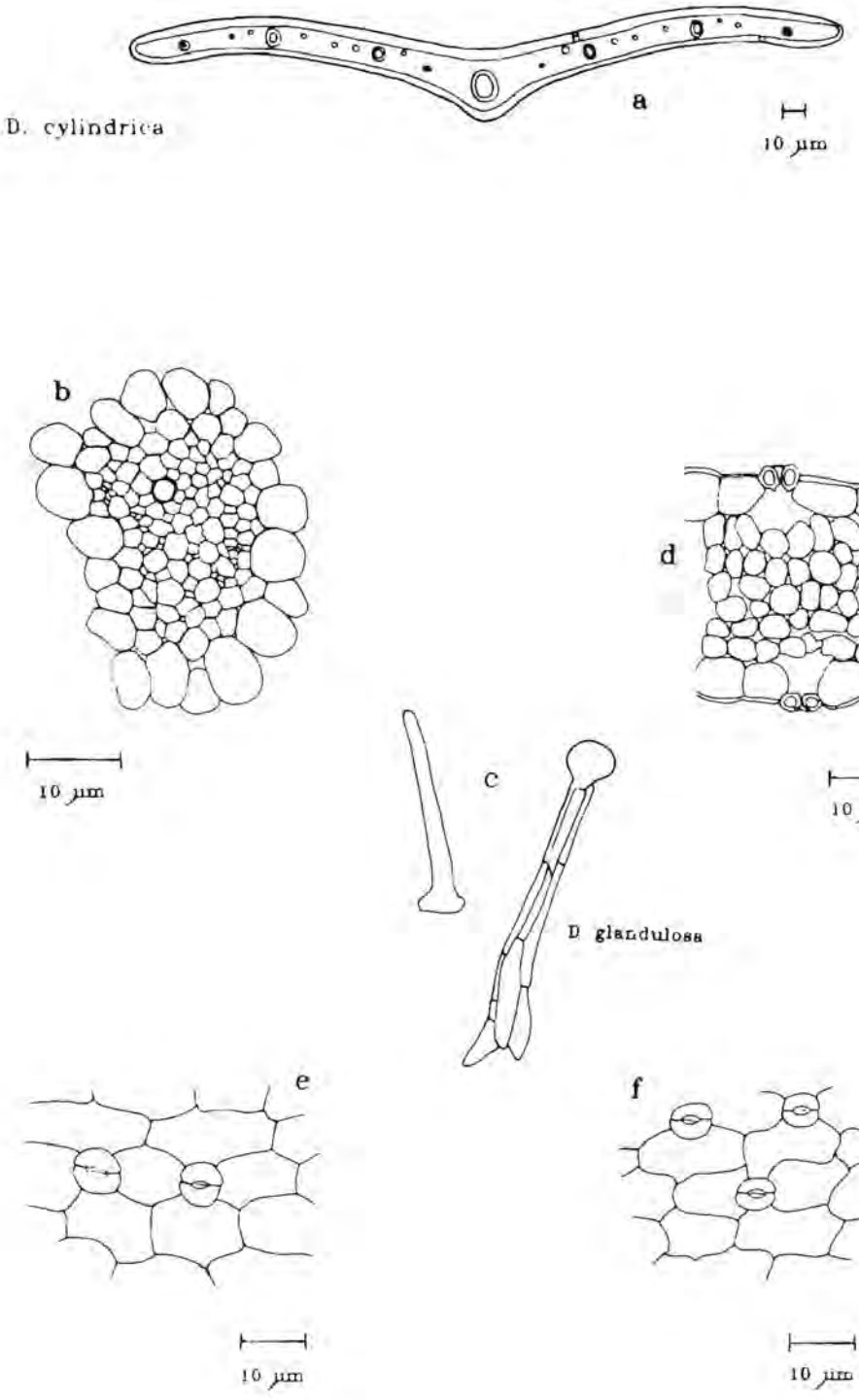

Figure 5.1.1.J

Leaf anatomy in the Disinae: Disa section Coryphaea. Amphistomatic (e, f) leaf with undifferentiated photosynthetic tissue (a, d). Primary vascular bundle with parenchymatous bundle sheath (b). Disa glandulosa has unicellular hairs and multicellular glands (c) on both epidermal surfaces.

DISINAE

DISA SECTION STENOCARPA

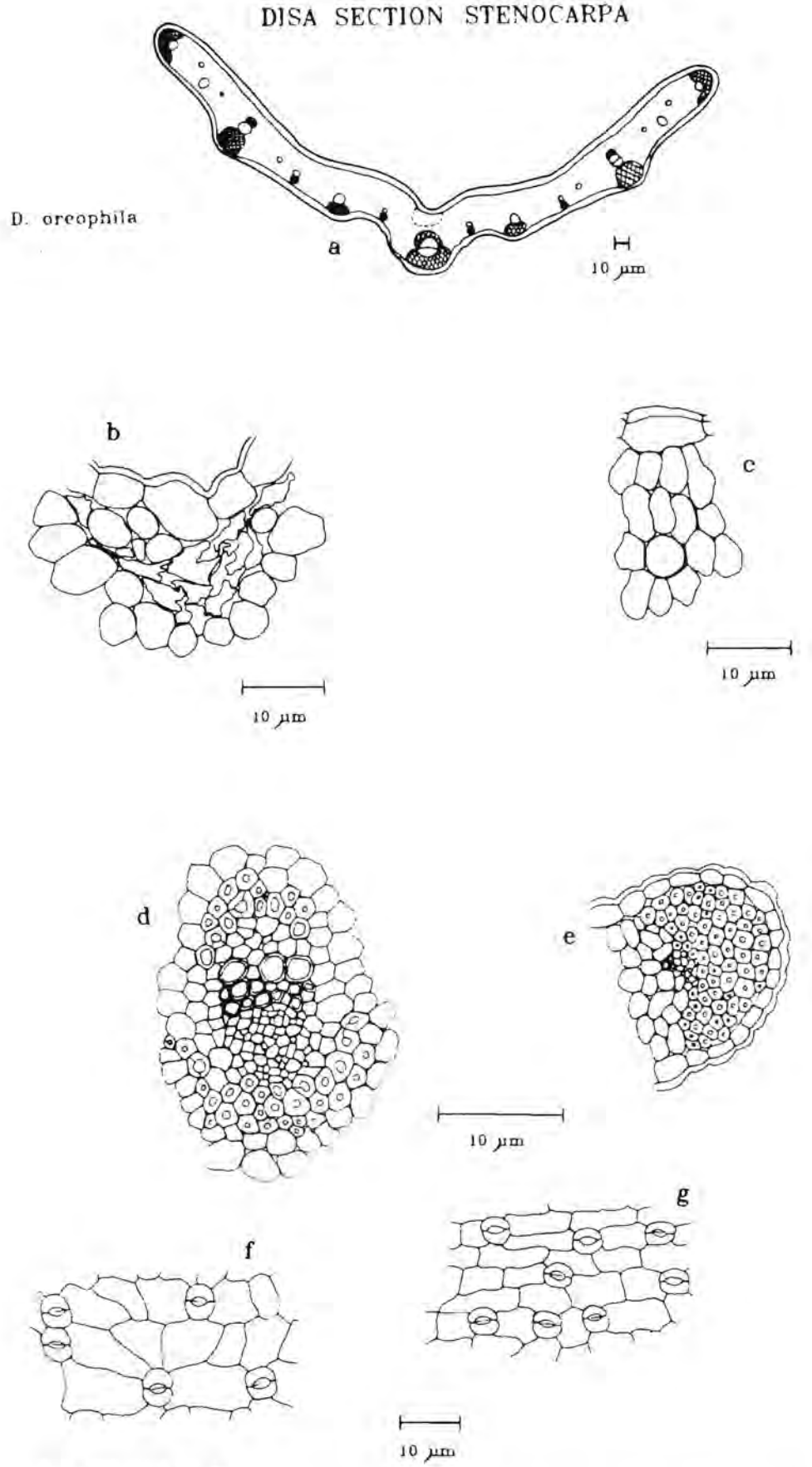

Figure 5.1.1.K

Leaf anatomy in the Disinae: Disa section Stenocarpa. The group is characterised by the shared possession of a suite of xeromorphic features. Leaves are sclerified, have a compact homogeneous mesophyll (c), thick cuticles and expansion cells at the midrib (b). Adaxial and abaxial fibres in primary vascular bundle (d), and leaf margins are sclerified (e). Cuticles are smooth or striate, and stomata occur on both leaf surfaces. (f, g)

DISINAE

DISA SECTION DISELLA

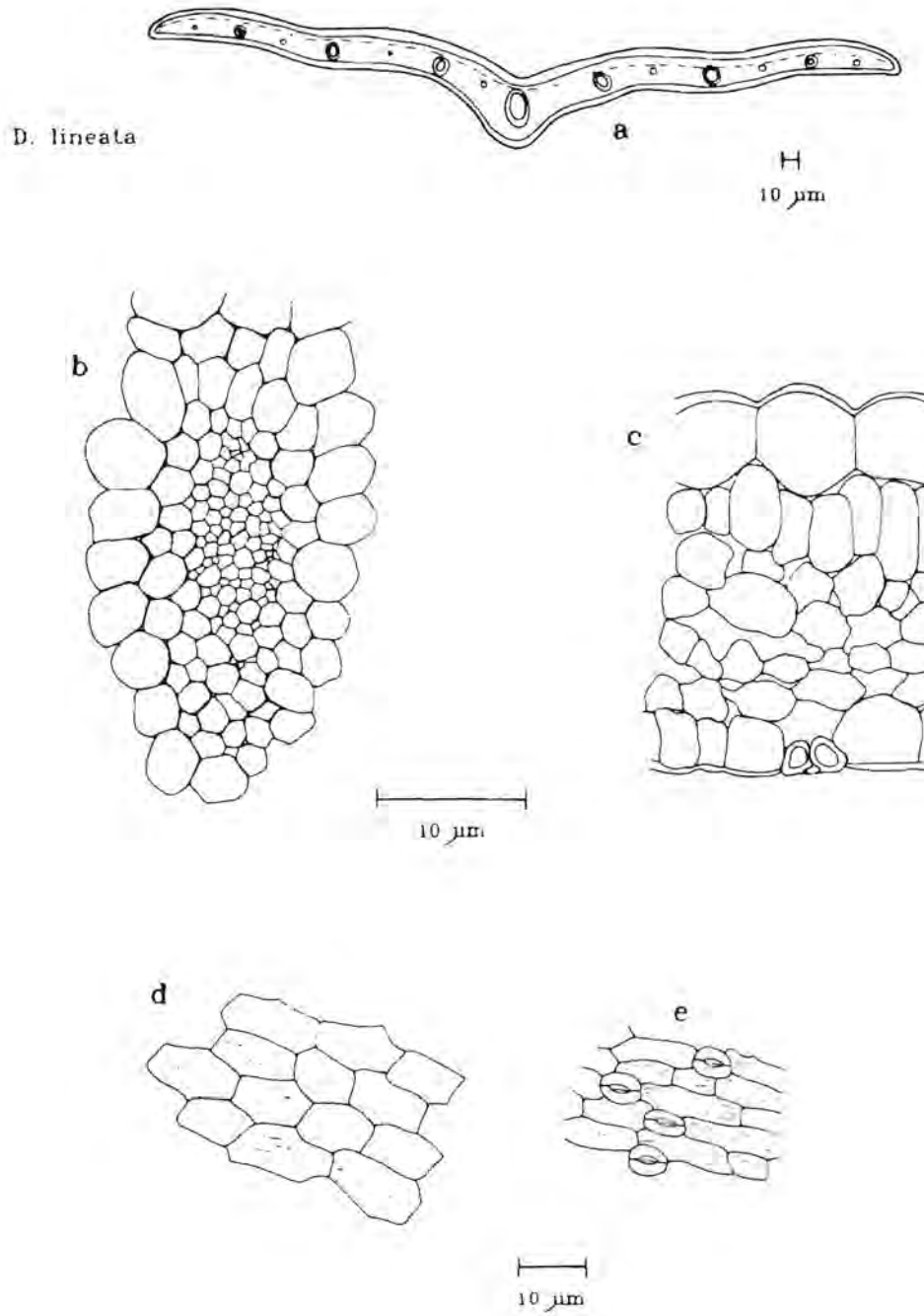

Figure 5.1.1.L

Leaf anatomy in the Disinae: Disa section Disella. Disa lineata has adaxial water storage tissue, differentiated photosynthetic tissue (a, c), primary vascular bundle with parenchymatous bundle sheath (b). Stomata are abaxial and cuticle is striate (d, e).

DISINAE

DISA SECTION REPANDRA

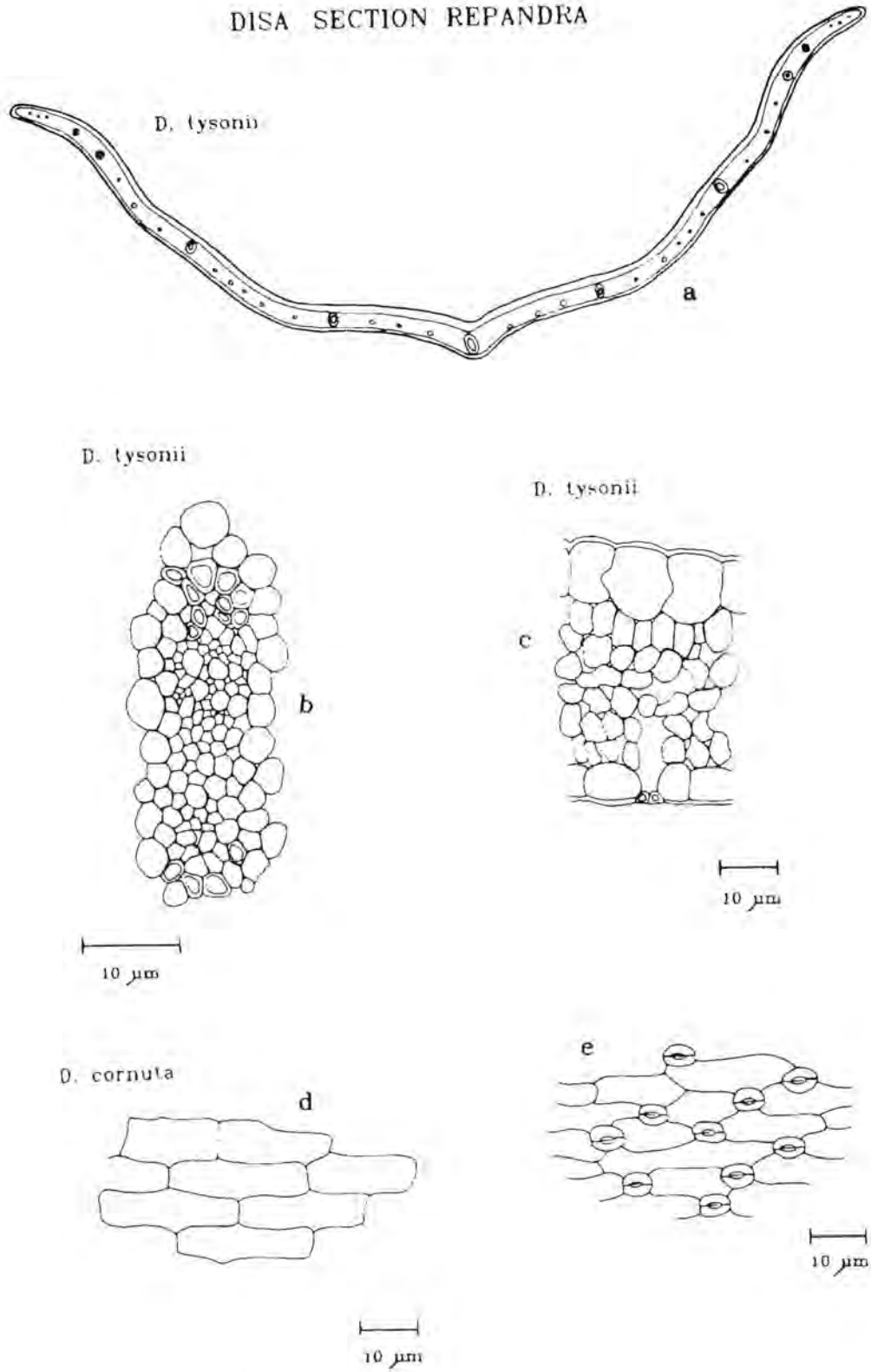

Figure 5.1.1.M

Leaf anatomy in the Disinae: Disa section Repandra.

Hypostomatic (d, e) leaves with enlarged adaxial epidermal cells and a single, or two tiered palisade layer. Sclerenchyma at the poles of the primary vascular bundle (b).

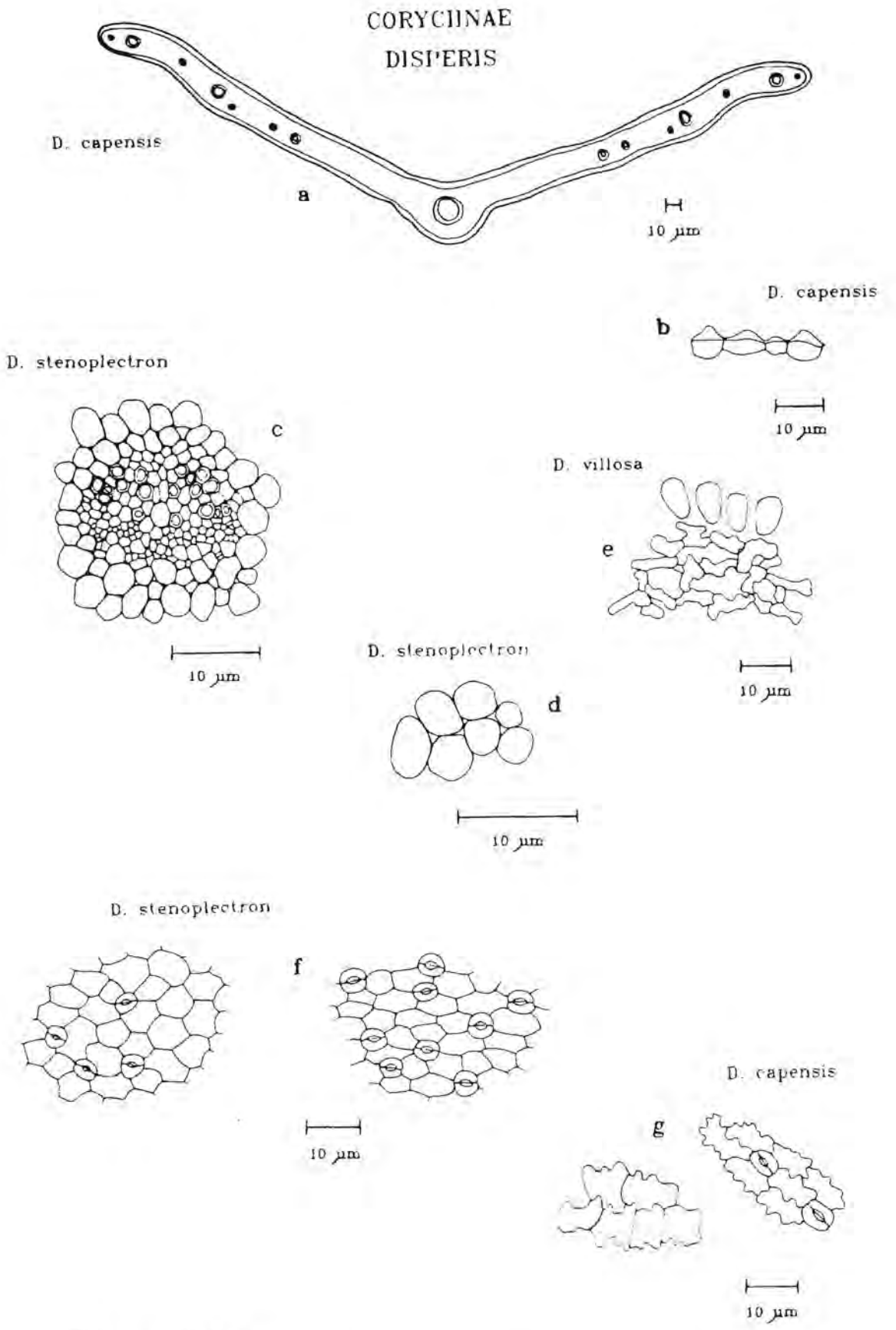

Figure 5.1.1.N

Leaf anatomy in the Coryciinae: Disperis. Mostly leaves have undifferentiated photosynthetic tissue (a) with the exception of D. villosa which has a palisade-like layer and extremely well developed arm cells in the mesophyll (e), whilstD. stenoplectron has rounded mesophyll cells (d). Epidermal cells are small, and often with papillae (b). Leaves may be amphi- or hypostomatic, and anticlinal epidermal walls are straight or undulated (f, g), and cuticles are mostly smooth.

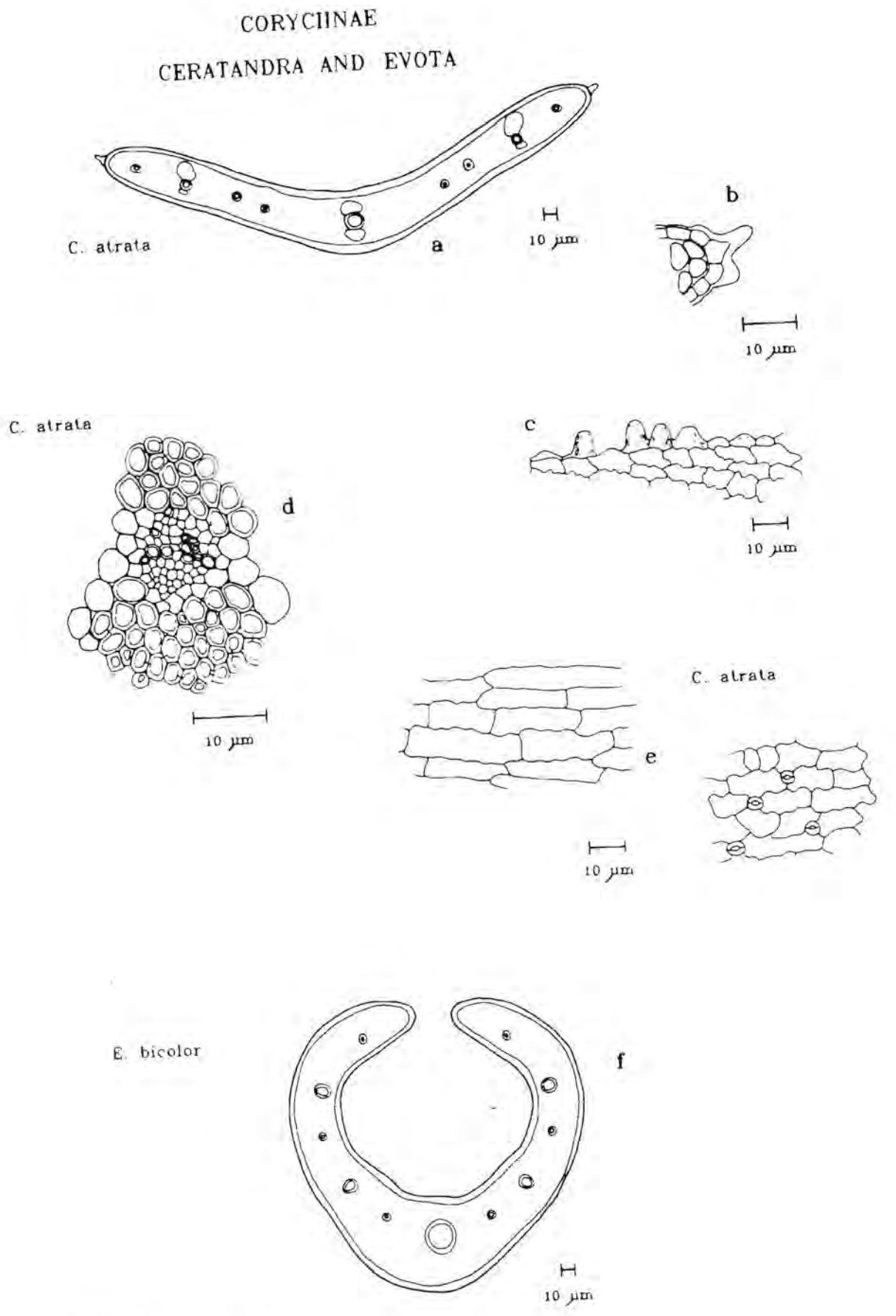

Figure 5.1.1.0

Leaf anatomy in the Coryciinae: Ceratandra and Evota. Leaves of these two genera can be distinguished by the presence of fibres at the poles of the primary vascular bundle of Ceratandra spp. (a, e, d), and epidermal papillae (b, c). Cuticles are mostly smooth with undulated anticlinal walls in the epidermis (e).

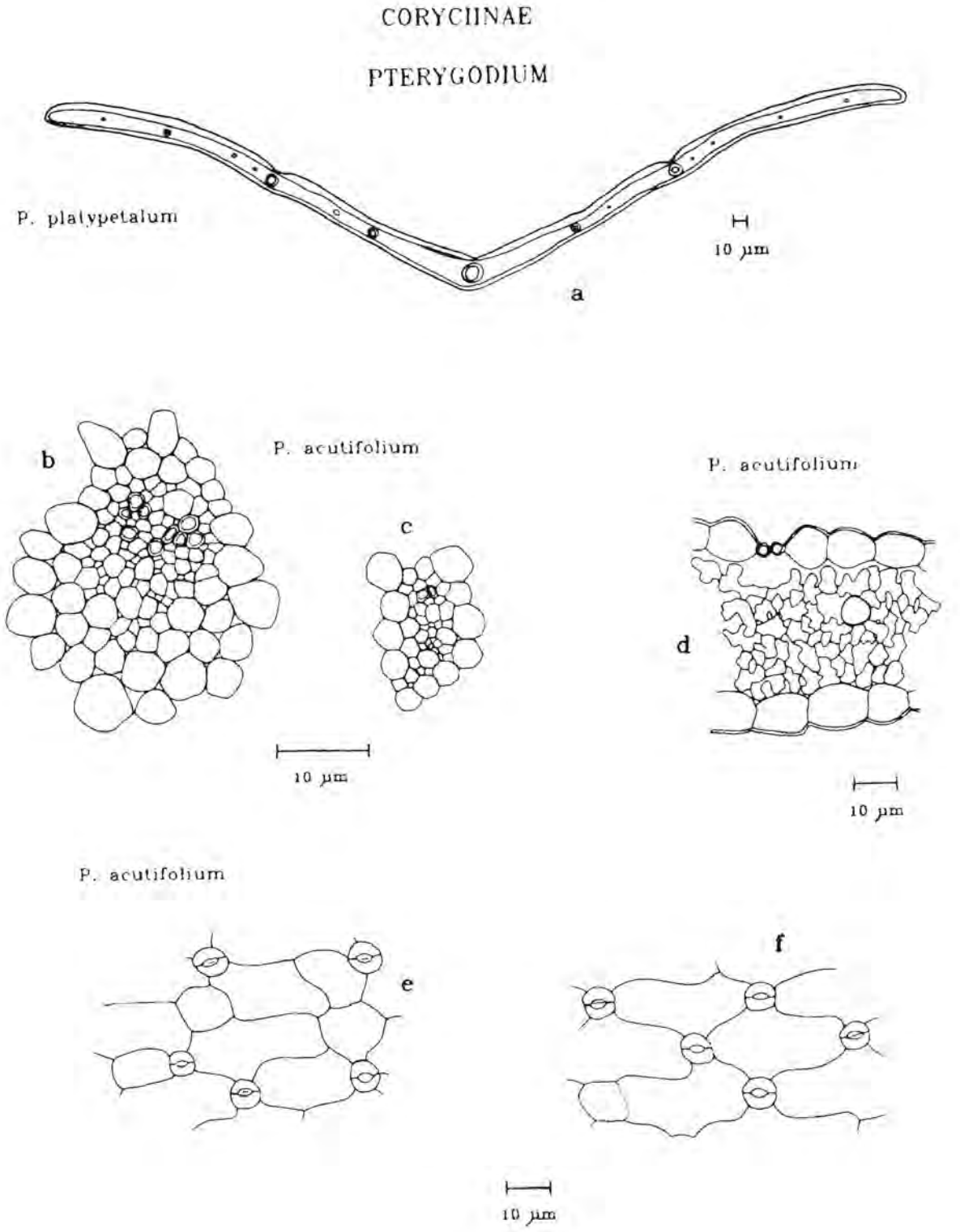

Figure 5.1.1.P

Leaf anatomy in the Coryciinae: Pterygodium. Adaxial epidermal cell size is often reduced at the primary and secondary veins (a), primary and seconadry vascular bundles (b, c) with parenchymatous bundle sheaths. Mesophyll composed of well developed arm cells (d), leaves mostly amphistomatic, with striate or smooth cuticles (e, f).

EPIDERMIS AND CUTICLE

Epidermis

The epidermis of all species investigated is uniseriate.

Anticlinal walls of epidermal cells

The anticlinal walls of epidermal cells may be straight or undulated. According to Rudall (1987), anticlinal walls are often more sinuous on the abaxial than the adaxial surface of the same leaf. In certain species of the Cypripedioideae, Rosso (1966) reports more or less straight walls on the adaxial surface and sinuous walls on the abaxial surface of the same leaf. In this study, abaxial anticlinal walls were found to be more undulated than adaxial ones in diverse genera such as Disa, Brownleea, Disperis and Ceratandra, and in Corycium rubiginosum and Disperis villosa, for example, the adaxial epidermal cells only have undulated anticlinal walls. Due to this variation, the character should probably not be coded as separate characters relating to each surface, but as a single character whether it be adaxial, abaxial or both.

In the Coryciinae, the genera Disperis, Evota and Ceratandra have undulated anticlinal walls. However, D. stenoplectron has straight walls. Corycium and Anochilus hallii typically have straight anticlinal walls with the exception of C. dracomontanum and C. rubiginosum. Straight and sinuous walls occurs in

Pterygodium, with P. acutifolium and P. volucris being straight-walled and P. alatum and P. caffrum sinuous.

In the Disinae this character also shows some trends. Sections Micranthae, Hircicornes, Ovalifoliae, Stoloniferae, Disella and Repandra are all straight-walled. Both states occur in sections Disa, Phlebidia, Stenocarpa and Coryphaea, as well as in the genera Monadenia, Brownleea and Schizodium.

On the basis of outgroup comparison, straight anticlinal walls of epidermal cells are regarded as the primitive state in the study group.

Depth of adaxial epidermal cells

Dimensional characteristics of epidermal cells also show some trends, particularly the depth of adaxial epidermal cells. Metzler (cited by Solereder and Meyer, 1930) reported that the main function of large adaxial cells is water storage. The outgroup species of the study group (with the exception of Pachites bodkinii (Pachites is in the Satyriinae), all possess enlarged adaxial epidermal cells, and on this basis it is possibly but not indisputably the plesiomorphic state in the study group. This character appears to be associated with the mesophytic leaves found in both the Disinae and Coryciinae. In the Coryciinae enlarged adaxial epidermal cells are absent in Disperis, Evota and Ceratandra, the latter two genera having

small crescent-shaped leaves similar to that of Pachites bodkinii.

In the Disinae, Brownleea and Schizodium lack enlarged adaxial epidermal cells. Monadenia, with the exception of Monadenia bracteata, possesses enlarged adaxial cells, but in this genus, they are always pierced by adaxial stomata which in other taxa do not co-occur with the adaxial water storage tissue. Disa section Micranthae typically possesses an enlarged adaxial epidermal layer whilst the other sections tend to be variable with regard to this character.

The remaining morphometric characters associated with the epidermis tend to vary considerably. No patterns consistent with the present phylogeny were found for the following characters: adaxial and abaxial epidermal cell lengths, adaxial and abaxial epidermal cell widths, adaxial and abaxial epidermal length to width ratios, abaxial epidermal cell length.

Unicellular hairs, multicellular glands and epidermal papillae
Additional anatomical features associated with the epidermis are the presence of unicellular hairs found in Disa vaginata and D. glandulosa, the latter also has multicellular stalked glands. Epidermal papillae were noted in species of Disperis and Ceratandra.

Cuticular sculpturing

In surface view the outer periclinal walls of the epidermis are covered with a cuticle which in many cases is sculptured. Several cuticular sculpturing patterns were observed in the study group. Two non-homologous sculpturing characters were identified. The first is the presence (or absence) of striations across the anticlinal walls of adjacent epidermal cells. These striations were observed in the outgroup species Habenaria laevigata and in several species of the ingroup including species of Disa sections Disa, Phlebidia, Hircicornes and Stenocarpa. They are also present in species of Monadenia i.e. M. ophrydea, M. atrorubens and M. bracteata. In the Coryciinae striations across anticlinal walls of the epidermis occur in conjunction with striate cuticular sculpturing in Corycium crispum and Anochilus hallii.

Cuticular sculpturing in the study group is variable, ranging from micropapillose to reticulate, striate or absent (psilate). The psilate cuticle is thought to be a derived condition and appears in several genera including Schizodium, Evota and Disperis (except D. fanniniae which is slightly striate). Psilate cuticles were also noted in C. dracomontanum, C. nigrescens, C. rubiginosum, Pterygodium volucris and P. acutifolium.

The Coryciinae can be characterized by the possession of either striate or smooth cuticles, whereas the Disinae show considerable variation in cuticular patterns with little pattern consistent with the present classification. Two sections of Disa, however, are uniform in their sculpturing patterns. Species of Micranthae have reticulate cuticles and in Stenocarpa cuticular sculpturing is striate.

The polarization of the different states of cuticular sculpturing was problematic as there is considerable variation in the outgroup species. Schizochiles flexuosus is micropapillose and Habenaria laevigata reticulate, with striations across anticlinal walls. In the Satyriinae, Satyrium erectum is striate and in Pachites bodkinii the cuticle is micropapillose.

PHOTOSYNTHETIC TISSUE AND STOMATA

Mesophyll

A range of variation was observed in the mesophyll of the study group. The outgroup species all have an undifferentiated mesophyll, consequently an homogeneous chlorenchyma is postulated to be the plesiomorphic condition. The Coryciinae also typically have undifferentiated photosynthetic tissue although there is considerable variation in the degree of arm cell development. Disperis villosa is exceptional in the

Coryciinae, as this species has a palisade-like layer of chlorenchyma and extremely well developed arm cells comprising the spongy mesophyll.

The chlorenchyma of the Disinae is variable. A single or two tiered palisade is characteristic of the section Micranthae and Schizodium. In Brownleea, Monadenia and the rest of Disa there is no consistent pattern with regard to the differentiation of the palisade layer(s). Disa section Stenocarpa, however, is characterized by the possession of an undifferentiated mesophyll, with compact rounded cells.

Mesophyll cells throughout the study group range from rounded cells to well developed arm cells with large intercellular spaces. In the Coryciinae, the mesophyll is often composed of well developed arm cells. The length of the long axis of mesophyll cells was used in the analyses and largely reflects the degree of arm cell development.

Stomata

Stomata in the Orchidoideae are anomocitic at maturity, lacking subsidiary cells. Developmental studies of stomata of the Orchidoideae (Rasmussen, 1981) indicate that both agenous and hemimesogenous developmental types occur in this group. These developmental types are indistinguishable at maturity, both being anomocytic. For Disa uniflora Rasmussen (1981) found the proportion of hemimesogenous to agenous development to be between 1:2 and 1:4.

Dimensional characters relating to stomatal lengths, widths and length to width ratios were omitted in the final analyses as they did not vary sufficiently between taxa to provide any worthwhile information.

Stomatal distribution did, however, show some trends. In the outgroup species, stomata were in most cases (with the exception of Pachites bodkinii) restricted to the lower leaf surface, and hypostomatic leaves are thought to be plesiomorphic in the study group. Anochilus, Brownleea and Disa sections Micranthae and Hircicornes have hypostomatic leaves. Amphistomatic leaves are characteristic of Monadenia, Schizodium and Evota. In the rest of the study group there was much variation in the distribution of stomata. It is only in Monadenia that stomata pierce the enlarged adaxial epidermal cell layer. In all other species which do possess an adaxial water storage tissue, stomata are restricted to the lower leaf surface.

VASCULAR BUNDLES

Vascular bundles, bundle sheaths and sclerification

Vascular bundles are collateral throughout the study group, mostly with parenchymatous bundle sheaths surrounding them. The subgenus Stenocarpa, of Disa, which includes the sections Amphigena, Stenocarpa, Coryphaea, Emarginatae and Austroalpinae have variously lignified vascular bundles and bundle sheaths. In Disa tenuis (Amphigena), the vascular bundles are entirely

surrounded by a fibrous bundle sheath. Disa tysonii (Repandra) has some sclerenchymatous cells at the poles of the primary vascular bundle. Disa section Stenocarpa consistently has fibre caps at the poles of primary and secondary vascular bundles. In smaller (tertiary) vascular bundles sclerification is either absent or reduced to phloem fibre caps. In section Stenocarpa, sclerification of vascular bundles is coupled with the presence of sclerified leaf margins. Herschelianthe spathulata also has sclerified vascular bundles and leaf margins. In all other species vascular bundles are unsclerified, and sclerification of vascular tissue is thus regarded as an apomorphic condition.

Sclerification associated with the vascular bundles is mostly absent in the Coryciinae, but Ceratandra is characterized by the possession of fibre caps at the poles of primary and secondary vascular bundles.

Size classes of veins

Veins were divided into three size classes: primary, secondary and tertiary. The number of veins were counted and included in the analysis although they probably reflect leaf size rather than show any pattern consistent with the present phylogeny of the study group.

Ribbed leaves and parenchymatous keels

Other characters associated with veins are the ribbed leaves found in Corycium dracomontanum and C. nigrescens and prominent parenchymatous keels at the midrib and secondary veins as noted in Disa uniflora. Parenchymatous tissue at the midrib and leaf margins was noted in Habenaria laevigata.

LEAF ARTICULATION MECHANISMS

Expansion cells

The presence of "expansion cells" on the adaxial side of the midrib is interpreted as functioning in leaf movement. These thin-walled parenchymatous cells are present on the adaxial side of the midrib and are thought to expand and contract in response to hydration status. The sclerophyllous leaves of Disa section Stenocarpa all have such cells at the midrib. In addition several other species of Disa (D. versicolor, D. tysonii, D. englerana, D. filicornis and D. sankeyi) also have this leaf-folding mechanism. Expansion cells were noted in Habenaria laevigata, Monadenia sabulosa and Brownleea parviflora and, in the Coryciinae, Corycium dracomontanum. With the exception of species of section Stenocarpa this character appears across the genera in some of the large-leaved species.

Reduced cell size at midrib and secondary veins

Another character which might be associated with folding of leaves is the presence of relatively small adaxial epidermal cells at the primary and secondary veins of species which possess enlarged adaxial epidermal cells. Although this reduction in cell size does not occur in the outgroup species it cuts across genera and sections of the in-group and is characteristic of the genera Corycium (with the exception of C. rubiginosum), Anochilus and Pterygodium.

RAPHIDE IDIOBLASTS

Idioblast cells containing raphide crystals are ubiquitous in leaves of the study group. They have also been noted in tubers and roots. Crystal raphides are mostly found in single idioblast cells not much larger than surrounding cells. They differ in Brownleea where they are enlarged and aggregated in files of tubular, mucilage-filled cells, each containing a cluster of raphides.

5.1.2 CLADISTIC AND PHENETIC ANALYSES OF LEAF ANATOMICAL DATA

In the cladistic analysis, the tree was rooted by specifying Habenaria laevigata, Schizochiles flexuosus and Satyrium erectum as outgroup taxa. The hypothetical ancestor to the study group was included simply to test hypotheses of character polarity used in initial analyses. The analysis placed this hypothetical taxon near the root of the tree.

Very little pattern emerged from this analysis using the MHENNIG* routine. The nelsen strict consensus tree, tree characteristics, and character consistency indices are shown in Fig. 5.1.2 A. Only species of Disa section Stenocarpa (D. cephalotes, D. cephalotes ssp. frigida and D. nivea) and species of Schizodium (S.cornutum, S. bifidum, S. obliquum) remained grouped in the consensus tree. The Coryciinae, particularly Corycium, Anochilus and Pterygodium tended to collapse into a single undifferentiated group when their leaf anatomical characters were subjected to cladistic analysis. This lack of resolution is due to the fact that taxa are virtually indistinguishable in their leaf anatomy.

Suites of correlated characters are lacking in the data set. In the Disinae in particular, there is little correlation between the various components of the photosynthetic apparatus e.g. leaves with differentiated palisade may be hypo- or amphistomatic. In the cladistic analysis, characters related to

Table 5.1.2.A

Matrix of leaf anatomy data for the Disinae.

Species	Characters 01234567890123456789012345678901234567
Disa cephalotes	01110100110031103010000?06824441660000
Ceratandra atrata	11001100110011011110010?21512231410000
Disa englerana	04111111311141114010111114545460250000
Pterygodium acutifolium	00110111311111111111001?30120020000000
Ceratandra globosa	11100100110111111111110?10801411420000
Disa nivea	01110200110011102011100?05815531760000
Disa telipogonis	00111011101120111111110?03533421320000
Monadenia comosa	01110111211141113111111124181070000000
Monadenia atrorubens	01110111111111111001010?02611400120000
Schizodium inflexum	00110011101110111111111101252250163000
Disa tysonii	04111100211051114011110?04275070220000
Brownleea coerula	02101111111121111110011137574521620000
Schizochiles flexuosus	02111111111110111111110?04184260310000
Disa rosea	02111111201120112111111035284160100000
Disa saxicola	01111200110031102000000?00501401650000
Disperis stenoplectron	20110111311121113111110?07686551760000
Disa maculata	01111111111101110101111033183240100000
Disa versicolor	04111111311151114000011116586170240000
Disa cephalotes frigida	01110000200020112010000?04556371560000
Evota bicolor	00000111111110111011111?06842501610000
Satyrium erectum	01111111411140114111110?30081060200000
Corycium nigrescens	02110111311141114110010?25383070100010
Corycium crispum	01110111???7111101001107112310503100000
Disa sagittalis	00101111211101110111111026486170120000
Disa filicornis	03111111211101110001111003715521350000
Disa vaginata	21000111211111111110001070656645152010?
Disa cylindrica	01110111211101110101110?04463340250000
Corycium dracomontanum	00100111111112111201001?21140130200010
Corycium rubiginosum	00010111131110111111111?36734431210000
Disa patens	02111111211111111111111?05564521350000
Disa fragrans	02111111211151115110011136382140110000
Habenaria laevigata	02111111111131113011110?34376270620000
Disa pillansii	02111111111101110111111036575360410000
Disa crassicornis	02111111311151115100011124361320310000
Disa aconotoides	00110111111131113111110?07675451560000
Disa patula	00111100110021111110000?06646560650000
Disa chrysostachya	04111111211131113110011011162140140000
Disa atricapilla	01100111111111111011111?01714431430000
Disa alticola	01111111211111111011110?02615601560000
Pterygodium volucris	00111111211111111110010?20052060330000
Schizodium bifidum	00000111111110111011111102777451166?0000
Pterygodium alatum	01101111211111111110010?21251310440000
Anochiles hallii	01111111311131113100010?30210210210000
Corycium orobanchoides	01111111111111111110000?20300120420000
Pterygodium caffrum	01001111211131113110010?22174260240000
Disa sankeyi	04111111111141114010011015383160110000
Monadenia sabulosa	02110111211131113011110?13543340000000
Disa longicornu	00101111111111110111111024532410320000
Schizodium cornutum	00000111311111110111111017856531760000

Corycium bicolorum	01111111111111111110010?0004003001000
Disperis villosa	20011111111111111111111043272140600000
Disperis capensis	00001111211111111111110?3563553165000
Disa glandulosa	20000111111111111111111016744531631100
Monadenia bracteata	03000111111121111100010?026124113500000
Disperis fanniniae	11101111111111111110110?17776561?600000
Brownleea parviflora	00111111211151114010010?17586641?70000
Disa fasciata	01000111211101110101111014542140210000
Schizodium obliquum	00010111111111111111111017853061550000
Disa draconis	01111111111131113110011010410400440000
Disa cornuta	01111111311141114100011023610401440000
Monadenia ophrydea	00110111211131113100011033441230210000
Disa uniflora	00111111211131113111110?12533430320001
Disa lineata	01111111111121111110111002533511650000

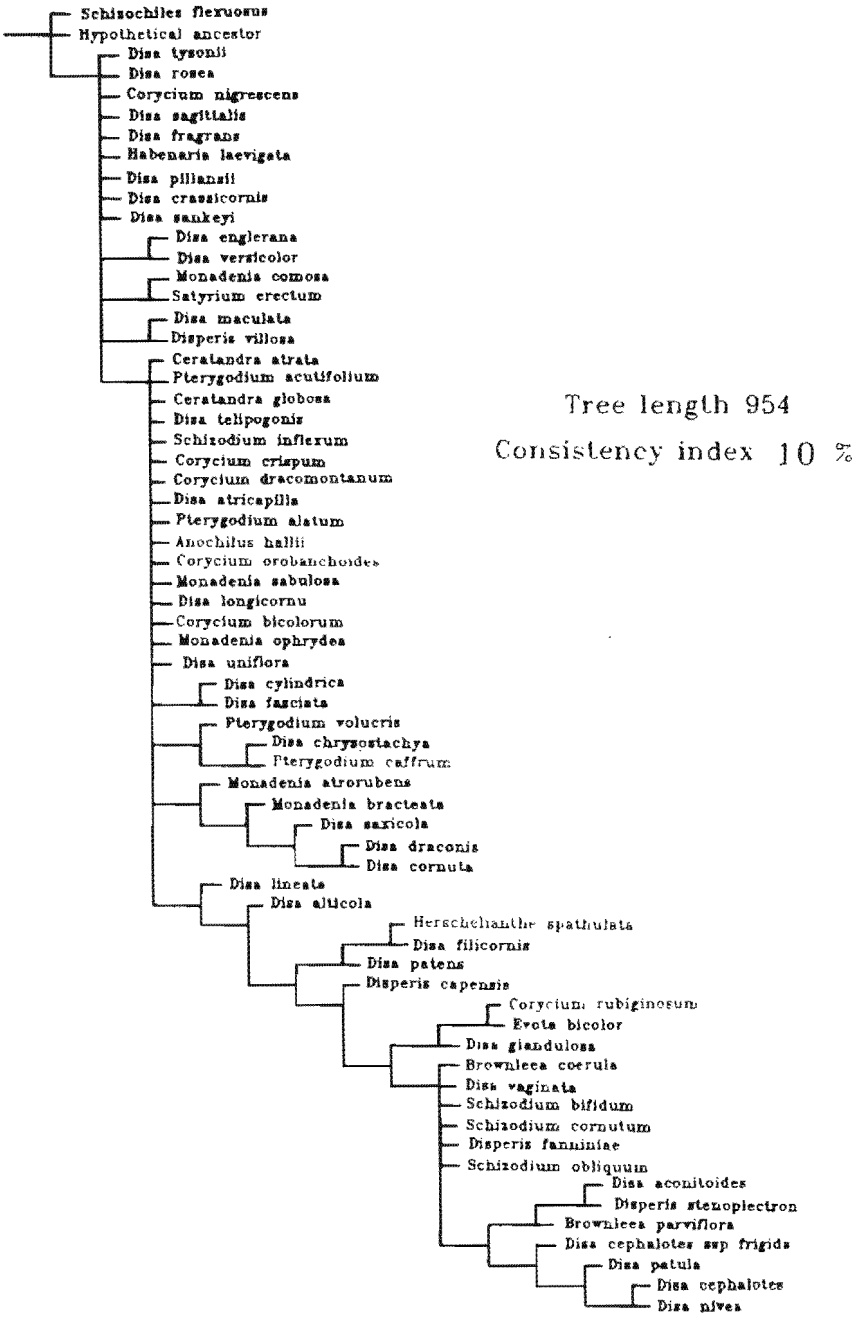

character	0	1	2	3	4	5	6	7	8	9	10	11	12	13	14	15	16	17	18
steps	12	35	9	14	19	6	6	6	35	5	4	5	53	6	1	2	50	13	12
ci	16	11	11	7	5	33	16	16	8	20	25	20	9	16	100	50	10	7	6

	19	20	21	22	23	24	25	26	27	28	29	30	31	32	33	34	35	36	37
	22	20	4	19	5	48	59	73	70	67	61	74	9	63	60	1	2	2	1
	4	5	25	5	20	8	11	10	11	6	9	9	11	5	11	100	50	50	100

Figure 5.1.2.A

Nelsen strict consensus tree, tree characteristics, and character consistency indices for anatomical data of species of the Diseae.

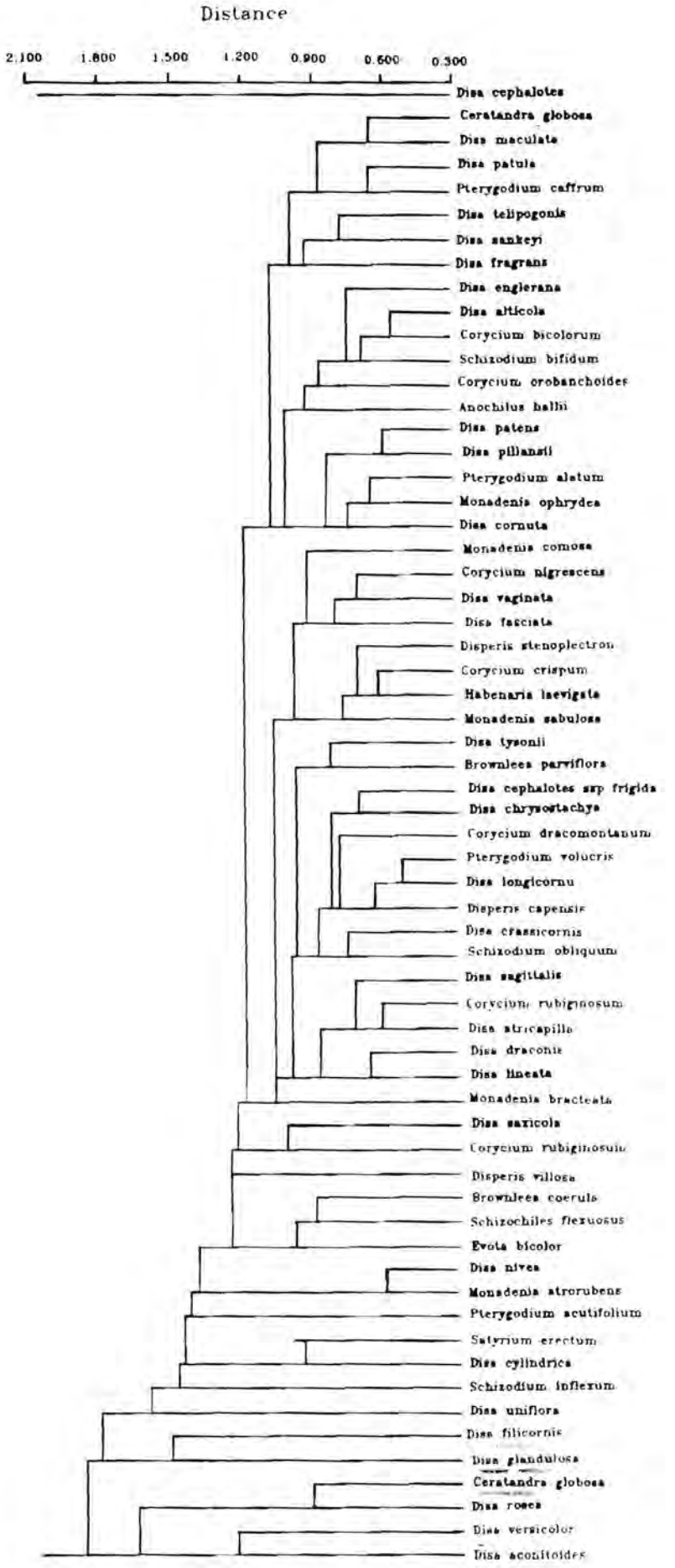

Figure 5.1.2.B

Phenogram generated using SIMINT for anatomical data of species of the Diseae.

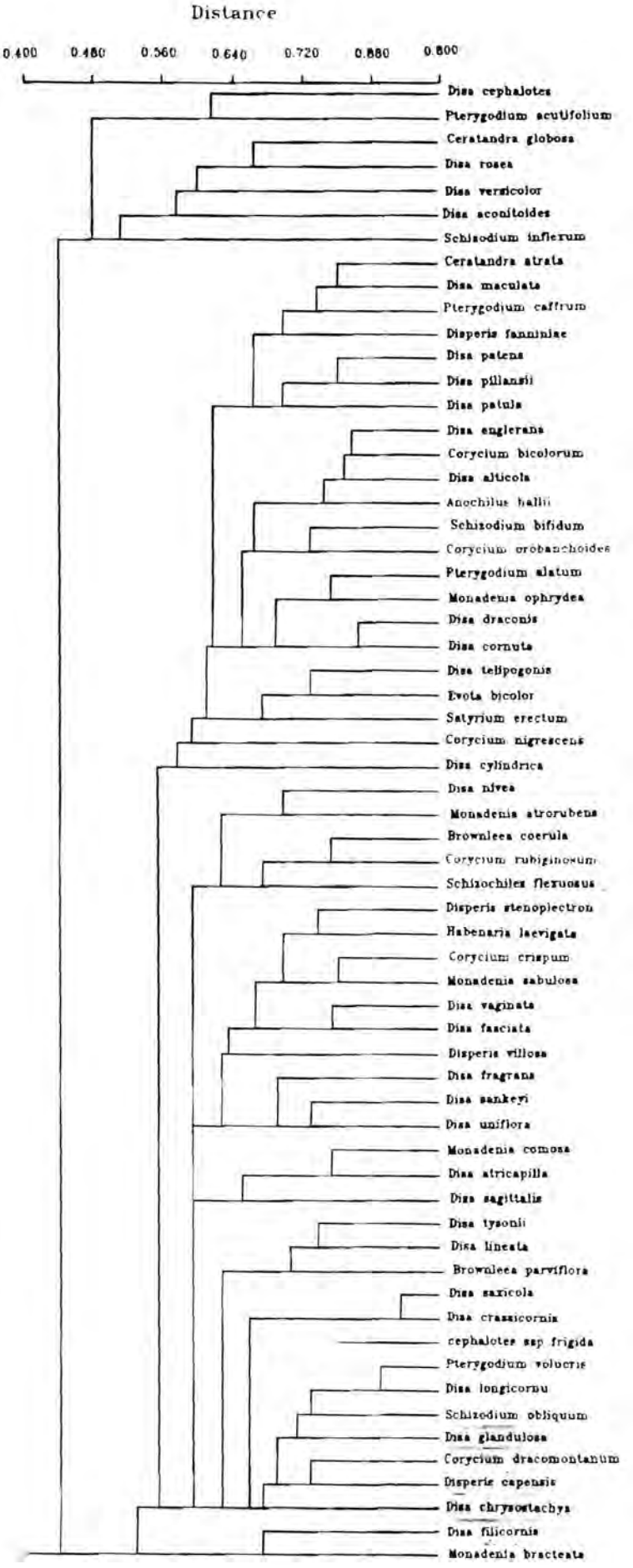

Figure 5.1.2.C

Phenogram generated using SIMQUAL for anatomical data of species of the Diseae.

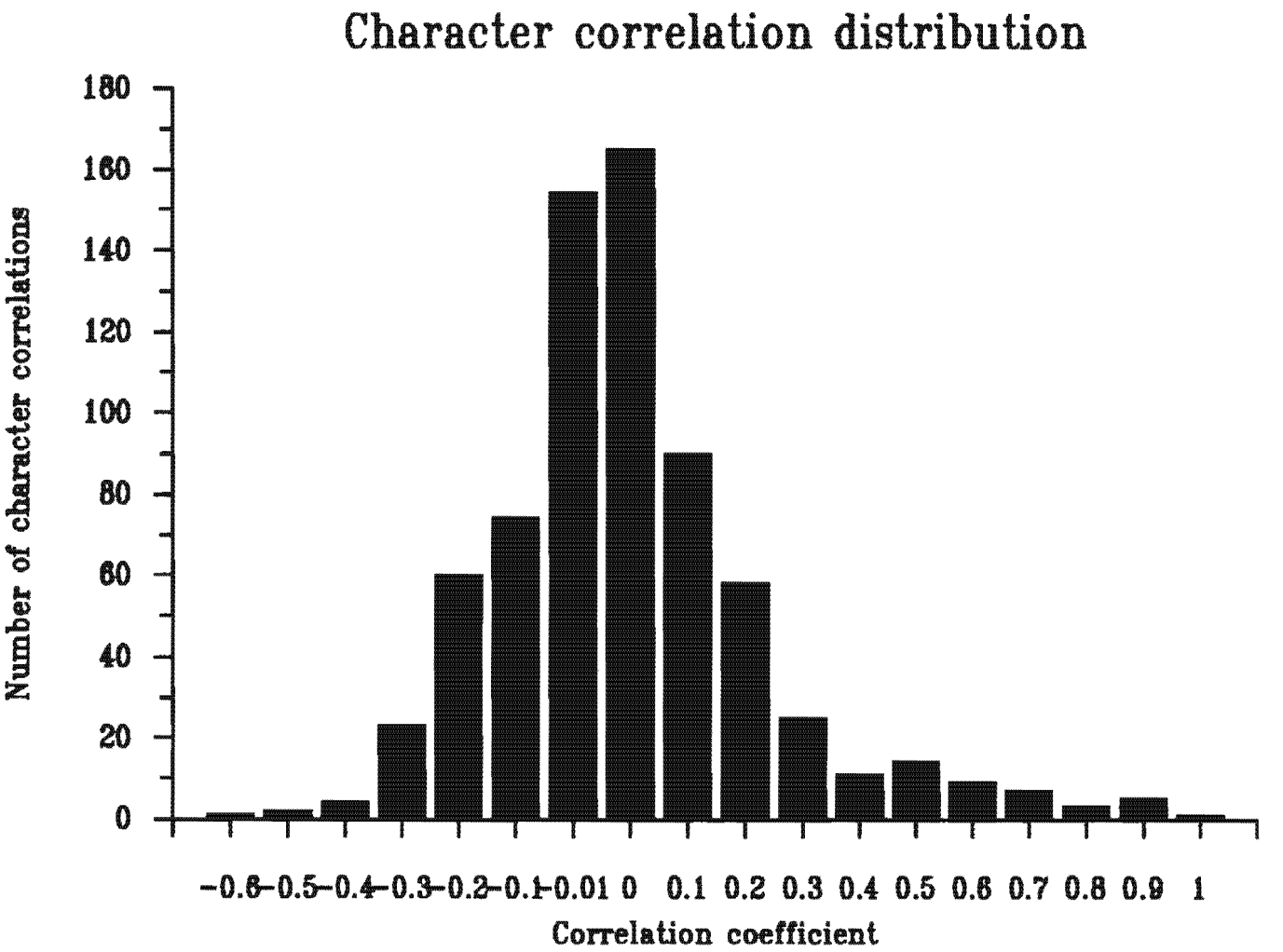

Figure 5.1.2.D

Number of character correlations in relation to correlation coefficient intervals.

the photosynthetic apparatus showed low consistency indices with respect to the cladogram (stomatal distribution 5 %, differentiation of photosynthetic tissue 5 %, degree of arm cell development 8 %, length of mesophyll cells 11 %). The presence of a leaf articulation mechanism in the form of expansion cells at the midrib, and reduced cell sizes at the midrib and secondary veins of leaves with enlarged adaxial epidermal cells, also proved to be "bad" characters with equally low consistency indices.

The only characters showing fairly high consistency indices were autapomorphies i.e. characters unique to a species, and characters relating to the sclerification of vascular bundles of species of Disa section Stenocarpa.

When morphometric characters alone were used during preliminary analyses, a chaining branching effect was produced. It was concluded that measurement data contained litte phylogenetic information.

Results of the phenetic analyses, which were used in an attempt to cluster similar leaf types or "adaptive syndromes", were unsuccessful and widely different leaf types were grouped together. Phenograms are shown in Figures 5.1.2.B & C.

Results of the cophenetic correlation which was used as a measure of goodness of fit for the cluster analysis indicated a high scatter in the data (matrix correlation r= 0.73633) which, according to Rohlf (1988), is a poor fit.

The correlation between each character and all the others did show some trends. The number of character correlations were plotted against correlation coefficients and are shown in Fig. 5.1.2.D. There is a high number of character correlations around the correlation coefficient of zero, indicating that most characters were independent of each other. Characters with a correlation coefficient near +1 indicate that a high value of one variable is associated with a high value of the other, and conversely, correlation coefficients near -1 imply association of high values of one variable with low values of the other.

Characters with correlation coefficients of between 0.5 and 1.0 were identified in the matrix. These include correlations between adaxial and abaxial sinuous anticlinal walls in epidermal cells, abaxial and adaxial sclerenchyma caps of the primary vascular bundle, the nature of bundle sheaths in the different size classes of veins, the co-occurrence of fibre caps adaxially and/or abaxially in different size classes of veins, the number of tertiary veins and total number of veins, reduced cell size at midrib and secondary veins. The seriation of palisade was indirectly correlated to leaf size (total number of veins (0.591) and number of tertiary vascular bundles (0.673).

Morphometric characters were correlated to each other in fairly obvious ways. Lengths and withs of cells of abaxial epidermis correlated with those of adaxial epidermis, the depth of the adaxial epidermis was correlated to the width of adaxial epidermal cells (0.737) (deep cells usually being wide). Unicellular hairs were correlated with the presence of multicellular glands but these two features co-occur on Disa glandulosa only, and can therefore be expected to be highly correlated.

As (Abbot et al, 1985) point out, high correlations may mean that the variables are simply redundant i.e. that they are two measures of the same phenomenon. This is probably the case in the sclerification of vascular bundles, which accounted for many of the high character correlations e.g. adaxial and abaxial fibre caps in the primary vascular bundle had a correlation coefficient of +1. Abbot et al (1985) further suggest that the use of correlated characters is essentially equivalent to weighting certain characters, and that using characters known to be correlated is essentially a form of a priori weighting. On the other hand, significant positive correlations between characters reflect a stable association which is presumably genetically based and might constitute desirable taxonomic information. If seemingly unrelated characters such as sclerification of vascular tissue were correlated with the presence of expansion cells at the midrib, and an homogeneous

chlorenchyma, this would serve to identify the xeromorphic syndrome shared by species of section Stenocarpa, for example. This form of character correlation would then be useful. However, possibly due to the large amount of taxa and use of many "bad" characters, noise in the data set precluded the identification of any "leaf types" or "adaptive syndromes" using numerical methods.

5.1.3. SYSTEMATIC IMPLICATIONS OF LEAF ANATOMY

Leaf anatomy does not provide many unequivocal apomorphies for resolving taxa at the three hierarchic levels considered here. Nevertheless, certain trends were identified. These are summarized in Fig. 5.1.3.A. where leaf anatomical characters are shown in the context of the present phylogeny of the group. The picture that emerges is unclear and reflects to some extent results obtained by the cladistic analyses. Only Disa sections Micranthae and Stenocarpa, and Schizodium have combinations of characters which may be interpreted as syndromes characteristic of the groups.

Anatomical data might provide evidence for treating Disa section Micranthae as a distinct group within the subtribe Disinae. In addition, the sclerification of vascular bundles and presence of marginal sclereids in section Stenocarpa does support the inclusion of Herschelianthe within Disa section Stenocarpa. In the rest of the Disinae, clear delimitations of taxa are impossible due to the high degree of heterobathmy, or differential character evolution, which may be related to the phylogenetic history of this speciose group.

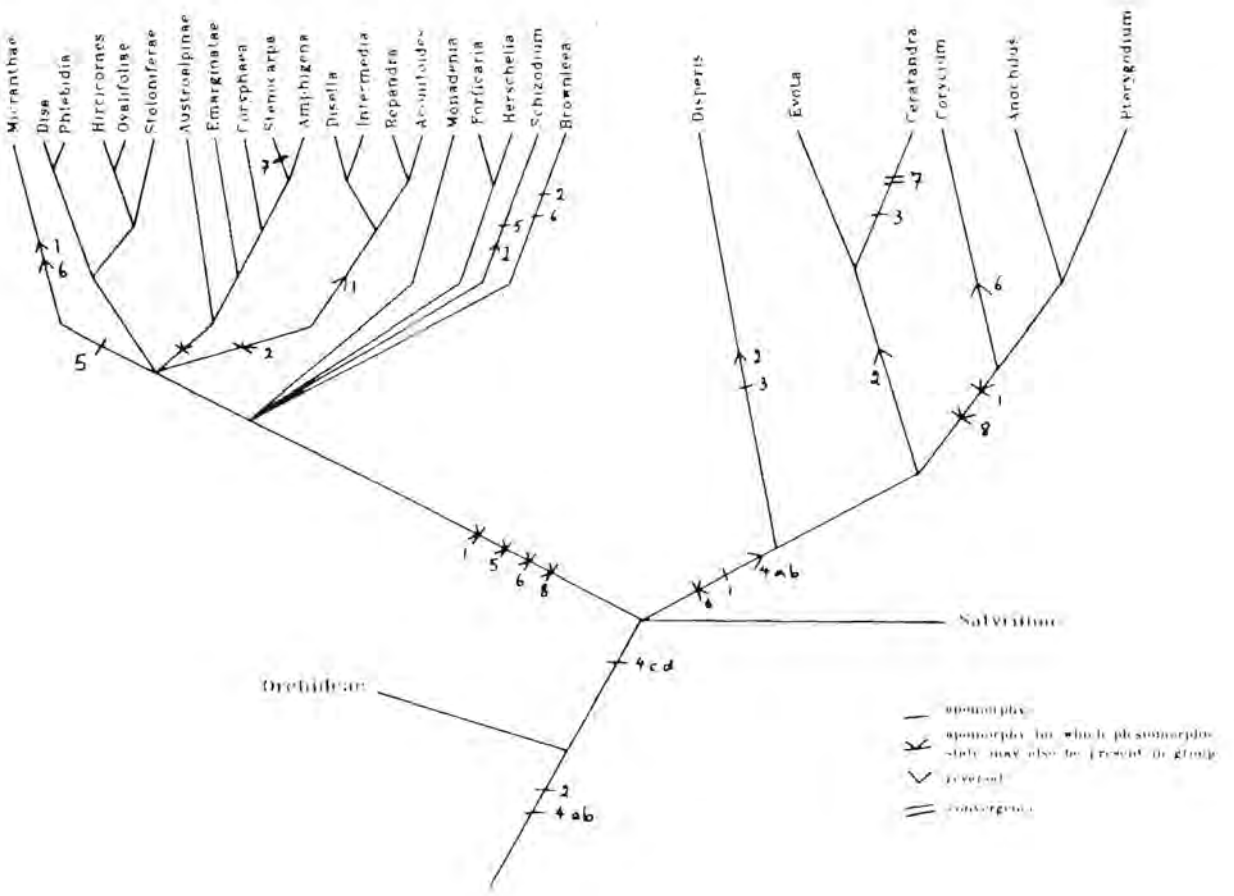

Figure 5.1.3.A

Leaf anatomy characters in relation to the present phylogeny of the Diseae. Characters used are: 1. sinuous anticlinal walls of epidermal cells; 2. enlarged adaxial epidermal cells; 3. epidermal papillae; 4. cuticular sculpture a) reticulate, b) micropapillose, c) striate, d) psilate; 5. differentiated photosynthetic tissue (palisade); 6. amphistomatic leaves; 7. sclerification associated with vascular bundles; 8. reduced adaxial epidermal cell size at primary and secondary veins.

In the Coryciinae, the genera Corycium, Anochilus and Pterygodium are virtually indistinguishable in terms of their leaf anatomy. This data set does therefore not provide sufficient evidence to treat Anochilus as a genus separate from Pterygodium. The presence of adaxial and abaxial fibre caps at the poles of primary and secondary vascular bundles of Ceratandra distinguish this genus from Evota.

Subtribal differences in leaf anatomical characters are also not clear as the same leaf types tends to occur in relatively unrelated taxa. For example, small crescent shaped leaves with undifferentiated chlorenchyma occur in diverse genera such as Evota, Disa, Monadenia and Pachites.

In addition to the observed differential nature of character evolution in the group, the equivocality with regards to character polarization is possibly one of the main problems in carrying out a cladistic analysis of leaf anatomical features. There appear to be two ancestral leaf types: the mesophytic broad leaf with adaxial water storage tissue and the small, relatively undifferentiated crescent-shaped leaf.

Results from other studies indicate that leaf anatomy can provide additional taxonomic information. For the subtribe Pleurothallidinae, Pridgeon (1982) found features of trichomes, cuticle, epidermis, hypodermis, spiral thickenings and number of veins series to be systematically useful. In placing the vandoid genus Ossiculum as most closely related to Calyptrochilum, Cribb and van der Laan (1986) found that only supporting evidence provided by leaf anatomy was the presence of water storage cells, the absence of hypodermal and mesophyll sclereids, and the palisade layer. Ayensu and Williams (1972) found the occurrence of adaxial fibre bundles to be unique in Palumbina and Osmoglossum, in the Oncidiinae.

Although leaf anatomy did serve to resolve some problematic taxa such as Herschelianthe, for example, on the basis of sclerification, results of this study show fairly conclusively that it has limited phylogenetic value in the Diseae.

5.2 PALYNOLOGY

5.2.1 GENERAL ACCOUNT OF POLLEN MORPHOLOGY AND ULTRASTRUCTURE

The pollinarium is the effective unit for pollen transfer in the Orchidoideae. In this subfamily, pollen is generally shed in sectile or massulate pollinia with tail-like, elastoviscin caudicles and viscidia which are basitonically attached (Burns-Balogh, 1986). Individual massulae are composed of tetrads which form the basic pollen unit. Only the tetrad walls on the outer surface of the massulum have a well developed sporopollenin exine. The relationship of components of the pollinarium is illustrated in Figure 5.2.1.A. Only the sporopollenin walls have been studied.

When pollen is united into functional masses, the structural functional aspects of the constituent parts of the compound pollen deviate from simpler systems such as monads or tetrads. Knox and McConchie (1986) emphasize this point by defining compound or composite grains as "the association of two to many grains, united in such a way that the properties of the whole are not necessarily those of its constituents." Walker and Doyle (1975) report composite pollen from more than 56 Angiosperm families.

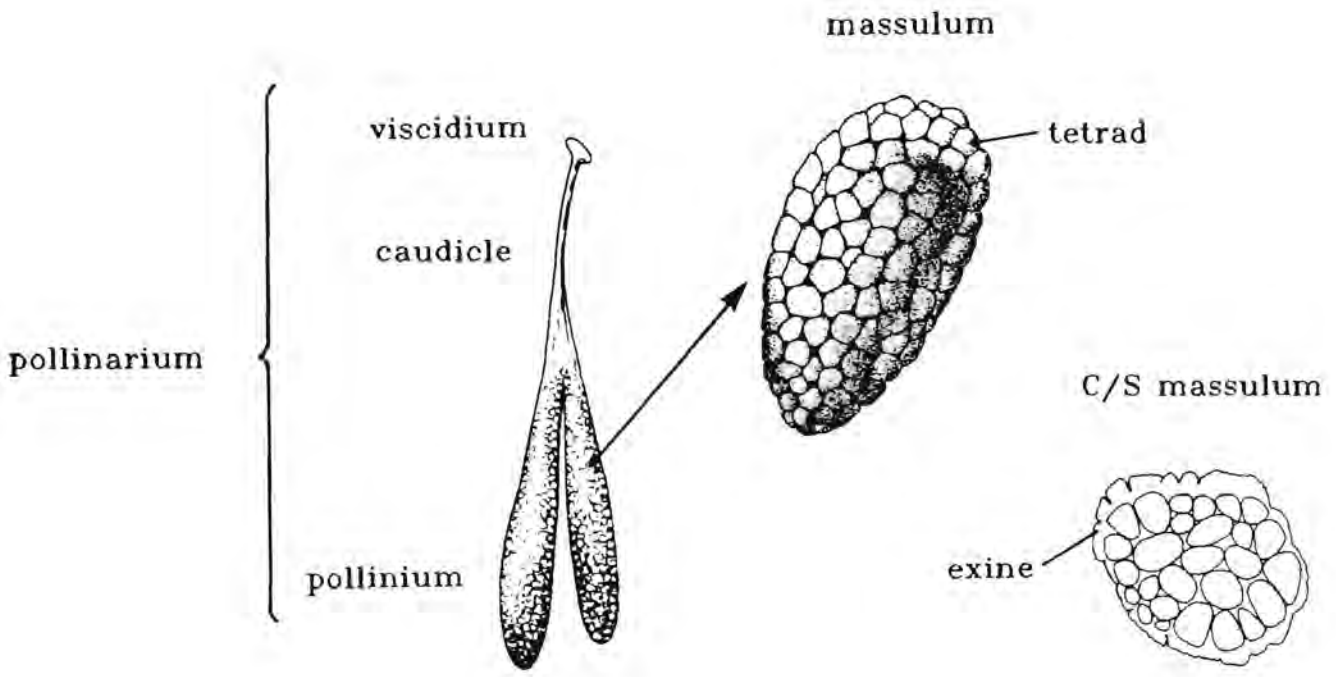

Figure 5.2.1.A

Relationship of components of pollinarium. Aggregated pollen with pollinarium comprising the sticky viscidium, the caudicle and pollinium. Pollinia are composed of basally attached massulae held within the sectile pollinium by connecting threads. Each massulum is a mass of compacted microspores, with the sculptured exine covering outer tetrads only. (not to scale).

5.2.1.1 POLLEN AGGREGATION

Single grains occur in the Apostasiodeae, Cypripedioideae, Vanillinae, some Diurideae, Neottieae and Pogoniinae (Dressler, 1981). In all other orchids, the pollen grains remain in tetrads or are aggregated into larger masses. Pollen aggregation is coupled with the large number of ovules contained in the orchid ovary. Seeds are small, lack endosperm and are released through the longitudinal slits of a twisted capsule. The transfer of pollen in masses effectively increases the number of ovules fertilized from a single pollination event. In the case of sectile pollinia, which are characteristic of the Diseae and Orchideae, a single pollinium can pollinate a number of flowers if the pollinator leaves one or more massulae on each stigma (Dressler, 1981).

In the scheme formulated by Van Campo and Guinet (1961) to describe the structural basis of wall cohesion of adjacent grains of compound pollen, two basic types of cohesion are distinguished. The simplest is the calymmate type. In this form, grains are fused by the tectum which surrounds the pollen unit, with the tectum absent from the internal walls. Pollen which has an interrupted tectum between the grains and a tectal layer which may be absent from the internal walls is classified as acalymmate.

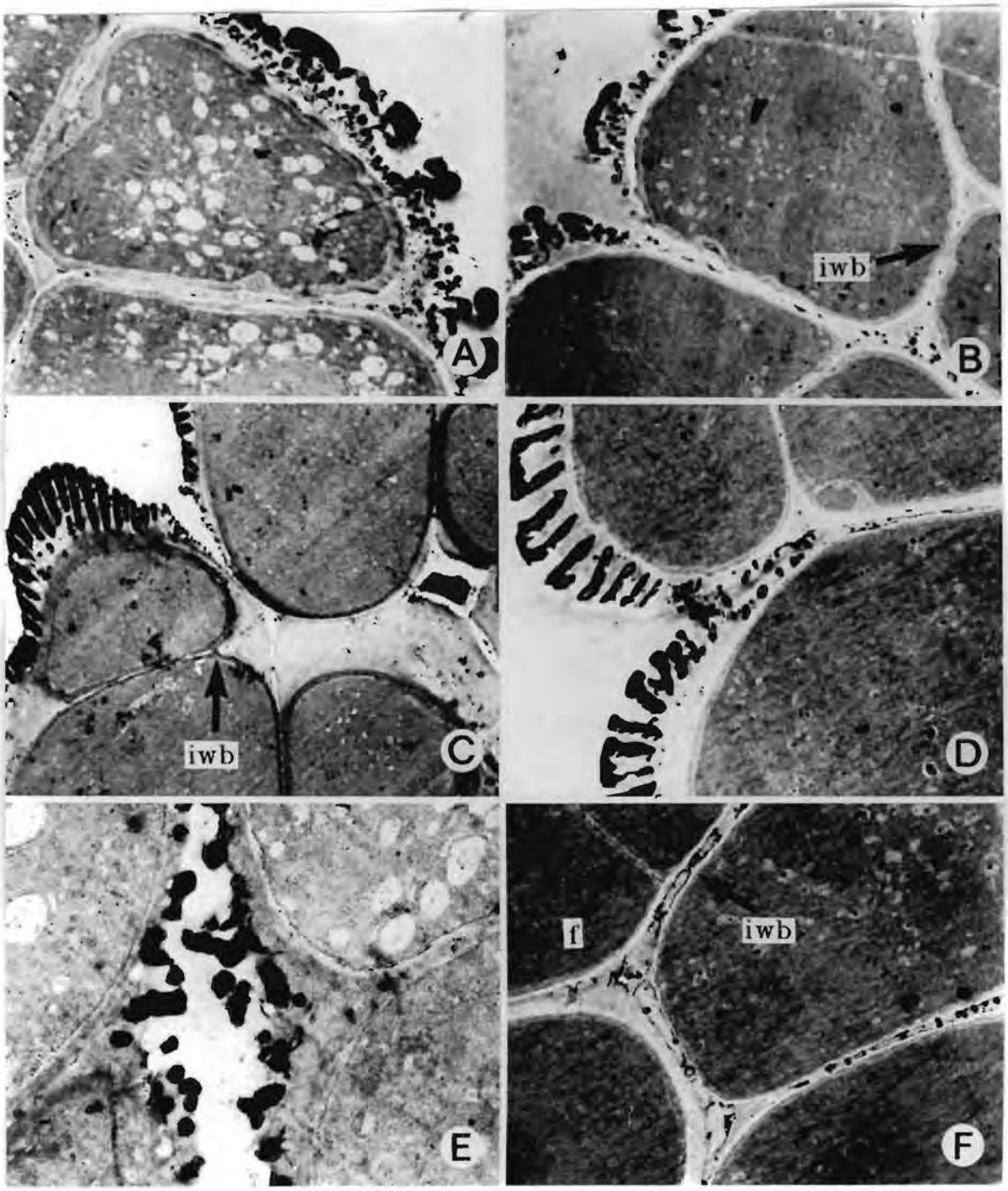

Figure 5.2.1.1.B.
Ultrathin sections through massulae of Disa lineata (A & B) (6800 X & 5000 X), Corycium orobanchoides (C) (5000 X), Pterygodium catholicum (D) (6800 X), Disa sagittalis (E) (14000 X), and Pterygodium catholicum (F) (6000 X). Calymmate and acalymmate forms occur in single species, as in D. lineata and C. orobanchoides. Intine wall bridges (iwb) connect adjacent microspores of D. lineata, C. orobanchoides and P. catholicum. Reduced sporopollenin deposition between inner tetrads (E & F). In D. sagittalis sporopollenous granules surround microspores of inner tetrad. Note partial fusion (f) between micropores, presumably of single tetrad, of P. catholicum.

In the light of the variation in pollen wall cohesion observed in recent years, the validity of this basic distinction has been questioned (Knox and McConchie, 1986). In this study both calymmate and acalymmate modes have been observed in single species. (Fig. 5.2.1.1.B a,b,c and d). In the compound pollen of orchids, Knox and McConchie (1986) report calymmate pollen held within a common exine or acalymmate massulae united by a common tectum.

On the basis of ultrastructural studies of compound pollen from 16 Angiosperm families, Knox and McConchie (1986) have identified two modes of cohesion between adjacent pollen units. These are simple cohesion, which is achieved through cohesion of the tectum, and crosswall cohesion in which connecting wall bridges occur between adjacent units. According to Knox and McConchie (1986), wall bridges may be composed of several wall layers although they are usually formed by the nexine. In Dactylorchis, Helsop-Harrison (1968) reports common internal walls comprised of the intine only. Crosswall cohesion through connecting wall bridges was observed between the pollen of Disa lineata, Corycium orobanchoides and Pterygodium catholicum (Fig. 5.2.1.1.B b,c and f). In all three species, these appear to be formed by the intine only.

In some orchid pollinia, such as Dactylorchis (Helsop-Harrison, 1968), Cleisostoma and Laelia (Zavada, 1983), the persistence of

cytoplasmic connections, which are characteristic of early developmental stages, have been noted. According to Knox and McConchie (1986), developmental and ultrastructural studies have shown the basic importance of the exine in determining the compound state. Fusion of the primexine matrix at tetrad period appears to initiate microspore cohesion in both calymmate and acalymmate (polyad) systems.

It is not clear from the literature what the exact nature of the "tetrads" of the study group is. Examination of the undersurface of the tetrad or "sculptured exine unit" of Disa patula revealed what appears to be evidence of a four-way division under the unit (Fig. 5.2.1.1.C a). This could be interpreted as evidence for four isobilateral microspore cells contained in each tetrad unit. If this were the case, the co-occurence of both calymate and acalymate tetrads in a single specimen can be explained as follows. The exine covering two adjacent cells contained within a single tetrad would be calymmate with a continuous tectum spanning the individual cells seen in TEM. In the case where the cells of two adjacent tetrads are viewed, one might expect them to be acalymmate, with a discontinuous tectum between the adjacent cells. Further investigation would be necessary to clarify this point as well as a closer correlation between SEM and TEM observations. In addition, a refinement of terms to suit these structures would be necessary. These observations are substantiated by L.M.

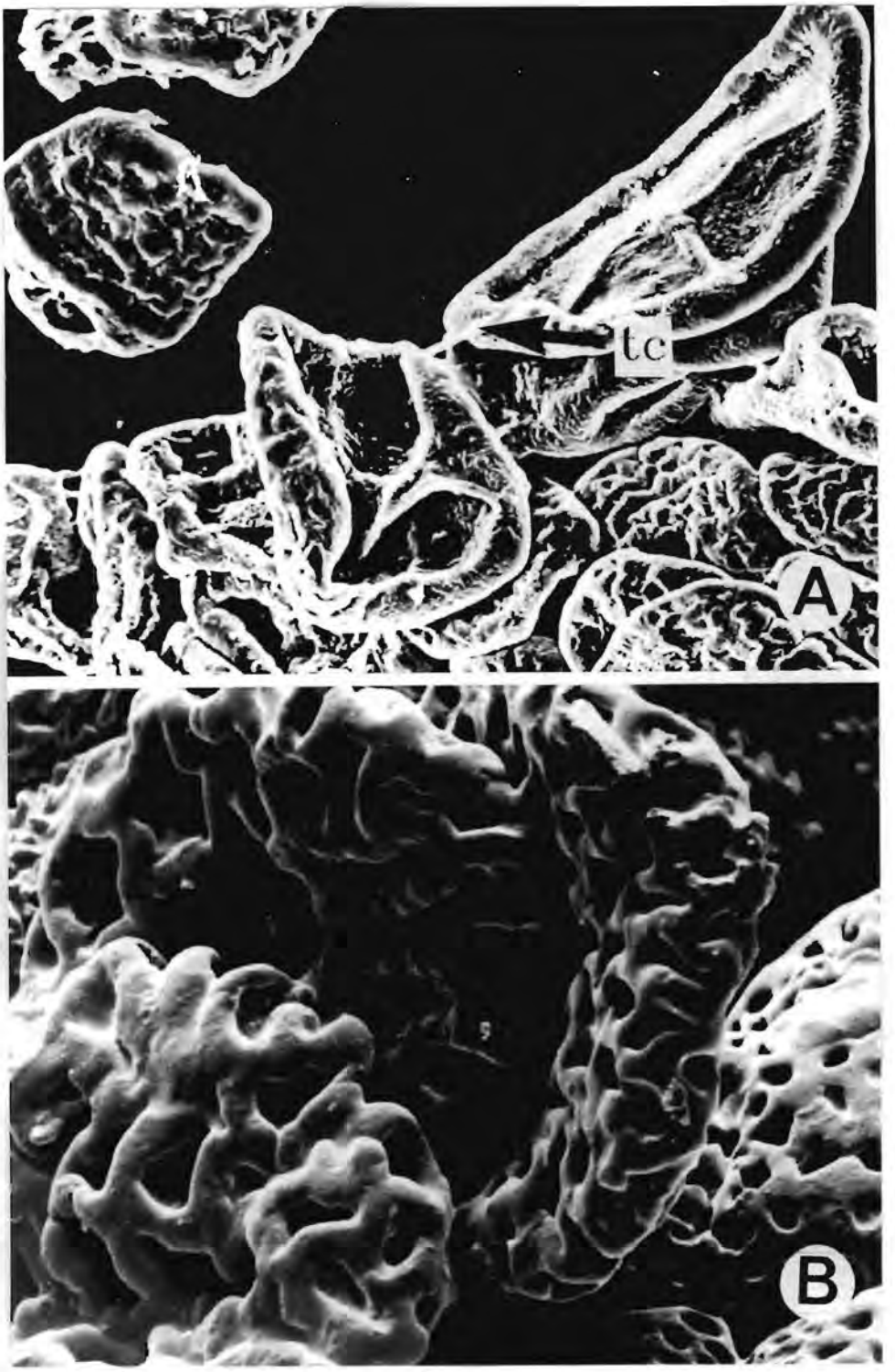

Figure 5.2.1.1.C
Inner surface of sculptured exine of Disa patula (A) (900 X) and Disperis lindleyana (B) (2400 X). Note tectal connection (tc) between tetrad units and what appears to be a four-way division, possibly indicating isobilateral tetrad configuration. In D. lindleyana the inner surface, as the outer one, is reticulate.

observations where linear tetrads were observed in Corycium crispum. In Disperis lindleyana, the undersurface of the exine is reticulate, without clear subdivisions (Fig. 5.2.1.1.C b). It is possible that these observations are artifacts.

A greatly reduced and sometimes almost absent sporopollenin layer, between the inner tetrads of the massulum, is associated with the compound state. There appears to be some variation in the amount of sporopollenin between inner tetrads of the study group. In Disa sagittalis tetrads appear to be less compact with more sporopollenin between them than in Pterygodium catholicum (Fig. 5.2.1.1.B e & f.). Sporopollenin deposition within the massulum appears to be variable within and between species.

Individual massulae are held together to form the pollinarium by connecting threads. Hesse (1986) identifies at least two different types of pollen connecting threads in the Orchidaceae. The most widely known are the tapetally derived elastoviscin threads, which are composed of sporopollenin (Burns-Balogh, 1986). Lipid threads are less well known. They have been noted in Habenaria (Hesse and Burns-Balogh, 1984) which belongs to the tribe Orchideae. Hesse and Burns-Balogh (1984) suggest that these sticky, inelastic lipid threads originate from immature degenerating cells in the transition region between the caudicle and the massulae. They are thought to be homologous to microspores. A third type of thread "cohesion strands" have been identified by Burns-Balogh (1983). These acetolysis-resistant structures are found in the Spiranthoideae and Neottioideae. Connecting threads were not investigated in this study and it remains an open question whether they are composed of elastoviscin or lipids as those reported for Habenaria.

5.2.1.2 POLLEN WALL STRATIFICATION, STRUCTURE AND SCULPTURE

The term pollen wall architecture was coined by Walker and Doyle (1976) to broadly define the various aspects of pollen wall morphology. These aspects are clearly defined by Walker (1976) who identifies three components to pollen wall architecture: wall stratification, structure and sculpture.

The stratification of the exine refers to the layers or strata in the wall. Wall structure describes the components present in the wall itself e.g. columellae. In terms of exine structure, angiosperm pollen grains are described as tectate (perforate or imperforate), semi-tectate or intectate. The sculpturing component of wall morphology can be fairly complex depending upon the wall structure. Walker and Doyle (1976) have distinguished two different types of sculpturing according to wall structure. In tectate pollen, the sculpturing is supra-tectate (or supra-ornate) whilst semi-tectate or intectate grains are per-ornate, their surface ornamentation simultaneously representing both structure and sculpture. If the exine forms a reticulum, for example, with the diameter of tectal perforations greater than the breadth of the pollen wall between them, the exine structure is semi-tectate (Walker, 1976). The sculptured exine (sexine) of intectate grains consists only of exposed columellae or their modified homologues. Sculpturing in tectate pollen describes any supra-tectal elements (Walker, 1976).

The stratification of a typical columellate angiosperm pollen grain consists of the three-layered exine which is derived from the tapetum (sporophyte) overlying the cellulosic intine, which is of gametophytic origin. The exine is comprised of the nexine (endexine and foot layer), columellae with interbacular spaces and the roof-like tectum (Walker, 1976). Schill and Pfeiffer (1977) report that the exine of orchid pollen is not comparable with the classical sporoderm. They found the tectum to be compact and homogenous and the intine more or less fibrillar.

The exine stratification and structure of those species where thin sections were prepared is shown in Fig. 5.2.1.2.A. The basal or foot layer is absent in all species investigated. This observation agrees with scheme of Burns-Balogh (1986), who reports the absence of a foot layer in the Orchidoideae, Cypripedioideae and most Epidendroideae. She interprets this absence as a loss representing three different apomorphies for these groups. In all species, two layers were noted. The electron-dense sexine (sculptured exine) and the less opaque endexine overlying the intine. The main feature which varies between groups is the nature of the tectum. Satyrium bracteatum, Disperis capensis, Schizodium inflexum, Disa sagittalis and Disa lineata are all interpreted as semi-tectate. This condition may be secondary in relation to the phylogeny of the orchids and the evolution of their pollen walls (Burns-Balogh, 1986). Nevertheless, it appears to be plesiomorphic in the context of the study group. Evota bicolor,

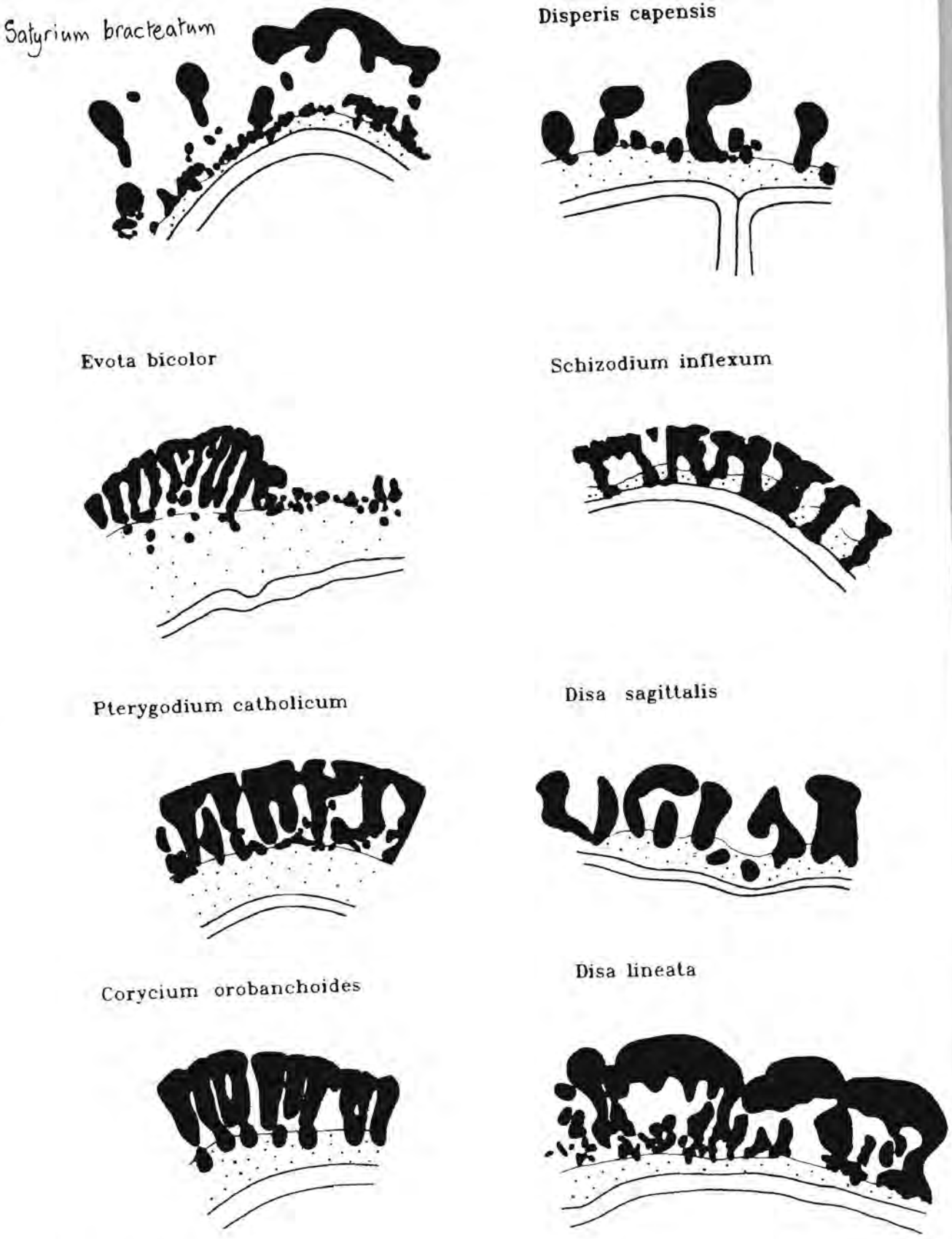

Figure 5.2.1.2.A

Exine stratification and wall structure of species used for TEM. Three wall layers were consitent throughout the group: the sculptured exine or sexine (black), the endexine (stippled), and the gametophytically-derived intine (white). The absence of a foot layer is characteristic of the group. In terms of wall structure, Satyrium bracteatum, Disperis capensis, Schizodium inflexum, Disa sagittalis, and Disa lineata are semi-tectate. In contrast, Evota bicolor, Pterygodium catholicum and Corycium orobanchoides have a tectate wall structure. (not to scale).

Pterygodium catholicum and Corycium orobanchoides are all interpreted as being secondarily tectate, with a more or less continuous tectum and well developed columellae supporting it. The size of interbacular spaces appears to be somewhat reduced in contrast with the semi-tectate forms.

5.2.2. OBSERVATIONS

Detailed descriptions of all species studied using SEM are given in Appendix 4.

The outgroups from the Tribe Orchidoideae were Habenaria laevigata and Bonatea pulchella (Fig. 5.2.2.A.). These have fairly rounded massulae and isodiametric tetrads. In H. laevigata, sculpturing is ornate with a semi-tectate exine structure. B. pulchella has a reticulate exine, with the muri of the reticulum almost absent, leaving free standing columellate structures. This latter species approaches the intectate state, in terms of exine structure. Huttonaea pulchra and H. grandiflora (Fig. 5.2.2.B) have elongated tetrads and reticulate exines. Satyrium bracteatum has fairly elongatedmassulae with isodiametric tetrads and a semi-tectate, reticulate exine (Fig. 5.2.2.C).

Representatives of the three minor genera of the sub-tribe Disinae are shown in Fig 5.2.2.D. Sculpturing in Schizodium is typically reticulate (hamulate) with either pilate lumina as in the loosely reticulate (ornate) Schizodium bifidum, or more tightly reticulate with ornate muri. Brownleea has a characteristically reticulate exine. A range of variation in exine sculpture is observed in Monadenia. Sculpturing is mostly

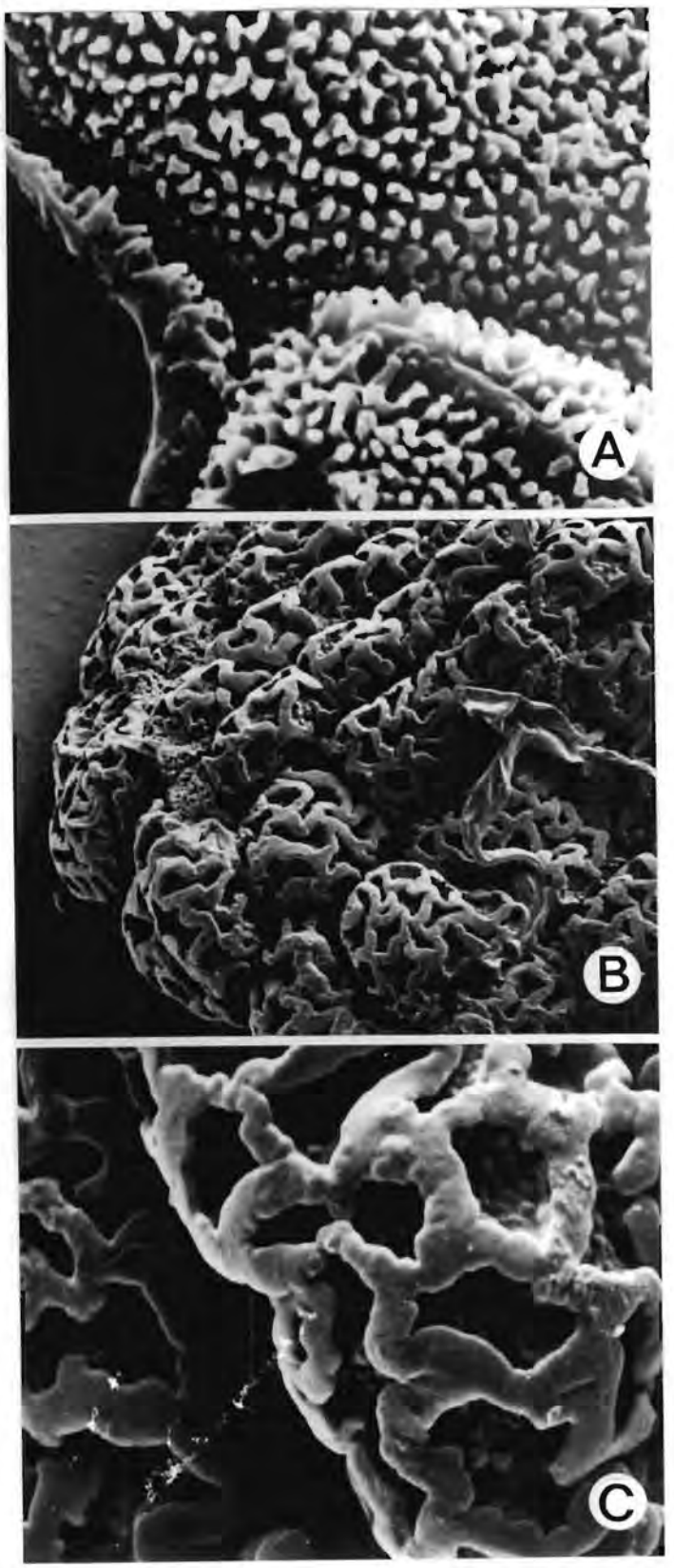

Figure 5.2.2.A.

Surface sculpturing in the Orchideae. Bonatea pulchella (A) (5000 X), Habenaria laevigata (B & C) (1500 X & 5700 X). Note fractured wall in B. pulchella showing columellae composing the virtually intectate structure of the reticulate exine, which has reduced muri. In H. laevigata, the ornate sculpturing pattern is a loose reticulum with pilate lumina.

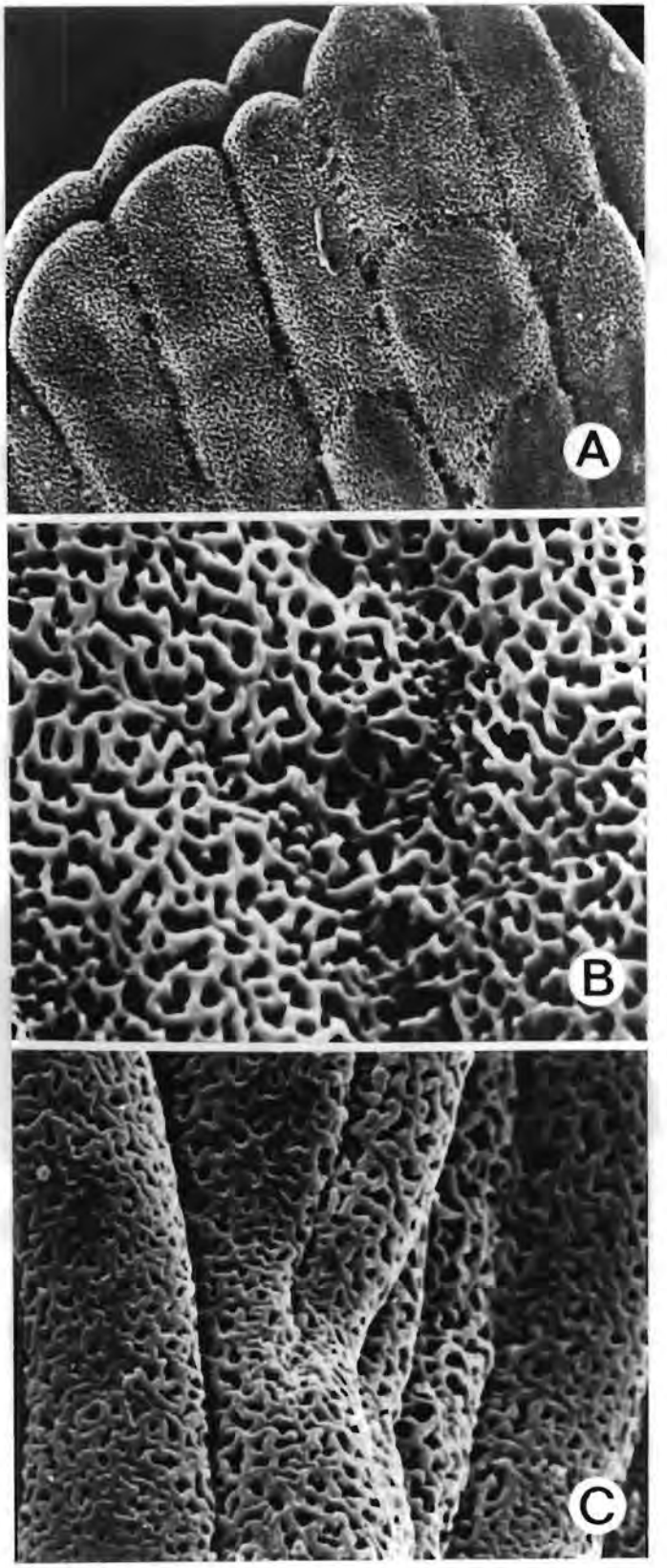

Figure 5.2.2.B

Pollen morphology of Huttonaea. Huttonaea pulchra (A&B) (1000 X & 5200 X) and Huttonaea grandiflora (C) (5100 X). Note elongated tetrads and reticulate sculpturing.

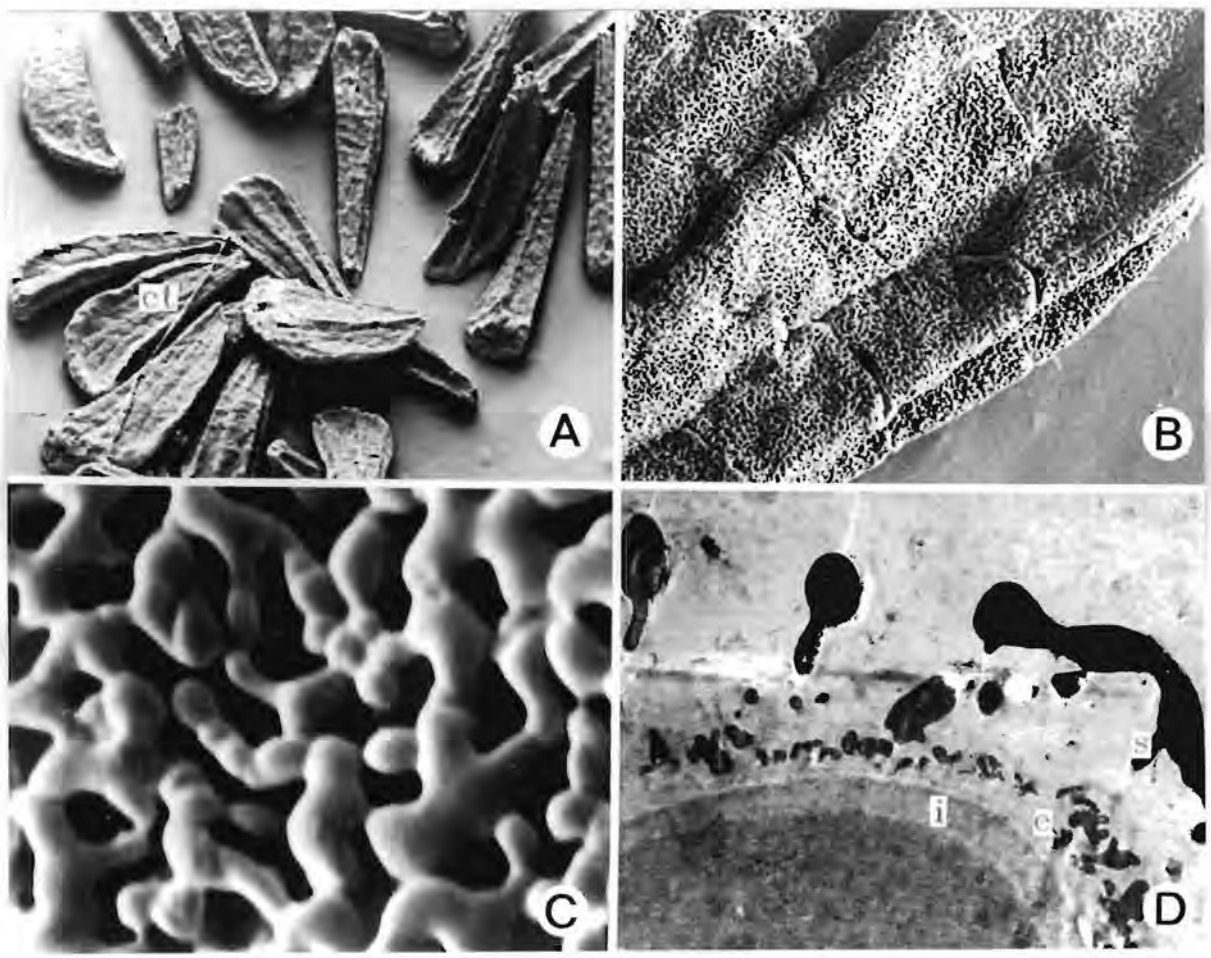

Figure 5.2.2.C

Pollen morphology of Satyrium bracteatum. Note connecting thread (ct) and fairly elongated massulae (A) (125 X), isodiametric tetrads (B) (1000 X) with reticulate sculpturing (C) (1500 X). Thin section through reticulum showing semi-tectate wall structure (D) (16000 X) (s=sculptured exine, e=endexine and i=intine).

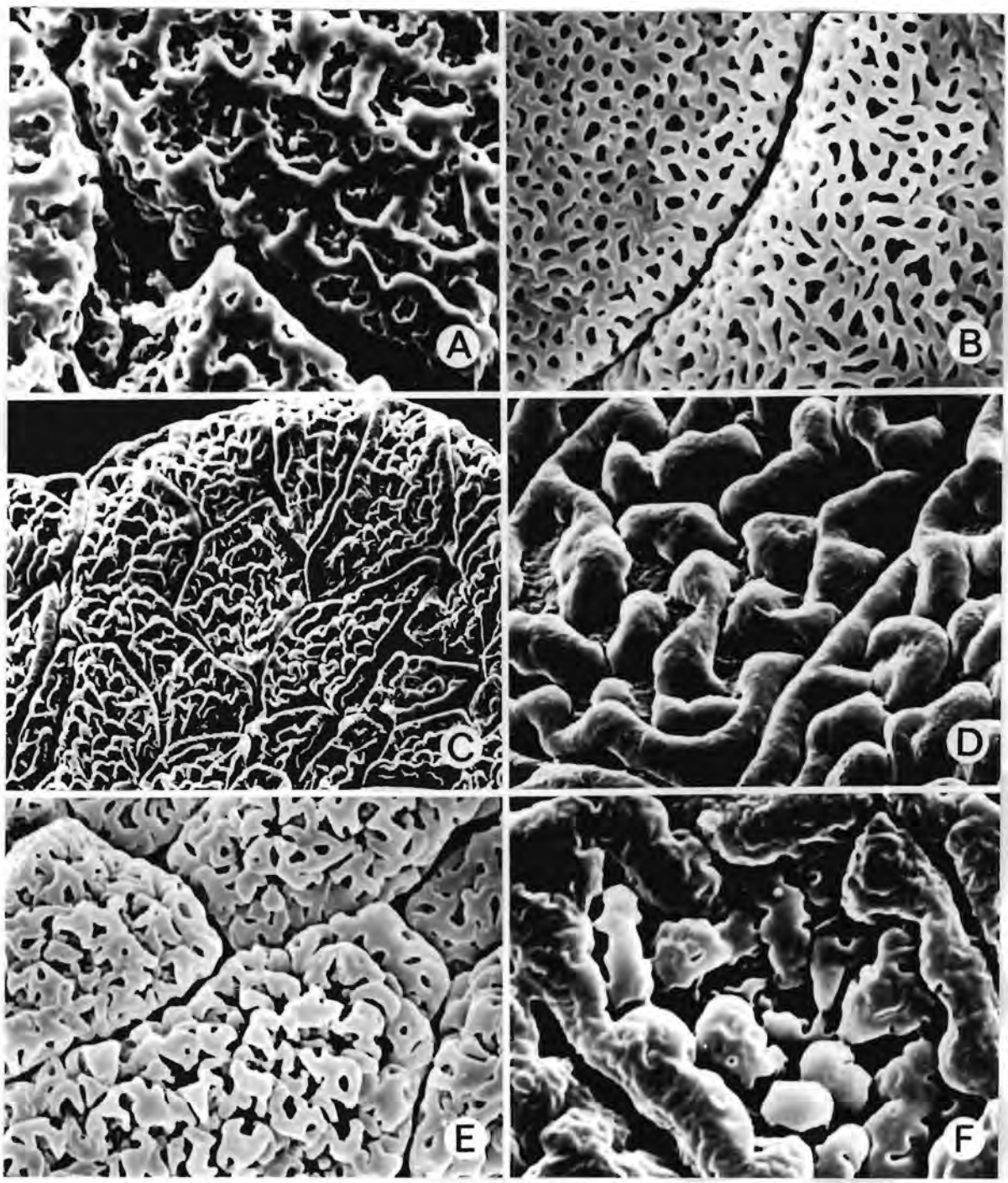

Figure 5.2.2.D.

Pollen surfaces of minor genera of the Disinae. Sculpturing is ornate in Schizodium bifidum (A) (5000 X), reticulate in Brownleea coerula (B) (5800 X), rugose in Monadenia atrorubens (C & D) (1 000 & 5 000 X), hamulate in Monadenia densiflora (E) (5100 X), and verrucose with a distinct tetrad margin in Monadenia sabulosa (F) (5100 X).

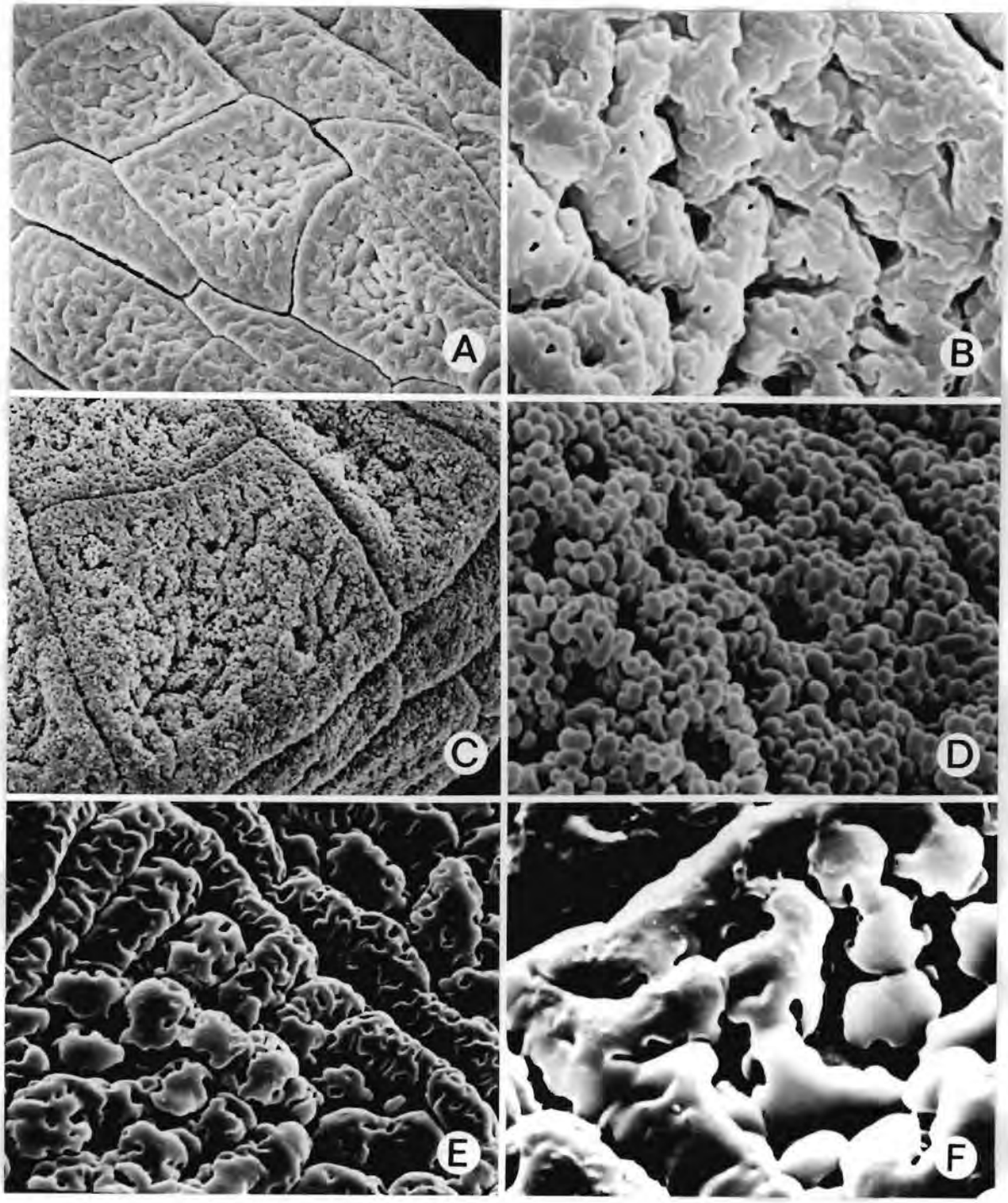

Figure 5.2.2.E.

Surface ornamentation in sections Disa (A-D) and Phlebidia (E & F). In Disa atricapilla (A & B) (1000 X & 5000 X) and Disa uniflora (C & D) (1100 X & 5100 X), sculpturing is typically rugose with variations in the supra-tectal ornamentation. Free standing baculate and pilate structures are interpreted as columella homologues. D. longicornu (E) (4400 X) and D. maculata (F) (5000 X) have verrucose sculpturing with distinct tetrad margin. Note convergence in exine sculpturing in D. maculata and Monadenia sabulosa (Fig. 5.2.2.D. F).

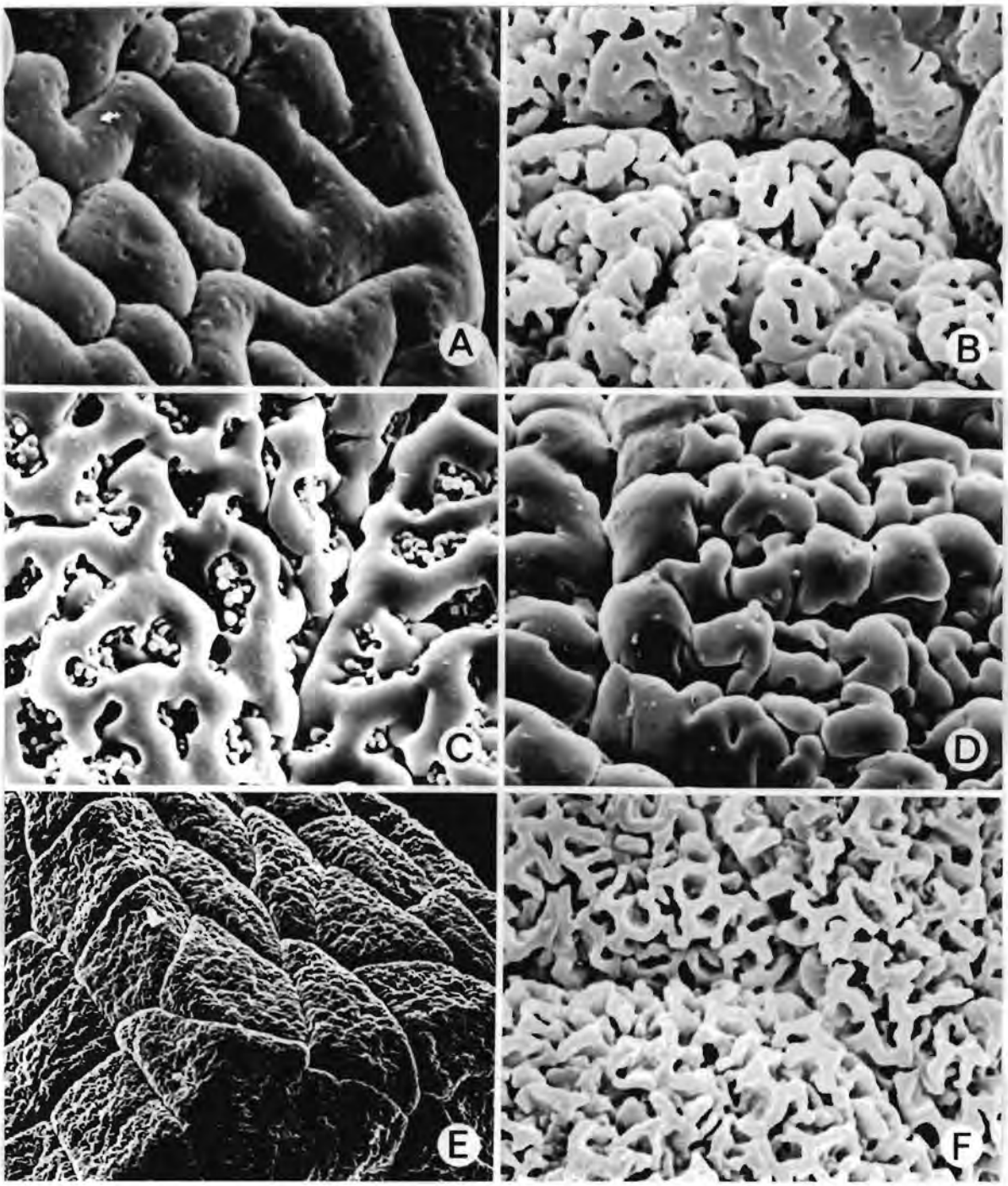

Figure 5.2.2.F

Surface ornamentation in sections Hircicornes (A–C), Ovalifoliae (D), and Amphigena (E & F). In section Hircicornes, sculpturing is extremely variable ranging from rugose-punctate, as in Disa versicolor (A) (5200 X), to rugose-foveolate in D. thodei (B) (5000 X). D. cooperi (C) (5000 X) is ornate, with pilate lumina. D. ovalifoliae (D) (5000 X) has verrucose sculpturing. D. salteri (E) (1000 X) and D. tenuis (F) (5000 X) are both interpreted as having an hamulate exine although they differ markedly from each other with D. salteri having an almost complete tectum.

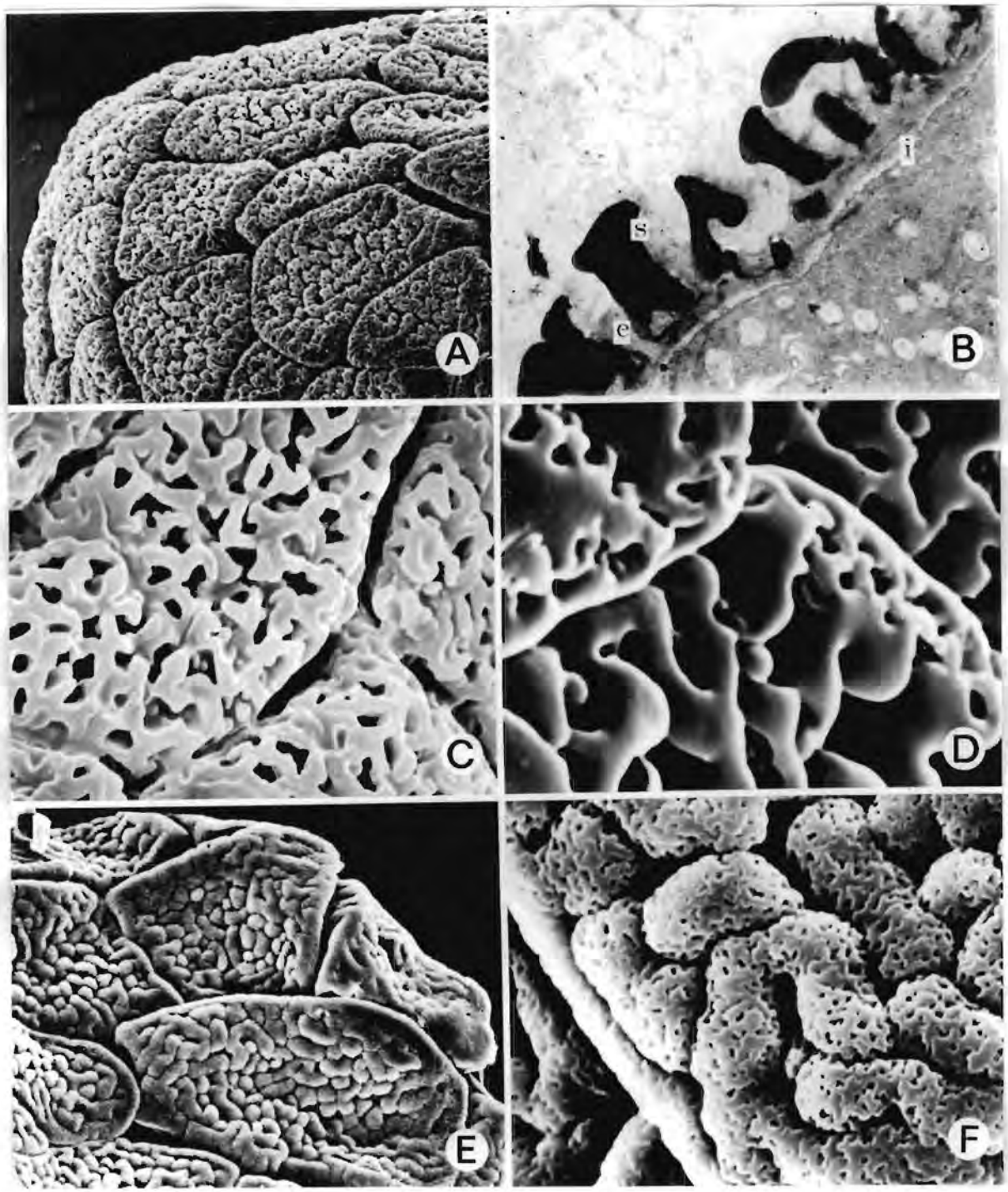

Figure 5.2.2.G

Disa gladioliflora (A) (1100 X), of the section Stenocarpa, is rugose with foveolae piercing the tectum. Disa sagittalis (B) (14000 X) (section Coryphaea) was used for TEM. Note semi-tectate exine structure (s=sculptured exine, e=endexine and i=intine). D. triloba (C) (5200 X) and D. marlothii (D) (5100 X) (section Coryphaea) have hamulate sculpturing. D. marlothii has unusual lace-like tetrad margins. Disa stachyoides (E & F) (1000 X & 5000 X) (section Emarginatae) has rugose-foveolate sculpturing and distinct tetrad margins which commonly occur in Disa.

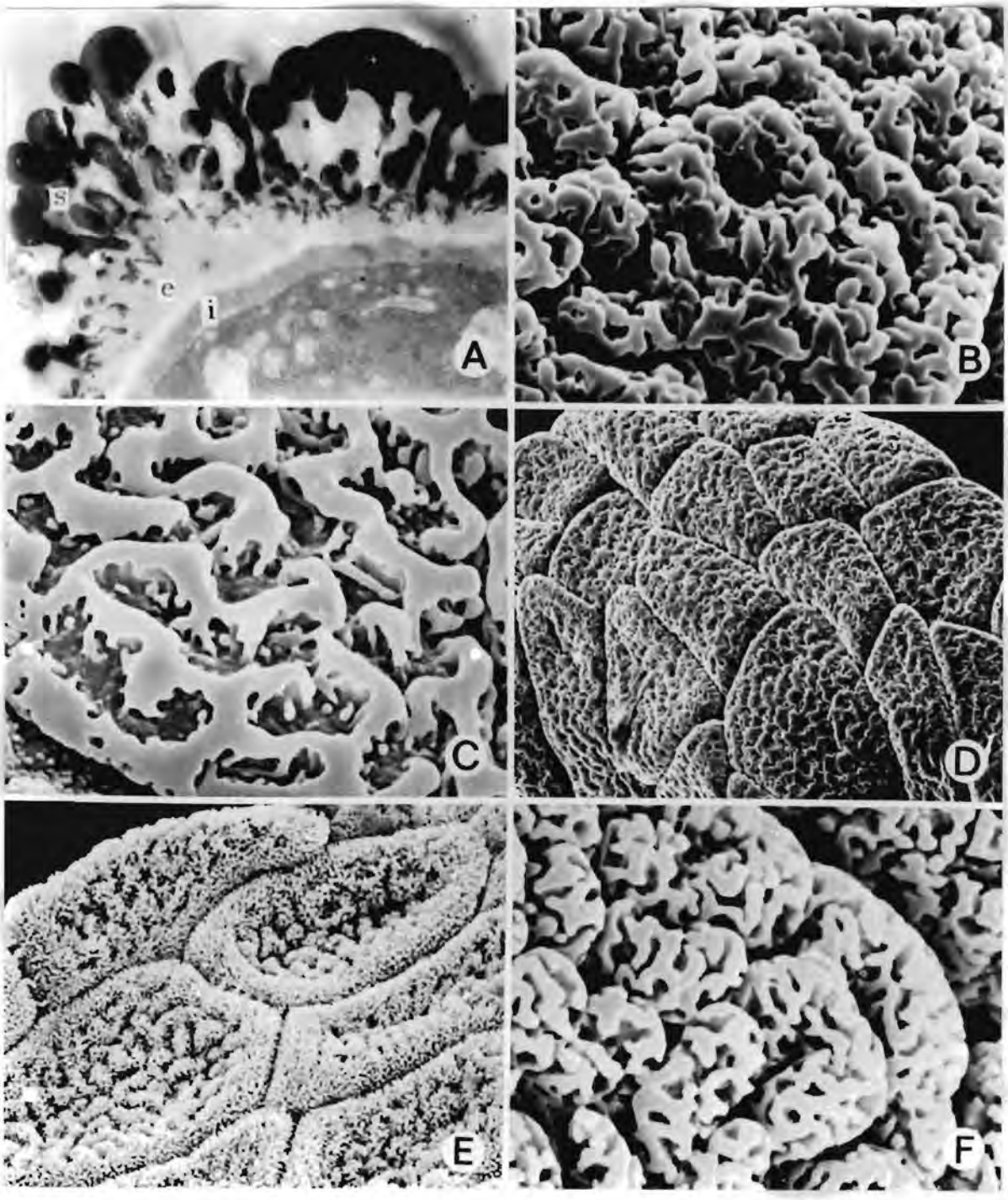

Figure 5.2.2.H

Thin section through pollen wall of D. lineata (A) (10000 X) (section Disella). Note rugae and baculate columella homologues. D. cornuta (B) (5100 X) (section Repandra) has rugose-foveolate sculpturing with supra-tectal granules. D. galpinii (C) (5200 X) (section Intermediae) has ornate sculpturing similar to Habenaria laevigata (Fig. 5.2.2.A. B & C), with a loose reticulum and pilate lumina. D. aconitoides (D) (1000 X) (section Aconitoideae) is very tightly verrucose with an almost complete tectum pierced by foveolae. Section Micranthae (E & F) is fairly distinctive. Mostly, rugae are pierced by foveolae as in D. ukingensis (F) (5100 X). Some species, e.g. D. englerana (E) (1000 X) have an intectate structure with free standing baculae supporting a greatly reduced tectum.

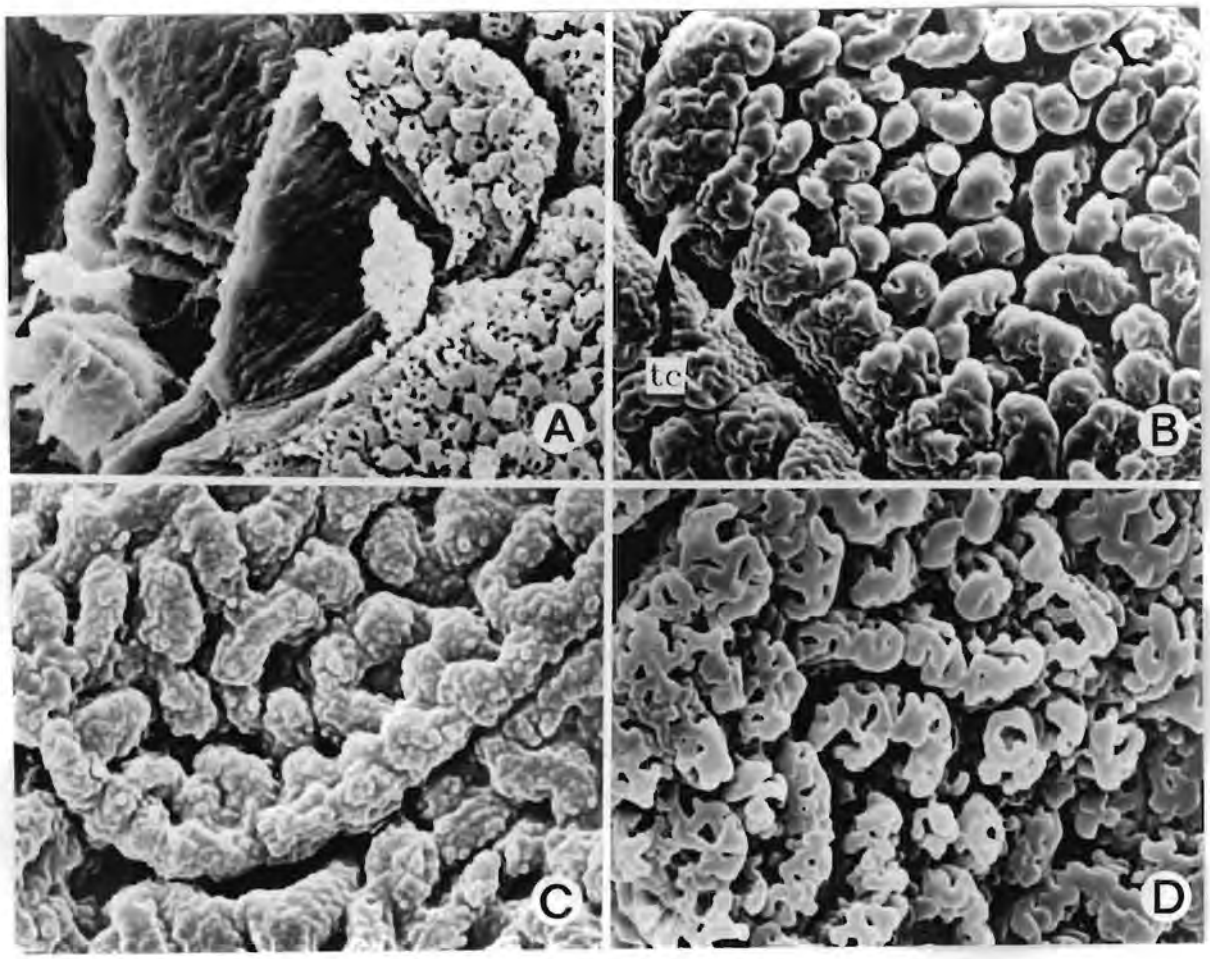

Figure 5.2.2.I

Exine sculpturing in Herschelianthe. A fractured massulum of H. hians (A) (3300 X) which has verrucose-foveolate sculpturing. H. schlechterana (B) (5000 X) is verrucose-foveolate with distinct tetrad margins. Note tectal connections (tc) between adjacent tetrads. H. spathulata (C) (5000 X) is unique, with granulate rugae and distinct tetrad margins. H. forficaria (D) (5000 X) has a rugose-foveolate sculpturing type common in Disa.

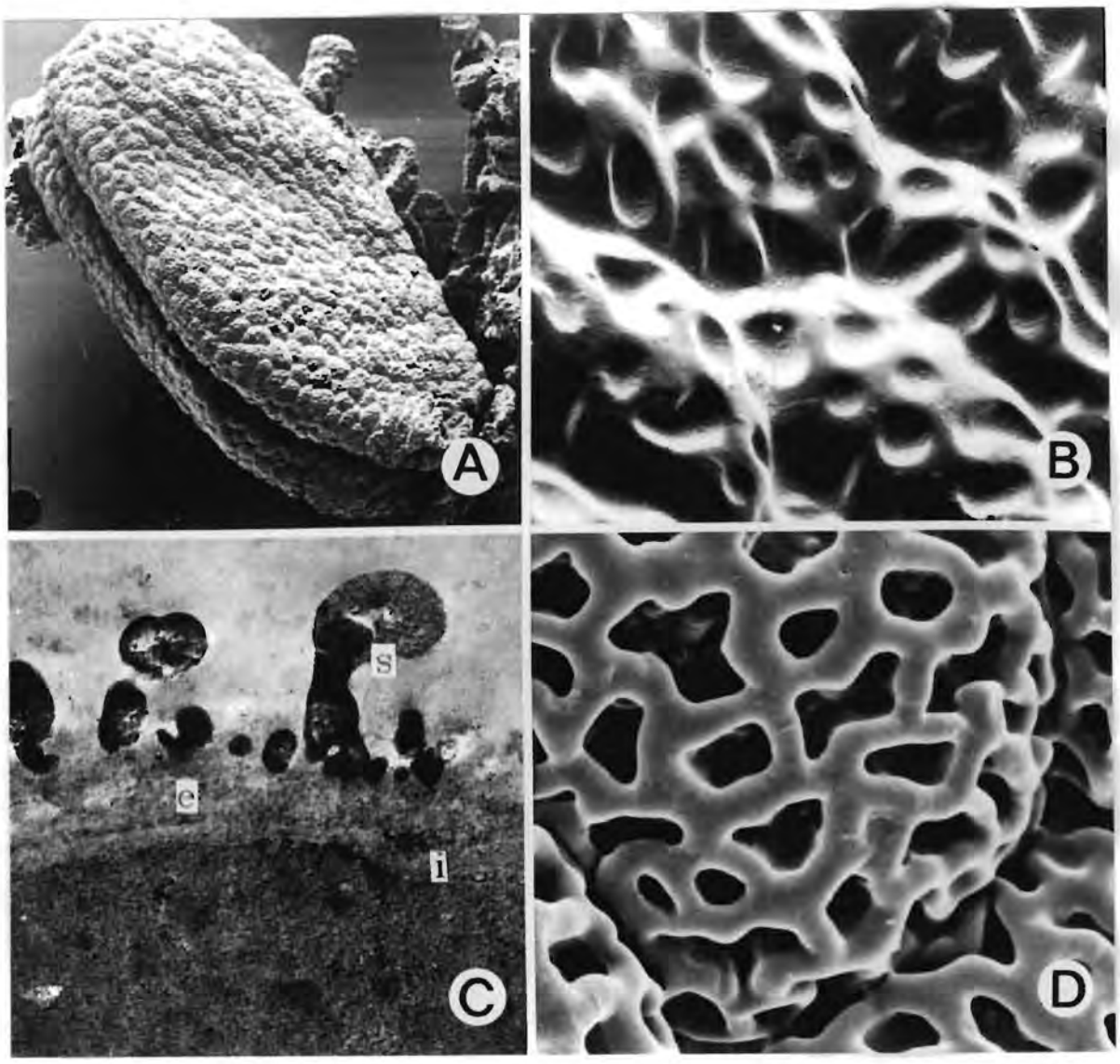

Figure 5.2.2.J

Rounded massulum with isodiametric tetrads (A) (162 X) of Disperis capensis, which has unusual, closed lumina in the reticulum (B) (3000 X), and a semi-tectate wall structure as can be seen in TEM (C) (27000 X) (s=sculptured exine, e=endexine and i=intine). Disperis lindleyana (D) (5000 X) is typical of the genus which characteristically has reticulate sculpturing.

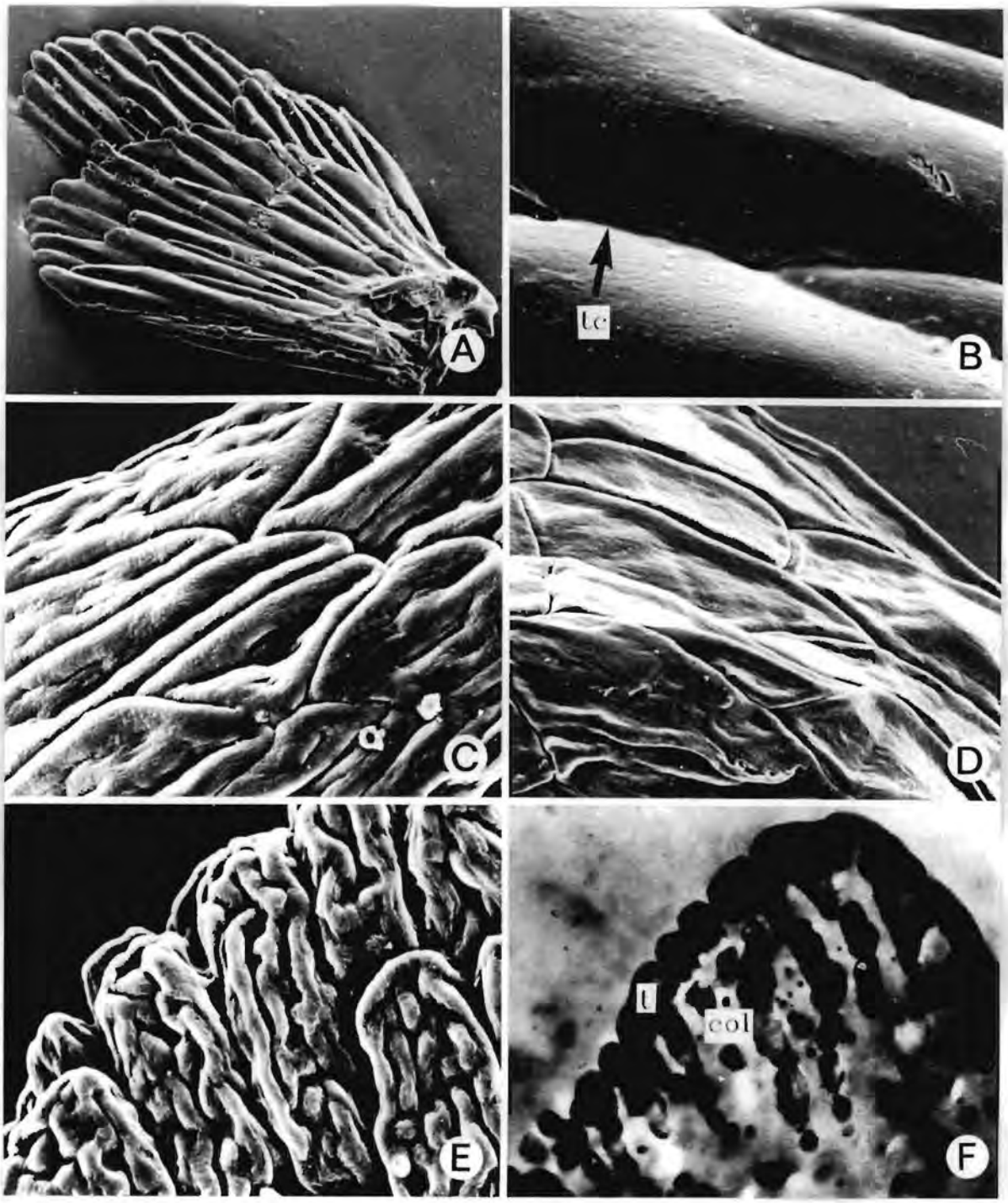

Figure 5.2.2.K.

Pollen morphology in minor genera of the Coryciinae. Anochilus halli (A & B) (300 X & 2800 X) has fan-shaped massulae, elongated tetrads, and a tectum perforated by fine punctae. Adjacent tetrads in this species are partially fused (f). Ceratandra grandiflora (C) (1200 X) and Evota venosa (D) (1200 X) have fasciculate massulae and elongated tetrads which are faintly striate and perforated by punctae. Evota bicolor (E) (1300 X) has unique rugulate exine sculpturing. Thin sections through these rugae (F) (20000 X) show that they are tectate-columellate structures.

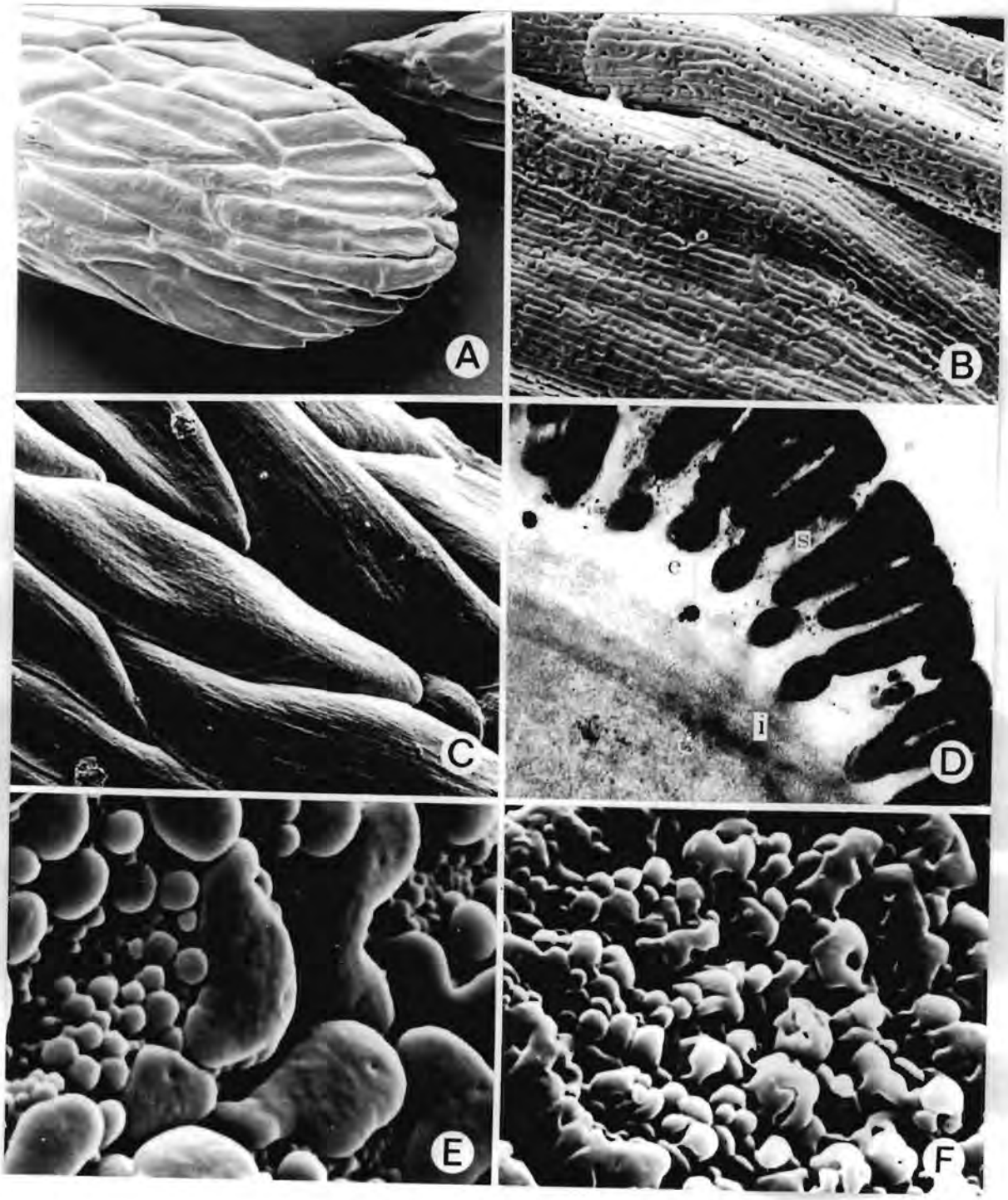

Figure 5.2.2.L

Pollen morphology in Corycium. Massulae of Corycium bifidum (A) (531 X) are fasciculate with elongated tetrads. Sculpturing is finely striate with foveolae or punctae piercing the tectum as in Corycium deflexum (B) (4900 X) and C. orobanchoides (C) (1500 X). In cross section, the wall of C. orobanchoides has well developed columellae supporting the tectum (D) (X). C. dracomontanum (E) (12500 X) and C. nigrescens (F) (5200 X) are exceptional in the Coryciinae, being convergent with the Disinae in their verrucose exine sculpturing and more or less isodiametric tetrad shape.

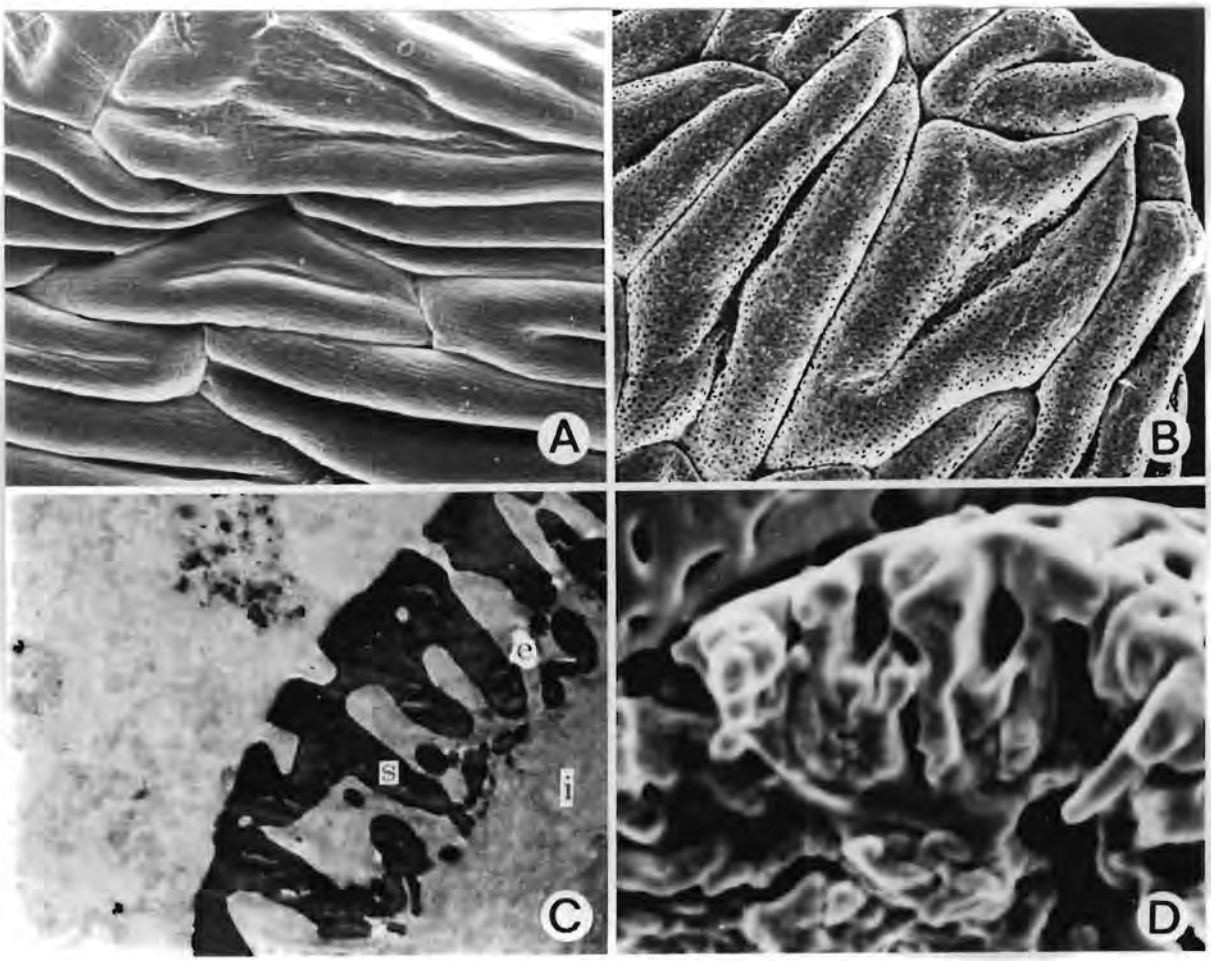

Figure 5.2.2.M.
Pollen wall morphology in Pterygodium. Sculpturing in this genus is striate with foveolate perforations in the tectum as can be seen in P. acutifolium (A) (1200 X) and P. catholicum (B) (X). The ultrathin section (C) (X) and the fracture (D) (17800 X) through the pollen wall of P. catholicum show columellae and interbacular spaces beneath the complete tectum.

rugose with distinct tetrad margins although sculpturing may tend to be verrucose, as in M. sabulosa, or hamulate, as in M. densiflora.

Exine sculpturing in Disa is diverse and often elaborate. Since sampling for SEM was done to represent sections of the Disinae and representative genera of the Coryciinae, these will be outlined below.

Section Disa, as represented here by D.atricapilla and D. uniflora, is typically rugose with variation in the supra-tectal ornamentation and free standing baculae or pilae which are interpreted as columella homologues (Fig 5.2.2.E. a-d). Section Phlebidia, represented by D. longicornis and D. maculata (Fig 5.2.2.E. e-f), is verrucose with distinct tetrad margins. Note the almost identical sculpturing of D. maculata and Monadenia sabulosa.

Section Hircicornes is extremely variable ranging from rugose-punctate to rugose-foveolate exine sculpturing as in D. versicolor and D. thodei respectively. D. cooperi is ornate with pilate lumina (Fig. 5.2.2.F. a-c). Disa ovalifoliae (Section Ovalifoliae), which belongs also to the subgenus Hircinornes has verrucose sculpturing (Fig. 5.2.2.F. d). D. salteri and D. tenuis represent the Section Amphigena, and although both are interpreted as having hamulate exine

sculpturing, they differ markedly from each other with D. salteri having an almost complete tectum. Section Stenocarpa, as represented here by D. gladioliflora is typically rugose with foveolae piercing the tectum (Fig. 5.2.2.G. a). D. sagittalis (Fig. 5.2.2.E. b) (Section Coryphaea) was used for ultrathin sectioning of the exine and is characteristically semi-tectate. D. triloba and D. marlothii (Fig. 5.2.2.G. c-d) (Section Coryphaea) have hamulate exine sculpturing, but D. marlothii is most unusual and has lace-like foveolate tetrad margins not observed in any other species of the genus. D. stachyoides (Fig. 5.2.2.G. e-f) has rugose-foveolate sculpturing and distinct margins, which commonly occur in Disa spp.

D. lineata (Section Disella) was used for TEM studies (Fig. 5.2.2.H. a). Rugae and baculate columella homologues can be seen in cross section.

D. cornuta (Section Repandra) has a very loose rugose sculpturing, with large foveolae and supra-tectal granules (Fig. 5.2.2.H. b).

D. galpinii (Fig 5.2.2.H. c) of the Section Intermediae appears to repeat the sculpturing found in the outgroup Habenaria laevigata. Sculpturing in this species is ornate with baculae in the lumina and punctate perforations in the tectum. D. aconitoides (Section Aconitoideae) is very tightly verrucose, with an almost complete tectum pierced by foveolae (Fig. 5.2.2.H. d).

Section Micranthae (Fig. 5.2.2.H. e-f) is fairly distinctive, usually rugose with the exception of D. chrysostachya which has verrucose sculpturing. In most cases the rugae are pierced by foveolae, as in D. ukingensis, in such a way that the tectum is mostly incomplete and bacculate columnmela homologues can be seen as in D. englerana.

The genus Herschelianthe (Fig. 5.2.2.I. a-d) has exine sculpturing types found in Disa. The outer tetrads of H. hians are covered with verrucae pierced by numerous large foveolae. H. schlechterana, which is also verrucose with foveolae and punctae has distinct tetrad margins. Between tetrads of this species, what appears to be "tectal bridges" connect adjacent tetrads. H. spathulata is unique in its sculpturing with fairly compact granulate rugae and distinct tetrad margins. H. forficaria has a rugose-foveolate exine sculpturing type most reminiscent of the genus Disa, and appears to be almost transitional between the rugose and verrucose character states.

Exine sculpturing in the subtribe Coryciinae was found to differ markedly from that of the Disinae. This is to be expected if one considers the basic differences shown in the TEM studies. The genus Disperis (Fig. 5.2.2.J. a-e) is quite distinctive and has fairly uniform exine sculpturing. The massulae are rounded with isodiametric tetrads and a semi-tectate exine. They are

mostly reticulate as in D. lindleyana, although in D. thorncroftii the muri of the reticulum are mostly absent, leaving free, exposed baculae (columella homologues) and approaching an intectate exine structure. D. circumflexa is exceptional, with elongated tetrads, it resembles other members of the Coryciinae in its pollen morphology.

The pollen of the minor genera Evota and Ceratandra is shown in Fig. 5.2.2.K. c-f. They characteristically have fasciculate massulae and elongated tetrads with a complete tectum which may be faintly striate and perforated by punctae. Evota bicolor is unique in its rugulate exine sculpturing. Thin sections through these rugae reveal they they also are composed of columellate structures supporting a complete tectum. In between these structures, the exine is reduced to short columellae, with the tectum absent from these parts.

Anochilus hallii (Fig 5.2.2.H. a & b) has fan-shaped massulae composed of psilate tetrads with a complete tectum perforated by fine punctae.

Features observed in the genus Corycium are shown in Fig. 5.2.2.L. The genus typically has fasciculate massulae with elongated tetrads with sculpturing mostly finely striate, and punctae or foveolae piercing the tectum. In cross section, as shown here for C. orobanchoides, one can note the well developed

columellae supporting the tectal layer. Two species, C. dracomontanum and C. nigrescens differ markedly from the rest of this fairly uniform genus. Both have the verrucose-baculate exines which occur commonly in the genus Disa.

The exine found in representatives of the genus Pterygodium does not differ greatly from that of Corycium. Sculpturing is striate with foveolate perforations piercing the tectum (Fig. 5.2.2.M).

5.2.3 IDENTIFICATION OF CHARACTERS AND ANALYSIS OF CHARACTER STATE DISTRIBUTION AMONG TAXA

From the TEM investigation it was apparent that exine stratification is consistent throughout the study group. Exine structure is clearly separated into two distinct types. On the basis of outgroup comparison it was concluded that the semi-tectate exine is plesiomorphic within the study group and that the tectate exine structure characteristic of the Coryciinae (excluding Disperis) is derived. This distinction is important in interpreting homologies amongst structures observed in SEM.

Three different shapes of massulae were identified. In the tribe Orchideae (Habenaria laevigata, Bonatea pulchella), and the Disinae, massulae are fairly rounded and composed of isodiametric tetrads. In the subtribe Satyriinae (Satyrium bracteatum) and in the genus Huttonaea, massulae are elongated, whilst fasciculate and fan-shaped massulae were noted in representatives of the subtribe Coryciinae. These three states are coded as non-additive as both rounded and elongated massulae are found in the outgroups.

Tetrad shape varies from more or less isodiametric (Orchideae, Disinae, Satyriinae and Disperis) to elongated (Coryciinae, Huttonaea).

0 - Reticulum with muri and inter-mural spaces evenly distributed

1 - Reticulum with depressions instead of open lumina

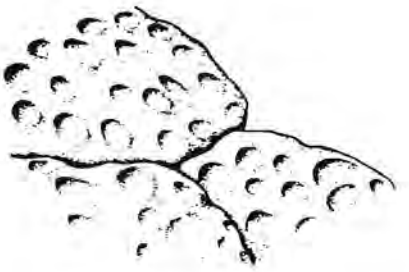

2 - Reticulum with reduced muri and free baculae

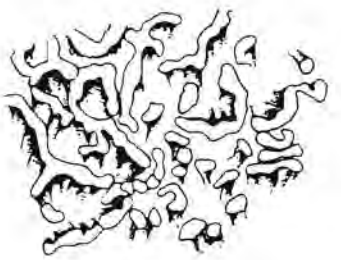

3 - Ornate, with large pilate lumina

4 - Hamulate, with supra-tectal elaborations on the muri

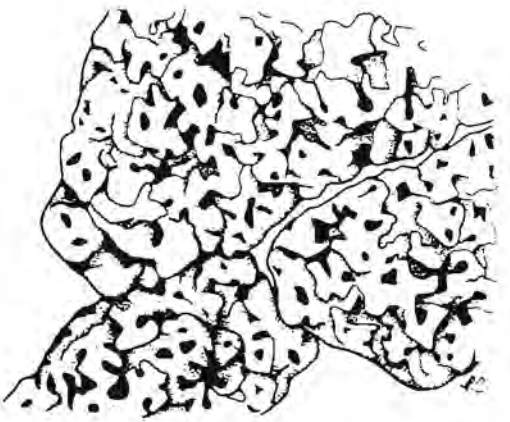

Figure 5.2.3.A.
Character states of the semi-tectate, reticulate exine.

0 - Rugose

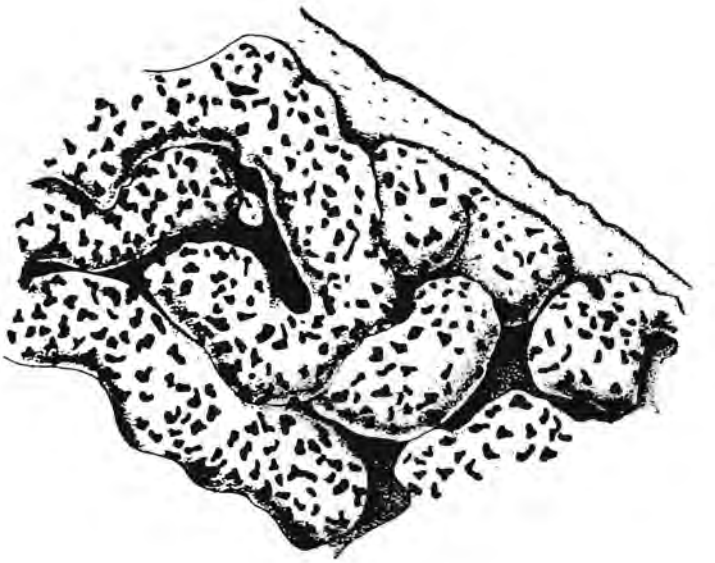

1 - Verrucose

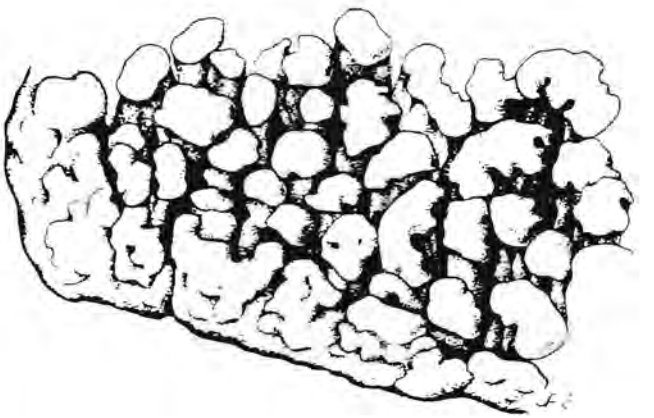

Figure 5.2.3.B.
Character states of semi-tectate exine which is other than reticulate.

0 – Psilate, perforated by fine punctae

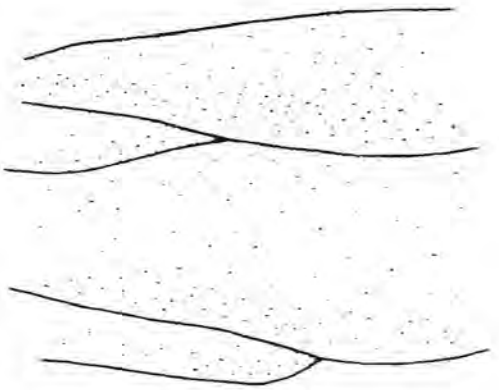

1 – Striate, perforated by punctae or foveolae

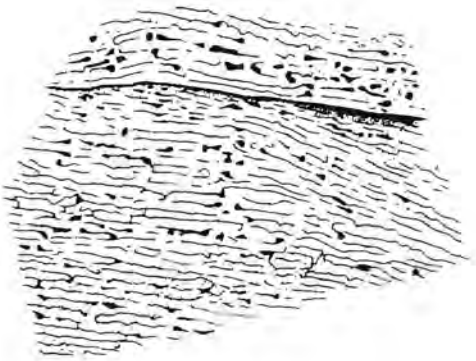

2 – Rugulate

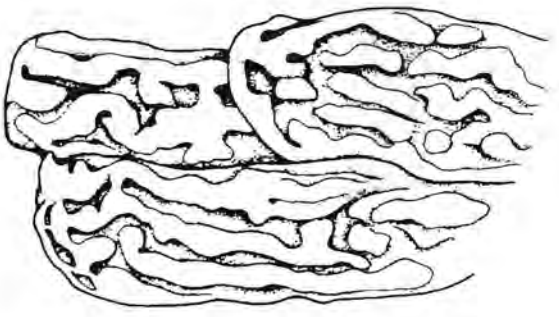

3 – Granulate

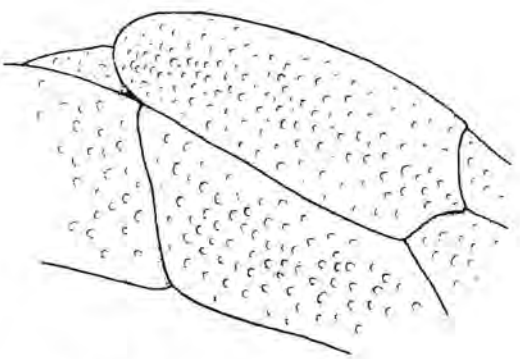

Figure 5.2.3.C.
Character states of secondarily tectate exine.

On the basis of combined observations of exine sculpturing (SEM) and exine structure (TEM), two basic structural categories were noted, and associated with these, three basic sculptural types. The Orchideae and Satyriinae possess a semi-tectate reticulate exine, and on this basis it is recognized as the ancestral state. The Disinae are also semi-tectate, but sculpturing is either rugose or verrucose, whilst the Coryciinae, excluding Disperis, have a complete tectum. These states are described in the character "basic exine sculpturing category" of which the first state is a semi-tectate reticulate exine. The character is non-additive as further polarization was not possible without a priori phylogenetic consideration.

The basic exine sculpturing types can be further subdivided. The types of reticulate sculpturing are illustrated in Fig. 5.2.3.A. The basic condition is a reticulum with evenly spaced muri and inter-mural spaces. In Disperis capensis and D. cardiophora, the reticulum seemed to have slight depressions instead of lumina. It is possible that pollenkitt or some other exine held substances filled the inter-mural spaces, and that this state may therefore be an artifact. In the third type of reticulum the muri appeared to be have broken down to a large extent, leaving free baculae as in Bonatea pulchella and Disperis thorncroftii. In ornate reticulate sculpturing the reticulum is open and the large lumina are often pilate or baculate. These inter-mural structures are interpreted as being

the homologues of columellae, or structural as opposed to sculptural elements. The last variation of the basically reticulate exine sculpturing type is termed hamulate, and is characterized by the possession of supra-tectal elaborations on the muri.

Semi-tectate, non-reticulate pollen may be either rugose or verrucose, and was noted in Disa, Monadenia and Herschelianthe. These two states are illustrtated in Fig. 5.2.3.B.

Variation in the sculpturing of secondarily tectate grains is illustrated in Fig. 5.2.3.C. Psilate surfaces are found in Anochilus, striate sculpturing is common to Corycium and Pterygodium, rugulate sculpturing is unique to Evota bicolor and a granulate surface, which unlike all other species of its genus, was found in Disperis circumflexa. This character was coded as non-additive as polarization was not possible. Due to the extreme variability in exine sculpturing and in an attempt to encompass all the observed detail into a character list, the following characters were added and refer to sculptural and structural details. These are: granulate or rugulate supra-tectal ornamentation; presence or absence of pilate or baculate structural sculpturing elements (columella homologues); foveolate and punctate perforations in either tectate or semi-tectate grains; presence of tetrad margins, in semi-tectate or tectate grain.

5.2.4 CLADOGRAMS BASED ON POLLEN DATA AND ASSESSMENT OF THE EFFECTS OF CHARACTER WEIGHTING

Results of species level analyses are presented in Figures 5.2.4 A, B, C and D. In the Disinae, the only group which is established by the consensus analysis is Disa section Micranthae (D. ukingensis, D. englerana, D. ochrostachya and D. ornithantha). In the Coryciinae, only Evota and Ceratandra persist as a separate group in the consensus tree. On this basis, one can conclude that pollen morphological characters do not provide evidence for resolving the phylogeny at the species level. Lack of resolution in the Coryciinae (excluding Disperis), reflects the relative homogeneity in pollen morphology in Corycium, Anochilus and Pterygodium. In contrast, it is the great diversity in pollen sculpturing in the Disinae which prevents resolution at the specific level.

Corycium dracomontanum and C. nigrescens are the only two species observed within the Coryciinae (excluding Disperis) which have highly elaborate exine sculpturing as is characteristic of many species of the Disinae. Corycium nigrescens and C. dracomontanum cause problems in the weighted tree, as the ancestral state at node 6 is the possession of a semi-tectate rugose or verrucose exine. Whether or not these two species have a semi-tectate exine structure is uncertain. TEM observations would be necessary to establish whether they have the columellate-tectate wall structure characteristic of

Table 5.2.4.A
Matrix of character states of pollen morphology data for species of the Disinae and outgroups.

Taxa	Characters													
	0	1	2	3	4	5	6	7	8	9	10	11	12	13
Monadenia physodes	0	0	1	?	0	?	?	0	0	?	?	1	0	0
Monadenia atrorubens	0	0	1	?	0	?	?	0	0	?	?	1	0	1
Monadenia sabulosa	0	0	1	?	1	?	?	1	0	?	?	1	1	1
Monadenia brevicornis	0	0	1	?	0	?	?	1	0	?	?	0	1	0
Monadenia densiflora	0	0	1	?	1	?	?	1	0	?	?	0	1	0
Brownleea galpinii ssp.major	0	0	0	0	?	?	0	0	0	?	?	0	0	0
Brownleea coerula	0	0	0	0	?	?	0	0	0	?	?	0	0	0
Schizodium bifidum	0	0	0	3	?	?	?	1	0	?	?	0	1	0
Schizodium inflexum	0	0	0	4	?	?	0	0	0	?	?	0	1	0
Disa welwitschii ssp.welwitschii	0	0	1	?	0	?	1	0	1	?	?	1	1	1
Disa ukingensis	0	0	1	?	0	?	?	0	1	?	?	0	2	0
Disa englerana	0	0	1	?	0	?	?	0	1	?	?	1	2	0
Disa ochrostachya	0	0	1	?	0	?	?	0	1	?	?	0	2	0
Disa ornithantha	0	0	1	?	0	?	?	1	1	?	?	0	2	0
Disa chrysostachya	0	0	1	?	1	?	0	1	0	?	?	1	1	1
Disa fragrans	0	0	1	?	1	?	0	1	0	?	?	0	1	0
Disa bivalvata	0	0	1	?	0	?	0	1	0	?	?	0	0	0
Disa atricapilla	0	0	1	?	0	?	1	0	0	?	?	1	1	0
Disa richardiana	0	0	1	?	0	?	0	0	0	?	?	0	1	0
Disa uniflora	0	0	1	?	0	?	0	0	0	?	?	1	0	0
Disa venosa	0	0	1	?	0	?	0	0	0	?	?	0	0	0
Disa filicornis	0	0	1	?	0	?	0	0	0	?	?	0	1	0
Disa maculata	0	0	1	?	1	?	?	0	0	?	?	1	1	1
Disa longicornu	0	0	1	?	1	?	?	0	0	?	?	1	1	1
Disa tenuis	0	0	0	2	?	?	?	1	0	?	?	0	0	0
Disa salteri	0	0	1	?	1	?	?	0	0	?	?	0	1	0
Disa saxicola	0	0	1	?	1	?	?	0	0	?	?	0	1	0
Disa gladioliflora ssp. gladiol.	0	0	1	?	0	?	?	0	0	?	?	0	1	0
Disa marlothii	0	0	0	4	?	?	0	0	0	?	?	0	1	0
Disa triloba	0	0	0	4	?	?	?	1	0	?	?	0	0	0
Disa patula	0	0	1	?	0	?	0	0	0	?	?	1	1	0
Disa stachyoides	0	0	1	?	0	?	0	0	0	?	?	1	1	0
Disa basutorum	0	0	1	?	1	?	0	1	0	?	?	0	0	0
Disa cooperi	0	0	1	?	0	?	?	1	0	?	?	0	0	0
Disa thodei	0	0	1	?	0	?	0	0	0	?	?	0	1	0
Disa crassicornis	0	0	1	?	0	?	1	0	0	?	?	0	0	0
Disa versicolor	0	0	1	?	0	?	?	0	0	?	?	1	0	1
Disa stairsii	0	0	1	?	1	?	?	0	0	?	?	0	0	1
Disa ovalifoliae	0	0	1	?	1	?	1	0	0	?	?	1	1	1
Disa tenuicornis	0	0	1	?	0	?	1	0	0	?	?	1	0	1
Disa obtusa ssp. picta	0	0	1	?	1	?	0	0	0	?	?	0	1	0
Disa aconotoides	0	0	1	?	1	?	0	0	0	?	?	0	1	0
Disa equestris	0	0	1	?	0	?	?	0	0	?	?	0	1	0
Disa aperta	0	0	1	?	0	?	?	0	0	?	?	1	1	0
Disa tysonii	0	0	1	?	0	?	?	0	0	?	?	0	1	0
Disa cornuta	0	0	1	?	0	?	0	0	0	?	?	0	1	0
Disa galpinii	0	0	0	3	?	?	?	1	0	?	?	0	0	1
Disa sanguinea	0	0	1	?	0	?	0	0	0	?	?	0	1	0

Table 5.2.4.A cont...

Taxa	Characters												
	0	1	2	3	4	5	6	7	8	9	10	11	12	13
Herschelianthe lugens	0	0	1	?	0	?	0	0	0	?	?	0	1	0
Herschelianthe forficaria	0	0	1	?	0	?	0	1	0	?	?	0	1	0
Herschelianthe chimanimaniensis	0	0	1	?	1	?	?	1	0	?	?	0	1	0
Herschelianthe baurii	0	0	1	?	1	?	?	1	1	?	?	0	1	1
Herschelianthe graminifolia	0	0	1	?	1	?	1	0	1	?	?	0	1	0
Herschelianthe hians	0	0	1	?	1	?	0	1	0	?	?	0	1	0
Herschelianthe praecox	0	0	1	?	1	?	0	0	1	?	?	0	0	0
Herschelianthe schlechterana	0	0	1	?	1	?	0	0	0	?	?	1	1	1
Disperis**	0	0	0	0	?	?	?	0	0	?	?	0	0	0
Coryciinae* **	2	1	2	?	?	1	?	0	0	1	1	0	?	?
Satyrium**	1	0	0	1	?	?	?	0	0	?	?	0	0	0
Habenaria**	0	0	0	3	?	?	?	1	0	?	?	0	0	0
Bonatea**	0	0	0	2	?	?	?	0	1	?	?	0	0	0
Huttonaea**	1	1	0	0	?	?	?	0	0	?	?	0	0	0

Coryciinae* represents a generic description based on a combination of Corycium and Pterygodium.
Taxon** represent outgroups used in combination.

Table 5.2.4.B
Matrix of character states for pollen morphology data of species of the Coryciinae excluding Disperis spp.

Taxa	Characters													
	0	1	2	3	4	5	6	7	8	9	10	11	12	13
Ceratandra atrata	2	1	2	?	?	2	0	0	0	0	1	2	?	?
Ceratandra grandiflora	2	1	2	?	?	2	1	0	0	0	1	2	?	?
Evota bicolor	2	1	2	?	?	2	1	0	0	0	0	2	?	?
Evota venosa	2	1	2	?	?	1	?	0	0	0	0	2	?	?
Anochilus hallii	2	1	2	?	?	0	?	0	0	0	1	0	?	?
Anochilus flanaganii	2	1	2	?	?	0	?	0	0	0	1	0	?	?
Anochilus inversus	2	1	2	?	?	0	?	0	0	0	1	0	?	?
Corycium bifidum	2	1	2	?	?	1	?	0	0	1	0	0	?	?
Corycium excisum	2	1	2	?	?	1	?	0	0	1	1	0	?	?
Corycium magnum	2	1	2	?	?	1	?	0	0	1	1	0	?	?
Corycium nigrescens	0	0	1	?	1	?	0	0	0	1	0	1	?	?
Corycium dracomontanum	0	0	1	?	1	?	?	1	0	0	1	0	?	?
Corycium orobanchoides	2	1	2	?	?	1	?	0	0	0	1	0	?	?
Pterygodium platypetalum	2	1	2	?	?	1	?	0	0	1	1	0	?	?
Pterygodium acutifolium	2	1	2	?	?	1	?	0	0	1	1	0	?	?
Pterygodium pantherianum	2	1	2	?	?	1	?	0	0	1	1	0	?	?
Pterygodium catholicum	2	1	2	?	?	1	?	0	0	1	1	0	?	?
Corycium deflexum	2	1	2	?	?	1	?	0	0	1	1	0	?	?
Huttonaea pulchra	1	1	0	0	?	?	?	0	0	?	?	0	0	0
Huttonaea grandiflora	1	1	0	0	?	?	?	0	0	?	?	0	0	0
Disperis**	0	0	0	0	?	?	?	0	0	?	?	0	0	0
Monadenia**	0	0	1	?	0	?	?	0	0	?	?	1	0	1
Brownleea**	0	0	0	0	?	?	?	0	0	?	?	0	0	0
Schizodium**	0	0	0	4	?	?	0	0	0	?	?	0	1	0
Micranthae**	0	0	1	?	0	?	?	0	1	?	?	0	2	0
Disa**	0	0	1	?	0	?	?	0	0	?	?	1	1	0
Herschelianthe**	0	0	1	?	1	?	?	0	1	?	?	0	1	0
Satyrium**	1	0	0	1	?	?	?	0	0	?	?	0	0	0
Habenaria**	0	0	0	3	?	?	?	1	0	?	?	0	0	0
Bonatea**	0	0	0	2	?	?	?	0	1	?	?	0	0	0

Taxon** are the outgroups used in combination.

Table 5.2.4.C
Matrix of character states for pollen morphology data for the subtribes of the Diseae and outgroups. Taxa are generic descriptions.

Taxa	Characters													
	0	1	2	3	4	5	6	7	8	9	10	11	12	14
Disperis	0	0	0	0	?	?	?	0	0	?	?	0	0	0
Coryciinae*	2	1	2	?	?	1	?	0	0	1	1	0	?	?
Monadenia	0	0	1	?	0	?	?	0	0	?	?	1	0	1
Brownleea	0	0	0	0	?	?	?	0	0	?	?	0	0	0
Schizodium	0	0	0	4	?	?	0	0	0	?	?	0	1	0
Micranthae	0	0	1	?	0	?	?	0	1	?	?	0	2	0
Disa	0	0	1	?	0	?	?	0	0	?	?	1	1	0
Herschelianthe	0	0	1	?	1	?	?	0	1	?	?	0	1	0
Satyrium**	1	0	0	1	?	?	?	0	0	?	?	0	0	0
Habenaria**	0	0	0	3	?	?	?	1	0	?	?	0	0	0
Bonatea**	0	0	0	2	?	?	?	0	1	?	?	0	0	0
Huttonaea	1	1	0	0	?	?	?	0	0	?	?	0	0	0

Coryciinae* represents a combination of the genera Corycium and Pterygodium.
Taxon** are the outgroups used in combination.

Figure 5.2.4.A.

Nelsen strict consensus tree, character consistency indices, and number of steps for pollen morphology data of species of the Disinae and outgroups. Characters defining nodes: 1) massulae rounded, 2) massulae elongated, 3) reticulate exine sculpturing with broken down muri and free baculae, 4) elongated tetrads, 5) baculate structural sculpturing elements, 6) Pilate structural sculpturing elements, 7) hamulate reticulum with supra-tectal elaborations on the muri, 8) finely rugulate supra-tectal ornamentation, 9) semi-tectate rugose or verrucose exine, 10) ornate exine sculpturing, 11) semi-tectate exine with distinct and slightly raised margins, punctate perforations in semi-tectate grains, granulate or finely rugulate supra-tectal ornamentation, 12) ?, 13) ?, 14) foveolate perforations in semi-tectate exine.

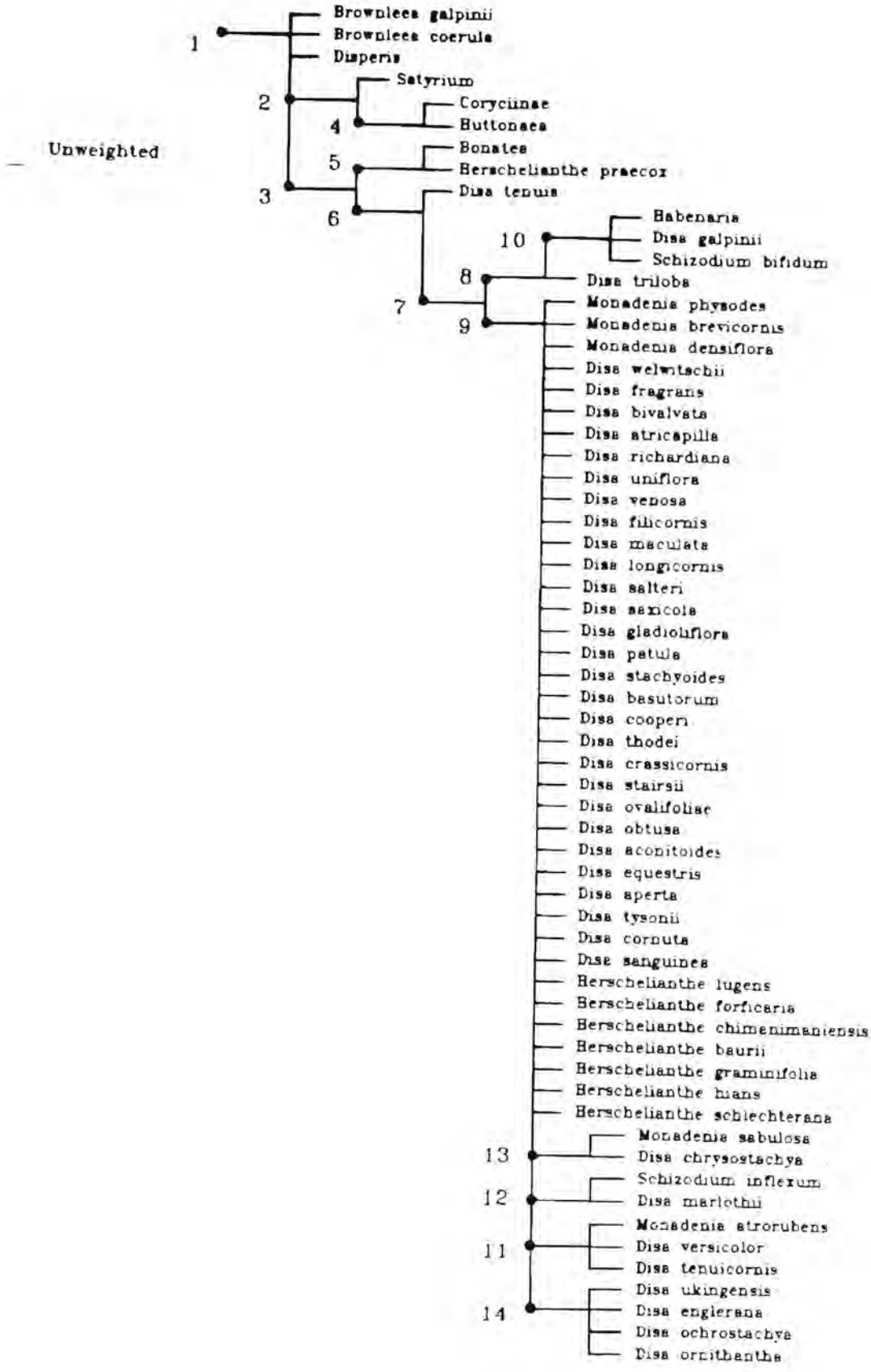

Character	0	1	2	3	4	5	6	7	8	9	10	11	12	13
number of steps	2	1	4	4	18	0	7	14	5	0	0	14	12	1
Unit character consistency index (%)	100	100	50	100	5	100	28	7	20	100	100	7	16	10 1

Figure 5.2.4.B.

Nelsen strict consensus tree, character consistency indices, and number of steps for pollen morphology data of species of the Disinae and outgroups. Characters weighted for equivalence. Characters defining nodes: 1) massulae rounded, 2) reticulate exine with broken down muri and free baculae, 3) massulae elongated, 4) pilate structural sculpturing elements, 5) tetrads elongated, 6) semi-tectate rugose or verrucose exine, 7) hamulate reticulate exine, with supra-tectal elaborations on the muri, 8) baculate structural sculpturing elements, 9) ?.

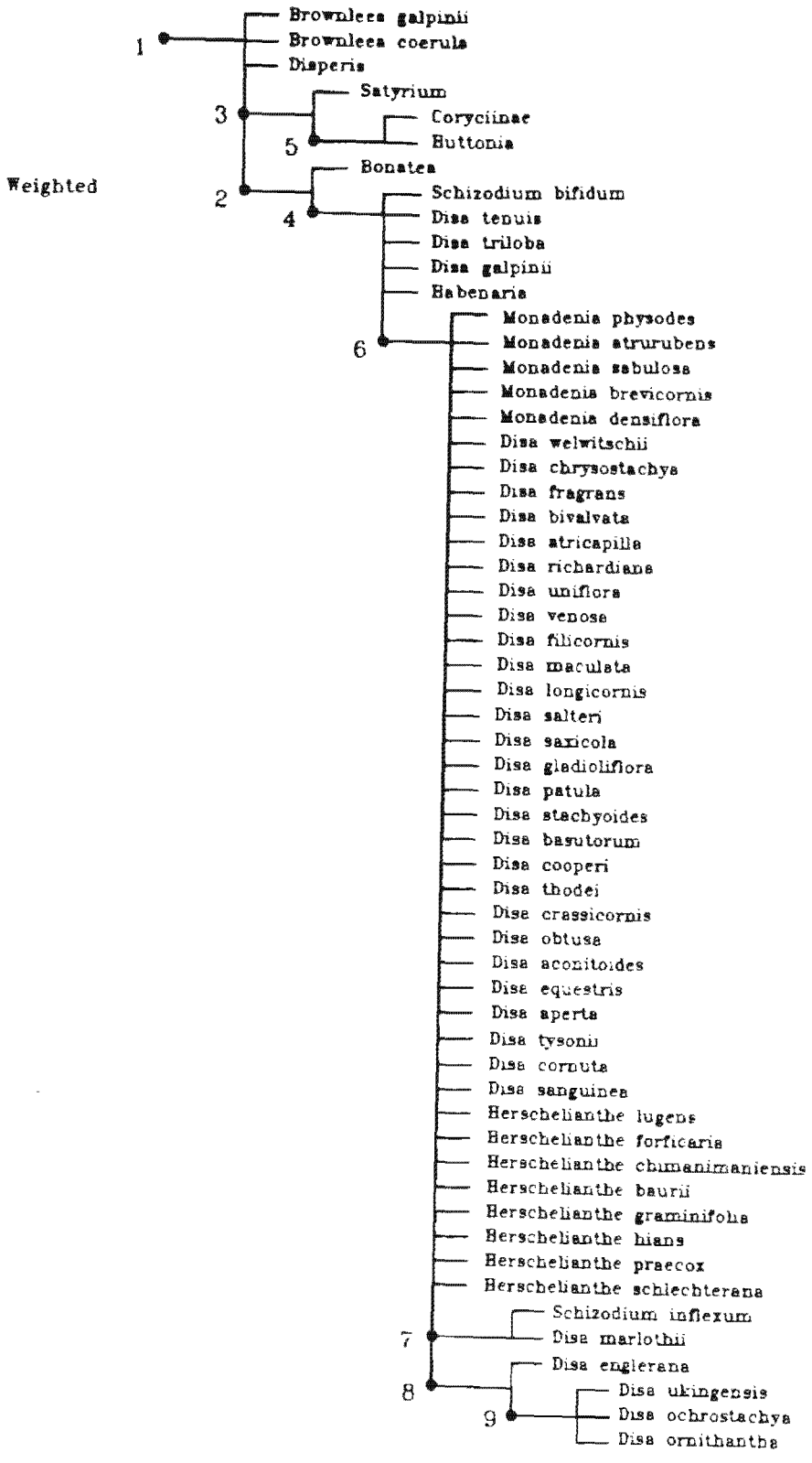

Character	0	1	2	3	4	5	6	7	8	9	10	11	12	13
Number of steps	2	1	3	6	19	0	6	15	6	0	0	17	15	13
Unit character consistency index (%)	100	100	66	66	5	100	16	6	16	100	100	5	13	7

Figure 5.2.4.C.

Nelsen strict consensus tree, character consistency indices, and number of steps for pollen morphology data for species of the Coryciinae (excluding Disperis) and outgroups. Characters defining nodes: 1) rounded massulae, 2) semi-tectate rugose or verrucose exine, baculate structural sculpturing elements, and foveolate perforations in semi-tectate pollen, 3) margins distinct and slightly raised in semi-tectate pollen, 4) fasciculate massulae, and elongated tetrads, 5) rugose exine sculpturing, 6) secondarily tectate exine (psilate, striate, rugulate, granulate), 7) rugulate secondarily tectate exine.

unweighted

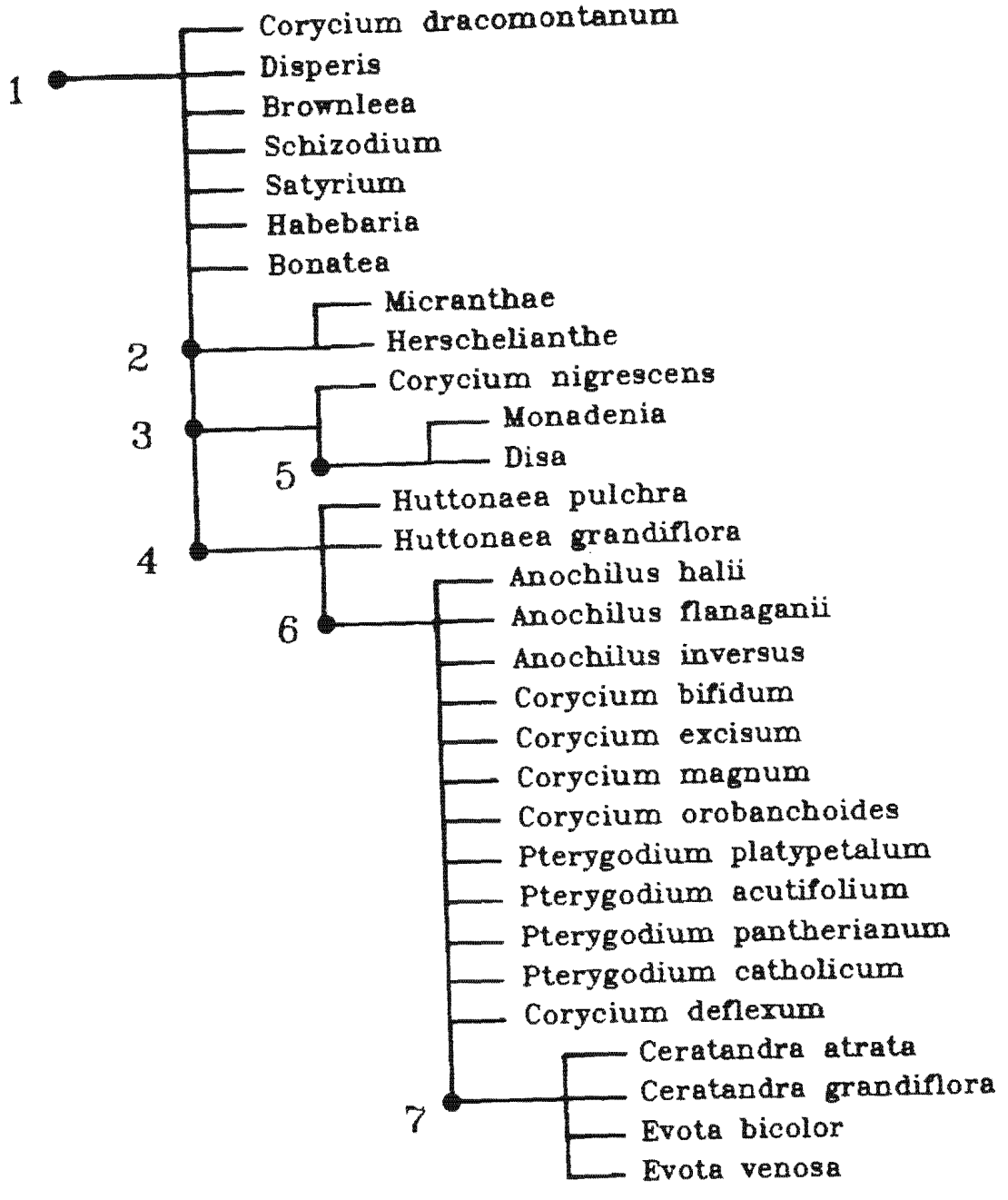

Character	0	1	2	3	4	5	6	7	8	9	10	11	12	13
Number of steps	3	1	4	4	2	5	2	2	2	6	4	2	4	1
Unit character consistency index (%)	66	100	50	100	50	40	50	50	50	16	25	100	50	100

Figure 5.2.4.D.

Nelsen strict consensus tree, character consistency indices, and number of steps for pollen morphology data for species of the Coryciinae (excluding Disperis) and outgroups. Characters weighted for equivalence. Characters defining nodes: 1) massulae elongated, 2) massulae rounded, 3) tetrads elongated, 4) foveolate perforations in semi-tectate exine, 5) massulae fasciculate, secondarily tectate exine (psilate, striate, rugulate, granulate), 6) semi-tectate rugose or verrucose exine, 7) secondarily tectate pollen with tetrad margins slightly raised, 8) baculate structural sculpturing elements (columella homologues), 9) ?, 10) rugulate exine in secondarily tectate pollen , 11) rugose exine in semi-tectate pollen, 12) fine, supra-tectal rugules.

weighted

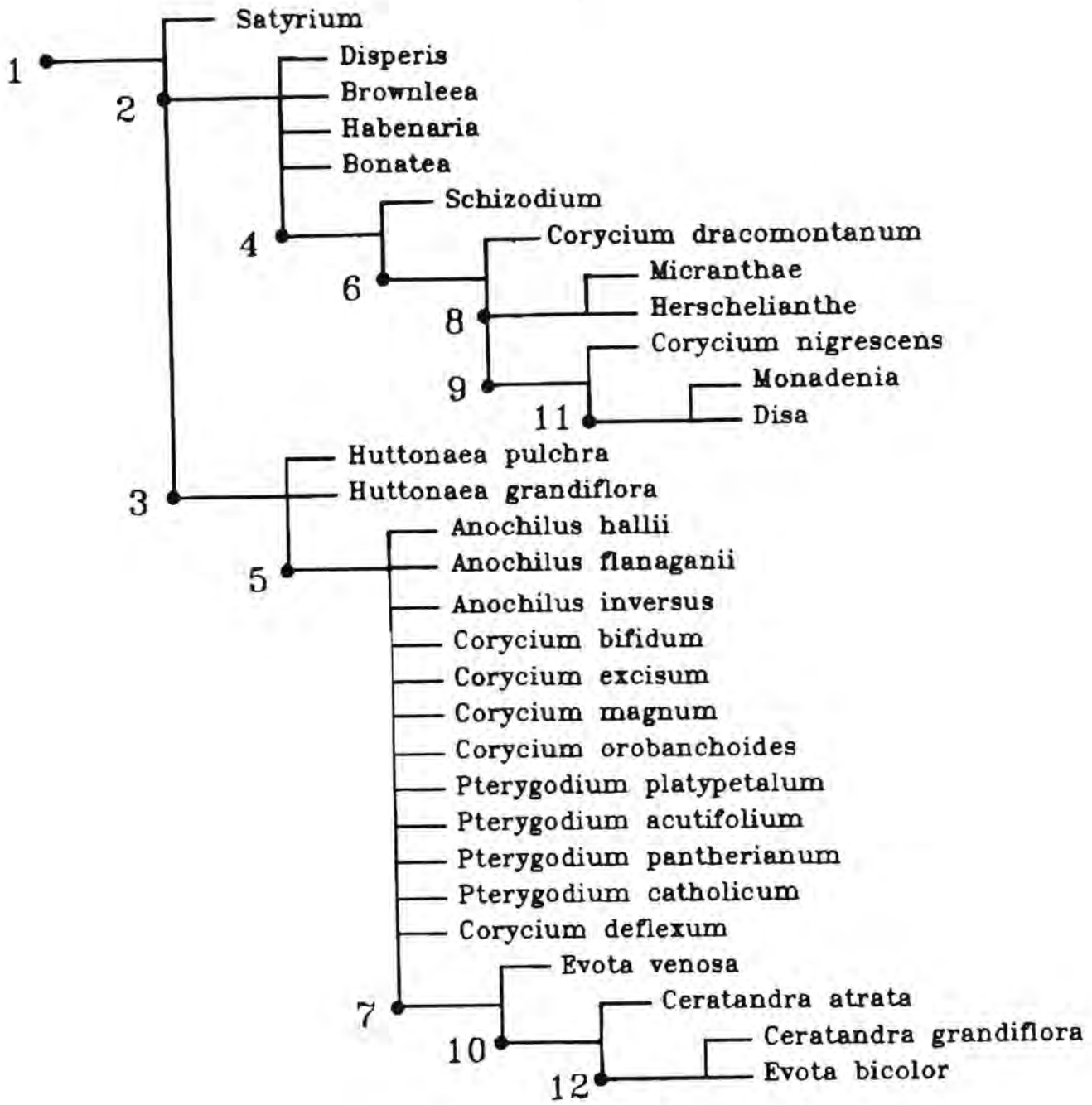

Character	0	1	2	3	4	5	6	7	8	9	10	11	12	13
Number of steps	2	1	2	4	2	4	1	2	2	6	4	2	3	1
unit character consistency index (%)	100	100	100	100	50	50	100	50	50	16	25	100	66	100

weighted and unweighted

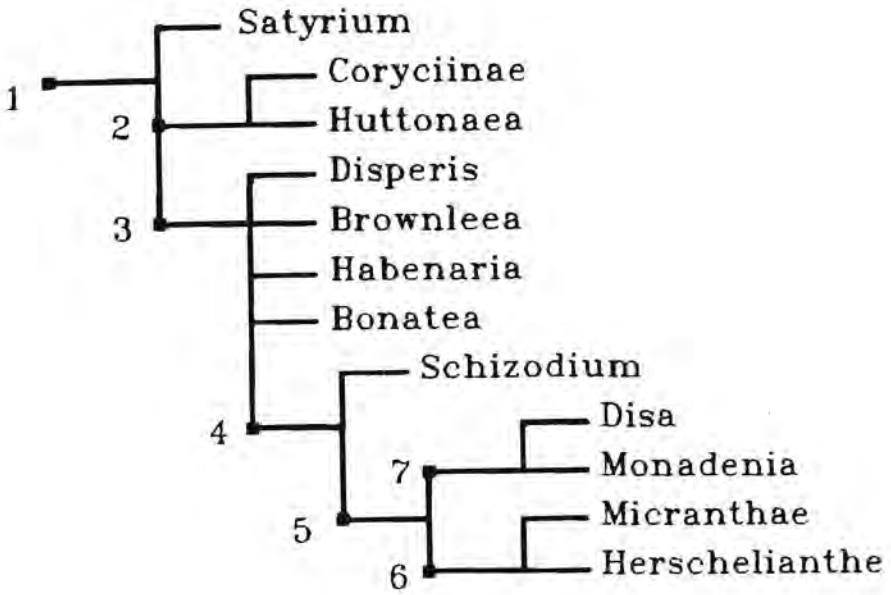

UNWEIGHTED

character	0	1	2	3	4	5	6	7	8	9	10	11	12	13
number of steps	2	1	2	4	1	0	0	1	2	0	0	1	3	1
Unit character consistency index (%)	100	100	100	100	100	100	100	100	50	100	100	100	66	100

WEIGHTED

Character	0	1	2	3	4	5	6	7	8	9	10	11	12	13
Number of steps	2	1	2	4	1	0	0	1	2	0	0	1	3	1
Unit character consistency index (%)	100	100	100	100	100	100	100	100	50	100	100	100	66	100

Figure 5.2.4.E.
Nelsen strict consensus tree, character consistency indices, and number of steps for pollen morphology data for the genera of the Diseae and outgroups. Weighted and unweighted characters yield the same cladogram. Characters defining nodes: 1) massulae elongated, 2) tetrads elongated, 3) massulae rounded, 4) foveolate perforations in semi-tectate pollen, and hamulate variation of reticulate sculpturing, 5) semi-tectate rugose or verrucose exine, 6) baculate structural sculpturing elements (columella homologues), tetrad margins distinct and slightly raised in semi-tectate grains.

Group and Number of taxa	Tree generating program	Tree diagnosis	Unweighted	Weighted
Species of the Disinae and outgroups 62 Taxa	m hennig* bb* Nelsen strict consensus tree	Effective number of characters	14	29
		Number of trees generated	1020	1014
		Tree length	91	201
		Consistency index (%)	19	23
Species of the Coryciinae and outgroups 30 Taxa	m hennig* bb* Nelsen strict consensus tree	Effective number of characters	14	29
		Number of trees generated	1904	105
		Tree length	42	82
		Consistency index (%)	52	73
Genera of the Diseae and outgroups 12 Taxa	m hennig* ie* Nelsen strict consensus tree	Effective number of characters	14	29
		Number of trees generated	7	7
		Tree length	18	50
		Consistency index (%)	88	92

Table 5.2.4.D

Effects of character weighting on the number of trees generated, tree length, and overall consistency indices.

the subtribe Coryciinae, and whether this convergence is also structural.

At the subtribal level however, a fair amount of resolution was obtained, and both weighted and unweighted characters yielded the same consensus tree (Fig. 5.2.4. E), although the tree was not fully resolved, and the taxa resolved on this basis do not coincide exactly with those in the present postulated phylogeny.

The weighting of characters for equivalence has several effects which are summarized in Table 5.2.4.D. Firstly, it results in a less parsimonious tree, with an increased number of steps for each character. Since tree length reflects the number of character changes in a tree, this increase, with weighting, indicates an increased number of evolutionary events or character transformations from one state to another, and is the effect of increasing the effective number of characters used, through weighting.

Weighting also affects the number of trees generated. This is particularly apparent in the analysis of the Coryciinae, where the number of trees is significantly reduced in the weighted data set (from 1904 to 105 trees). In addition, weighting for equivalence resulted in an increase in the overall character consistency index. In the species-level analyses of the Disinae

and Coryciinae, this increase was from 19% to 23%, and 52% to 73% respectively. In the generic analysis, the overall character consistency index increased from 88% to 92%, with a corresponding increase in tree length from 18 to 50.

The Coryciinae showed a fairly considerable increase in overall character consistency with weighting. This increase is related to reduced ratio of outgroup taxa to ingroup taxa, as resolution was not increased for species of the Coryciinae as such. In the Disinae, this effect is greatly reduced and can be attributed to the large number of taxa used i.e. the ratio of characters to taxa was still fairly low, thereby producing more than a thousand equally parsimonious trees for unweighted and weighted data sets. At the subtribal level, the consensus tree has very high consistency indices in spite of being not fully resolved into branching dichotomies. This also relates to the ratio of characters to taxa used in the analysis and relates to the limited number of possibilities in terms of characters and taxa used. The fact that the tree is not fully resolved and yet has a high consistency index can also be expected since mostly non-additive characters were used for the analysis, and since evolutionary information is lost, potential resolution is diminished.

Weighting for equivalence, rather than improving resolution of taxa has shed some light on the interrelationship between the

number of characters and number of trees generated; the more characters the less number of possible trees, increased tree length and the fit of characters to the tree i.e. higher consistency indices. Also, character weighting had little effect on the tree generated for the subtribal level classification. This is due to the fact that relationships are stronger, since the tree was founded on characters that do give resolution at that level of the hierarchy.

5.2.5 SYSTEMATIC IMPLICATIONS OF POLLEN DATA AND POSTULATED EVOLUTION OF POLLEN WALLS

Cladistic analyses indicate that pollen wall morphology does not resolve taxa at the species level. In the Disinae, variability is too great and in the Coryciinae (excluding Disperis) pollen is too uniform for taxonomic resolution. Pollen characters did, however, provide some apomorphies at the subtribal level. Pollen character distribution in relation to the present phylogeny is summarized in Fig. 5.2.5.A. Pollen data provide a suite of synapomorphies for the Coryciinae i.e. fasciculate massulae, elongated tetrads (linear tetrad configuration) and a secondarily tectate exine.

The elongated tetrads of Huttonaea provide some evidence of closer affinities with the Coryciinae, although the reticulate sculpturing characteristic of this genus is plesiomorphic with respect to the study group.

The shared possession of a reticulate exine in Disperis and Brownleea could provide evidence for a closer relationship between these two genera which are presently classified in different subtribes.

Pollen morphology in the Disinae is commonly either rugose or verrucose, and does not distinguish the genera Monadenia, Herschelianthe and Disa. This may partly be due to the extreme

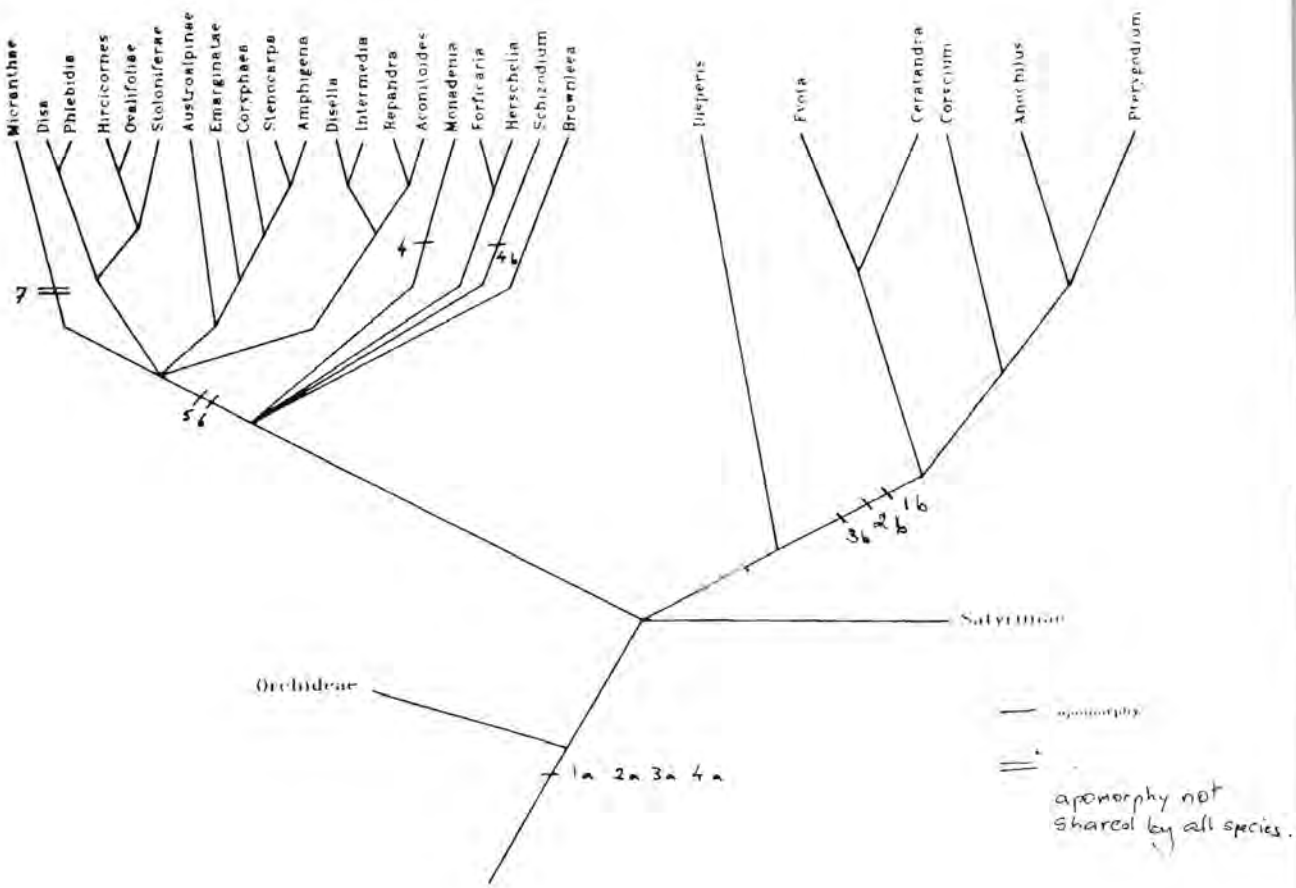

Figure 5.2.5.A

Pollen character distribution in relation to the phylogeny of the Diseae. Characters are: 1a. massulae rounded; 1b. massulae fasciculate; 1c. massulae elongated; 2a. tetrads isodiametric; 2b. tetrads elongated; 3a. semi-tectate exine; 3b. secondarily tectate exine; 4a. reticulate sculpturing; 4b. hamulate sculpturing; 5. rugose sculpturing; 6. verrucose sculpturing; 7. intectate exine structure.

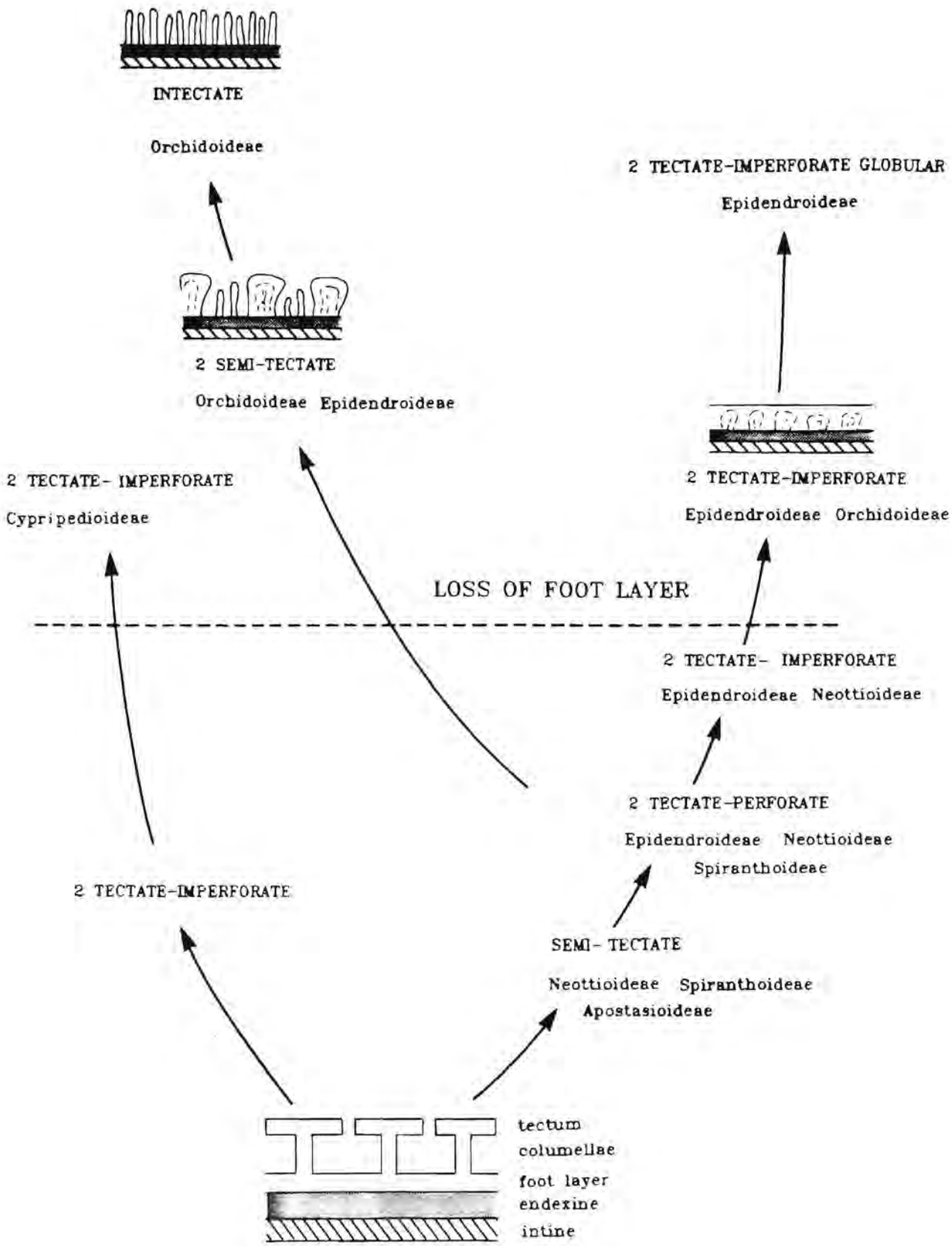

Figure 5.2.5.B
Postulated evolution of orchid exine development. (modified from Burns-Balogh, 1983).

variation in supra-tectal elaborations and tectal perforations in these two exine sculpturing types. However, Brownleea differs by being reticulate and Schizodium by being hamulate. Sculpturing in Disa spp. may, in some cases, be hamulate (e.g. Disa triloba) or ornate (e.g. Disa galpinii). Such plesiomorphic exines can be interpreted as reversals. Disa section Micranthae form the only corroborated group; their rugose exines with free baculae and pilae often approaching the intectate state. Pollen data may therefore support the separation of section Micranthae from Disa as a group on its own.

Burns-Balogh (1983) has postulated a "possible evolutionary theory" on orchid exine development adapted from the work of Walker (1976) on the pollen of primitive dicotyledonous angiosperms. The basis of her inference was reached through a cladistic study of column and pollen characters (Burns-Balogh and Funk, 1986), and placing each exine type according to phylogenetic position. It is her opinion that in the majority of the Orchidaceae, the structure of the pollen wall is secondarily derived, and for this reason she regards evolutionary models of dicot or even monocot pollen inapplicable to that of orchids.

In an attempt to synthesize what is already known about orchid pollen ultrastructure into a possible evolutionary theory, she

recognizes three evolutionary lines, all derived from a possibly tectate perforate ancestral type. These trends are summarized in Fig. 5.2.5.B

These lines culminate in a tectate-imperforate exine with incipient columellae (Cypripedioideae), an intectate exine lacking a foot layer (Orchidoideae), and a tectate-imperforate exine with globular masses of sporopollenin (Vandoid Epidendroideae).

She postulated that the most modified and unique type of monocot exine in the orchids was found in the Cypripedioideae, higher Epidendroideae and Orchidoideae. She also postulates a trend towards a loss of the exinous basal (foot) layer. This loss is confirmed by observations in this study. She attributes the loss of the foot layer and columellae to the specialized life habits of orchids, without testing or specifying further the adaptational inferences made. She states: "the specialized life habits and habitats in which orchids live have resulted in the loss of the foot layer, the loss of a well defined columellate structure and the secondarily derived exine types of the higher orchids". She qualifies these statements by adding that the most primitive exine types are found in the primarily terrestrial orchid groups, while the more advanced exines are found in the primarily epiphytic orchids, stating that the latter have a reduced or absent foot layer. This appears to be

a contradiction as the Orchidoideae are primarily terrestrial, have a reduced or missing foot layer and represent the culmination of one of her "evolutionary lines".

According to Burns-Balogh (1983), the line which gave rise to the secondarily semi-tectate condition of the Orchidoideae and primitive Epidendroideae had a semi-tectate structure composed of only the tectum and endexine, rarely with baculae. This postulate is not confirmed by TEM observations in this study, where semi-tectate exines are composed of columellae (or homologous baculae) supporting a tectum layer. She further suggests that the secondarily semi-tectate condition then gave rise to the intectate condition of the Orchidoideae, including an SEM micrograph of a Disa sp. to illustrate this point. Results of this study indicate that the exine of Disa is in most cases semi-tectate; intectate forms having been observed only in some species of section Micranthae, where the rugose-foveolate structure appears to have given rise to an intectate condition with free baculate columella homologues. Schill and Pfeiffer (1977) also report that intectate forms occur almost exclusively in the Orchidoideae. In Bonatea pulchella the reticulate exine has reduced muri and the structure approaches the intectate state. In general, intectate exines are the exception and not the rule in the study group.

With regard to the evolution of the exine in the study group two lines are evident, one being semi-tectate with rugose or verrucose exines, rarely becoming intectate as observed in some species of Disa section Micranthae. The other line is the secondarily tectate exine of the Coryciinae (excluding Disperis), which in combination with tetrad configuration, tetrad shape, and massulum shape represent a suite of synapomorphies for the group.

5.2.8 FUNCTIONAL INTERPRETATION OF POLLEN FORM.

The striking differences in pollen form in the Disinae and Coryciinae raise several questions. With the exception of the genus Disperis, the Coryciinae are characterised, palynologically, by the possession of a secondarily tectate exine, elongated tetrads, and fasciculate massulae. One may raise questions regarding the adaptive significance of this combination of apomorphic character states. In contrast, the Disinae have retained the plesiomorphic semi-tectate exine, but this speciose group manifests extreme variation and elaboration of mostly rugose or verrucose exine sculpture.

In cladistic terms, adaptation can be regarded as apomorphic function, promoted by natural selection (Coddington, 1988). In this context, it may be important to relate the extreme variation of sculpturing in the Disinae, and the fairly uniform sculpture of the Coryciinae, to functional aspects in the determination the form of pollen. Nevertheless, several factors need be considered in addition to invoking adaptational hypotheses and selective forces in determining pollen form. The topics of functional morphology and adaptation are amongst the more controversial issues in modern evolutionary biology.

Gould and Lewontin (1979) have criticised what they have termed the "adaptationist programme" which views the force of natural

selection as an optimizing agent, with non-optimality resulting from trade-offs amongst competing demands only, therefore also mediated by natural selection. They claim that adaptive explanations have overriden other potential influences on form, and criticise the trend amongst evolutionary biologists to focus exclusively on immediate adaptation to local conditions, through the atomization of organisms into traits which are tested on a one-to-one basis in relation to the environment. They stress that "organisms must be analysed as integrated wholes, with Bauplane so constained by phyletic heritage, pathways of development and general architecture that the constaints themselves become more interesting and important in delimiting pathways of change than the selective force that may mediate change when it occurs."

The lack of testability, use of loose analogies, and ad hoc rationalizations when theoretical predictions of adaptive analyses are not fulfilled, are major criticisms of adaptational explanations put foward by Fisher (1985) and Crane (1986). Fisher (1985) defines adaptation in terms of its contribution to the organism's current fitness, by enhancing the reproductive potential of an organism bearing a particular adaptive feature, rather than resulting from the effects of natural selection. Crane (1986) points out that, so defined, adaptation becomes intimately dependent on the ecological and evolutionary context in which it is viewed. This he emphasises to point out the

potential shortcomings inherent in simplistic "explanations" of pollen morphological features. Crane (1986) stresses that grains are not optimally designed for a specific function, but are merely structures that work with varying efficiency in a specific ecological and evolutionary context. He identifies a need to integrate knowledge of floral biology, phylogeny and ecology in attempting to disentangle the relationship between pollen form and function.

Several functional factors have been evoked as influencing pollen form, and exine sculpturing in particular. Genetic factors, however, impose a phylogenetic constraint which is embodied in the ontogenetic process. This historic component undoubtedly encompasses many aspects which relate to pollen function, and is probably the overriding factor determining pollen form. As Punt (1986) points out, the response of a pollen grain to functional factors is limited by the original gene pool present. Blackmore (1981) views the interplay of three main functional aspects of the exine, and possibly others, as reflected in the form of pollen. These are harmomegathy, pollination biology and the role of the exine as a repository for physiologically active substances. The columellar interstices of the chambered exine function in the storage and release of sporophytically and gametophytically derived substances (Helsop-Harrison, 1976) which become physiologically active in pollen-stigma interactions. Exine held substances

include the superficial pollenkitt and pigmented (carotenoid) lipid fraction which seal the pollen during dehydration. In addition, wall-held proteins which are released during early period of attachment to the stigma, are recognition substances which play a part in compatability mechanisms. Since there is no way to assess these complex biochemical factors in the present study, I shall not discuss them any further. Bolick (1978, 1981) evokes factors such as mechanical efficiency combined with economy of materials as having a role in determining pollen wall morphology.

Pollination biology is regarded as a potential selective factor in questions relating to the adaptive significance of the exine. Grayum (1986) views pollinator type as a potent selective factor in the evolution of exine sculpture in the Araceae. Ferguson and Skvarla (1982) found very significant correlations between pollen mode and exine sculpturing in papillionoid legumes, to the extent that distantly related genera with the same pollination syndrome exhibited strikingly similar exine patterns. Correlations have been noted between anemophyly and psilate exines, entomophyly and sculptured exines (Fisher, 1890, Chaloner, 1976). However, there is a paucity of data on pollination, and according (Grayum, 1986) this generalization might apply in the case of temperate zones, it needs to be reconsidered for tropical species .

In the study group, as in all Orchidoideae, adhesion of pollen to pollinating agent is through the sticky viscidium. A direct relation between surface ornamentation and pollinator would therefore not be expected. There is, however, a fundamental difference between the Disinae and Coryciinae (excluding Disperis) in their pollination biology. Species of the genus Disa are pollinated mostly by flies (Vogel, 1959), or butterflies as in the case of D. uniflora (Marloth, 1915). Certain species of Disa, in the Drakensberg region, are bee pollinated (K. Steiner pers. comm.). The Coryciinae, in contrast, with the exception of Disperis, are all bee pollinated. Flies and moths have been noted to pollinate Satyrium and Habenaria respectively (Vogel, 1959).
On the basis of these observations one could speculate that the presence of a secondarily tectate exine may confer additional strength to pollen of the Coryciinae, and that a requirement of additional mechanical protection may be associated with mel itophylous pollination.

Another factor which is recognized as influencing pollen form is the requirement for harmomegathic mechanisms which accomodate volume changes in the cytoplasm, in response to hydration status of the pollen. The term harmomegathy was introduced by Wodehouse (1935) and is probably one of the most studied functional aspects of pollen. Harmomegathic mechanisms are considered as essential for the extended survival of pollen in

air (Barnes and Blackmore, 1986). These mechanisms involve the reaction of the complete pollen wall to turgor pressure in the cytoplasm. The resulting changes in size and shape reflect localized variations in the ability of the pollen wall to yield or to resist changing pressure. Payne (1981) regards volume change one of the main determinants of pollen form. This requirement is related to aperture characteristics (in aperturate pollen), internal structural features of the exine (Grayum, 1986) and to some extent exine sculpturing (Payne, 1981).

In considering the differences between the pollen of the Disinae and the Coryciinae in the light of harmomegathic mechanisms, the question of harmomegathy must be framed differently. Rather than considering individual microspores, the massulum should be considered as the basic "harmomegathic unit". Consequently, the entire massulum would expand and contract in relation to hydration status. If one relates features of the exine and tetrad shape to the structure of the massulum, one might expect that the two subtribes differ considerably in their harmomegathic response. In the Disinae, which have fairly rounded massulae, isodiametric tetrads, and are semi-tectate, I would expect an expansion of the massulum in all directions, in response to hydration. In contrast, the Coryciinae, which have fasciculate massulae, elongated tetrads and a tectate exine, might expand longitudinally upon hydration. Low Temperature SEM

(Barnes and Blackmore, 1986) would be required to observe harmomegathic responses of massulae, although a preliminary assessment might be obtainable using a light microscopy. This postulated difference in harmomegathic response could then be related to the tectate nature of the exine in the bee pollinated Coryciinae. On this basis a pollinator mediated set of interactions could be evoked in partly explaining the observed differences in pollen form between the Disinae and Coryciinae.

In terms of harmomegathy, ecological context may also be a factor to which pollen form is related. Barnes and Blackmore (1986) point out that just as whole plants differ in their tolerance of water stress, there may also be xeromorphic or mesomorphic pollen grains. They do point out, however, that there is little evidence of a correlation between harmomegathic mechanisms and the natural environment of plants.

Questions regarding the extreme variability in the taxically diverse Disinae are more difficult to attempt to answer. There is insufficient information regarding pollination biology, and whether the diversity in exine sculpturing in this group is related to pollinators is not known. The observed diversity may be related to compatibility systems, but this also cannot be ascertained. Van Campo (1976) points out that intraspecific pollen polymorphism occurs in addition to the variability

encountered at all taxonomic levels. She adds that " the amplitude of pollen variation within a homogeneous assemblage prefigures, in some cases, the possible pollen types within an assemblage higher in the classification."

On the basis of ontogenic studies of pollen and spores, Blackmore and Crane (1988) conclude that "pollen ontogeny is not a highly structured and contingent process in which the modification of one structure into another can very frequently be observed. It is instead continuous and itself controlled by the duration and rate of predominantly intracellular processes operating at the level of organelles and molecules."

For the above reasons and the interplay of factors determining pollen form, and exine sculpturing in particular, it is not surprising that the sculpturing in the Disinae may not provide characters for taxonomic resolution at the species level.

6.0 CONCLUSION

Leaf anatomy data has little systematic value in the Diseae.

Morphometric characters, when used exclusively, produced a chaining branching effect in the cladograms generated, and are thought to contain little phylogenetic information.

Sclerification associated with vascular bundles is the only useful source of phylogenetic information in the leaf anatomy data set. It represents a synapomorphy for Disa section Stenocarpa, and supports the inclusion of Herschelianthe in this section. The presence of fibre caps at the poles of vascular bundles of Ceratandra serve to distinguish this genus from Evota.

The Disinae show a high degree of heterobathmy, or differential character evolution, which may reflect the phylogenetic history of this speciose group. In contrast, in the Coryciinae, Pterygodium, Anochilus and Corycium are virtually indistinguishable on the basis of leaf anatomy. Data from this source does not support the removal of Anochilus from Pterygodium.

Phenetic analyses did not force the grouping of similar leaves, and the hypothesis that environmentally rather than

phylogenetically determined "adaptive syndromes" were present, was refuted. Most characters were found to be independent of each other, and where they were correlated, they were mostly found to reflect the same feature, and should have been coded as a single character.

The large amount of taxa, use of "bad" characters, and problems relating to the polarization of character states contributed to the lack of resolution of cladograms based on leaf anatomy data.

Cohesion of compound pollen in the Disinae and Coryciinae is achieved through simple cohesion of the tectum, and crosswall cohesion through intine wall bridges.

Stratification of the exine in the Diseae is uniform, with the pollen wall composed of the sculptured exine and the endexine overlying the intine. The foot layer is absent.

The structure of the exine varies, with semi-tectate forms in Orchideae, Satyriinae, Disinae and Disperis. The Coryciinae (excluding Disperis) have a secondarily tectate exine structure. Some intectate forms occur in Disa section Micranthae and in the Orchideae.

Cladistic analyses indicate that pollen wall morphology data does not resolve taxa at the species level. The Disinae are too diverse, with only species of Disa section Micranthae remaining grouped, and the Coryciinae (excluding Disperis) are too

homogeneous for taxonomic resolution based on pollen characters.

Weighting characters for equivalence, rather than improving resolution of taxa, highlighted the relationship between the numbers of characters and taxa used in analyses using HENNIG 86. Weighting resulted in longer and fewer equally parsimonious trees with higher consistency indices.

Pollen data does provide evidence for the inclusion of Huttonaea in the Coryciinae. Elongated tetrads are found only in these two groups.

Two evolutionary lines are recognized for the exine of the Diseae. The plesiomorphic semi-tectate reticulate exine is thought to have given rise to 1) a semi-tectate rugose or verrucose exine, rarely becoming intectate (Disinae), and 2) to the secondarily tectate exine of Coryciinae (excluding Disperis), for which the linear tetrad configuration, elongated tetrad shape and fasciculate massulae provide a suite of synapomorphies.

Structural-functional interpretations of compound pollen differ from those applicable to single grains. The massulum is interpreted as a single "harmomegathic unit". The Coryciinae are thought to differ from the rest of the study group in their harmomegathic responses.

Adams, E.N. (1972). Consensus techniques and the comparison of taxonomic trees. Systematic Zoology 21: 390-399.

Ackerman, J.D. and Williams, N.H. (1980). Pollen morphology of the tribe Neottieae and its impact on the classification of the Orchidaceae. Grana 19: 7-18.

Archie, J.W. (1985). Methods for coding variable morphological features for numerical taxonomic analysis. Systematic Zoology 34(3): 326-345.

Ayensu, E.S. and Williams, N.H. (1972). Leaf Anatomy of Palumbina and Odontoglossum Subgenus Osmoglossum. American Orchid Society Bulletin. August 1972.

Bentham, G. and Hooker, J.D. (1883). Genera Plantarum. Vol. 3. London.

Blackmore, S. (1981). A Functional Interpretation of Lactuceae (Compositae) Pollen. Plant Systematics and Evolution 141: 153-168.

Blackmore, S. and Barnes, S.H. (1986). Harmomegathic mechanisms in pollen grains. In S. Blackmore and I.K. Ferguson (eds.). Pollen and Spores: Form and Function. Linnean Society Symposium Series 12. Academic Press, London. pp. 137-150.

Blackmore, S. and Crane P.R. (1988). The systematic implications of pollen and spore ontogeny. In: C.J. Humphries (ed.). Ontogeny and Systematics. British Museum London; Columbia University Press, U.S.A. pp. 83-116

Bock, W. J. (1974). Philosophical foundations of classical evolutionary classification. Systematic Zoology 22: 375-392.

Bolick, M.R. (1978). Taxonomic, evolutionary and functional considerations of Compositae pollen ultrastructure and systematics. Plant Systematics and Evolution 130: 209-218.

Bolick, M.R. (1981). Mechanics as an aid to interpreting pollen structure and function. Review of Palaeobotany and Palynology 35: 61-79.

Brooks, D.R. , O'Grady, R.T. and E.O. Wiley (1986). A measure of the information content of phylogenetic trees, and its use as an optimality criterion. Systematic Zoology 35: 571-581.

Burns-Balogh, P. (1983). A theory on the evolution of the exine in the Orchidaceae. American Journal of Botany 70(9): 1304-1302.

Burns-Balogh, P. and Funk, V.A. (1986). A phylogenetic analysis of the Orchidaceae. Smithsonian Contributions to Botany 61, Smithsonian Institution Press, Washington.

Camus, E.G. (1908). Monographie des Orchidees de l' Europe, de l'Afrique septentrionale, de l'Asie Mineure et des Provinces Russe transcapiennes. Paris.

Cantino, P.D. (1982). Affinities of the Lamiales: A Cladistic Analysis. Systematic Botany 7(3): 237-248.

Carpenter, J.M. (1988). Choosing Among Multiple Equally Parsimonious Cladograms. Cladistics 4(3): 291-296.

Chaloner, W.G. (1976). The evolution of adaptive features in fossil exines. In I.K. Ferguson and J. Muller (eds.). The Evolutionary Significance of the Exine. Linnean Society Symposium Series 1. Academic Press, London. pp. 1-14.

Chardard, R. (1969). Aspects infrastructuraux de la maturation des grains de pollen de quelques Orchidacees. Revue de Cytologie et Biologie Vegetale 32: 67-100.

Clifford, H.T. and Lavarack, P.S. (1974). The role of vegetative and reproductive attributes in the classification of the Orchidaceae. Botanical Journal of the Linnean Society 6: 97-110.

Coddington, J.A. (1988). Cladistic tests of adaptational hypotheses. Cladistics 4: 3-22

Crane, P.R. (1986). Form and function in wind dispersed pollen. In: S. Blackmore and I.K. Ferguson (eds.). Pollen and Spores: Form and Function. Linnean Society Symposium Series 12. Academic Press, London. pp. 179-202.

Cutler, D.F. (1978). Applied Plant Anatomy. Longman, London and New York.

Darwin, C.H. (1862). On the various contrivances by which British and foreign orchids are fertilized by insects. John Murray, London.

Dallwitz, M.J. and Paine, T.A. (1986). User's guide to the DELTA system - a general system for processing taxonomic descriptions. Third Edition CSIRO. Australian Division of Entomology Report 13.

Donoghue, M.J. and Cantino, P.D. (1984). The Logic and Limitations of the Outgroup Substitution Approach to Cladistic Analysis. Systematic Botany 9(2): 192-202.

Dressler, R.L. (1981). The Orchids. Nataral History and Classification. Harvard University Press, London.

Eldredge, N. and Cracraft, J. (1980). Phylogenetic Patterns and the Evolutionary Process. Columbia University Press, New York.

Farris, J.S. (1972). The hypothesis of non-specificity and taxonomic congruence. Annual Review of Ecology and Systematics 2: 277-302.

Farris, J.S. (1969). A successive approximations approach to character weighting. Systematic Zoology 18: 374-385.

Farris, J.S. (1988). Hennig 86 Version 1.5.

Ferguson, I.K. and Skvarla, J.J. (1982). Pollen morphology in relation to pollinators in Papilionoideae (Leguminosae). Botanical Journal of the Linnean Society 84: 183-193

Fischer, H. (1890). Beitrage zur vergleichenden Morphologie der Pollenkorner. Thesis, Breslau.

Fisher, D.C. (1985). Evolutionary morphology: beyond the analogous, the anecdotal, and the ad hoc. Paleobiology 11: 120-138.

Gaffney, E.S. (1979). An introduction to the logic of phylogeny reconstruction. In: J. Cracraft and N. Eldredge (eds.). Phylogenetic Analysis and Paleontology. Columbia University Press, New York. pp. 79-111.

Glauert, A.M. (1975). Fixation, Dehydration and Embedding of Biological Specimens. North- Holland Publishing Company, Amsterdam.

Goldman, N. (1988). Methods for discrete coding of morphological characters for numerical analysis. Cladistics 4: 59-71.

Gould, S.J. and Lewontin, R. (1979). The spandrels of San Marco and the Panglossan paradigm: a critique of the adaptationist programme. Proceedings of the Royal Society (London) B 205: 581-598.

Gould, S.J. and Vrba, E.S. (1982). Exaptation- a missing term in the science of form. Paleobiology 8: 4-15.

Grayum, M.H. (1986). Correlations between pollination biology and pollen morphology in the Araceae, with some implications for angiosperm evolution. In: S. Blackmore and I.K. Ferguson (eds.). Pollen and Spores. Form and Function. Linnean Society Symposium Series 12. Academic Press, London. pp. 313-328.

Hayat, M.A. (1981). Principles and Techniques of Electron Microscopy. Biological Applications. Edward Arnold, London.

Hall, A.V. (1982). A revision of the southern African Species of Satyrium. Contributions to the Bolus Herbarium 10: 1-137.

Hecht, M.K. (1976). Phylogenetic inference and methodology applied to the vertebrate record. Evolutionary Biology 9: 353-363.

Hecht, M.K. and Edwards, J.L. (1977). The methodology of phylogenetic inference above the species level. In: Hecht, M.K., Goody, P.C. and Hecht, B.M. (eds.). Major Patterns in Vertebrate Evolution. Plenum Press, New York. pp. 3-51.

Helsop-Harrison, J. (1976). The adaptive significance of the exine. In: I.K. Ferguson and J. Muller eds. The Evolutionary Significance of the Exine. Linnean Society Symposium Series 1. Academic Press, London. pp. 27-38.

Hennig, W. (1965). Phylogenetic systematics. Annual Review of Entomology 10: 97-116

Hennig, W. (1966). Phylogenetic systematics. University of Illinois Press, Urbana.

Hesse, M. (1986). Nature, form and function of pollen-connecting threads in angiosperms. In: S. Blackmore and I.K. Ferguson (eds.). Pollen and Spores: Form and Function. Linnean Society Symposium Series 12. Academic Press, London. pp. 109-118.

Hill, C.R. and Crane, P.R. (1982). Evolutionary cladistics and the origin of the angiosperms. In: K.A. Joysey and A.E. Friday (eds.). Problems of Phylogenetic Reconstruction. Academic Press, New York. pp 269-362.

Holm, T. (1904). The root structure of North american terrestrial Orchideae. American Journal of Science 168: 197-212.

Hull, D.L. (1984). Cladistic theory: hypotheses that blur and glow. Ch 1. In: Duncan, T and Stuessy, T.F. (eds.). Cladistics: perspectives on the reconstruction of evolutionary history.

Hunecke, G. (1904). Zur Anatomie der Pleurothallidinae. Horning & Berkenbusch, Heidelberg.

Jefferies, R.P.S. (1979). The origin of chordates- a methodological essay. In: M.R. House (ed.). The Origin of Major Invertebrate Groups. Academic Press, London. pp. 443-477.

Johansen, D.A. (1940). Plant Microtechnique. Mcgraw-Hill, London; New York.

Knox, R.B and McConchie, C.A. (1986). Structure and function of compound pollen. In: S. Blackmore and I.K. Ferguson (eds.) Pollen and Spores. Form and Function. Linnean Society Symposium Series 12. Academic Press, London. pp. 265-282.

Kremp, G.O.W. (1965). Morphologic Encyclopedia of Palynology. The University of Arizona Press, Tucson.

Kurzweil, H. (1989). Floral morphology and ontogeny in Huttonaea pulchra. Lindleyana 4(1): 1-5.

Linder, H.P. (1981a). Taxonomic studies on the Disinae: 1. A revision of the genus Brownleea Lindl. Journal of South African Botany 47: 13-48.

Linder, H.P. (1981b). Taxonomic studies on the Disinae: 2. A revision of the genus Schizodium Lindl. Journal of South African Botany 47: 339-371.

Linder, H.P. (1981c). Taxonomic studies on the Disinae: III. A revision of Disa Berg. excluding sect. Micranthae Lindl. Contributions to the Bolus Herbarium 9: 1-370.

Linder, H.P. (1981d). Taxonomic studies on the Disinae: V. A revision of the genus Monadenia Lindl. Bothalia 13: 339-363.

Linder, H.P. (1981e). Taxonomic studies on the Disinae: VI. A revision of the genus Herschelia Lindl. Bothalia 13: 365-388.

Linder, H.P. (1981f). Taxonomic studies on the Disinae: IV. A revision of Disa Berg. sect. Micranthae Lindl. Bulletin ?des Jardins Botaniques National Belge 51: 255-346.

Linder, H.P. (1986). Notes on the phylogeny of the Orchidoideae, with particular reference to the Diseae. Lindleyana 1(1): 51-64.

Linder, H.P. (1988). A review of cladistics for botanists. South African Journal of Botany 54(3): 208-220.

Lovtrup, S. (1977). The Phylogeny of Vertebrata. Wiley, London.

Maddison, W.P., Donoghue, M.J. and Maddison, D.R. (1984). Outgroup analysis and parsimony. Systematic Zoology 33: 83-103.

Mayr, E. (1969). Principles of Systematic Zoology. McGraw-Hill, New York.

Mickevich, M.F. (1978). Taxonomic congruence. Systematic Zoology 27 : 143-158.

Mickevich, M.F. and Farris, F.J. (1981). The implications of congruence in Menidia. Systematic Zoology 30: 351-370

Mobius, M. (1887). Anatomischer Bau der Orchideenblatter. Pringsheims Jahrb. 18: 530-607.

Neff, N.A. (1986). A rational basis for a priori character weighting. Systematic Zoology 35: 110-123.

Newton, G.D. and Williams, N.H. (1978). Pollen morphology of the Cyprepedioideae and the Apostasioideae (Orchidaceae). Selbyana 2: 169-182.

Patterson, G. (1982). Morphological characters and homology. In K.A. Joysey and A.E. Friday (eds.). Problems of Phylogenetic Reconstruction. Academic Press, London. pp.21-74.

Payne, W.W. (1972). Observations of harmomegathy in pollen of Anthophyta. Grana 12: 93-98

Payne, W.W. (1981). Structure and function in Angiosperm pollen wall evolution. Review of Palaeobotany and Palynology 35: 39-59.

Pfitzer, E. (1889). Orchidaceae. In: Engler, A. and Prantl, K. (eds.). Die Naturlichen Pflantzenfamilien 2.6.

Platnik, N.I. (1977). Cladograms, phylogenetic trees and hypothesis testing. Systematic Zoology 26: 438-442.

Pridgeon, A.M. (1981). Shoot anatomy of two additional species of Dresslerella (Orchidaceae). Selbyana 5: 274-278.

Pridgeon, A.M. (1982 a). Diagnostic anatomical characters in the Pleurothallidinae (Orchidaceae). American Journal of Botany 69: 921-938.

Pridgeon, A.M. (1982 b). Numerical analyses in the classification of the Pleurothallidinae (Orchidaceae). Botanical Journal of the Linnean Society 85: 103-131.

Pridgeon, A.M. and Stern, W.L. (1982). Vegetative anatomy of Myoxanthus (Orchidaceae). Selbyana 7: 55-63.

Punt, W. (1986). Functional factors influencing pollen form. In: S. Blackmore and I.K. Ferguson (eds.). Pollen and Spores: Form and Function. Linnean Society Symposium Series 12. Academic Press, London. pp. 97-102.

Rasmussen, H. (1981). The diversity of stomatal development in Orchidaceae subfamily Orchidoideae. Botanical Journal of the Linnean Society 82: 381-393.

Rasmussen, F.N. (1985). Orchids. In R.M.T. Dahlgren, H.T. Clifford and P.F. Yeo (eds.). The families of the monocotyledons: structure, evolution and taxonomy. Springer Verlag, Berlin. pp. 249-274.

Reynolds, E.S. (1963). The use of lead citrate at high pH as an electron opaque stain in electron microscopy. Journal of Cell Biology 17: 208.

Rohlf, F.J. (1988). NTSYS-pc. Numerical Taxonomy and Multivariate Analysis System. Version 1.40. Exeter Publishing Company, New York.

SAS Institute (1985). SAS/STAT Guide for personal Computers. Version 6 ed. SAS Institute, Cary, North Carolina.

Schill, R. and Pfeiffer, W. (1977). Untersuchungen an orchideenpollinien unter besonderen Beruecksichtigung ihrer Feinskulpturen. Pollen et Spores 19: 5-118.

Schlechter, R. (1926). Das System der Orchidaceen. Notizblad Botanischen Garten Berlin-Dahlem 9: 563-591.

Simon, C. (1983). A new coding procedure for morphometric data with an example fromperiodical cicada wing veins. In: J. Felsenstein (ed.). Numerical Taxonomy. Proceedings of the NATO Advanced Study Institute Series G (Ecological Sciences) No. 1. Springer-Verlag, Berlin.

Sneath, P.H.A. (1971). Numerical taxonomy: criticism and critiques. Biological Journal of the Linnean Society 3 (2): 147-158.

Sokal, R.R. and Sneath, P.H.A. (1963). Principles of Numerical Taxonomy. Freeman Press, San Francisco.

Spurr, A.R. (1969). A low viscosity epoxy resin embedding medium for electron microscopy. Journal of Ultrastructural Research 26: 31-43.

Stewart, J.H., Linder, H.P., Schelpe, E.A. and A.V. Hall. (1982). Wild orchids of southern Africa. Macmillan South Africa, Johannesburg.

Takhtajan, A. (1969). Flowering plants: Origin and Dispersal. Smithsonian Institution Press, Washington, DC.

Thiele, K. and Ladiges, P. (1988). A Cladistic analysis of Angophora Cav. (Myrtaceae). Cladistics 4: 23-42.

Tolivia, D. and Tolivia J. (1987). Fasga: a new polychromatic method for simultaneous and differential staining of plant tissue. Journal of Microscopy 148: 113-117.

Van Campo, M. and Guinet, P. (1961). Les pollens composees. L'example des Mimosacees. Pollen et Spores 3: 201-218

Van Campo, M. (1976). Patterns of pollen morphological variation within taxa. In: I.K. Ferguson and J. Muller (eds.). The Evolutionary Significance of the Exine. Linnean Society Symposium Series 1. Academic Press, London. pp.125-138.

Walker, J.W. (1974). Evolution of exine structure in the pollen of primitive angiosperms. American Journal of Botany 61: 891-902.

Walker, J.W. and Doyle, J.A. (1975). The Bases of Angiosperm Phylogeny: Palynology. Annals of the Missouri Botanic(al) Gardens 62: 664-723.

Walker, J.W. (1976). Evolutionary significance of the exine in the pollen of primitive angiosperms. In I.K. Ferguson and J. Muller (eds.). The Evolutionary Significance of the Exine. Linnean Society Symposium Series 1, Academic Press, London. pp. 251-308.

Watrous, L.E. and Wheeler, Q.D. (1981). The outgroup comparison method of character analysis. Systematic Zoology 30: 1-11 16?.

Wheeler, Q.D. (1986). Character weighting and cladistic analysis. Systematic Zoology 35: 102-109.

Wiley, E.O. (1981). Phylogenetics: The Theory and Practice of Phylogenetic Systematics. John Wiley and Sons, New York. 439pp.

Williams, N.H. and Broome, C.R. (1976). Scanning electron microscope studies of orchid pollen. American Orchid Society Bulletin 45: 699-707.

Williams, N.H. (1982). Scanning Electron Microscope Studies of Orchid Pollen. American Orchid Society Bulletin 45: 699-707.

Witcomb, M.J. (1985). The suitability of various adhesives as mounting media for scanning electron microscopy. II. General purpose glues. Journal of Microscopy 139: 75-114.

Wodehouse, R.P. (1935). Pollen Grains. McGraw-Hill, New York, London.

Zavada, M.S. (1984). The Relation Between Pollen Exine Sculpturing and Self-Incompatability Mechanisms. Plant Systematics and Evolution 147: 63-78.

Appendix 1

Vouchered specimens used in leaf anatomy and pollen studies.

SPECIES		SEM	TEM	ANATOMY
Schizochilus flexuosus				Linder 4661
Bonatea pulchella		?		
Habenaria laevigata		?		Linder 4670
Satyrium bracteatum		?		
Satyrium erectum				NBG 30785
Huttonaea pulchra		Gerstner 553		
Huttonaea grandiflora		McLoughlin 193		
Monadenia physodes		H.Bolus 4336		
Monadenia atrorubens		H.Bolus 9938		Linder 4396
Monadenia sabulosa		Linder 1508		Hall 1208
Monadenia brevicornis		Boardman 49		
Monadenia densiflora		Page 16232		
Monadenia ophrydea				?
Monadenia comosa				Linder 4409
Monadenia bracteata				P.Chesselet 1
Brownleea galpinii		Boardman 55		
Brownleea coerula		McLoughlin 68		Linder 4639
Brownleea parviflora				NBG s.n.
Schizodium obliquum			P.Chesselet 24	P.Chesselet 2
Schizodium bifidum		Boardman 1158		Hall 1034
Schizodium inflexum		Linder 4398		Linder 4396
Schizodium cornutum				Hall 1051
Disa welwitschii	Micranthae	Best 1255		
Disa ukingensis	Micranthae	La Croix 996		
Disa englerana	Micranthae	La Croix 1008		La Croix 1008
Disa ochrostachya	Micranthae	Stolz 2450		
Disa ornithantha	Micranthae	Williamson 1397		
Disa chrysostachya	Micranthae	Boardman 297		Courtney-Lati
Disa fragrans	Micranthae	Linder 960		Linder 4638
Disa sankeyi	Micranthae			Hall 1090
Disa bivalvata	Disa	Muir s.n.	?	
Disa atricapilla	Disa	Vlok 90		H.Kurzweil 98
Disa richardiana	Disa	McLoughlin 5		
Disa uniflora	Disa	Leipold 602		P.Chesselet 3
Disa venosa	Disa	Keet 1057		
Disa filicornis	Disa	s.n.		
Disa rosea	Disa			Linder 4406
Disa pillansii	Disa			Olivier s.n.
Disa fasciata	Disa			P.Chesselet 2
Disa patens	Disa			H.Kurzweil 10
Disa filicornis	Disa			Linder 4399
Disa maculata	Phlebidia	Linder 1675		Linder 4405
Disa longicornis	Phlebidia	Linder 1675		P.Chesselet 8
Disa tenuis	Amphigena	Schlechter 7550		
Disa salteri	Amphigena	Esterhuysen 35200		
Disa saxicola	Stenocarpa	Hall 930		La Croix 983
Disa gladioliflora	Stenocarpa	Linder 1766		
Disa nivea	Stenocarpa			Linder 4647
Disa oreophila	Stenocarpa			Linder 4666
Disa cephalotes	Stenocarpa			?
Disa cephalotes ssp frigi	Stenocarpa			Linder 4690
Disa sagittalis	Coryphaea		NBG 450/82	NBG 456/82
Disa vaginata	Coryphaea			Linder 4515
Disa cylindrica	Coryphaea			Linder 4401
Disa draconis	Coryphaea			P.Chesselet 1
Disa glandulosa	Coryphaea			P.Chesselet 9
Disa marlothii	Coryphaea	Esterhuysen 27406A		
Disa triloba	Coryphaea	Esterhuysen 30017		
Disa patula	Emarginatae	Widdicombe 31		M.Rutgers 30
Disa stachyoides	Emarginatae	Rutgers 12		
Disa alticola	Emarginatae			Linder 2063
Disa basutorum	Austroalpine	Linder 959		

Disa cooperi	Hircicornes	Boardman 214		
Disa thodei	Hircicornes	Boardman 19		
Disa crassicornis	Hircicornes	Linder 1073		A.Batten s.n.
Disa versicolor	Hircicornes	Linder 999		Linder 4652
Disa stairsii	Stoloniferae	Esterhuysen 25156		
Disa ovalifoliae	Ovalifoliae	Schlechter 8892		
Disa tenuicornis	Disella	Linder 1523		
Disa obtusa sp. picta	Disella	Linder 1594		
Disa lineata	Disella		Linder 4722	
Disa telipogonis	Disella			Linder 4489
Disa aconitoides	Aconotoideae	Franeeld 1034		
Disa equestris	Aconotoideae	Eccles 59		
Disa aperta	Aconotoideae	Linder s.n.		
Disa aconotoides	Aconotoideae			Hall 826
Disa tysonii	Repandra	Hall 790		Linder 4664
Disa cornuta	Repandra	Kurzweil 961		P.Chesselet 1
Disa galpinii	Intermediae	Boardman 59		
Disa sanguinea	Intermediae	McLoughlin 644		
Herschelianthe lugens		Linder s.n.		
Herschelianthe forficaria		Gillet 718		
Herschelianthe chimanimaniensis		s.n.		
Herschelianthe baurii		Linder s.n.		
Herschelianthe graminifolia		s.n.		
Herschelianthe hians		Buhr 5		
Herschelianthe praecox		Linder s.n.		
Herschelianthe schlerterana		Luyt 10571		
Herschelianthe spathulata		Leipold 601		?
Disperis capensis		?	H.Kurzweil s.n.	H.Kurzweil 90
Disperis cardiophora		?		
Disperis lindleyana		Hall 902		
Disperis villosa		Hall 957		Hall 957
Disperis cuculata		Linder 1137		
Disperis thorncroftii		Schnell 22861		
Disperis circumflexa		Hall 1045		
Disperis fanniniae				H.Kurzweil 10
Disperis stenoplectron				Linder 4668
Ceratandra atrata		Taylor 248		Linder 4473
Ceratandra grandiflora		Middlemost 1806		
Ceratandra globosa				Linder 4485
Evota venosa		H.Bolus 5281		
Evota bicolor		Esterhuysen 11216	?	Steiner s.n./
Anochilus flanagani		?		
Anochilus inversus		?		
Anochilus hallii		Winter 182		Linder 4227
Corycium bifidum		Stokoe 17854		
Corycium orobanchoides		Lewis 22241	P.Chesselet 16	Linder 4227
Corycium excisum		Linder 1805		
Corycium magnum		Linder 938		
Corycium nigrescens		Hall 841		Linder 4665
Corycium dracomontanum		McLoughlin 200		Linder 4666
Corycium deflexum		Schelpe 8088		
Corycium bicolorum				I.B.Walters 5
Corycium rubiginosum				Linder 4442
Corycium crispum				Linder 4314
Pterygodium volucris				Hall 953
Pterygodium alatum				Linder 4296
Pterygodium caffrum				Linder 4220
Pterygodium catholicum		Linder 4216	P.Chesselet 11	
Pterygodium platypetalum		Linder 4219		
Pterygodium acutifolium		Linder 1679		Linder 4449
Pterygodium pantherianum		Linder 4198		

Appendix 2

Homogeneous subset grouping for leaf anatomy measurement data.

adaxial epidermal cell length

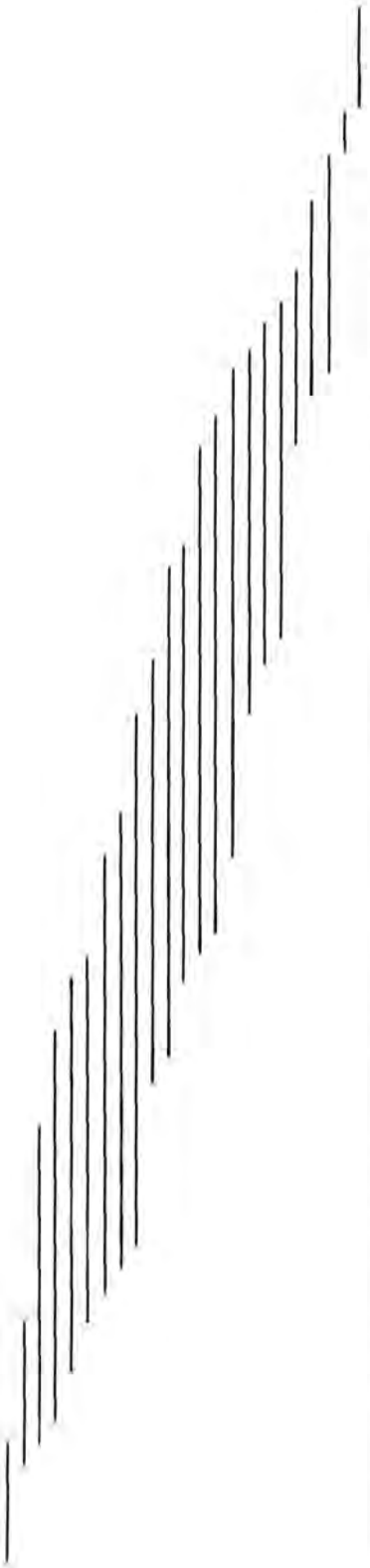

homogeneous subset code	actual code	
1	0	Corycium orobanchoides
1	0	Anochilus hallii
1	0	Satyrium erectum
1	0	Corycium bicolorum
2	0	Pterygodium acutifolium
2	0	Disa saxicola
3	0	Disa draconis
3	0	Pterygodium volucris
3.5	0	Ceratandra globosa
4	1	Corycium crispum
4	1	Ceratandra atrata
4.5	1	Corycium dracomontanum
5	1	Disa chrysostachya
5.5	1	Pterygodium alatum
6	1	Disa atricapilla
7	2	Disa alticola
7.5	2	Pterygodium caffrum
8.5	2	Disa linearis
9.5	2	Monadenia atrorubens
9.5	2	Monadenia bracteata
9.5	2	Schizodium inflexum
9.5	2	Disa uniflora
10	3	Disa telipogonis
10.5	3	Disa cornuta
10.5	3	Disperis villosa
10.5	3	Monadenia ophrydea
11.5	3	Disa filicornis
12	3	Monadenia sabulosa
12	3	Disa maculata
13	4	Disa longicornu
13	4	Disa crassicornis
13	4	Habenaria laevigata
13	4	Schizochilus flexuosus
13.5	4	Disa tysonii
13.5	4	Monadenia comosa
14.5	4	Disa fasciata
14.5	4	Disa englerana
14.5	4	Disa cylindrica
15	4	Disa cephalotes ssp frigida
16	5	Disa sankeyi
17	5	Disperis capensis
17	5	Disa nivea
17.5	5	Disa rosea
18	5	Disa patens
18.5	5	Corycium nigrescens
18.5	5	Evota bicolor
19	6	Disa fragrans
19	6	Disa cephalotes
19	6	Disa patula
19	6	Disa pillansii
19	6	Corycium rubiginosum
19.5	6	Disa glandulosa
20	6	Disa vaginata
20.5	6	Disa sagittalis
21.5	6	Evota bicolor
21.5	6	Disa versicolor
22	7	Brownleea coerula
22	7	Disa aconitoides
22.5	7	Schizodium obliquum
23.5	7	Brownleea parviflora
24	7	Disperis fanniniae
24	7	Schizodium cornutum
24	7	Schizodium bifidum
24	7	Disperis stenoplectron

abaxial epidermal cell depth

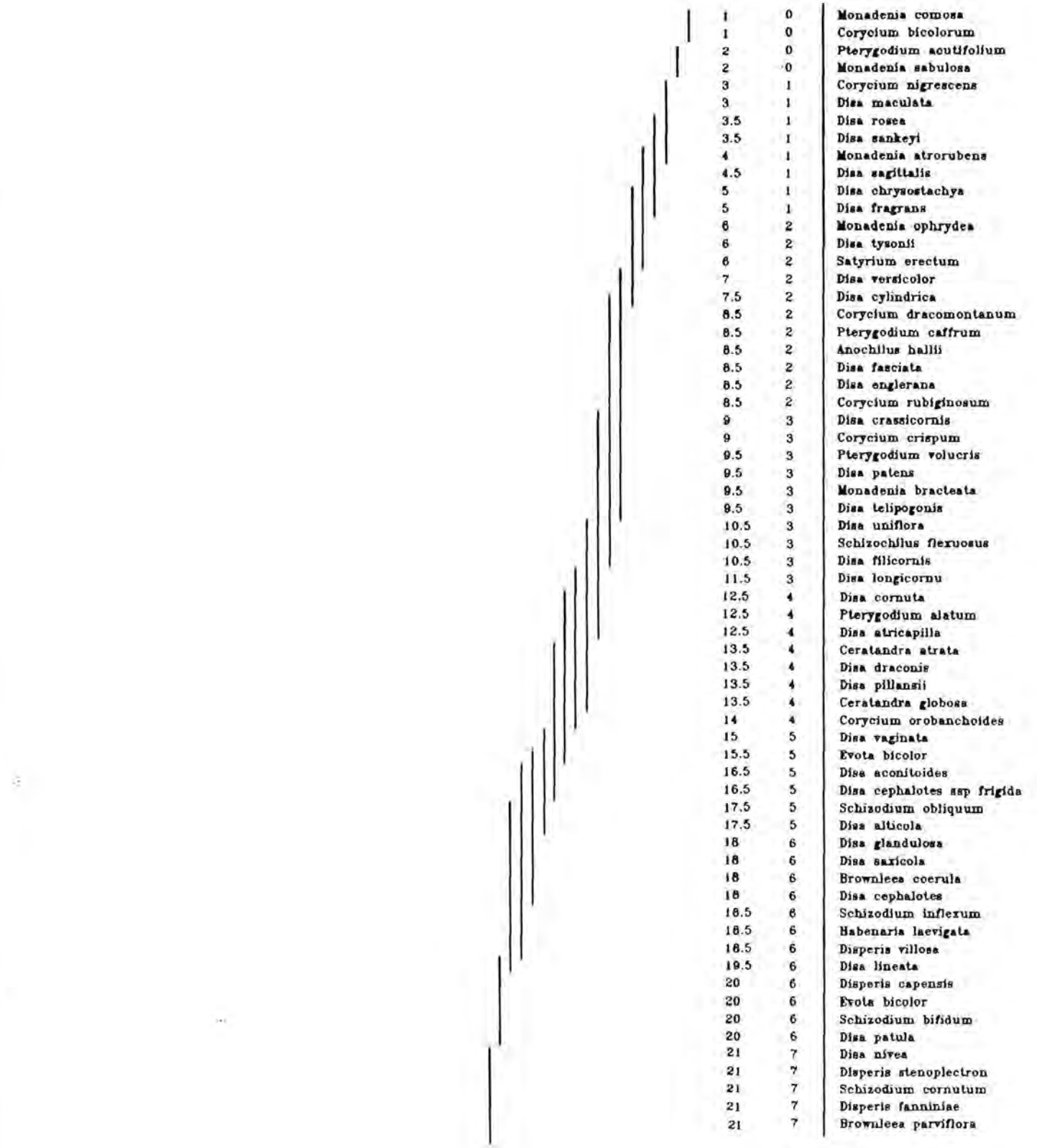

homogeneous subset code	actual code	
1	0	Monadenia comosa
1	0	Corycium bicolorum
2	0	Pterygodium acutifolium
2	0	Monadenia sabulosa
3	1	Corycium nigrescens
3	1	Disa maculata
3.5	1	Disa rosea
3.5	1	Disa sankeyi
4	1	Monadenia atrorubens
4.5	1	Disa sagittalis
5	1	Disa chrysostachya
5	1	Disa fragrans
6	2	Monadenia ophrydea
6	2	Disa tysonii
6	2	Satyrium erectum
7	2	Disa versicolor
7.5	2	Disa cylindrica
8.5	2	Corycium dracomontanum
8.5	2	Pterygodium caffrum
8.5	2	Anochilus hallii
8.5	2	Disa fasciata
8.5	2	Disa englerana
8.5	2	Corycium rubiginosum
9	3	Disa crassicornis
9	3	Corycium crispum
9.5	3	Pterygodium volucris
9.5	3	Disa patens
9.5	3	Monadenia bracteata
9.5	3	Disa telipogonis
10.5	3	Disa uniflora
10.5	3	Schizochilus flexuosus
10.5	3	Disa filicornis
11.5	3	Disa longicornu
12.5	4	Disa cornuta
12.5	4	Pterygodium alatum
12.5	4	Disa atricapilla
13.5	4	Ceratandra atrata
13.5	4	Disa draconis
13.5	4	Disa pillansii
13.5	4	Ceratandra globosa
14	4	Corycium orobanchoides
15	5	Disa vaginata
15.5	5	Evota bicolor
16.5	5	Disa aconitoides
16.5	5	Disa cephalotes ssp frigida
17.5	5	Schizodium obliquum
17.5	5	Disa alticola
18	6	Disa glandulosa
18	6	Disa saxicola
18	6	Brownleea coerula
18	6	Disa cephalotes
18.5	6	Schizodium inflexum
18.5	6	Habenaria laevigata
18.5	6	Disperis villosa
19.5	6	Disa lineata
20	6	Disperis capensis
20	6	Evota bicolor
20	6	Schizodium bifidum
20	6	Disa patula
21	7	Disa nivea
21	7	Disperis stenoplectron
21	7	Schizodium cornutum
21	7	Disperis fanniniae
21	7	Brownleea parviflora

abaxial epidermal cell length

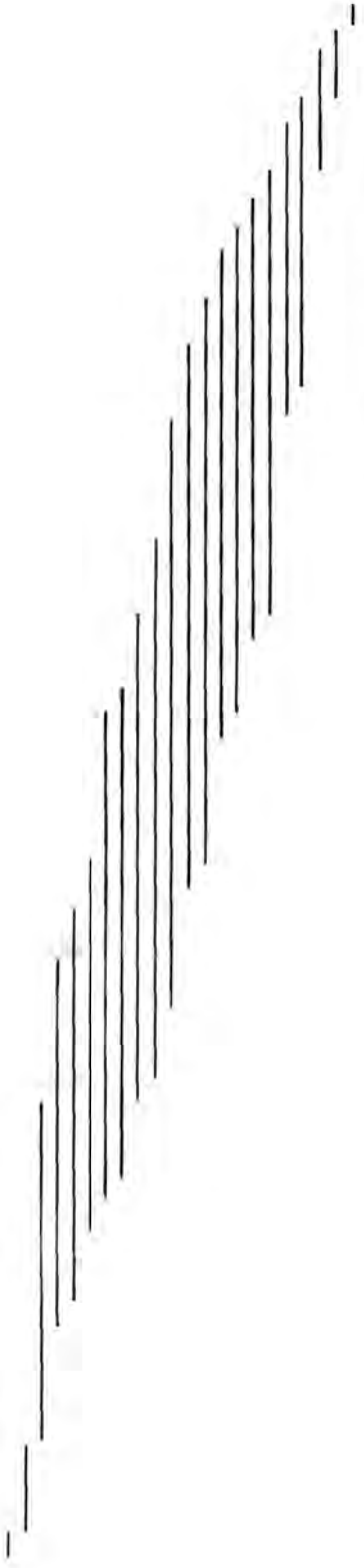

homogeneous subset code	actual code	
1	0	Pterygodium acutifolium
2	0	Disa draconis
2.5	0	Corycium bicolorum
2.5	0	Anochilus hallii
3.5	0	Corycium dracomontanum
4	0	Corycium orobanchoides
4	0	Disa cornuta
5	1	Satyrium erectum
5.5	1	Disa saxicola
6	1	Monadenia comosa
6.5	1	Monadenia atrorubens
6.5	1	Pterygodium alatum
7	1	Ceratandra globosa
7	1	Corycium crispum
7.5	1	Disa crassicornis
7.5	1	Monadenia ophrydea
8	2	Evota bicolor
9	2	Monadenia bracteata
9	2	Disa longicornu
9	2	Disperis villosa
9	2	Disa chrysostachya
9	2	Ceratandra atrata
9.5	2	Schizodium inflexum
9.5	2	Disa fasciata
9.5	2	Pterygodium volucris
10.5	2	Disa fragrans
11	3	Corycium nigrescens
11	3	Schizodium obliquum
11.5	3	Disa telipogonis
12.5	3	Disa maculata
13	3	Disa uniflora
13	3	Disa sankeyi
13	3	Disa lineata
13	3	Monadenia sabulosa
13	3	Disa cylindrica
14	4	Disa atricapilla
14.5	4	Disa cephalotes
15	4	Disa rosea
15	4	Corycium rubiginosum
15.5	4	Schizochilus flexuosus
15.5	4	Pterygodium caffrum
16	4	Disa patens
16	4	Brownleea coerula
16	4	Schizodium bifidum
17	4	Disa glandulosa
17.5	5	Disa tysonii
17.5	5	Disa filicornis
17.5	5	Evota bicolor
18	5	Disa alticola
18.5	5	Disa nivea
18.5	5	Disa pillansii
19	5	Disperis capensis
19	5	Disa englerana
19.5	5	Disa aconitoides
20	6	Disa versicolor
20	6	Schizodium cornutum
20	6	Disa sagittalis
20	6	Habenaria laevigata
20	6	Disa vaginata
21	6	Disa cephalotes ssp. frigida
21	6	Brownleea parviflora
21	6	Disperis stenoplectron
21	6	Disperis fanniniae
22	6	Disa patula

abaxial stomatal length

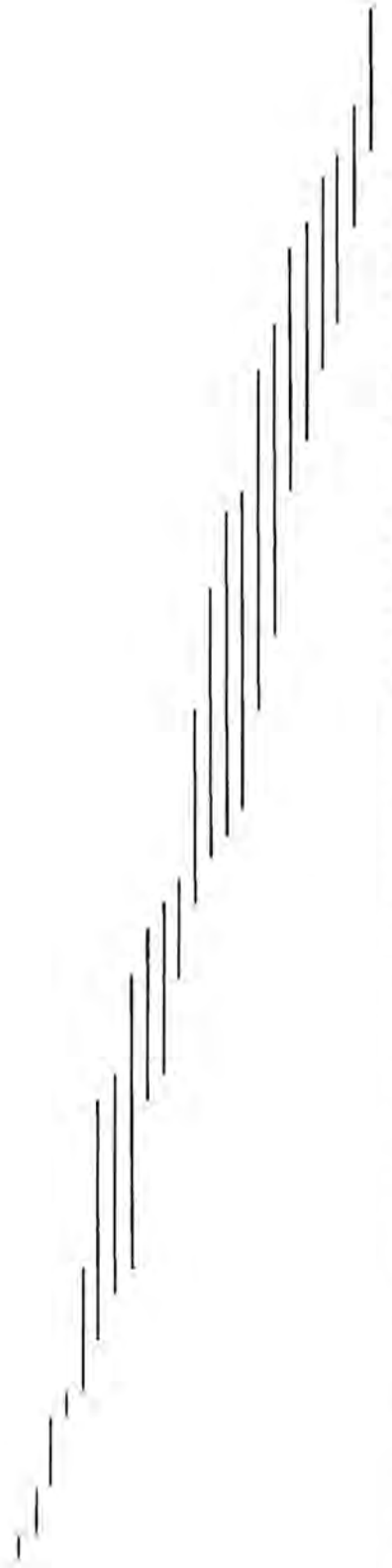

homogeneous subset code	actual code	
1	0	Disa crassicornis
1	0	Corycium dracomontanum
1	0	Disa chrysostachya
1	0	Disa maculata
1.5	0	Monadenia comosa
1.5	0	Satyrium erectum
2.5	0	Disa tulipogonis
3	0	Pterygodium acutifolium
3	0	Corycium orobanchoides
4	1	Corycium crispum
4.5	1	Corycium nigrescens
4.5	1	Disa tysonii
4.5	1	Disa sankeyi
5.5	1	Anochilus hallii
5.5	1	Disa versicolor
6.5	1	Disa rosea
6.5	1	Monadenia atrorubens
6.5	1	Brownleea coerula
7	2	Disa uniflora
7	2	Pterygodium alatum
8	2	Corycium bicolorum
8.5	2	Disa longicornu
8.5	2	Disa fasciata
8.5	2	Disa lineata
9	2	Disa fragrans
9	2	Disa cornuta
9.5	2	Disa draconis
9.5	2	Disperis capensis
9.5	2	Schizodium obliquum
10.5	3	Evota bicolor
10.5	3	Pterygodium caffrum
10.5	3	Disa cylindrica
10.5	3	Disa englerana
11	3	Schizochilus flexuosus
11.5	3	Pterygodium volucris
12	3	Ceratandra globosa
12.5	3	Schizodium inflexum
13.5	4	Disa saxicola
13.5	4	Monadenia ophrydea
14	4	Evota bicolor
14	4	Disa aconitoides
15	4	Disa cephalotes
15	4	Disa cephalotes ssp frigida
15	4	Disa pillansii
15	5	Monadenia bracteata
16.5	5	Disa atricapilla
17	5	Corycium rubiginosum
17	5	Disa alticola
17	5	Disa glandulosa
17	5	Ceratandra atrata
17	5	Disperis fanniniae
17	5	Habenaria laevigata
18	5	Disperis villosa
18.5	5	Disperis stenoplectron
18.5	5	Disa filicornis
19	6	Monadenia sabulosa
19	6	Disa nivea
20	6	Disa sagittalis
21	6	Schizodium bifidum
21	6	Disa patula
21	6	Disa vaginata
22	7	Disa patens
22	7	Brownleea parviflora
23	7	Schizodium cornutum

abaxial stomatal width

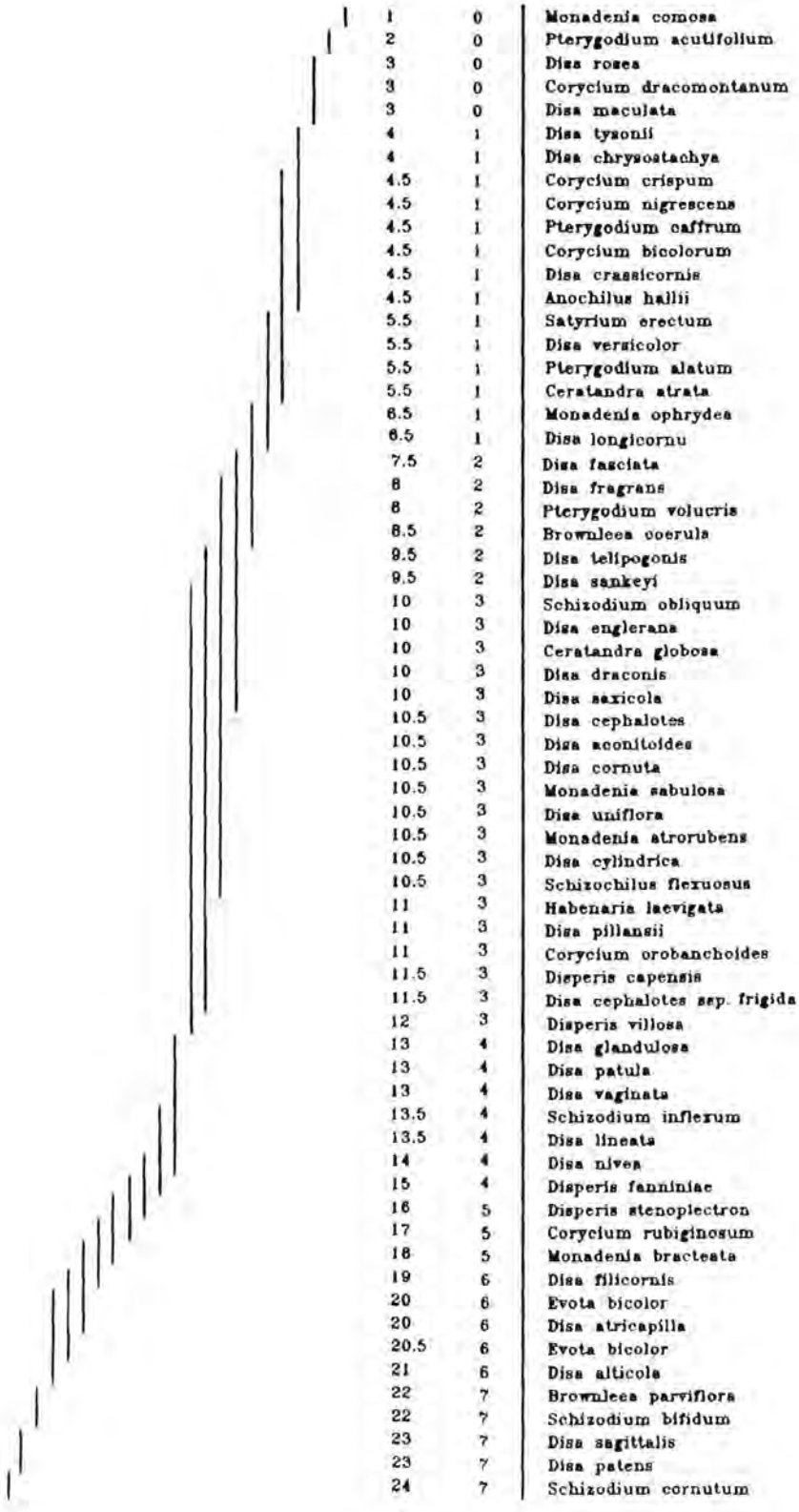

homogeneous subset code	actual code	
1	0	Monadenia comosa
2	0	Pterygodium acutifolium
3	0	Disa rosea
3	0	Corycium dracomontanum
3	0	Disa maculata
4	1	Disa tysonii
4	1	Disa chrysostachya
4.5	1	Corycium crispum
4.5	1	Corycium nigrescens
4.5	1	Pterygodium caffrum
4.5	1	Corycium bicolorum
4.5	1	Disa crassicornis
4.5	1	Anochilus hallii
5.5	1	Satyrium erectum
5.5	1	Disa versicolor
5.5	1	Pterygodium alatum
5.5	1	Ceratandra atrata
6.5	1	Monadenia ophrydea
6.5	1	Disa longicornu
7.5	2	Disa fasciata
8	2	Disa fragrans
8	2	Pterygodium volucris
8.5	2	Brownleea coerula
9.5	2	Disa telipogonis
9.5	2	Disa sankeyi
10	3	Schizodium obliquum
10	3	Disa englerana
10	3	Ceratandra globosa
10	3	Disa draconis
10	3	Disa saxicola
10.5	3	Disa cephalotes
10.5	3	Disa aconitoides
10.5	3	Disa cornuta
10.5	3	Monadenia sabulosa
10.5	3	Disa uniflora
10.5	3	Monadenia atrorubens
10.5	3	Disa cylindrica
10.5	3	Schizochilus flexuosus
11	3	Habenaria laevigata
11	3	Disa pillansii
11	3	Corycium orobanchoides
11.5	3	Disperis capensis
11.5	3	Disa cephalotes ssp. frigida
12	3	Disperis villosa
13	4	Disa glandulosa
13	4	Disa patula
13	4	Disa vaginata
13.5	4	Schizodium inflexum
13.5	4	Disa lineata
14	4	Disa nivea
15	4	Disperis fanniniae
16	5	Disperis stenoplectron
17	5	Corycium rubiginosum
18	5	Monadenia bracteata
19	6	Disa filicornis
20	6	Evota bicolor
20	6	Disa atricapilla
20.5	6	Evota bicolor
21	6	Disa alticola
22	7	Brownleea parviflora
22	7	Schizodium bifidum
23	7	Disa sagittalis
23	7	Disa patens
24	7	Schizodium cornutum

adaxial epidermal cell width

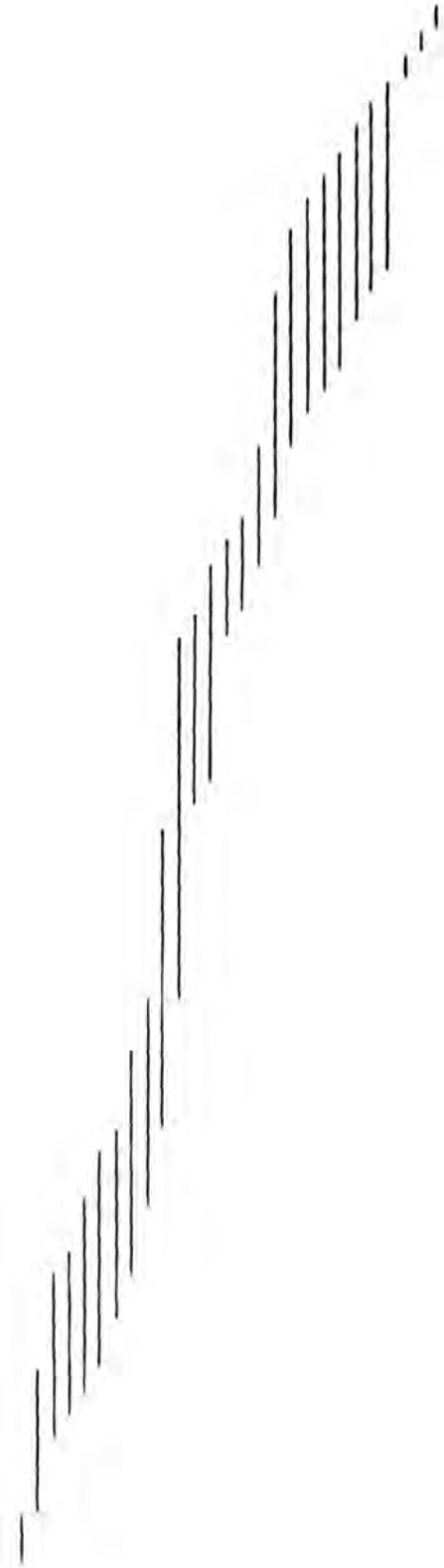

homogeneous subset code	actual code	
1	0	Satyrium erectum
2	0	Corycium bicolorum
3	0	Pterygodium volucris
4	1	Disa maculata
4.5	1	Pterygodium caffrum
5	1	Monadenia comosa
5.5	1	Disa chrysostachya
6	1	Pterygodium acutifolium
6.5	1	Shizochilus flexuosus
7	2	Anochilus hallii
7	2	Pterygodium alatum
7.5	2	Corycium dracomontanum
8.5	2	Disperis villosa
9	2	Disa tysonii
9	2	Disa rosea
9.5	2	Corycium crispum
10	3	Corycium nigrescens
10.5	3	Disa sankeyi
11.5	3	Corycium orobanchoides
11.5	3	Disa fragrans
11.5	3	Habenaria laevigata
12.5	3	Disa crassicornis
13	4	Disa draconis
14	4	Monadenia ophrydea
14	4	Disa cylindrica
15	4	Disa sagittalis
16	5	Monadenia sabulosa
16	5	Disa versicolor
16	5	Disa uniflora
16	5	Disa telipogonis
16	5	Disa pillansii
16	5	Disa patens
16.5	5	Disa lineata
17	5	Disa cephalotes ssp frigida
17.5	5	Ceratandra atrata
17.5	5	Disa fasciata
17.5	5	Schizodium inflexum
17.5	5	Disa englerana
17.5	5	Disa longicornu
17.5	5	Disa saxicola
17.5	5	Brownleea parviflora
18.5	5	Disa vaginata
18.5	5	Brownleea coerula
19	6	Monadenia atrorubens
19	6	Monadenia bracteata
19	6	Disa aconitoides
20	6	Disa cornuta
20.5	6	Disa patula
20.5	6	Disa alticola
21	6	Disperis stenoplectron
21.5	6	Disperis capensis
22	7	Disa atricapilla
23	7	Disperis fanniniae
23	7	Disa glandulosa
23.5	7	Disa filicornis
23.5	7	Schizodium bifidum
24.5	7	Corycium rubiginosum
25	8	Schizodium obliquum
25.5	8	Evota bicolor
26	8	Ceratandra globosa
26	8	Disa nivea
26	8	Disa cephalotes
27	8	Schizodium cornutum
27	8	Evota bicolor

adaxial epidermal cell length: width ratio

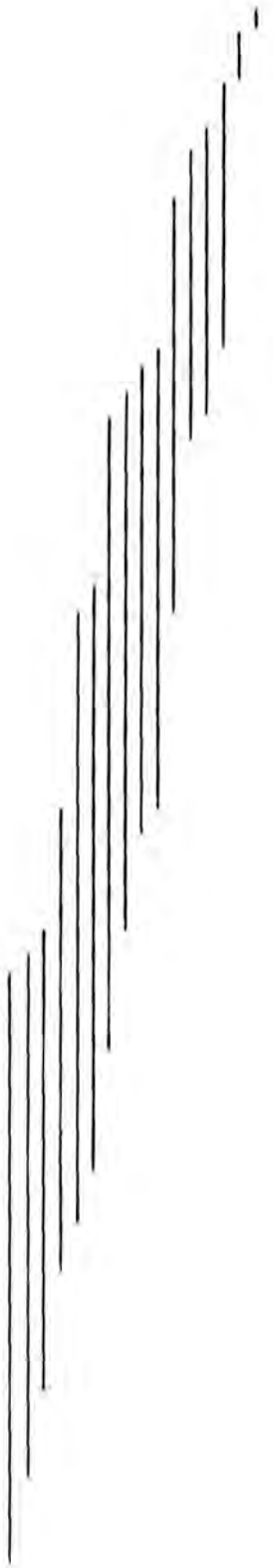

homogeneous subset code	actual code	
1	0	Ceratandra globosa
2	0	Disa saxicola
2	0	Corycium orobanchoides
3	1	Disa atricapilla
3	1	Anochilus hallii
3.5	1	Disa alticola
4	1	Ceratandra atrata
4	1	Disa filicornis
4.5	1	Evota bicolor
4.5	1	Monadenia atrorubens
4.5	1	Disa nivea
4.5	1	Monadenia bracteata
4.5	1	Disa cornuta
4.5	1	Disa draconis
5.5	2	Pterygodium acutifolium
6	2	Disa cephalotes
6.5	2	Schizodium inflexum
7.5	3	Disa lineata
8.5	3	Disperis capensis
8.5	3	Disa uniflora
8.5	3	Disa telipogonis
8.5	3	Corycium rubiginosum
8.5	3	Corycium crispum
8.5	3	Disa longicornu
9	4	Corycium bicolorum
10	4	Disa glandulosa
10.5	4	Monadenia sabulosa
10.5	4	Evota bicolor
10.5	4	Corycium dracomontanum
10.5	4	Disa fasciata
10.5	4	Disa patula
10.5	4	Disa englerana
10.5	4	Monadenia ophrydea
11.5	5	Disa cephalotes ssp. frigida
12	5	Schizodium obliquum
12	5	Pterygodium alatum
12	5	Pterygodium volucris
12	5	Schizodium cornutum
13	6	Disa chrysostachya
14	6	Disa vaginata
14.5	6	Disa patens
14.5	6	Disa crassicornis
14.5	6	Disa cylindrica
15	7	Disa aconitoides
15	7	Habenaria laevigata
15	7	Brownleea coerula
15	7	Disperis villosa
15	7	Disa pillansii
15.5	7	Pterygodium caffrum
15.5	7	Disperis fanniniae
16	7	Schizodium bifidum
16.5	7	Disa tysonii
17	8	Satyrium erectum
17	8	Disa sankeyi
17	8	Disperis stenoplectron
17	8	Schizochilus flexuosus
17	8	Disa versicolor
17.5	8	Disa sagittalis
17.5	8	Disa maculata
17.5	8	Disa fragrans
17.5	8	Brownleea parviflora
18	8	Monadenia comosa
18	8	Disa rosea
18	8	Corycium nigrescens

abaxial stomatal length:width ratio

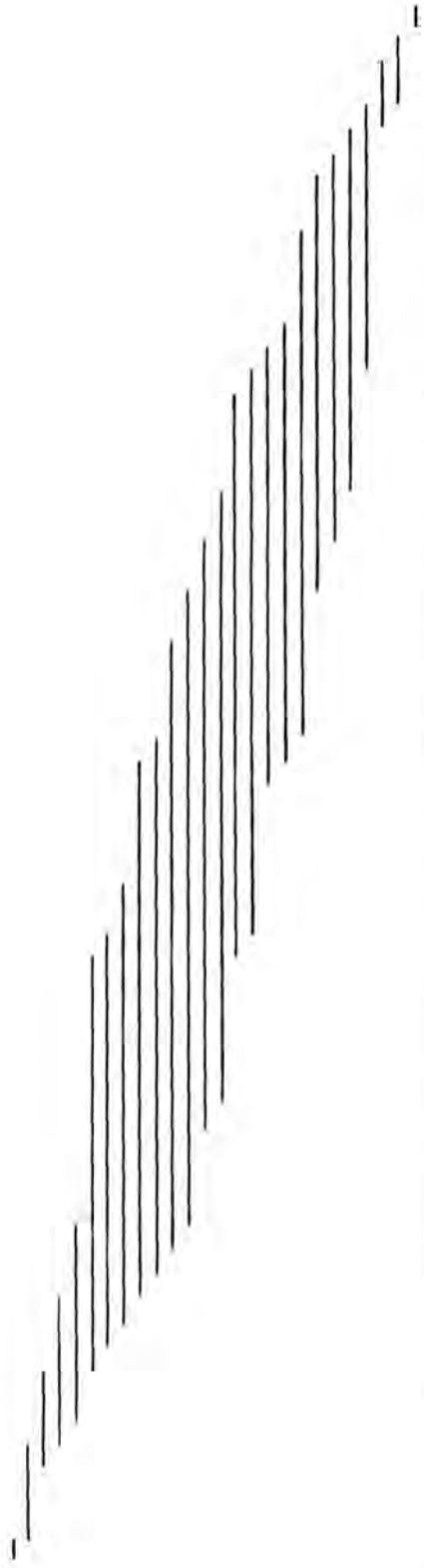

homogeneous subset code	actual code	
1	0	Evota bicolor
2	0	Corycium orobanchoides
2.5	0	Evota bicolor
2.5	0	Disa lineata
3.5	0	Disa telipogonis
4.5	1	Disa alticola
5	1	Disa atricapilla
5.5	1	Disa sankeyi
5.5	1	Monadenia atrorubens
6	1	Monadenia bracteata
6	1	Disa uniflora
6	1	Disa crassicornis
6	1	Disperis capensis
6.5	1	Schizodium inflexum
7	2	Disa sagittalis
8	2	Satyrium erectum
8.5	2	Brownleea coerula
8.5	2	Corycium rubiginosum
8.5	2	Disa cornuta
8.5	2	Schizodium cornutum
9.5	2	Disa draconis
9.5	2	Disa chrysostachya
10.5	3	Disa filicornis
10.5	3	Disa cylindrica
11.5	3	Schizodium obliquum
11.5	3	Disperis fanniniae
12	3	Disa patens
12	3	Schizochilus flexuosus
12	3	Corycium dracomontanum
12	3	Schizodium bifidum
13	4	Disa maculata
14	4	Disa fragrans
14.5	4	Disa englerana
14.5	4	Disperis stenoplectron
15.5	4	Disa fasciata
14.5	4	Disa versicolor
15	4	Disa longicornu
15	4	Corycium nigrescens
16	5	Corycium crispum
17	5	Pterygodium alatum
17	5	Anochilus hallii
17	5	Ceratandra globosa
17	5	Disa glandulosa
17	5	Disa oephalotes ssp. frigida
17	5	Pterygodium volucris
17.5	5	Disa tysonii
18	5	Brownleea parviflora
18	5	Disa saxicola
18	5	Disa pillansii
18	5	Disa nivea
19	6	Disa aconitoides
19.5	6	Corycium bicolorum
20	6	Disa cephalotes
21	6	Pterygodium acutifolium
21.5	6	Habenaria laevigata
22	7	Disperis villosa
23	7	Pterygodium caffrum
23	7	Disa rosea
23.5	7	Monadenia ophrydea
24.5	7	Monadenia comosa
25	8	Monadenia sabulosa
25	8	Disa patula
25	8	Disa vaginata
26	8	Ceratandra atrata

adaxial epidermal cell depth

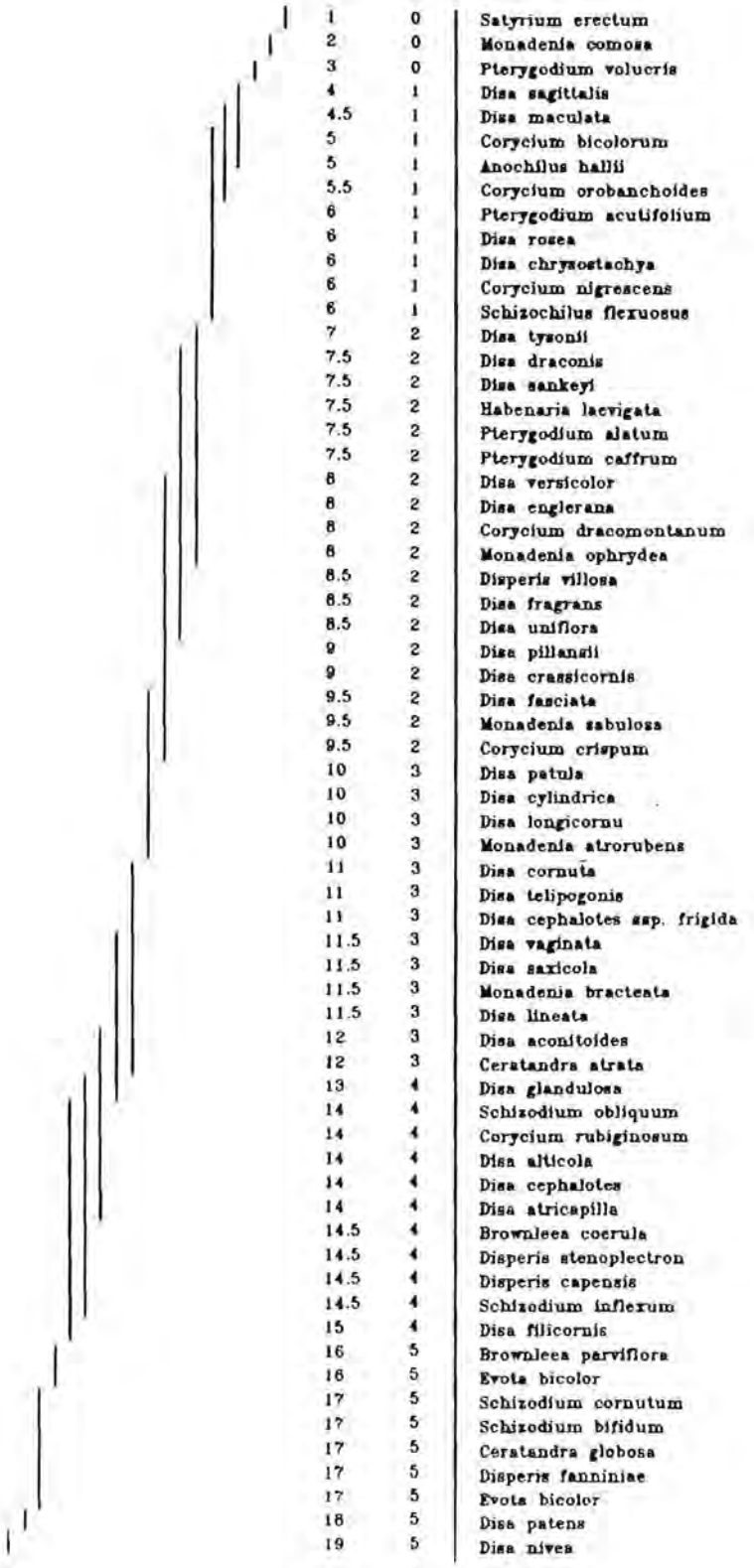

abaxial epidermal cell width

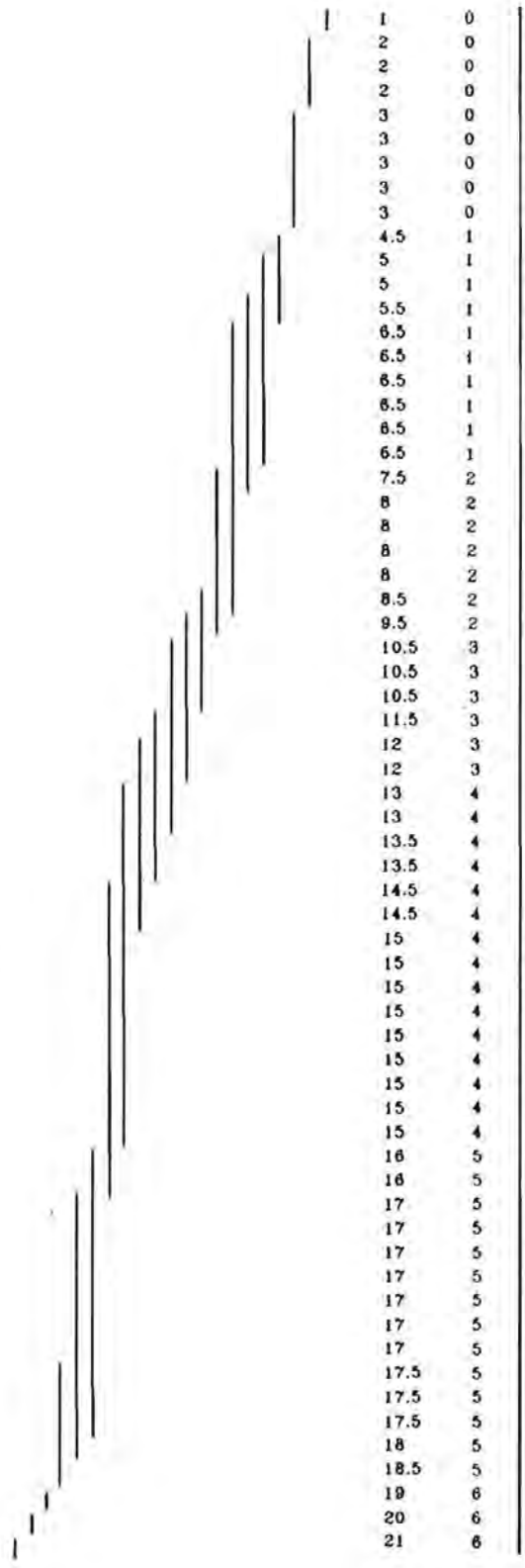

homogeneous subset code	actual code	
1	0	Monadenia comosa
2	0	Pterygodium acutifolium
2	0	Corycium nigrescens
2	0	Satyrium erectum
3	0	Schizodium obliquum
3	0	Corycium bicolorum
3	0	Corycium crispum
3	0	Pterygodium volucris
3	0	Disa tysonii
4.5	1	Corycium dracomontanum
5	1	Disa versicolor
5	1	Disa sagittalis
5.5	1	Disa sankeyi
6.5	1	Corycium orobanchoides
6.5	1	Disperis villosa
6.5	1	Disa fasciata
6.5	1	Disa fragrans
6.5	1	Disa rosea
6.5	1	Disa chrysostachya
7.5	2	Schizochilus flexuosus
8	2	Habenaria laevigata
8	2	Pterygodium caffrum
8	2	Anochilus hallii
8	2	Disa maculata
8.5	2	Monadenia ophrydea
9.5	2	Ceratandra atrata
10.5	3	Disa crassicornis
10.5	3	Disa pillansii
10.5	3	Monadenia sabulosa
11.5	3	Disa cylindrica
12	3	Pterygodium alatum
12	3	Disa cephalotes ssp. frigida
13	4	Disa englerana
13	4	Disa cephalotes
13.5	4	Disa uniflora
13.5	4	Disa atricapilla
14.5	4	Disa longicornu
14.5	4	Disa telipogonis
15	4	Disa draconis
15	4	Monadenia bracteata
15	4	Corycium rubiginosum
15	4	Monadenia atrorubens
15	4	Disa aconitoides
15	4	Ceratandra globosa
15	4	Disa cornuta
15	4	Disa saxicola
15	4	Disa vaginata
16	5	Disa glandulosa
16	5	Brownleea coerula
17	5	Disa patens
17	5	Schizodium inflexum
17	5	Disa lineata
17	5	Evota bicolor
17	5	Disperis capensis
17	5	Disa nivea
17	5	Disa filicornis
17.5	5	Disperis fanniniae
17.5	5	Disa patula
17.5	5	Disperis stenoplectron
18	5	Schizodium cornutum
18.5	5	Schizodium bifidum
19	6	Brownleea parviflora
20	6	Evota bicolor
21	6	Disa alticola

adaxial stomatal length: width ratio

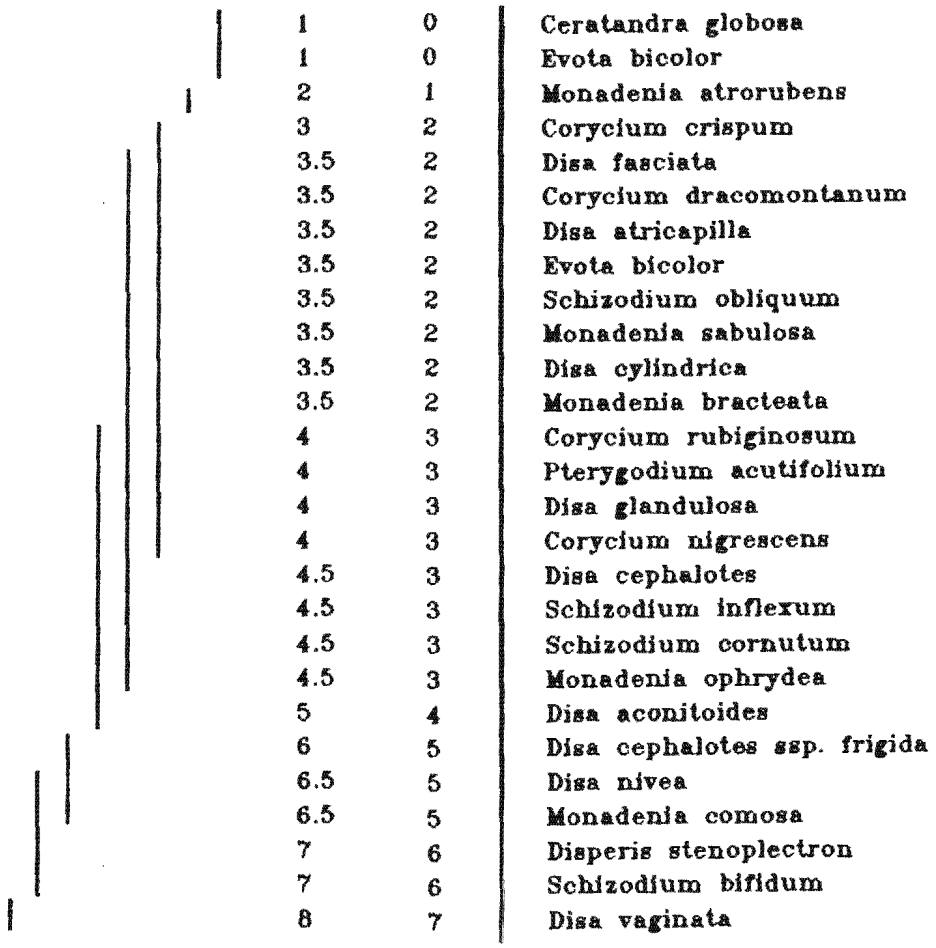

adaxial stomatal length

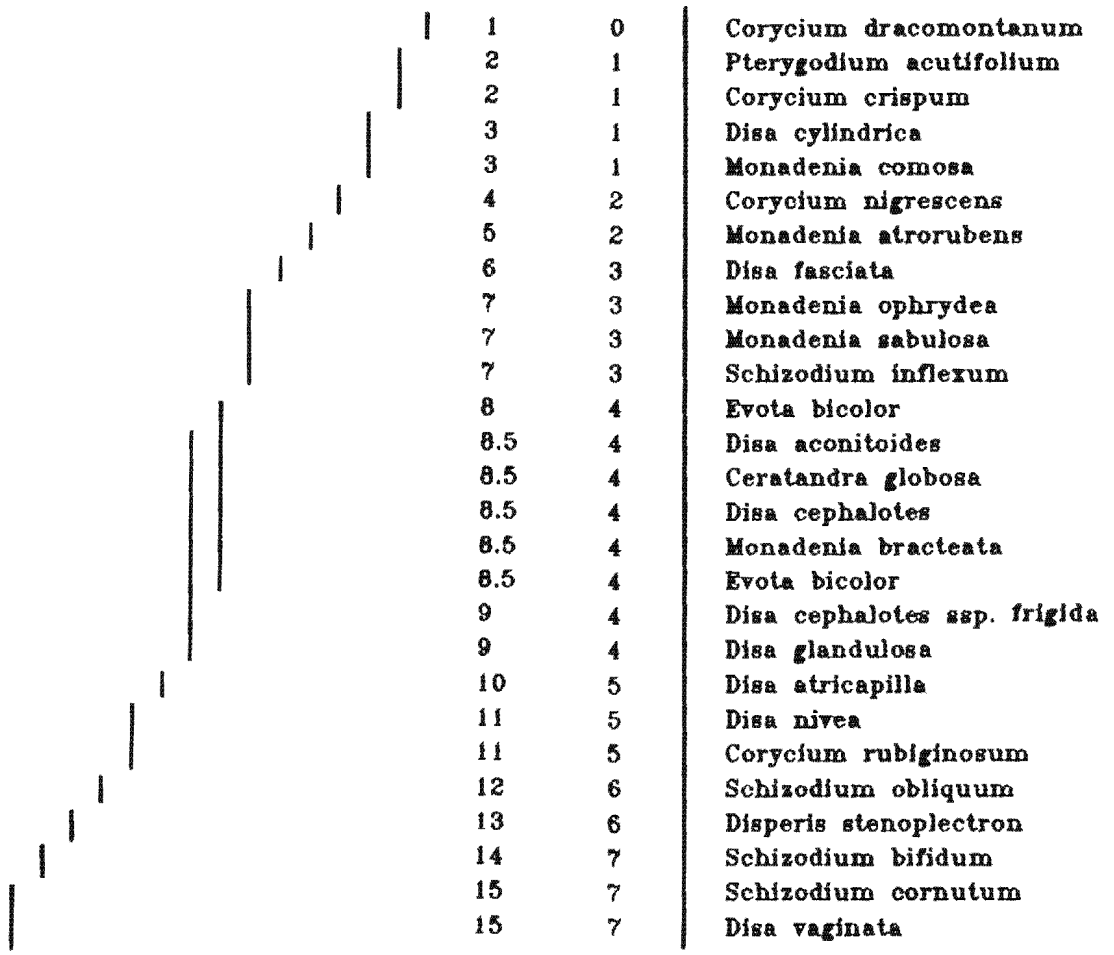

homogeneous subset code	actual code	
1	0	Corycium dracomontanum
2	1	Pterygodium acutifolium
2	1	Corycium crispum
3	1	Disa cylindrica
3	1	Monadenia comosa
4	2	Corycium nigrescens
5	2	Monadenia atrorubens
6	3	Disa fasciata
7	3	Monadenia ophrydea
7	3	Monadenia sabulosa
7	3	Schizodium inflexum
8	4	Evota bicolor
8.5	4	Disa aconitoides
8.5	4	Ceratandra globosa
8.5	4	Disa cephalotes
8.5	4	Monadenia bracteata
8.5	4	Evota bicolor
9	4	Disa cephalotes ssp. frigida
9	4	Disa glandulosa
10	5	Disa atricapilla
11	5	Disa nivea
11	5	Corycium rubiginosum
12	6	Schizodium obliquum
13	6	Disperis stenoplectron
14	7	Schizodium bifidum
15	7	Schizodium cornutum
15	7	Disa vaginata

palisade cell width

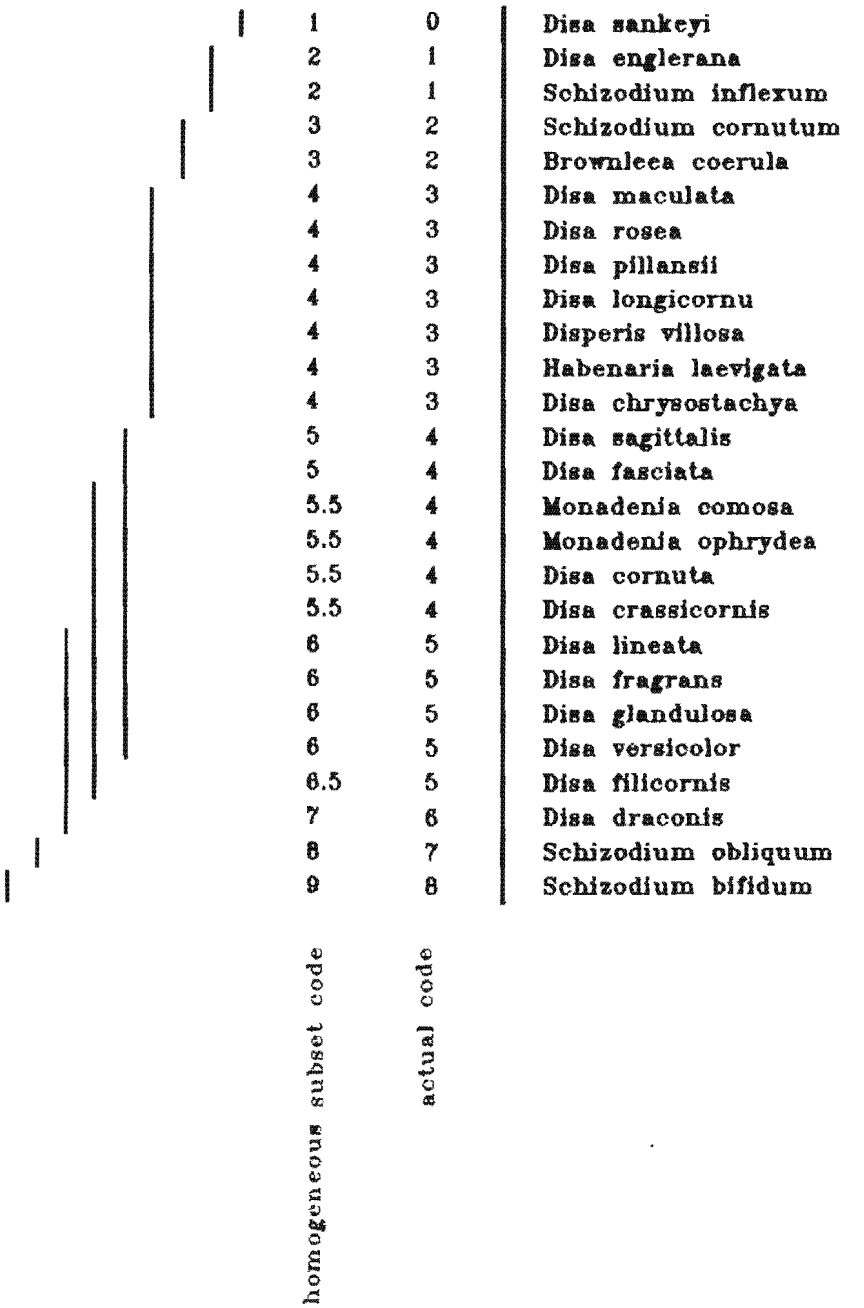

adaxial stomatal width

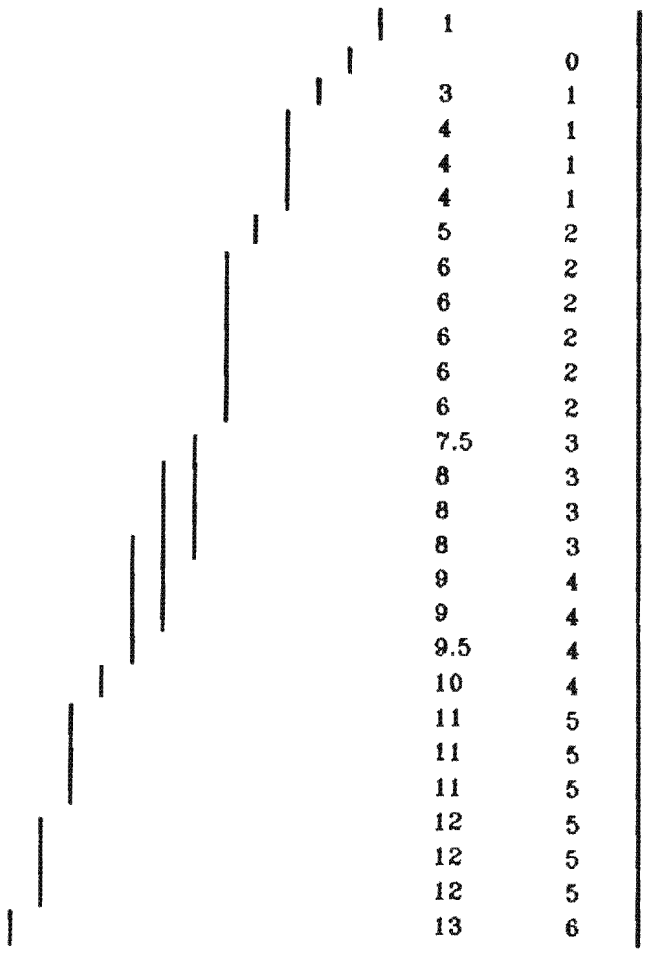

homogeneous subset code	actual code	
1		Monadenia comosa
	0	Corycium dracomontanum
3	1	Pterygodium acutifolium
4	1	Corycium crispum
4	1	Disa cylindrica
4	1	Corycium nigrescens
5	2	Monadenia ophrydea
6	2	Disa fasciata
6	2	Schizodium inflexum
6	2	Disa aconitoides
6	2	Disa cephalotes ssp. frigida
6	2	Monadenia sabulosa
7.5	3	Monadenia atrorubens
8	3	Disa cephalotes
8	3	Evota bicolor
8	3	Disa nivea
9	4	Monadenia bracteata
9	4	Disa glandulosa
9.5	4	Disperis stenoplectron
10	4	Disa atricapilla
11	5	Schizodium bifidum
11	5	Disa vaginata
11	5	Corycium rubiginosum
12	5	Schizodium obliquum
12	5	Ceratandra globosa
12	5	Evota bicolor
13	6	Schizodium cornutum

palisade cell length: width ratio

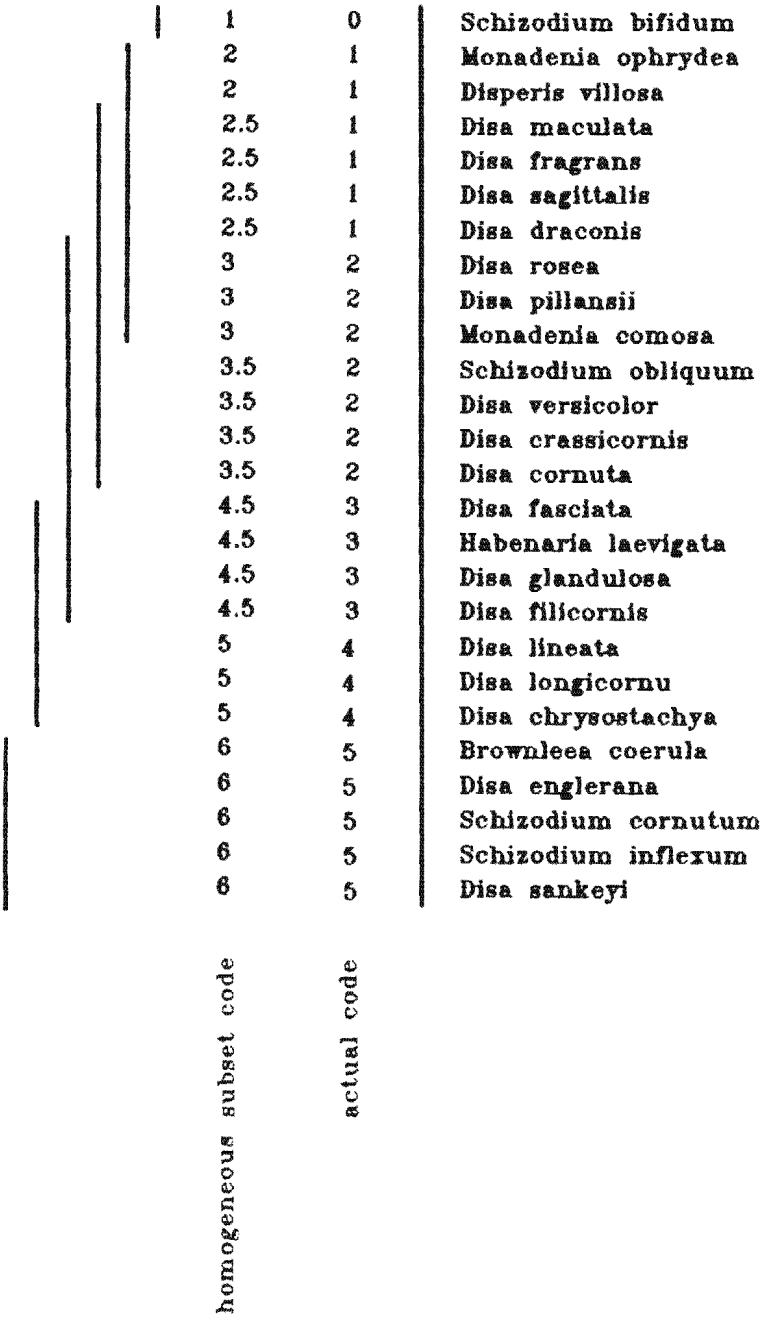

palisade cell length

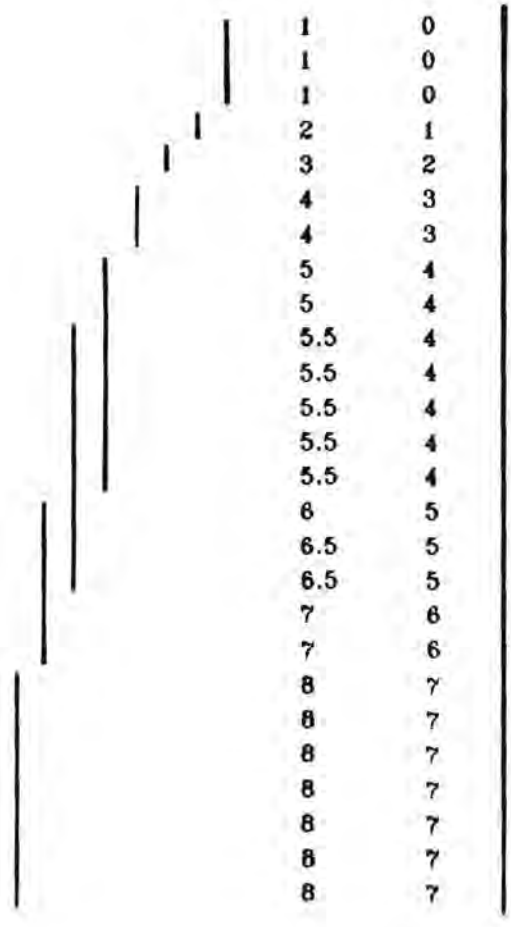

homogeneous subset code	actual code	
1	0	Disa maculata
1	0	Disperis villosa
1	0	Disa rosea
2	1	Disa pillansii
3	2	Monadenia ophrydea
4	3	Disa sankeyi
4	3	Disa sagittalis
5	4	Habenaria laevigata
5	4	Monadenia comosa
5.5	4	Disa fragrans
5.5	4	Disa crassicornis
5.5	4	Disa longicornu
5.5	4	Disa englerana
5.5	4	Disa cornuta
6	5	Schizodium inflexum
6.5	5	Disa chrysostachya
6.5	5	Disa fasciata
7	6	Disa versicolor
7	6	Disa draconis
8	7	Schizodium bifidum
8	7	Disa lineata
8	7	Disa glandulosa
8	7	Schizodium cornutum
8	7	Schizodium obliquum
8	7	Disa filicornis
8	7	Brownleea coerula

abaxial epidermal cell length:width ratio

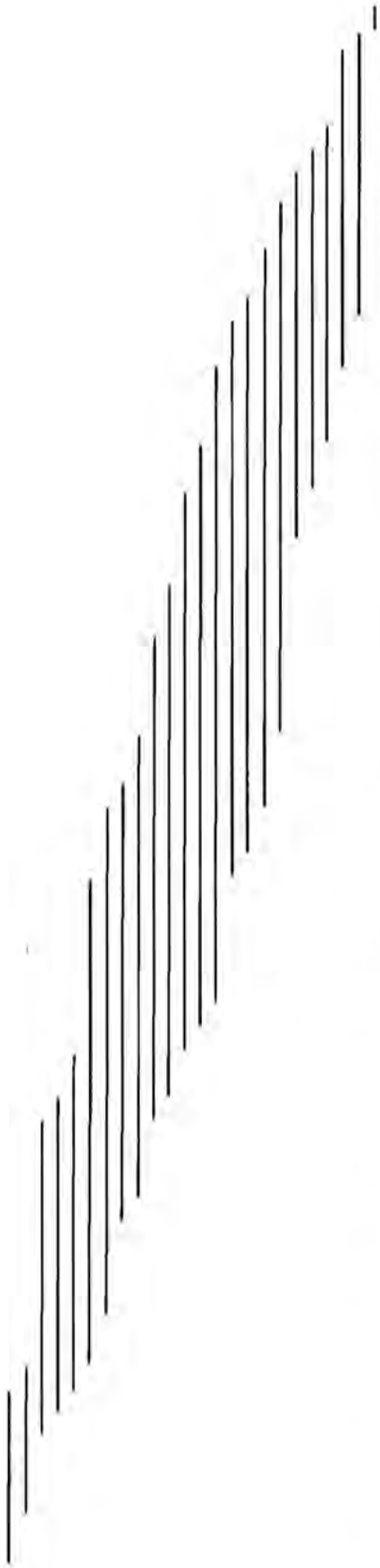

homogeneous subset code	actual code	
1	0	Disa draconis
2	0	Disa cornuta
2.5	0	Evota bicolor
2.5	0	Disa alticola
2.5	0	Disa saxicola
3	0	Schizodium inflexum
3.5	0	Monadenia atrorubens
4	1	Ceratandra globosa
4.5	1	Evota bicolor
4.5	1	Anochilus hallii
5	1	Schizodium bifidum
5	1	Disa lineata
5.5	1	Monadenia bracteata
6.5	1	Pterygodium alatum
6.5	1	Disa longicornu
7.5	2	Disa crassicornis
7.5	2	Disa patens
7.5	2	Disa tellpogonis
8.5	2	Corycium orobanchoides
8.5	2	Disa filicornis
9.5	2	Pterygodium acutifolium
9.5	2	Brownleca coerula
10	3	Monadenia ophrydea
10	3	Disa uniflora
10.5	3	Disa nivea
10.5	3	Disa glandulosa
11	3	Corycium rubiginosum
11	3	Disa atricapilla
11	3	Corycium dracomontanum
11	3	Ceratandra atrata
12	3	Disperis capensis
12	3	Corycium bicolorum
12.5	3	Schizodium cornutum
13.5	3	Disa cephalotes
13.5	4	Disa cylindrica
14	4	Monadenia sabulosa
15	4	Brownleca parviflora
15	4	Disa chrysostachya
15	4	Disperis villosa
15	4	Disa maculata
15	4	Disa fasciata
15.5	4	Disa fragrans
16	5	Disa aconitoides
17	5	Disa vaginata
17	5	Disperis stenoplectron
18	5	Corycium crispum
19	6	Disa englerana
19	6	Pterygodium caffrum
19	6	Disperis fanniniae
19.5	6	Schizochilus flexuosus
20	6	Disa sankeyi
20	6	Disa rosea
20	6	Disa pillansii
20	6	Satyrium erectum
20.5	6	Disa patula
20.5	6	Pterygodium volucris
21.5	6	Schizodium obliquum
22.5	7	Monadenia comosa
23	7	Disa cephalotes ssp. frigida
23.5	7	Habenaria laevigata
23.5	7	Corycium nigrescens
23.5	7	Disa tysonii
24	7	Disa versicolor
24	7	Disa sagittalis

mesophyll long axis

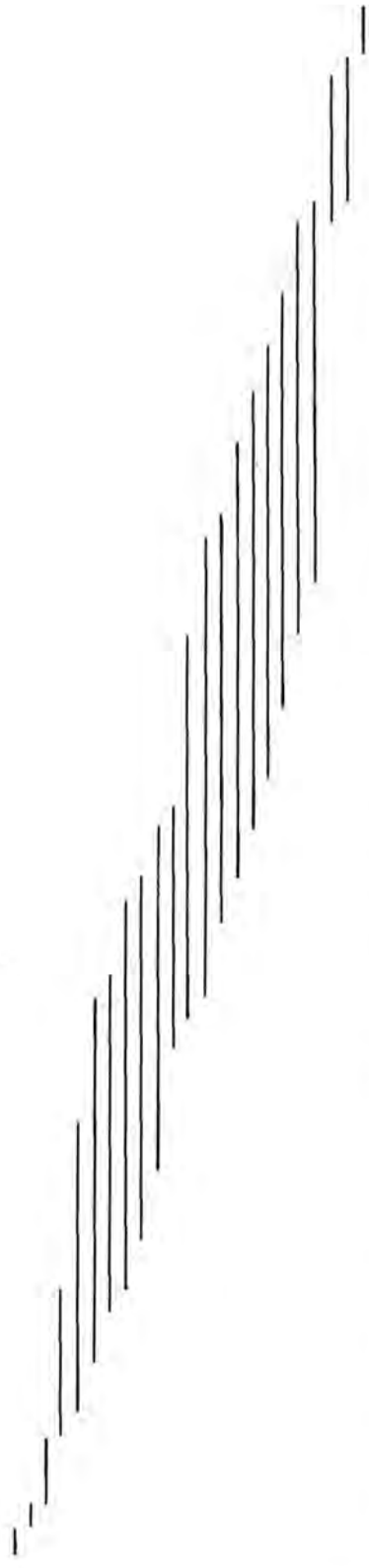

homogeneous subset code	actual code	
1	0	Disperis villosa
1	0	Monadenia comosa
2	0	Corycium dracomontanum
2.5	0	Satyrium erectum
2.5	0	Pterygodium acutifolium
2.5	0	Corycium nigrescens
2.5	0	Disa maculata
2.5	0	Disa rosea
3.5	0	Monadenia sabulosa
4.5	1	Evota bicolor
4.5	1	Corycium crispum
4.5	1	Corycium rubiginosum
5	1	Disa crassicornis
5	1	Anochilus hallii
5.5	1	Disa pillansii
5.5	1	Ceratandra atrata
6	1	Corycium bicolorum
6	1	Disa fragrans
6.5	1	Disa sankeyi
6.5	1	Monadenia ophrydea
6.5	1	Disa fasciata
7	2	Corycium orobanchoides
7.5	2	Monadenia atrorubens
7.5	2	Ceratandra globosa
8	2	Disa telipogonis
8	2	Brownleea coerula
9	2	Disa tysonii
9	2	Disa sagittalis
9	2	Habenaria laevigata
9.5	2	Disa uniflora
9.5	2	Disa vaginata
9.5	2	Disa longicornu
10	3	Evota bicolor
10.5	3	Disa atricapilla
11.5	3	Schizodium inflexum
11.5	3	Disa glandulosa
12.5	3	Pterygodium volucris
13	4	Disa cornuta
13.5	4	Disa draconis
13.5	4	Pterygodium alatum
14	4	Disa versicolor
15	4	Disa chrysostachya
15.5	4	Pterygodium caffrum
16	5	Disa cylindrica
16	5	Disa patula
16	5	Disa filicornis
16.5	5	Schizodium obliquum
16.5	5	Disa englerana
17	5	Schizochilus flexuosus
17	5	Disa saxicola
17	5	Monadenia bracteata
17.5	5	Disperis capensis
17.5	5	Disa lineata
18.5	5	Disa patens
19	6	Disa cephalotes ssp. frigida
19	6	Disa cephalotes
19.5	6	Disperis stenoplectron
19.5	6	Disperis fanniniae
20	6	Disa aconitoides
21	6	Schizodium bifidum
21	6	Disa alticola
21	6	Schizodium cornutum
22	7	Disa nivea
23	7	Brownleea parviflora

Appendix 3

Descriptions of leaf anatomy.

Anatomy Descriptions

Habenaria laevigata

Epidermis and cuticle

Length of adaxial epidermal cells Ø.Ø61 mm; width of adaxial epidermal cells Ø.1Ø3 mm; length to width ratio of adaxial epidermal cells 1.563 ; length of abaxial epidermal cells Ø.Ø98 mm; width of abaxial epidermal cells Ø.Ø69 mm; length to width ratio of abaxial epidermal cells 1.42; depth of adaxial epidermal cells Ø.119 mm; depth of abaxial epidermal cells Ø.Ø4 mm; reticulate cuticle sculpturing; striate cuticle over anticlinal walls of adjacent epidermal cells.

Stomatal apparatus

Hypostomatic; superficial stomata; length of abaxial stomata Ø.Ø51 mm; width of abaxial stomata Ø.Ø51 mm; length to width ratio of abaxial stomata 1.

Vascular bundles

Primary vascular bundle with parenchymatous bundle sheath; 2 secondary vascular bundles with parenchymatous bundle sheaths; 18 tertiary vascular bundles with parenchymatous bundle sheaths.

Leaf articulation mechanism

Expansion cells present at midrib.

Photosynthetic tissue

Heterogenous chlorenchyma; 2 tiers of palisade cells; well developed arm cells in mesophyll; length of longest axis of

mesophyll cells Ø.Ø58 mm; length of palisade cells Ø.Ø77 mm; width of palisade cells Ø.Ø41 mm; length to width ratio of palisade cells 1.878.

Satyrium erectum

Epidermis and cuticle

Length of adaxial epidermal cells Ø.456 mm; width of adaxial epidermal cells Ø.35 mm; length to width ratio of adaxial epidermal cells 1.3Ø3; length of abaxial epidermal cells Ø.22 mm; width of abaxial epidermal cells Ø.116 mm; length to width ratio of abaxial epidermal cells 1.897; depth of adaxial epidermal cells Ø.43 mm; depth of abaxial epidermal cells Ø.Ø76 mm; striate cuticle sculpturing

Stomatal apparatus

Hypostomatic; slightly raised stomata; length of abaxial stomata Ø.Ø79 mm; width of abaxial stomata Ø.Ø63 mm; length to width ratio of abaxial stomata 1.254

Vascular bundles

Primary vascular bundle with parenchymatous bundle sheath; 8 secondary vascular bundles with parenchymatous bundle sheaths; 24 tertiary vascular bundles without bundle sheaths.

Photosynthetic tissue

Homogenous chlorenchyma; well developed arm cells in mesophyll; length of longest axis of mesophyll cells Ø.Ø93 mm.

Schizochilus flexuosus

Epidermis and cuticle

Length of adaxial epidermal cells Ø.15 mm; width of adaxial epidermis cells Ø.116 mm; length to width ratio of adaxial epidermal cells 1.293 mm; length of abaxial epidermal cells Ø.13 mm; width of abaxial epidermal cells Ø.Ø65; length to width ratio of abaxial epidermal cells 2; depth of adaxial epidermal cells Ø.13 mm; depth of abaxial epidermal cells Ø.Ø54 mm; papillose cuticle sculpturing.

Vascular bundles

Primary vascular bundles with parenchymatous bundle sheath; 2 secondary vascular bundles with parenchymatous bundles sheaths; 8 tertiary vascular bundles without bundle sheaths.

Photosynthetic tissue

Homogenous chlorenchyma; rounded cells in mesophyll; length of longest axis of mesophyll cells Ø.Ø4 mm.

Corycium bicolorum

Epidermis and cuticle

Length of adaxial epidermal cells Ø.445 mm; width of adaxial epidermal cells Ø.194 mm; length to width ratio of adaxial epidermal cells 2.294; length of abaxial epidermal cells Ø.276 mm; width of abaxial epidermal cells Ø.1Ø1 mm; length to width ratio of abaxial epidermal cells 2.733; depth of adaxial

epidermal cells Ø.16 mm; depth of abaxial epidermal cells Ø.116 mm; striate cuticle sculpturing.

Stomatal apparatus

Hypostomatic; slightly sunken stomata; length of abaxial stomata Ø.Ø67 mm; width of abaxial stomata Ø.Ø65 mm; length to width ratio of abaxial stomata 1.Ø31.

Vascular bundles

Primary vascular bundle with parenchymatous bundle sheath; 2 secondary vascular bundles with parenchymatous bundle sheaths; 1Ø tertiary vascular bundles with with parenchymatous bundle sheaths.

Leaf articulation mechanism

Adaxial epidermal cell size reduced at midrib; adaxial epidermal cell size reduced at secondary veins.

Photosynthetic tissue

Homogenous chlorenchyma; rounded cells in mesophyll; length of longest axis of mesophyll cells Ø.Ø71 mm

Corycium orobanchoides

Epidermis and cuticle

Length of adaxial epidermal cells Ø.517 mm; width of adaxial epidermal cells Ø.1Ø4 mm; length to width ratio of adaxial epidermal cells 4.971; length of abaxial epidermal cells Ø.249 mm; width of abaxial epidermal cells Ø.Ø75 mm; length to width ratio of abaxial epidermal cells 3.32; depth of adaxial epidermal

cells Ø.151 mm; depth of abaxial epidermal cells Ø.Ø51 mm; striate cuticle sculpturing.

Stomatal apparatus

Hypostomatic; superficial stomata; length of abaxial stomata Ø.Ø75 mm; width of abaxial stomata Ø.Ø51 mm; length to width ratio of abaxial stomata 1.471.

Vascular bundles

Primary vascular bundle with parenchymatous bundle sheath; 2 secondary vascular bundles with parenchymatous bundle sheaths; 8 tertiary vascular bundles with parenchymatous bundle sheaths.

Leaf articulation mechanism

Adaxial epidermal cell size reduced at midrib; adaxial epidermal cell size reduced at secondary veins.

Photosynthetic tissue

Homogenous chlorenchyma; mesophyll cells arm-like; length of longest axis of mesophyll cells Ø.Ø67 mm.

Corycium dracomontanum

Epidermis and cuticle

Llength of adaxial epidermal cells Ø.254 mm; width of adaxial epidermal cells Ø.12 mm; length to width ratio of adaxial epidermal cells 2.117; length of abaxial epidermal cells Ø.16 mm; width of abaxial epidermal cells Ø.Ø88 mm; length to width ratio of abaxial epidermal cells 1.86; depth of adaxial epidermal cells Ø.1Ø5 mm; depth of abaxial epidermal cells Ø.Ø68 mm; Psilate

cuticle; anticlinal walls of abaxial epidermal cells slightly undulated.

Stomatal apparatus

Amphistomatic; slightly sunken stomata; length of adaxial stomata Ø.Ø86 mm; width of adaxial stomata Ø.Ø77 mm; length to width ratio of adaxial stomata 1.117; length of abaxial stomata Ø.Ø82 mm; width of abaxial stomata Ø.Ø7 mm; length to width of abaxial stomata 1.171.

Vascular bundles

Primary vascular bundle with parenchymatous bundle sheath; 2 secondary vascular bundles with parenchymatous bundle sheaths; 14 tertiary vascular bundles with parenchymatous bundle sheaths; leaf ribbed.

Leaf articulation mechanism

Expansion cells present at midrib; adaxial epidermal cell size reduced at midrib; adaxial epidermal cell size reduced at secondary vein.

Photosynthetic tissue

Homogenous chlorenchyma; arm-like mesophyll cells; length of longest axis of mesophyll cells Ø.1Ø2 mm.

Corycium nigrescens

Epidermis and cuticle

Length of adaxial epidermal cells Ø.126 mm; width of adaxial epidermal cells Ø.11Ø mm; length to width ratio of adaxial

epidermal cells 1.145 mm; length of abaxial epidermal cells Ø.161 mm; width of abaxial epidermal cells Ø.115 mm; length to width ratio of abaxial epidermal cells 1.4; depth of adaxial epidermal cells Ø.142 mm; depth of abaxial epidermal cells Ø.Ø94 mm; papillose sculpturing of cuticle.

Stomatal apparatus

Amphistomatic; slightly raised stomata; length of adaxial stomata Ø.Ø7Ø mm; width of adaxial stomata Ø.Ø67 mm; length to width ratio of adaxial stomata 1.Ø45; length of abaxial stomata Ø.Ø74 mm; width of abaxial stomata Ø.Ø66 mm; length to width ratio of abaxial stomata 1.121;

Vascular bundles

primary vascular bundle with parenchymatous bundle sheath; 8 secondary vascular bundles with parenchymatous bundle sheaths; 26 tertiary vascular bundles with parenchymatous bundle sheaths; leaf ribbed.

Leaf articulation mechanism

Adaxial epidermal cell size reduced at midrib; adaxial epidermal cell size reduced at secondary veins.

Photosynthetic tissue

Homogenous chlorenchyma; arm-like mesophyll cells; length of longest axis of mesophyll cells Ø.Ø92 mm.

Corycium rubiginosum

Epidermis and cuticle

Length of adaxial epidermal cells 0.124 mm; width of adaxial epidermal cells 0.051 mm; length to width ratio of adaxial epidermal cells 2.431; length of abaxial epidermal cells 0.044 mm; width of abaxial epidermal cells 0.041 mm; length to width ratio of abaxial epidermal cells 1.073; depth of adaxial epidermal cells 0.057; depth of abaxial epidermal cells 0.066 mm; psilate cuticle; anticlinal walls of adaxial epidermal cells undulated.

Stomatal apparatus

Amphistomatic; slightly sunken stomata; length of adaxial stomata 0.044 mm; width of adaxial stomata 0.041 mm; length to width ratio of adaxial stomata 1.073 mm; length of abaxial stomata 0.138 mm; width of abaxial stomata 0.048 mm; length to width ratio of abaxial stomata 2.875.

Vascular bundles

Primary vascular bundle with parenchymatous bundle sheath; 6 secondary vascular bundles with parenchymatous bundle sheaths; 4 tertiary vascular bundles with parenchymatous bundles sheaths.

Photosynthetic tissue

Homogenous chlorenchyma; mesophyll with well developed arm cells; length of longest axis of mesophyll cells 0.074 mm.

Corycium crispum

Epidermis and cuticle

length of adaxial epidermal cells Ø.269 mm; width of adaxial epidermal cells Ø.113 mm; length to width ratio of adaxial epidermal cells 2.381; length of abaxial epidermal cells 1.195 mm; width of abaxial epidermal cells Ø.Ø97 mm; length to width ratio of abaxial epidermal cells 2.Ø1; depth of adaxial epidermal cells Ø.Ø92 mm; depth of abaxial epidermal cells Ø.Ø65 mm; striate cuticle sculpturing; striate cuticle over anticlinal walls of adjacent epidermal cells.

Stomatal apparatus

Amphistomatic; slightly raised stomata; length of adaxial stomata Ø.Ø79 mm; width of adaxial stomata Ø.Ø68 mm; length to width ratio of adaxial stomata 1.162; length of abaxial stomata Ø.Ø74 mm; width of abaxial stomata Ø.Ø66 mm; length to width ratio of abaxial stomata 1.121.

Vascular bundles

Primary vascular bundle with parenchymatous bundle sheath; 8 tertiary vascular bundles with parenchymatous bundle sheaths.

Leaf articulation mechanism

Adaxial cell size reduced at midrib.

Photosynthetic tissue

Homogenous chlorenchyma; less rounded mesophyll cells.

Pterygodium caffrum

Epidermis and cuticle

Length of adaxial epidermal cells Ø.2Ø9 mm; width of adaxial epidermal cells Ø.137 mm; length to width ratio of adaxial epidermal cells 1.526; length of abaxial epidermal cells Ø.135 mm; width of abaxial epidermal cells Ø.Ø68 mm; length to width ratio of abaxial epidermal cells 1.985; depth of adaxial epidermal cells Ø.117 mm; depth of abaxial epidermal cellsØ.Ø68 mm; striate cuticle sculpturing; anticlinal walls of adaxial epidermal cells slightly undulated; anticlinal walls of abaxial epidermal cells slightly undulated.

Stomatal apparatus

Hypostomatic; slightly raised stomata; length of abaxial stomata Ø.Ø63 mm; width of abaxial stomata Ø.Ø65 mm; length to width ratio of abaxial stomata Ø.969.

Vascular bundles

Primary vascular bundle with parenchymatous bundle sheath; 4 secondary vascular bundles with parenchymatous bundle sheaths; 16 tertiary vascular bundles with parenchymatous bundle sheaths.

Leaf articulation mechanism

Adaxial epidermal cell size reduced at midrib; adaxial epidermal cell size reduced at secondary veins.

Photosynthetic tissue

Homogenous chlorenchyma; mesophyll with arm-like cells; length of longest axis of mesophyll cells Ø.Ø45 mm.

Pterygodium alatum

Epidermis and cuticle

Length of adaxial epidermal cells 0.241 mm; width of adaxial epidermal cells 0.123 mm; length to width ratio of adaxial epidermal cells 1.959; length of abaxial epidermal cells 0.212 mm; width of abaxial epidermal cells 0.057 mm; length to width ratio of abaxial epidermal cells 3.719 mm; depth of adaxial epidermal cells 0.118 mm; depth of abaxial epidermal cells 0.054 mm; striate cuticle sculpturing; anticlinal walls of abaxial epidermal cells undulated.

Stomatal apparatus

Hypostomatic; superficial stomata; length of abaxial stomata 0.068 mm; width of abaxial stomata 0.061 mm; length to width ratio of abaxial stomata 1.115.

Vascular bundles

Primary vascular bundle with parenchymatous bundle sheath; 4 secondary vascular bundles with parenchymatous bundle sheaths; 10 tertiary vascular bundles with parenchymatous bundle sheaths;

Leaf articulation mechanism

Adaxial epidermal cell size reduced at midrib; adaxial epidermal cell size reduced at secondary veins.

Photosynthetic tissue

Homogenous chlorenchyma; arm-like cells in mesophyll; length of longest axis of mesophyll cells 0.051 mm.

Pterygodium volucris

Epidermis and cuticle

Length of adaxial epidermal cells Ø.286 mm; width of adaxial epidermal cells Ø.149 mm; length to width ratio of adaxial epidermal cells 1.919; length of abaxial epidermal cells Ø.172 mm; width of abaxial epidermal cells Ø.095 mm; length to width ratio of abaxial epidermal cells 1.811; depth of adaxial epidermal cells Ø.194 mm; depth of abaxial epidermal cells Ø.063 mm; psilate cuticle.

Stomatal apparatus

Hypostomatic; superficial stomata; length of abaxial stomata Ø.Ø81 mm; width of abaxial stomata Ø.Ø57 mm; length to width ratio of abaxial stomata 1.Ø7 mm.

Vascular bundles

Primary vascular bundle with parenchymatous bundle sheath; 4 secondary vascular bundles with parenchymatous bundle sheaths; 10 tertiary vascular bundles with parenchymatous bundle sheaths.

Leaf articulation mechanism

Adaxial epidermal cell size reduced at midrib; adaxial epidermal cell size reduced at secondary veins.

Photosynthetic tissue

Homogenous chlorenchyma, arm-like cells in mesophyll; length of longest axis of mesophyll cells Ø.Ø52 mm.

Pterygodium acutifolium

Epidermis and cuticle

Length of adaxial epidermal cells 0.365 mm; width of adaxial epidermal cells 0.12 mm; length to width ratio of adaxial epidermal cell 3.042; length of abaxial epidermal cells 0.350 mm; width of abaxial epidermal cells 0.115 mm; length to width ratio of abaxial epidermal cells 3.043; depth of adaxial epidermal cells 0.13 mm; depth of abaxial epidermal cells 0.1 mm; psilate cuticle.

Stomatal apparatus

Amphistomatic; slightly sunken stomata; length of adaxial stomata 0.08 mm; width of adaxial stomata 0.07 mm; length to width ratio of adaxial stomata 1.143; length of abaxial stomata 0.072 mm; width of abaxial stomata 0.06 mm; length to width ratio of abaxial stomata 1.2 mm.

Vascular bundles

Primary vascular bundle with parenchymatous bundle sheath, 6 secondary vascular bundles with parenchymatous bundle sheaths; 6 tertiary vascular bundles with parenchymatous bundle sheaths.

Leaf articulation mechanism

Adaxial epidermal cell size reduced at midrib; adaxial epidermal cell size reduced at secondary veins.

Photosynthetic tissue

Homogenous chlorenchyma; well developed arm cells in mesophyll; length of longest axis of mesophyll cells 0.09 mm.

Anochilus hallii

Epidermis and cuticle

Length of adaxial epidermal cells Ø.5Ø2 mm; width of adaxial epidermal cells Ø.122 mm; length to width ratio of adaxial epidermal cells 4.115 mm; length of abaxial epidermal cells Ø.271 mm; width of abaxial epidermal cells Ø.Ø67 mm; length to width ratio of abaxial epidermal cells 4.Ø45 mm; depth of adaxial epidermal cells Ø.156 mm; depth of abaxial epidermal cells Ø.Ø67 mm; striate cuticle sculpturing; striate cuticle over anticlinal wall of adjacent epidermal cells.

Stomatal apparatus

Hypostomatic; slightly raised stomata; length of abaxial stomata Ø.Ø71 mm; width of abaxial stomata Ø.Ø65 mm; length to width ratio of abaxial stomata 1.Ø92.

Vascular bundles

Primary vascular bundle with parenchymatous bundle sheath; 6 secondary vascular bundles with parenchymatous bundle sheaths; 18 tertiary vascular bundles with parenchymatous bundle sheaths.

Leaf articulation mechanism

Adaxial epidermal cell size reduced at midrib; adaxial epidermal cell size reduced at secondary veins.

Photosynthetic tissue

Homogeneous chlorenchyma; well developed arm cells in mesophyll; length of longest axis of mesophyll cells Ø.Ø73 mm.

Evota bicolor

Epidermis and cuticle

Length of adaxial epidermal cells 0.127 mm; width of adaxial epidermal cells 0.039 mm; length to width of adaxial epidermal cells 3.256; length of abaxial epidermal cells 0.120 mm; width of abaxial epidermal cells 0.030 mm; length to width ratio of abaxial epidermal cells 4; depth of adaxial epidermal cells 0.036 mm; depth of abaxial epidermal cells 0.004 mm; psilate cuticle; anticlinal wall sof adaxial epidermal cells undulated ; anticlinal walls of abaxial epidermal cells undulated

Stomatal apparatus

Amphistomatic; superficial stomata; length of adaxial stomata 0.052 mm; width of adaxial stomata 0.037 mm; length to width ratio of adaxial stomata 1.405; length of abaxial stomata 0.056 mm; width of abaxial stomata 0.039 mm; length to width ratio of abaxial stomata 1.436 mm.

Vascular bundles

Primary vascular bundle with parenchymatous bundle sheath; 2 secondary vascular bundles with p[arenchymatous bundle sheaths; 4 tertiary vascular bundles with parenchymatous bundle sheaths.

Photosynthetic tissue

Homogenous chlorenchyma arm-like cells in mesophyll; length of longest axis of mesophyll cells 0.083 mm

Evota bicolor

Epidermis and cuticle

Length of adaxial epidermal cells 0.107 mm; width of adaxial epidermal cells 0.049 mm; length to width ratio of adaxial epidermal cells 2.184 mm; length of abaxial epidermal cells 0 056 mm; width of abaxial epidermal cells 0.051 mm; length to width ratio of abaxial epidermal cells 1.098; depth opf adaxial epidermal cells 0.044 mm; depth of abaxial epidermal cells 0.047 mm; psilate cuticle; anticlinal walls of adaxial epidermal cells undulated; anticlinal walls of abaxial epidermal cells undulated.

Stomatal apparatus

Amphistomatic; superficial stomata; length of adaxial stomata 0.056 mm; width of adaxial stomata 0.051 mm; length to width ratio of adaxial stomata 1.098; length of abaxial stomata 0.063 mm; width of abaxial stomata 0.040 mm; length to width ratio of abaxial stomata 1.575.

Vascular bundles

Primary vascular bundle with parenchymatous bundle sheath; 4 secondary vascular bundles with parenchymatous bundle sheaths; 6 tertiary vascular bundles with parenchymatous bundle sheaths.

Photosynthetic tissue

Homogenous chlorenchyma; arm-like cells in mesophyll; length of longest axis of mesophyll cells 0.077 mm.

Ceratandra globosa

Epidermis and cuticle

Papillae present on leaf margin; length of adaxial epidermal cells 0.268 mm; width of adaxial epidermal cells 0.040 mm; length to width ratio of adaxial epidermal cells 6.70 mm; length of abaxial epidermal cells 0.190 mm; width of abaxial epidermal cells 0.048 mm; length to width ratio of abaxial epidermal cells 3.958 mm; papillose sculpturing of cuticle; anticlinal walls of abaxial epidermal cells undulated.

Stomatal apparatus

Amphistomatic; slightly raised stomata; length of adaxial stomata 0.051 mm; width of adaxial stomata 0.035 mm; length to width ratio of adaxial stomata 1.457; length of abaxial stomat 0.055 mm; width of abaxial stomata 0.051 mm; length to width ratio of abaxial stomata 1.078.

Vascular bundles

Primary vascular bundle with parenchymatous bundle sheath; adaxial and abaxial schlerenchyma caps at poles of primary vascular bundle; 2 secondary vascular bundles with parenchymatous bundle sheaths; schlerenchyma caps at adaxial pole of secondary vascular bundles; 8 tertiary vascular bundles with parenchymatous bundle sheaths.

Photosynthetic tissue

Homogenous chlorenchyma; less rounded cells in mesophyll; length of longest axis of mesophyll cells 0.058 mm.

Ceratandra atrata

Epidermis and cuticle

Papillae present at leaf margins; length of adaxial epidermal cells 0.310 mm; width of adaxial epidermal cells 0.067 mm; length to width ratio of adaxial epidermal cells 4.627; length of abaxial epidermal cells 0.170 mm; width of abaxial epidermal cells 0.058 mm; length to width ratio of abaxial epidermal cells 2.931; depth of adaxial epidermal cells 0.066 mm; depth of abaxial epidermal cells 0.050 mm; papillose cuticle sculpturing.

Stomatal apparatus

Hypostomatic; superficial stomata; length of abaxial stomata 0.05 mm; width of abaxial stomata 0.040 mm; length to width ratio of abaxial stomata 1.25.

Vascular bundles

Primary vascular bundle with parenchymatous bundle sheath; adaxial and abaxial schlerenchyma caps present at the poles of the primary vascular bundle; 2 secondary vascular bundles with parenchymatous bundle sheaths; adaxial and abaxial schlerenchyma caps present at poles of secondary vascular bundles; 6 tertiary vascular bundles with parenchymatous bundle sheaths; adaxial schlerenchyma caps present at poles of 2 of the 6 tertiary vascular bundles.

Photosynthetic tissue

Homogenous chlorenchyma; arm-like cells in the mesophyll; length of longest axis of mesophyll cells 0.066 mm.

Disperis fanniniae

Epidermis and cuticle.

Papillae on adaxial epidermis; length of adaxial epidermal cells 0.082 mm; width of adaxial epidermal cells 0.054 mm; length to width ratio of adaxial epidermal cells 1.519 mm; length of abaxial epidermal cells 0.074 mm; width of adaxial epidermal cells 0.038 mm; length to width ratio of abaxial epidermal cells 1.947; depth of adaxial epidermal cells 0.037 mm; depth of abaxial epidermal cells 0.021 mm.

Stomatal apparatus

Hypostomatic; slightly raised stomata; length of abaxial stomata 0.052 mm; width of abaxial stomata 0.044 mm; length to width of abaxial stomata 1.182.

Vascular bundles

Primary vascular bundle with parenchymatous bundle sheath; 2 secondary vascular bundles with parenchymatous bundle sheaths; 6 tertiary vascular bundles with parenchymatous bundle sheaths.

Leaf articulation mechanism

Adaxial epidermal cell size reduced at midrib.

Photosynthetic tissue

Homogenous chlorenchyma; less rounded cells in mesophyll; length of longest axis of mesophyll cells 0.035 mm.

Disperis villosa

Epidermis and cuticle

Hairs present on leaf margin; length of adaxial epidermal cells 0.184 mm; width of adaxial epidermal cells 0.118 mm; length to width ratio of adaxial epidermal cells 1.559; length of abaxial epidermal cells 0.179 mm; width of abaxial epidermal cells 0.075 mm; length to width ratio of abaxial epidermal cells 2.387; depth of adaxial epidermal cells 0.105 mm; depth of abaxial epidermal cells 0.040 mm, psilate cuticle; anticlinal walls of adaxial epidermal cells undulated.

Stomatal apparatus

Hypostomatic; superficial stomata; length of abaxial stomata 0.054 mm; width of abaxial stomata 0.050 mm; length to width ratio of abaxial stomata 1.08.

Vascular bundles

Primary vascular bundle with parenchymatous bundle sheath; 2 secondary vascular bundles with parenchymatous bundle sheaths; 10 tertiary vascular bundles with parenchymatous bundle sheaths.

Photosynthetic tissue

"Heterogenous" chlorenchyma; single tier of tapered palisade-like cells; well developed arm cells in mesophyll; length of longest axis of mesophyll cells 0.122 mm; length of palisade cells 0.108 mm; width of palisade cells 0.042 mm; length to width ratio of palisade cells 2.524.

Disperis capensis

Epidermis and cuticle

Length of adaxial epidermal cells 0.138 mm; width of adaxial epidermal cells 0.056 mm; length to width ratio of adaxial epidermal cells 2.464; length of abaxial epidermal cells 0.107 mm; width of abaxial epidermal cells 0.040 mm; length to width ratio of abaxial epidermal cells 2.675; depth of adaxial epidermal cells 0.052 mm; depth of abaxial epidermal cells 0.035 mm; psilate cuticle; anticlinal walls of adaxial epidermal cells undulated; anticlinal walls of abaxial epidermal cells undulated.

Stomatal apparatus

Hypostomatic; superficial stomata; length of abaxial stomata 0.065 mm; width of abaxial stomata 0.051 mm; length to width of abaxial stomata 1.275.

Vascular bundles

Primary vascular bundle with parenchymatous bundle sheath; 4 secondary vascular bundles with parenchymatous bundle sheaths; 6 tertiary vascular bundles with parenchymatous bundle sheaths.

Photosynthetic tissue

Homogenous chlorenchyma with palisade-like cells towards the leaf margins; well developed arm cells in the mesophyll; length of longest axis of mesophyll cells 0.043 mm.

Disperis stenoplectron

Epidermis and cuticle

Epidermal hairs present; length of adaxial epidermal cells 0.068 mm; width of adaxial epidermal cells 0.054 mm; length to width

ratio of adaxial epidermal cells 1.259; length of abaxial epidermal cells 0.070 mm; width of abaxial epidermal cells 0.038 mm; length to width ratio of abaxial epidermal cells 1.842; depth of adaxial epidermal cells 0.058 mm; depth of abaxial epidermal cells 0.028 mm; psilate cuticle.

Stomatal apparatus

Amphistomatic; superficial stomata; length of adaxial stomata 0.040 mm; width of adaxial stomata 0.0450 mm; length to width ratio of adaxial stomata 0.889; length of abaxial stomata 0.048 mm; width of abaxial stomata 0.042 mm; length to width ratio of abaxial stomata 1.143.

Vascular bundles

Primary vascular bundles with parenchymatous bundle sheath; 6 secondary vascular bundles with parenchymatous bundle sheaths; 14 tertiary vascular bundles with parenchymatous bundle sheaths.

Photosynthetic tissue

Homogenous chlorenchyma; rounded mesophyll cells; length of longest axis of mesophyll cells 0.032 mm.

Schizodium cornutum

Epidermis and cuticle

Length of adaxial epidermal cells 0.075 mm; width of adaxial epiderma cells 0.040 mm; length to width ratio of adaxial epidermal cells 1.875; length of abaxial epidermal cells 0.099 mm; width of abaxial epidermal cells 0.037 mm; length to width

ratio of abaxial epidermal cells 2.676; depth of adaxial epidermal cells 0.038 mm; depth of abaxial epidermal cells 0.028 mm; psilate cuticle; anticlinal walls of adaxial epidermal cells undulated; anticlinal walls of abaxial epidermal cells undulated.

Stomatal apparatus

Amphistomatic; superficial stomata; length of adaxial stomata 0.034 mm; width of adaxial stomata 0.033 mm; length to width ratio of adaxial stomata 1.030; length of abaxial stomata 0.038 mm; width of abaxial stomata 1.226; length to width ratio of abaxial stomata 1.226.

Vascular bundles

Primary vascular bundle with parenchymatous bundle sheath; 6 secondary vascular bundles with parenchymatous bundle sheaths; 2 tertiary vascular bundles with parenchymatous bundle sheaths.

Photosynthetic tissue

Heterogenous chlorenchyma; 1 tier of palisade cells; less rounded mesophyll cells; length of longest axis of mesophyll cells 0.029 mm; length of palisade cells 0.053 mm; width of palisade cells 0.023 mm; length to width ratio of palisade cells 2.304.

Schizodium obliquum

Epidermis and cuticle

length of adaxial epidermal cells 0.094 mm; width of adaxial epidermal cells 0.049 mm; length to width ratio of adaxial epidermal cells 1.918; length of abaxial epidermal cells 0.158

mm; width of abaxial epidermal cells Ø.1Ø1 mm; length to width ratio of abaxial epidermal cells 1.564; depth of adaxial epidermal cells Ø.Ø56 mm; depth of abaxial epidermal cells Ø.Ø44 mm; psilate cuticle; anticlinal walls of adaxial epidermal cells undulated.

Stomatal apparatus

Amphistomatic; slightly raised stomata; length of adaxial stomata Ø.Ø43 mm; width of adaxial stomata Ø.Ø39 mm; length to width ratio of adaxial stomata 1.1Ø3; length of abaxial stomata Ø.Ø85 mm; width of abaxial stomata Ø.Ø55 mm; length to width of abaxial stomata 1.182.

Vascular bundles

Primary vascular bundle with parenchymatous bundle sheath; 2 secondary vascular bundles with parenchymatous bundle sheaths; 8 tertiary vascular bundles with parenchymatous bundle sheaths.

Photosynthetic tissue

Heterogenous chlorenchyma; 1 tier of palisade cells; less rounded mesophyll cells; length of longest axis of mesophyll cells Ø.Ø35 mm; length of palisade cells Ø.Ø51 mm; width of palisade cells Ø.Ø51 mm; length to width ratio of palisade cells Ø.Ø51.

Schizodium bifidum

Epidermis and cuticle

Length of adaxial epidermal cells Ø.Ø76 mm; width of adaxial epidermal cells Ø.Ø51 mm; length to width ratio of adaxial

epidermal cells 1.490; length of abaxial epidermal cells 0.112 mm; width of abaxial epidermal cells 0.034 mm; length to width ratio of abaxial epidermal cells 3.294; depth of adaxial epidermal cells 0.038 mm; depth of abaxial epidermal cells 0.034 mm; psilate cuticle; anticlinal walls of adaxial epidermal cells undulated; anticlinal walls of abaxial epidermal cells undulated.

Stomatal apparatus

Amphistomatic; superficial stomata; length of adaxial stomata 0.037 mm; width of adaxial stomata 0.043 mm; length to width ratio of adaxial stomata 0.860; length of abaxial stomata 0.043 mm; width of abaxial stomata 0.037 mm; length to width ratio of abaxial stomata 1.162.

Vascular bundles

Primary vascular bundle with parenchymatous bundle sheath; 2 secondary vascular bundles with parenchymatous bundle sheaths; 2 tertiary vascular bundles with parenchymatous bundle sheaths

Photosynthetic tissue

Heterogenous chlorenchyma; arm-like mesophyll cells; 1 tier of palisade cells; length of longest axis of mesophyll cells 0.030 mm; length of palisade cells 0.054 mm; width of palisade cells 0.015 mm; length to width ratio of palisade cells 3.600.

Schizodium inflexum

Epidermis and cuticle

Length of adaxial epidermal cells 0.192 mm; width of adaxial epidermal cells 0.068 mm; length to width ratio of adaxial epidermal cells 2.824; length of abaxial epidermal cells 0.173 mm; width of abaxial epidermal cells 0.039 mm; length to width ratio of abaxial epidermal cells 4.436; depth of adaxial ep[idermal cells 0.050 mm; depth of abaxial epidermal cells 0.039 mm; psilate cuticle.

Stomatal apparatus

Amphistomatic; superficial stomata; length of adaxial stomata 0.057 mm; width of adaxial stomata 0.055 mm; length to width ratio of adaxial stomata 1.036 mm; length of abaxial stomata 0.055 mm; width of abaxial stomata 0.045 mm; length to width ratio of abaxial stomata 1.222.

Vascular bundles

Primary vascular bundle without distinct bundle sheath; 2 secondary vascular bundles without distinct bundle sheaths; 8 tertiary vascular bundles without distinct bundle sheaths.

Photosynthetic tissue

Heterogenous chlorenchyma; 1 tier of palisade cells, less rounded mesophyll cells; length of longest axis of mesophyll cells 0.051 mm; length of palisade cells 0.065 mm; width of palisade cells 0.030 mm; length to width ratio of palisade cells 2.167.

Brownlees parviflora

Epidermis and cuticle

Length of adaxial epidermal cells 0.083 mm; width of adaxial epidermal cells 0.070 mm; length to width ratio of adaxial epidermal cells 1.186; length of abaxial epidermal cells 0.079 mm; width of abaxial epidermal cells 0.032 mm; length to width ratio of abaxial epidermal cells 2.469; depth of adaxial epidermal cells 0.043 mm; depth of abaxial epidermal cells 0.020 mm; psilate cuticle;

Stomatal apparatus

Hypostomatic; superficial stomata; length of abaxial stomata 0.039 mm; width of abaxial stomata 0.037 mm; length to width ratio of abaxial stomata 1.054;

Vascular bundles

Primary vascular bundle with parenchymatous bundle sheath; 4 secondary vascular bundles with parenchymatous bundle sheaths; 32 tertiary vascular bundles with parenchymatous bundle sheaths.

Leaf articulation mechanism

Expansion cells present at midrib (not very clear); adaxial epidermal cell size reduced at midrib; adaxial epidermal cell size reduced at secondary veins.

Photosynthetic tissue

Homogenous chlorenchyma; less rouded cells in mesophyll; length of longest axis of mesophyll cells 0.047 mm;

Brownlesa coerula

Epidermis and cuticle

Length of adaxial epidermal cells 0.097 mm; width of adaxial epidermal cells 0.060 mm; length to width ratio of adaxial epidermal cells 1.617; length of abaxial epidermal cells 0.130 mm; width of abaxial epidermal cells 0.040 mm; length to width ratio of abaxial epidermal cells 3.250; depth of adaxial epidermal cells 0.051 mm; depth of abaxial epidermal cells 0.040 mm; papillose cuticle; anticlinal walls of adaxial epidermal cells undulated.

Stomatal apparatus

Hypostomatic; slightly raised stomata; length of abaxial stomata 0.087 mm; width of abaxial stomata 0.054 mm; length to width ratio of abaxial stomata 1.241;

Vascular bundles

Primary vascular bundle with parenchymatous bundle sheath; 2 secondary vascular bundles with parenchymatous bundle sheaths; 12 tertiary vascular bundles with parenchymatous bundle sheaths.

Leaf articulation mechanism

Adaxial epidermal cell size reduced at midrib

Photosynthetic tissue

Heterogenous chlorenchyma; well developed arm cells in mesophyll; length of longest axis of mesophyll cells 0.057 mm; 2 tiers of palisade cells; length of palisade cells 0.049 mm; width of palisade cells 0.032 mm; length to width ratio of palisade cells 1.531.

Monadenia ophrydea

Epidermis and cuticle

Length of adaxial epidermal cells 0.184 mm; width of adaxial epidermal cells 0.092 mm; length to width ratio of adaxial epidermal cells 2; length of abaxial epidermal cells 0.180 mm; width of abaxial epidermal cells 0.065 mm; length to width ratio of abaxial epidermal cells 2.769; depth of adaxial epidermal cells 0.105 mm; depth of abaxial epidermal cells 0.075 mm; psilate cuticle; striate cuticle over anticlinal walls of adjacent epidermal cells.

Stomatal apparatus

Amphistomatic; superficial stomata; length of adaxial stomata 0.060 mm; width of adaxial stomata 0.060 mm; length to width ratio of adaxial stomata 1; length of abaxial stomata 0.057 mm; width of abaxial stomata 0.059 mm; length to width ratio of abaxial stomata 0.966.

Vascular bundles

Primary vascular bundle with parenchymatous bundle sheath; 4 secondary vascular bundles with parenchymatous bundle sheaths; 20 tertiary vascular bundles with parenchymatous bundle sheaths.

Leaf articulation mechanism

Adaxial epidermal cell size reduced at midrib; adaxial epidermal cell size reduced at secondary veins.

Photosynthetic tissue

Heterogenous chlorenchyma; well developed arm cells in mesophyll; length of longest axis of mesophyll cells 0.068 mm; 1 tier of palisade cells; length of palisade cells 0.091 mm; width of palisade cells 0.036 mm; length to width ratio of palisade cells 2.528.

Monadenia comosa

Epidermis and cuticle

Length of adaxial epidermal cells 0.150 mm; width of adaxial epidermal cells 0.125 mm; length to width ratio of adaxial epidermal cells 1.200; length of abaxial epidermal cells 0.197 mm; width of abaxial epidermal cells 0.132 mm; length to width ratio of abaxial epidermal cells 1.492; depth of adaxial epidermal cells 0.215 mm; depth of abaxial epidermal cells 0.112 mm; cuticle partly psilate, striate and reticulate.

Stomatal apparatus

Amphistomatic although stomata are scarce on adaxial surface; superficial stomatal apparatus: length of adaxial stomata 0.070 mm; width of adaxial stomata 0.080 mm; length to width ratio of adaxial stomata 0.875; length of abaxial stomata 0.078 mm; width of abaxial stomata 0.082 mm; length to width ratio of abaxial stomata 0.951.

Vascular bundles

Primary vascular bundle with parenchymatous bundle sheath; 4 secondary vascular bundles with parenchymatous bundle sheaths; 24 tertiary vascular bundles with parenchymatous bundle sheaths.

Photosynthetic tissue

Heterogenous chlorenchyma; arm-like cells in mesophyll; length of longest axis of mesophyll cells 0.055 mm; 2 tiers of palisade cells; length of palisade cells 0.070 mm; width of palisade cells 0.030 mm; length to width ratio of palisade cells 2.33.

Monadenia atrorubens

Epidermis and cuticle

Length of adaxial epidermal cells 0.190 mm; width of adaxial epidermal cells 0.060 mm; length to width ratio of adaxial epidermal cells 3.167; length of abaxial epidermal cells 0.190 mm; width of abaxial epidermal cells 0.049 mm; length to width ratio of abaxial epidermal cells 3.878; depth of adaxial epidermal cells 0.080 mm; depth of abaxial epidermal cells 0.070 mm; striate cuticle; striate cuticle over anticlinal walls of adjacent epidermal cells

Stomatal apparatus

Amphistomatic; superficial stomata; length of adaxial stomata 0.062 mm; width of adaxial stomata 0.050 mm; length to width ratio of adaxial stomata 1.240; length of abaxial stomata 0.064 mm; width of abaxial stomata 0.050 mm; length to width ratio of abaxial stomata 1.280.

Vascular bundles

Primary vascular bundle with parenchymatous bundle sheath; 2 secondary vascular bundles with parenchymatous bundle sheaths; 8 tertiary vascular bundles with parenchymatous bundle sheaths.

Leaf articulation mechanism

Expansion cells present at midrib (not very clear).

Photosynthetic tissue

Homogenous chlorenchyma; rounded cells in mesophyll; length of longest axis of mesophyll cells 0.061 mm;

Monadenia sabulosa

Epidermis and cuticle

Length of adaxial epidermal cells 0.199 mm; width of adaxial epidermal cells 0.081 mm; length to width ratio of adaxial epidermal cells 2.457; length of abaxial epidermal cells 0.151 mm; width of abaxial epidermal cells 0.060 mm; length to width ratio of abaxial epidermal cells 2.517; depth of adaxial epidermal cells 0.092 mm; depth of abaxial epidermal cells 0.106 mm; papillose sculpturing of cuticle.

Stomatal apparatus

Amphistomatic; slightly sunken stomata; length of adaxial stomata 0.059 mm; width of adaxial stomata 0.054 mm; length to width ratio of adaxial stomata 1.093; length of abaxial stomata 0.048 mm; width of abaxial stomata 0.053 mm; length to width ratio of abaxial stomata 0.906.

Vascular bundles

Primary vascular bundle with parenchymatous bundle sheath; 4 secondary vascular bundles with parenchymatous bundle sheaths; 18 tertiary vascular bundles with parenchymatous bundle sheaths.

Leaf articulation mechanism

Expansion cells present at midrib although not very distinct.

Photosynthetic tissue

Homogenous chlorenchyma; rounded cells in mesophyll; length of longest axis of mesophyll cells mm.

Monadenia bracteata

Epidermis and cuticle

Length of adaxial epidermal cells Ø.197 mm; width of adaxial epidermal cells Ø.Ø64 mm; length to width ratio of adaxial epidermal cells 3.Ø78; length of abaxial epidermal cells Ø.181 mm; width of abaxial epidermal cells Ø.Ø49 mm; length to width ratio of abaxial epidermal cells 3.694; depth of adaxial epidermal cells Ø.Ø68 mm; depth of abaxial epidermal cells Ø.Ø61 mm; cuticle sculpturing reticulate; cuticle overlying anticlinal walls of adjacent epidermal cells striate; anticlinal walls of adaxial epidermal cells undulated; anticlinal walls of abaxial epidermal cells undulated.

Stomatal apparatus

Amphistomatic; superficial stomata; length of adaxial stomata Ø.Ø52 mm; width of adaxial stomata Ø.Ø48 mm; length to width ratio of adaxial stomata 1.Ø83; length of abaxial stomata Ø.Ø54 mm; width of abaxial stomata Ø.Ø41 mm; length to width ratio of abaxial stomata 1.317.

Vascular bundles

Primary vascular bundle with parenchymatous bundle sheath; 2 secondary vascular bundles with parenchymatous bundle sheaths; 12 tertiary vascular bundles with parenchymatous bundle sheaths.

Leaf articulation mechanism

Adaxial epidermal cell size slightly reduced at midrib; adaxial epidermal cell size slightly reduced at secondary veins.

Photosynthetic tissue

Homogenous chlorenchyma; rounded cells in mesophyll; length of longest axis of mesophyll cells 0.042 mm.

Disa fragrans

Epidermis and cuticle

Length of adaxial epidermal cells 0.124 mm; width of adaxial epidermal cells 0.103 mm; length to width ratio of adaxial epidermal cells 1.204; length of abaxial epidermal cells 0.162 mm; width of abaxial epidermal cells 0.074 mm; length to width ratio of abaxial epidermal cells 2.188; depth of adaxial epidermal cells 0.104 mm; depth of abaxial epidermal cells 0.078 mm; reticulate and psilate cuticle sculpturing.

Stomatal apparatus

Hypostomatic; superfgicial stomata; length of abaxial stomata 0.066 mm; width of abaxial stomata 0.057 mm; length to width ratio of abaxial stomata 1.158.

Vascular bundles

Primary vascular bundle with parenchymatous bundle sheath; 4 secondary vascular bundles with parenchymatous bundle sheaths; 40 tertiary vascular bundles with parenchymatous bundle sheaths.

Leaf articulation mechanism

Adaxial epidermal cell size reduced at midrib; adaxial epidermal cell size reduced at secondary veins.

Photosynthetic tissue

Heterogenous chlorenchyma; well developed arm cells in mesophyll; length of longest axis of mesophyll cells 0.070 mm; 2 tiers of palisade cells; length of palisade cells 0.072 mm; width of palisade cells 0.029 mm; length to width ratio of palisade cells 2.483.

Diss sankeyi

Epidermis and cuticle

Length of adaxial epidermal cells 0 141 mm; width of adaxial epidermal cells 0.109 mm; length to width ratio of adaxial epidermal cells 1.294; length of abaxial epidermal cells 0.150 mm; width of abaxial epidermal cells 0.082 mm; length to width ratio of abaxial epidermal cells 1.829; depth of adaxial epidermal cells 0.119 mm; depth of abaxial epidermal cells 0.089 mm; reticulate cuticle sculpturing; striate cuticle over anticlinal walls of adjacent epidermal cells.

Stomatal apparatus

Hypostomatic; slightly sunken stomata; length of abaxial stomata 0.073 mm; width of abaxial stomata 0.055 mm; length to width ratio of abaxial stomata 1.327.

Vascular bundles

Primary vascular bundle with parenchymatous bundle sheath; 2 secondary vascular bundles with parenchymatous bundle sheaths; 28 tertiary vascular bundles with parenchymatous bundle sheaths.

Leaf articulation mechanism

Adaxial epidermal cell size reduced at midrib; adaxial epidermal cell size reduced at secondary veins.

Photosynthetic tissue

Heterogenous chlorenchyma; less rounded cells in mesophyll; length of longest axis of mesophyll cells 0.068 mm; 1 tier of palisade cells; length of palisade cells 0.085 mm; width of palisade cells 0.030 mm; length to width ratio of palisade cells 2.833.

Diss englerana

Epidermis and cuticle

Length of adaxial epidermal cells 0.140 mm; width of adaxial epidermal cells 0.068 mm; length to width ratio of adaxial epidermal cells 2.059; length of abaxial epidermal cells 0.106 mm; width of abaxial epidermal cells 0.052 mm; length to width ratio of abaxial epidermal cells 2.038; depth of adaxial epidermal cells 0.100 mm; depth of abaxial epidermal cells 0.064

mm; reticulate cuticle sculpturing; striate cuticle over anticlinal walls of adjacent epidermal cells.

Stomatal apparatus

Hypostomatic; slightly raised stomata; length of abaxial stomata 0.060 mm; width of abaxial stomata 0.053 mm; length to width ratio of abaxial stomata 1.132.

Vascular bundles

Primary vascular bundle with parenchymatous bundle sheath; 6 secondary vascular bundles with parenchymatous bundle sheaths; 28 tertiary vascular bundles with parenchymatous bundle sheaths.

Leaf articulation mechanism

Expansion cells present at midrib; adaxial epidermal cell size reduced at midrib.

Photosynthetic tissue

Heterogenous chlorenchyma; less rounded cells in mesophyll; length of longest axis of mesophyll cells 0.045 mm; 2 tiers of palisade cells; length of palisade cells 0.067 mm; width of palisade cells 0.021 mm; length to width ratio of palisade cells 3.190.

Disa chrysostachya

Epidermis and cuticle

Length of adaxial epidermal cells 0.348 mm; width of adaxial epidermal cells 0.122 mm; length to width ratio of adaxial epidermal cells 2.836; length of abaxial epidermal cells 0.190

mm; width of abaxial epidermal cells 0.069 mm; length to width ratio of abaxial epidermal cells 2.754; depth of adaxial epidermal cells 0.112 mm; depth of abaxial epidermal cells 0.072 mm; reticulate cuticle sculpturing.

Stomatal apparatus

Hypostomatic; slightly sunken stomata; length of abaxial stomata 0.077 mm; width of abaxial stomata 0.066 mm; length to width ratio of abaxial stomata 1.167.

Vascular bundles

Primary vascular bundle with parenchymatous bundle sheath; 4 secondary vascular bundles with parenchymatous bundle sheaths; 18 tertiary vascular bundles with parenchymatous bundle sheaths.

Leaf articulation mechanism

Adaxial epidermal cell size reduced at midrib; adaxial epidermal cell size reduced at secondary veins.

Photosynthetic tissue

Heterogenous chlorenchyma; less rounded cells in mesophyll; length of longest axis of mesophyll cells 0.037 mm; 1 tier of palisade cells; length of palisade cells 0.065 mm; width of palisade cells 0.024 mm; length to width ratio of palisade cells 2.708.

Disa chrysostachya

Epidermis and cuticle

Length of adaxial epidermal cells 0.172 mm; width of adaxial epidermal cells 0.142 mm; length to width ratio of adaxial epidermal cells 1.211; length of abaxial epidermal cells 0.165 mm; width of abaxial epidermal cells 0.079 mm; length to width ratio of abaxial epidermal cells 2.089; depth of adaxial epidermal cells 0.182 mm; depth of abaxial epidermal cells 0.089 mm; reticulate cuticle sculpturing.

Stomatal apparatus

Hypostomatic; slightly sunken stomata; length of abaxial stomata 0.086 mm; width of abaxial stomata 0.069 mm; length to width ratio of abaxial stomata 1.246.

Vascular bundles

Primary vascular bundle with parenchymatous bundle sheath; 4 secondary vascular bundles with parenchymatous bundle sheaths; 16 tertiary vascular bundles with parenchymatous bundle sheaths.

Leaf articulation mechanism

Adaxial epidermal cell size reduced at midrib; adaxial epidermal cell size reduced at secondary veins.

Photosynthetic tissue

Heterogenous chlorenchyma; arm-like cells in mesophyll; length of longest axis of mesophyll cells 0.061 mm; 2 tiers of palisade cells; length of palisade cells 0.067 mm; width of palisade cells 0.021 mm; length to width ratio of palisade cells 2.68.

Disa stricapilla

Epidermis and cuticle

Length of adaxial epidermal cells 0.226 mm; width of adaxial epidermal cells 0.058 mm; length to width ratio of adaxial epidermal cells 4.048; length of abaxial epidermal cells 0.148 mm; width of abaxial epidermal cells 0.052 mm; length to width ratio of abaxial epidermal cells 2.846; depth of adaxial epidermal cells 0.056 mm; depth of abaxial epidermal cells 0.054 mm; striate cuticle sculpturing; anticlinal walls of abaxial epidermal cells undulated

Stomatal apparatus

Amphistomatic; superficial stomata; length of adaxial stomata 0.050 mm; width of adaxial stomata 0.045 mm; length to width ratio of adaxial stomata 1.111; length of abaxial stomata 0.052 mm; width of abaxial stomata 0.040 mm; length to width ratio of abaxial stomata 1.3.

Vascular bundles

Primary vascular bundle with parenchymatous bundle sheath; 2 secondary vascular bundles with parenchymatous bundle sheaths; 6 tertiary vascular bundles with parenchymatous bundle sheaths.

Photosynthetic tissue

Homogeneous chlorenchyma; rounded cells in mesophyll; length of longest axis of mesophyll cells 0.055 mm.

Disa uniflora

Epidermis and cuticle

Length of adaxial epidermal cells 0.192 mm; width of adaxial epidermal cells 0.080 mm; length to width ratio of adaxial epidermal cells 2.4; length of abaxial epidermal cells 0.153 mm; width of abaxial epidermal cells 0.051 mm; length to width ratio of abaxial epidermal cells 3.0; depth of adaxial epidermal cells 0.102 mm; depth of abaxial epidermal cells 0.059 mm; psilate cuticle;

Stomatal apparatus

Hypostomatic; slightly raised stomata; length of abaxial stomata 0.069 mm; width of abaxial stomata 0.053 mm; length to width ratio of abaxial stomata 1.302.

Vascular bundles

Primary vascular bundle with parenchymatous bundle sheath; 4 secondary vascular bundles with parenchymatous bundle sheaths(prominent parenchymatous midrib and secondary ribs; 18 tertiary vascular bundles with parenchymatous bundle sheaths

Photosynthetic tissue

Homogenous chlorenchyma; less rounded cells in mesophyll; length of longest axis of mesophyll cells 0.058 mm.

Disa rosea

Epidermis and cuticle

Length of adaxial epidermal cells 0.125 mm; width of adaxial epidermal cells 0.109 mm; length to width ratio of adaxial epidermal cells 1.147; length of abaxial epidermal cells 0.140

mm; width of abaxial epidermal cells 0.068 mm; length to width ratio of abaxial epidermal cells 2.059; depth of adaxial epidermal cells 0.134 mm; depth of abaxial epidermal cells 0.081 mm; papillose cuticle sculpturing.

Stomatal apparatus

Hypostomatic; slightly raised stomata; length of abaxial stomata 0.068 mm; width of abaxial stomata 0.066 mm; length to width ratio of abaxial stomata 1

Vascular bundles

Primary vascular bundle with parenchymatous bundle sheath; 4 secondary vascular bundles; 14 tertiary vascular bundles.

Photosynthetic tissue

Heterogenous chlorenchyma; well developed arrm cells in mesophyll; length of longest axis of mesophyll cells 0.095 mm; 1 tier of palisade cells; length of palisade cells 0.098 mm; width of palisade cells 0.045 mm; length to width ratio of palisade cells 2.178.

Disa pillansii

Epidermis and cuticle

Length of adaxial epidermal cells 0.121 mm; width of adaxial epidermal cells 0.079 mm; length to width ratio of adaxial epidermal cells 1.532; length of abaxial epidermal cells 0.113 mm; width of abaxial epidermal cells 0.025 mm; length to width ratio of abaxial epidermal cells 4.520; depth of adaxial

epidermal cells mm 0.098; depth of abaxial epidermal cells 0.050 mm; papillose cuticle sculpturing.

Stomatal apparatus

Hypostomatic; slightly raised stomata; length of abaxial stomata 0.054 mm; width of abaxial stomata 0.051 mm; length to width ratio of abaxial stomata 1.059.

Vascular bundles

Primary vascular bundle with parenchymatous bundle sheath; 2 secondary vascular bundles with parenchymatous bundle sheaths; 2 tertiary vascular bundles with parenchymatous bundle sheaths.

Photosynthetic tissue

Heterogenous chlorenchyma; well developed arm cells in mesophyll; length of longest axis of mesophyll cells 0.073 mm; 1 tier of palisade cells; length of palisade cells 0.098 mm; width of palisade cells 0.043 mm; length to width ratio of palisade cells 2.279.

Disa fasciata

Epidermis and cuticle

Length of adaxial epidermal cells 0.157 mm; width of adaxial epidermal cells 0.073 mm; length to width ratio of adaxial epidermal cells 2.151; length of abaxial epidermal cells 0.172 mm; width of abaxial epidermal cells 0.075 mm; length to width ratio of abaxial epidermal cells 2.293; depth of adaxial epidermal cells 0.094 mm; depth of abaxial epidermal cells 0.067

mm; striate (papillose in parts) cuticle sculpturing; striate cuticle over anticlinal walls of adjacent epidermal cells (more pronounced adaxially); anticlinal walls of adaxial epidermal cells undulated, anticlinal walls of abaxial epidermal cells undulated.

Stomatal apparatus

Amphistomatic; superficial stomata; length of adaxial stomata Ø.Ø64 mm; width of adaxial stomata Ø.Ø57 mm; length to width ratio of adaxial stomata 1.123; length of abaxial stomata Ø.Ø68 mm; width of abaxial stomata Ø.Ø59 mm; length to width ratio of abaxial stomata 1.138.

Vascular bundles

Primary vascular bundle with parenchymatous bundle sheath; 4 secondary vascular bundles with parenchymatous bundle sheaths; 4 tertiary vascular bundles with parenchymatous bundle sheaths.

Photosynthetic tissue

Heterogenous chlorenchyma; less rounded cells in mesophyll, length of longest axis of mesophyll cells Ø.Ø49 mm; 1 tier of palisade cells; length of palisade cells Ø.Ø65 mm; width of palisade cells Ø.Ø34 mm; length to width ratio of palisade cells 1.912.

Disa patens

Epidermis and cuticle

Length of adaxial epidermal cells 0.134 mm; width of adaxial epidermal cells 0.079 mm; length to width ratio of adaxial epidermal cells 1.696; length of abaxial epidermal cells 0.137 mm; width of abaxial epidermal cells 0.041 mm; length to width ratio of abaxial epidermal cells 3.341; depth of adaxial epidermal cells 0.033 mm; depth of abaxial epidermal cells 0.062 mm; papillose cuticle sculpturing.

Stomatal apparatus

Hypostomatic; slightly sunken stomata; length of abaxial stomata 0.040 mm; width of abaxial stomata 0.034 mm; length to width ratio of abaxial stomata 1.176

Vascular bundles

Primary vascular bundle with parenchymatous bundle sheath; 4 secondary vascular bundles with parenchymatous bundle sheaths; 6 tertiary vascular bundles with parenchymatous bundle sheaths.

Photosynthetic tissue

Homogenous chlorenchyma; rounded cells in mesophyll; length of longest axis of mesophyll cells 0.041 mm.

Disa filicornis

Epidermis and cuticle

Length of adaxial epidermal cells 0.177 mm; width of adaxial epidermal cells 0.051 mm; length to width ratio of adaxial epidermal cells 3.471; length of abaxial epidermal cells 0.124 mm; width of abaxial epidermal cells 0.039 mm; length to width

ratio of abaxial epidermal cells 3.179; depth of adaxial epidermal cells 0.05 mm; depth of abaxial epidermal cells 0.058 mm; psilate cuticle; striate cuticle over anticlinal walls of adjacent epidermal cells.

Stomatal apparatus

Hypostomatic; superficial stomata; length of abaxial stomata 0.049 mm; width of abaxial stomata 0.041 mm; length to width ratio of abaxial stomata 1.195.

Vascular bundles

Primary vascular bundle with parenchymatous bundle sheath; 4 secondary vascular bundles with parenchymatous bundle sheaths; 2 tertiary vascular bundles with parenchymatous bundle sheaths.

Leaf articulation mechanism

Epandion cells present at midrib.

Photosynthetic tissue

Heterogenous chlorenchyma; rounded cells in mesophyll; length of longest axis of mesophyll cells 0.044 mm; 1 tier of palisade cells; length of palisade cells 0.051 mm; width of palisade cells 0.027 mm; length to width ratio of palisade cells 1.889.

Disa longicornu

Epidermis and cuticle

Length of adaxial epidermal cells 0.164 mm; width of adaxial epidermal cells 0.070 mm; length to width ratio of adaxial epidermal cells 2.343; length of abaxial epidermal cells 0.180

mm; width of abaxial epidermal cells 0.050 mm; length to width ratio of abaxial epidermal cells 3.6; depth of adaxial epidermal cells 0.082 mm; depth of abaxial epidermal cells 0.057 mm; psilate cuticle; anticlinal walls of abaxial epidermal cells slightly undulated.

Stomatal apparatus

Hypostomatic; slightly raised stomata; length of abaxial stomata 0.068 mm; width of abaxial stomata 0.059 mm; length to width ratio of abaxial stomata 1.119.

Vascular bundles

Primary vascular bundle with parenchymatous bundle sheath; 2 secondary vascular bundles with parenchymatous bundle sheaths; 6 tertiary vascular bundles with parenchymatous bundle sheaths.

Photosynthetic tissue

Heterogenous chlorenchyma; arm-like cells in mesophyll; length of longest axis of mesophyll cells 0.056 mm; 1 tier of palisade cells; length of palisade cells 0.071 mm; width of palisade cells 0.042 mm; length to width ratio of palisade cells 1.69.

Disa maculata

Epidermis and cuticle

Length of adaxial epidermal cells 0.165 mm; width of adaxial epidermal cells 0.130 mm; length to width ratio of adaxial epidermal cells 1.269; length of abaxial epidermal cells 0.150 mm; width of abaxial epidermal cells 0.063 mm; length to width

ratio of abaxial epidermal cells 2.381; depth of adaxial epidermal cells Ø.158 mm; depth of abaxial epidermal cells Ø.Ø9Ø mm; striate cuticle sculpturing; striate cuticle over anticlinal walls of adjacent epidermal cells

Stomatal apparatus

Hypostomatic; raised stomata; length of abaxial stomata Ø.Ø75 mm; width of abaxial stomata Ø.Ø65 mm; length to width ratio of abaxial stomats 1.154.

Vascular bundles

Primary vascular bundle with parenchymatous bundle sheath; 2 secondary vascular bundles with parenchymatous bundle sheaths; 4 tertiary vascular bundles with parenchymatous bundle sheaths.

Photosynthetic tissue

Heterogenous chlorenchyma; well developed arm cells in mesophyll; length of longest axis of mesophyll cells Ø.Ø88 mm; 1 tier of palisade cells; length of palisade cells Ø.11Ø mm; width of palisade cells Ø.Ø28 mm; length to width ratio of palisade cells 3.929.

Disa maculata

Epidermis and cuticle

Length of adaxial epidermal cells Ø.165 mm; width of adaxial epidermal cells Ø.13Ø mm; length to width ratio of adaxial epidermal cells 1.269; length of abaxial epidermal cells mm Ø.15Ø; width of abaxial epidermal cells Ø.Ø6? mm; length to width

ratio of abaxial epidermal cells 2.381; depth of adaxial epidermal cells 0.158 mm; depth of abaxial epidermal cells 0.090 mm; striate cuticle sculpturing; striate cuticle over anticlinal walls of adjacent epidermal cells.

Stomatal apparatus

Hypostomatic; raised stomata; length of abaxial stomata 0.075 mm; width of abaxial stomata 0.065 mm; length to width ratio of abaxial stomata 1.154.

Vascular bundles

Primary vascular bundle with parenchymatous bundle sheath; 2 secondary vascular bundles with parenchymatous bundle sheaths; 4 tertiary vascular bundles with parenchymatous bundle sheaths.

Photosynthetic tissue

Heterogeneous chlorenchyma; well developed arm cells in mesophyll; length of longest axis of mesophyll cells 0.088 mm; 1 tier of palisade; length of palisade cells 0.110 mm; width of palisade cells 0.028 mm; length to width ratio of palisade cells 3.929.

Disa crassicornis

Epidermis and cuticle

Length of adaxial epidermal cells 0.184 mm; width of adaxial epidermal cells 0.096 mm; length to width ratio of adaxial epidermal cells 1.708; length of abaxial epidermal cells 0.198 mm; width of abaxial epidermal cells 0.060 mm; length to width ratio of abaxial epidermal cells 3.3; depth of adaxial epidermal

cells 0.098 mm; depth of abaxial epidermal cells 0.064 mm; papillose cuticle sculpturing; striate cuticle over anticlinal walls of adjacent epidermal cells.

Stomatal apparatus

Hypostomatic; slightly raised stomata; length of abaxial stomata 0.083 mm; width of abaxial stomata 0.065 mm; length to width ratio of abaxial stomata 1.277.

Vascular bundles

Primary vascular bundle with parenchymatous bundle sheath; 6 secondary vascular bundles with parenchymatous bundle sheaths; 36 tertiary vascular bundles with parenchymatous bundle sheaths.

Leaf articulation mechanism

Adaxial epidermal cell size reduced at midrib; adaxial epidermal cell size reduced at secondary veins.

Photosynthetic tissue

Heterogeneous chlorenchyma; arm-like cells in mesophyll; length of longest axis of mesophyll cells 0.074 mm; 2 tiers of palisade cells; length of palisade cells 0.072 mm; width of palisade cells 0.033 mm; length to width ratio of palisade cells 2.182.

Disa versicolor

Epidermis and cuticle

Length of adaxial epidermal cells 0.098 mm; width of adaxial epidermal cells 0.067 mm; length to width ratio of adaxial epidermal cells 1.463; length of abaxial epidermal cells 0.096

mm; width of abaxial epidermal cells 0.080 mm; length to width ratio of abaxial epidermal cells 1.2; depth of adaxial epidermal cells 0.105 mm; depth of abaxial epidermal cells 0.067 mm; reticulate cuticle sculpturing.

Stomatal apparatus

Amphistomatic; slightly raised stomata; length of abaxial stomata 0.07 mm; width of abaxial stomata 0.06 mm; length to width ratio of abaxial stomata 1.167.

Vascular bundles

Primary vascular bundle with parenchymatous bundle sheath; 6 secondary vascular bundles with parenchymatous bundle sheaths; 32 tertiary vascular bundles with parenchymatous bundle sheaths.

Leaf articulation mechanism

Expansion cells present at midrib; adaxial epidermal cell size reduced at midrib; adaxial epidermal cell size reduced at secondary veins.

Photosynthetic tissue

Heterogenous chlorenchyma; less rounded cells in mesophyll; length of longest axis of mesophyll cells 0.048 mm; 2 tiers of palisade cells; length of palisade cells 0.058 mm; width of palisade cells 0.030 mm; length to width ratio of palisade cells 1.933.

Disa alticola

Epidermis and cuticle

Length of adaxial epidermal cells Ø.217 mm; width of adaxial epidermal cells Ø.Ø58 mm; length to width ratio of adaxial epidermal cells 3.741; length of abaxial epidermal cells Ø.118 mm; width of abaxial epidermal cells Ø.Ø25 mm; length to width ratio of abaxial epidermal cells 4.72; depth of adaxial epidermal cells Ø.Ø57 mm; depth of abaxial epidermal cells Ø.Ø43 mm; striate cuticle sculpturing.

Stomatal apparatus

Hypostomatic; superficial stomata; length of abaxial stomata Ø.Ø52 mm; width of abaxial stomata Ø.Ø38 mm; length to width ratio of abaxial stomata 1.368.

Vascular bundles

Primary vascular bundle with parenchymatous bundle sheath; 4 secondary vascular bundles with parenchymatous bundle sheaths; 10 tertiary vascular bundles with parenchymatous bundle sheaths.

Leaf articulation mechanism

Expansion cells present at midrib.

Photosynthetic tissue

Homogeneous chlorenchyma; rounded cells in mesophyll; length of longest axis of mesophyll cells Ø.Ø29 mm.

Disa patula

Epidermis and cuticle

Length of adaxial epidermal cells Ø.124 mm; width of adaxial epidermal cells Ø.Ø58 mm; length to width ratio of adaxial

epidermal cells 2.138; length of abaxial epidermal cells 0.069 mm; width of abaxial epidermal cells 0.038 mm; length to width ratio of abaxial epidermal cells 1.816; depth of adaxial epidermal cells 0.085 mm; depth of abaxial epidermal cells 0.034 mm; psilate cuticle.

Stomatal apparatus

Hypostomatic; superficial stomata; length of abaxial stomata 0.042 mm; width of abaxial stomata 0.047 mm; length to width ratio of abaxial stomata 0.894.

Vascular bundles

Primary vascular bundle with parenchymatous bundle sheath; adaxial and abaxial schlerenchyma caps present at poles of primary vascular bundle; 2 secondary vascular bundles with parenchymatous bundle sheaths; adaxial and abaxial schlerenchyma caps present at poles of secondary vascular bundles; 12 tertiary vascular bundles with parenchymatous bundle sheaths; schlerenchymatous leaf margins present.

Leaf articulation mechanism

Adaxial epidermal cell size reduced at midrib; adaxial peidermal cell size reduced at secondary veins.

Photosynthetic tissue

Homogeneous chlorenchyma; rounded cells in mesophyll; length of longest axis of mesophyll cells 0.044 mm.

Disa saxicola

Epidermis and cuticle

Length of adaxial epidermal cells 0.215 mm; width of adaxial epidermal cells 0.065 mm; length to width ratio of adaxial epidermal cells 3.308; length of abaxial epidermal cells 0.200 mm; width of abaxial epidermal cells 0.042 mm; length to width ratio of abaxial epidermal cells 4.762; depth of adaxial epidermal cells 0.065 mm; depth of abaxial epidermal cells 0.040 mm; striate cuticle; striate cuticle over anticlinal walls of adjacent epidermal cells.

Stomatal apparatus

Hypostomatic; slightly raised stomata; length of abaxial stomata 0.055 mm; width of abaxial stomata 0.052 mm; length to width ratio of abaxial stomata 1.058.

Vascular bundles

Primary vascular bundle with schlerotic bundle sheath; abaxial and adaxial schlerenchyma caps present at poles of primary vascular bundle; secondary vascular bundles with parenchymatous and schlerotic bundle sheaths; adaxial and abaxial schlerenchyma caps at poles of secondary vascular bundles; 16 tertiary vascular bundles with parenchymatous bundle sheaths; abaxial schlerenchyma caps present in 8 of the 16 tertiary vascular bundles; schlereidal leaf margins present.

Leaf articulation mechanism

Expansion cells present at midrib; adaxial epidermal cell size reduced at midrib; adaxial epidermal cell size reduced at secondary veins.

Photosynthetic tissue

Homogeneous chlorenchyma; rounded cells in mesophyll; length of longest axis of mesophyll cells 0.043 mm

Disa nivea

Epidermis and cuticle

Length of adaxial epidermal cells 0.130 mm; width of adaxial epidermal cells 0.043 mm; length to width ratio of adaxial epidermal cells 3.171; length of abaxial epidermal cells 0.112 mm; width of abaxial epidermal cells 0.035 mm; length to width ratio of abaxial epidermal cells 3.2; depth of adaxial epidermal cells 0.030 mm; depth of abaxial epidermal cells 0.029 mm; striate cuticle sculpturing.

Stomatal apparatus

Amphistomatic; superficial stomata; length of adaxial stomata 0.044 mm; width of adaxial stomata 0.048 mm; length to width ratio of adaxial stomata 0.917; length of abaxial stomata 0.045 mm; width of abaxial stomata 0.042 mm; length to width ratio of abaxial stomata 1.071.

Vascular bundles

Primary vascular bundle with sclerotic bundle sheath; adaxial and abaxial fibre caps present at poles of primary bundle; 2 secondary vascular bundles with parenchymatous and sclerotic bundle sheaths; adaxial and abaxial fibre caps present at poles of secondary vascular bundles; 10 tertiary vascular bundles with parenchymatous bundle sheaths; abaxial fibre caps present at

poles of teriary vascular bundles; Schlereidal leaf margins present.

Leaf articulation mechanism

Expansion cells present at midrib.

Photosynthetic tissue

Homogenous chlorenchyma; rounded cells in mesophyll; length of longest axis of mesophyll cells 0.028 mm.

Disa oreophila

Epidermis and cuticle

Length of adaxial epidermal cells 0.153 mm; width of adaxial epidermal cells 0.091 mm; length to width ratio of adaxial epidermal cells 1.681; length of abaxial epidermal cells 0.095 mm; width of abaxial epidermal cells 0.054 mm; length to width ratio of abaxial epidermal cells 1.759; depth of adaxial epidermal cells 0.056 mm; depth of abaxial epidermal cells 0.051 mm; striate cuticle sculpturing; striate cuticle over anticlinal walls of adjacent epidermal cells.

Stomatal apparatus

Amphistomatic; superficial stomata; length of adaxial stomata 0.054 mm; width of adaxial stomata 0.056 mm; length to width ratio of adaxial stomata 0.964; length of abaxial stomata 0.053 mm; width of abaxial stomata 0.053 mm; length to width ratio of abaxial stomata 1.

Vascular bundles

Primary vascular bundle with slightly sclerified bundle sheath; adaxial and abaxial sclerenchyma caps present at poles of primary vascular bundle; 4 secondary vascular bundles with slightly sclerified bundle sheaths; adaxial sclerenchyma caps present in 2 of 4 secondary vascular bundles; abaxial fibre caps present in secondary vascular bundles; 8 tertiary vascular bundles; abaxial fibre caps present at 4 of 8 tertiary vascular bundles.

Leaf articulation mechanism

Expansion cells present at midrib.

Photosynthetic tissue

Homogeneous chlorenchyma; less rounded cells in mesophyll; length of longest axis of mesophyll cells 0.040 mm.

Disa cephalotes

Epidermis and cuticle

Length of adaxial epidermal cells 0.115 mm; width of adaxial epidermal cells 0.045 mm; length to width ratio of adaxial epidermal cells 2.556; length of abaxial epidermal cells 0.130 mm; width of abaxial epidermal cells 0.052 mm; length to width ratio of abaxial epidermal cells 2.524; depth of adaxial epidermal cells 0.042 mm; depth of abaxial epidermal cells 0.040 mm; striate cuticle sculpturing.

Stomatal apparatus

Amphistomatic;slightly raised stomata; length of adaxial stomata 0.040 mm; width of adaxial stomata 0.037 mm; length to width ratio of adaxial stomata 1.081; length of abaxial stomata 0.050 mm; width of abaxial stomata 0.039 mm; length to width ratio of abaxial stomata 1.282.

Vascular bundles

Primary vascular bundle with parenchymatous bundle sheath; adaxial and abaxial schlerenchyma caps present at poles of primary vascular bundle; 2 secondary vascular bundles with parenchymatous bundle sheaths; adaxial and abaxial schlerenchyma caps present at the poles of secondary vascular bundles; 20 tertiary vascular bundles with parenchymatous bundle sheaths; abaxial schlerenchyma caps present in 8 of 20 tertiary vascular bundles; schlereidal leaf margins present.

Leaf articulation mechanism

Epansion cells present at midrib.

Photosynthetic tissue

Homogeneous chlorenchyma; rounded cells in mesophyll; length of longest axis of mesophyll cells 0.037 mm.

Diss cephalotes ssp. frigida

Epidermis and cuticle

Length of adaxial epidermal cells 0.140 mm; width of adaxial epidermal cells 0.068 mm; length to width ratio of adaxial epidermal cells 2.059; length of abaxial epidermal cells 0.065

mm; width of abaxial epidermal cells 0.054 mm; length to width ratio of abaxial epidermal cells 1.204; depth of adaxial epidermal cells 0.070 mm; depth of abaxial epidermal cells 0.043 mm; striate cuticle sculpturing.

Stomatal apparatus

Amphistomatic; slightly raised stomata; length of adaxial stomata 0.050 mm; width of adaxial stomata 0.054 mm; length to width ratio of adaxial stomata 0.926; length of abaxial stomata 0.054 mm; width of abaxial stomata 0.049 mm; length to width ratio of abaxial stomata 1.102.

Vascular bundles

Primary vascular bundle with parenchymatous bundle sheath; adaxial and abaxial schlerenchyma caps at poles of primary vascular bundle; 4 secondary vascular bundles with parenchymatous bundle sheaths; adaxial and abaxial schlerenchyma caps at poles of secondary vascular bundles; 14 tertiary vascular bundles with parenchymatous bundle sheaths; schlereidal leaf margins present.

Leaf articulation mechanism

Expansion cells present at midrib.

Photosynthetic tissue

Homogeneous chlorenchyma; rounded cells in mesophyll; length of longest axis of mesophyll cells 0.038 mm.

Disa glandulosa

Epidermis and cuticle

Epidermis with multicellular hairs and stalked glands; length of adaxial epidermal cells 0.117 mm; width of adaxial epidermal cells 0.054 mm; length to width ratio of adaxial epidermal cells 2.167; length of abaxial epidermal cells 0.126 mm; width of abaxial epidermal cells 0.043 mm; length to width ratio of abaxial epidermal cells 2.930; depth of adaxial epidermal cells 0.061 mm; depth of abaxial epidermal cells 0.041 mm; psilate cuticle; anticlinal walls of adaxial epidermal cells undulated; anticlinal walls of abaxial epidermis undulated.

Stomatal apparatus

Amphistomatic; raised stomata; length of adaxial stomata 0.051 mm; width of adaxial stomata 0.048 mm; length to width ratio of adaxial stomata 1.063; length of abaxial stomata 0.052 mm; width of abaxial stomata 0.048 mm; length to width ratio of abaxial stomata 1.083.

Vascular bundles

Primary vascular bundle with parenchymatous bundle sheath; 2 secondary vascular bundles with parenchymatous bundle sheaths; 8 tertiary vascular bundles with parenchymatous bundle sheaths.

Photosynthetic tissue

Heterogeneous chlorenchyma; less rounded cells in mesophyll; length of longest axis of mesophyll cells 0.054 mm; 1 tier of palisade cells; length of palisade cells 0.053 mm; width of palisade cells 0.029 mm; length to width ratio of palisade cells 1.828.

Disa draconis

Epidermis and cuticle

Length of adaxial epidermal cells 0.285 mm; width of adaxial epidermal cells 0.093 mm; length to width ratio of adaxial epidermal cells 3.065; length of abaxial epidermal cells 0.284 mm; width of abaxial epidermal cells 0.049 mm; length to width ratio of abaxial epidermal cells 5.798; depth of adaxial epidermal cells 0.121 mm; depth of abaxial epidermal cells 0.051 mm; striate cuticle sculpturing.

Stomatal apparatus

Hypostomatic; superficial stomata; length of abaxial stomata 0.065 mm; width of abaxial stomata 0.054 mm; length to width ratio of abaxial stomata 1.204.

Vascular bundles

Primary vascular bundle with parenchymatous bundle sheath; 2 secondary vascular bundles with parenchymatous bundle sheaths; 18 tertiary vascular bundles with parenchymatous bundle sheaths.

Leaf articulation mechanism

Adaxial epidermal cell size reduced at midrib; adaxial epidermal cell size reduced at secondary veins.

Photosynthetic tissue

Heterogeneous chlorenchyma; less rounded cells in mesophyll; length of longest axis of mesophyll cells 0.050 mm; 1 tier of palisade cells; length of palisade cells 0.060 mm; width of

palisade cells 0.026 mm; length to width ratio of palisade cells 2.308.

Disa cylindrica

Epidermis and cuticle

Length of adaxial epidermal cells 0.149 mm; width of adaxial epidermal cells 0.089 mm; length to width ratio of adaxial epidermal cells 1.674; length of abaxial epidermal cells 0.151 mm; width of abaxial epidermal cells 0.058 mm; length to width ratio of abaxial epidermal cells 2.603; depth of adaxial epidermal cells 0.084 mm; depth of abaxial epidermal cells 0.070 mm; psilate cuticle.

Stomatal apparatus

Amphistomatic; slightly raised stomata; length of adaxial stomata 0.074 mm; width of adaxial stomata 0.068 mm; length to width ratio of adaxial stomata 1.088; length of abaxial stomata 0.063 mm; width of abaxial stomata 0.053 mm; length to width ratio of abaxial stomata 1.189.

Vascular bundles

Primary vascular bundle with parenchymatous bundle sheath; 4 secondary vascular bundles with parenchymatous bundle sheaths; 4 tertiary vascular bundles with parenchymatous bundle sheaths.

Photosynthetic tissue

Homogeneous chlorenchyma; rounded cells in mesophyll; length of longest axis of mesophyll cells 0.044 mm.

Disa vaginata

Epidermis and cuticle

Epidermal hairs present; length of adaxial epidermal cells 0.115 mm; width of adaxial epidermal cells 0.066 mm; length to width ratio of adaxial epidermal cells 1.742; length of abaxial epidermal cells 0.096 mm; width of abaxial epidermal cells 0.046 mm; length to width ratio of abaxial epidermal cells 2.087; depth of adaxial epidermal cells 0.069 mm; depth of abaxial epidermal cells 0.049 mm; striate cuticle sculpturing; striate cuticle over anticlinal walls of adjacent epidermal cells.

Stomatal apparatus

Amphistomatic; superficial stomata; length of adaxial stomata 0.033 mm; width of adaxial stomata 0.042 mm; length to width ratio of adaxial stomata 0.786; length of abaxial stomata 0.042 mm; width of abaxial stomata 0.047 mm; length to width ratio of abaxial stomata 0.894.

Vascular bundles

Primary vascular bundle with parenchymatous bundle sheath; 4 secondary vascular bundles with parenchymatous bundle sheaths; 6 tertiary vascular bundles with parenchymatous bundle sheaths.

Leaf articulation mechanism

Adaxial epidermal cell size reduced at midrib; adaxial epidermal cell size reduced at secondary veins.

Photosynthetic tissue

Homogeneous chlorenchyma; rounded cells in mesophyll; length of longest axis of mesophyll cells 0.057 mm.

Disa sagittalis

Epidermis and cuticle

Length of adaxial epidermal cells 0.107 mm; width of adaxial epidermal cells 0.088 mm; length to width ratio of adaxial epidermal cells 1.244; length of abaxial epidermal cells 0.098 mm; width of abaxial epidermal cells 0.082 mm; length to width ratio of abaxial epidermal cells 1.195; depth of adaxial epidermal cells 0.177 mm; depth of abaxial epidermal cells 0.081 mm; psilate cuticle; anticlinal walls of abaxial epidermal cells undulated.

Stomatal apparatus

Hypostomatic; slightly raised stomata; length of abaxial stomata 0.044 mm; width of abaxial stomata 0.035 mm; length to width ratio of abaxial stomata 1.257.

Vascular bundles

Primary vascular bundle with parenchymatous bundle sheath; 4 secondary vascular bundles with parenchymatous bundle sheaths; 5 tertiary vascular bundles with parenchymatous bundle sheaths.

Photosynthetic tissue

Heterogeneous chlorenchyma; arm-like cells in mesophyll; length of longest axis of mesophyll cells 0.059 mm; 1 tier of palisade

cells; length of palisade cells 0.084 mm; width of palisade cells 0.035 mm; length to width ratio of palisade cells 2.4.

Disa lineata

Epidermis and cuticle

Length of adaxial epidermal cells 0.204 mm; width of adaxial epidermal cells 0.076 mm; length to width ratio of adaxial epidermal cells 2.684; length of abaxial epidermal cells 0.150 mm; width of abaxial epidermal cells 0.040 mm; length to width ratio of abaxial epidermal cells 3.75; depth of adaxial epidermal cells 0.067 mm; depth of abaxial epidermal cells 0.037 mm; striate cuticle sculpturing.

Stomatal apparatus

Hypostomatic; slightly raised stomata; length of abaxial stomata 0.066 mm; width of abaxial stomata 0.046 mm; length to width ratio of abaxial stomata 1.435.

Vascular bundles

Primary vascular bundle with parenchymatous bundle sheath; 2 secondary vascular bundles with parenchymatous bundle sheaths; 12 tertiary vascular bundles with parenchymatous bundle sheaths.

Leaf articulation mechanism

Adaxial epidermal cell size slightly reduced at midrib.

Photosynthetic tissue

Heterogenous chlorenchyma; rounded cells in mesophyll; length of longest axis of mesophyll cells 0.041 mm; 1 tier of palisade

cells; length of palisade cells 0.054 mm; width of palisade cells 0.031 mm; length to width ratio of palisade cells 1.742.

Disa telipogonis

Epidermis and cuticle

Length of adaxial epidermal cells 0.180 mm; width of adaxial epidermal cells 0.075 mm; length to width ratio of adaxial epidermal cells 2.4; length of abaxial epidermal cells 0.115 mm; width of abaxial epidermal cells 0.042 mm; length to width ratio of abaxial epidermal cells 2.738; depth of adaxial epidermal cells 0.088 mm; depth of abaxial epidermal cells 0.057 mm; psilate cuticle.

Stomatal apparatus

Hypostomatic; superficial stomata; length of abaxial stomata 0.074 mm; width of abaxial stomata 0.053 mm; length to width ratio of abaxial stomata 1.396.

Vascular bundles

Primary vascular bundle without bundle sheath; 2 secondary vascular bundles without bundle sheaths; 12 tertiary vascular bundles without bundle sheaths.

Photosynthetic tissue

Homogeneous chlorenchyma; rounded cells in mesophyll; length of longest axis of mesophyll cells mm.

Disa aconitoides

Epidermis and cuticle

Length of adaxial epidermal cells Ø.100 mm; width of adaxial epidermal cells Ø.Ø83 mm; length to width ratio of adaxial epidermal cells 1.587; length of abaxial epidermal cells Ø.105 mm; width of abaxial epidermal cells Ø.Ø48 mm; length to width ratio of abaxial epidermal cells 2.188; depth of adaxial epidermal cells Ø.Ø64 mm; depth of abaxial epidermal cells Ø.Ø45 mm; psilate cuticle;

Stomatal apparatus

Amphistomatic; superficial stomata; length of adaxial stomata Ø.Ø55 mm; width of adaxial stomata Ø.Ø56 mm; length to width ratio of adaxial stomata Ø.982; length of abaxial stomata Ø.Ø56 mm; width of abaxial stomata Ø.Ø53 mm; length to width ratio of abaxial stomata 1.Ø57.

Vascular bundles

Primary vascular bundle with parenchymatous bundle sheath; 2 secondary vascular bundles with parenchymatous bundle sheaths; 18 tertiary vascular bundles with parenchymatous bundle sheaths.

Photosynthetic tissue

Homogeneous chlorenchyma; rounded cells in mesophyll; length of longest axis of mesophyll cells Ø.Ø34 mm.

Disa cornuta

Epidermis and cuticle

Length of adaxial epidermal cells 0.182 mm; width of adaxial epidermal cells 0.059 mm; length to width ratio of adaxial epidermal cells 3.085; length of abaxial epidermal cells 0.233 mm; width of abaxial epidermal cells 0.047 mm; length to width ratio of abaxial epidermal cells 4.957; depth of adaxial epidermal cells 0.074 mm; depth of abaxial epidermal cells 0.054 mm; striate cuticle sculpturing; striate cuticle over anticlinal walls of adjacent epidermal cells.

Stomatal apparatus

Hypostomatic; slightly raised stomata; length of abaxial stomata 0.068 mm; width of abaxial stomata 0.053 mm; length to width ratio of abaxial stomata 1.245.

Vascular bundles

Primary vascular bundle with parenchymatous bundle sheath; 6 secondary vascular bundles with parenchymatous bundle sheaths; 28 tertiary vascular bundles with parenchymatous bundle sheaths.

Leaf articulation mechanism

Adaxial epidermal cell size reduced at midrib; adaxial epidermal cell size reduced at secondary veins.

Photosynthetic tissue

Heterogenous chlorenchyma; arm-like cells in mesophyll; length of longest axis of mesophyll cells 0.052 mm; 1 tier of palisade cells; length of palisade cells 0.069 mm; width of palisade cells 0.033 mm; length to width ratio of palisade cells 2.091.

Disa tysonii

Epidermis and cuticle

Length of adaxial epidermal cells 0.14 mm; width of adaxial epidermal cells 0.11 mm; length to width ratio of adaxial epidermal cells 1.273; length of abaxial epidermal cells 0.115 mm; width of abaxial epidermal cells 0.090 mm; length to width ratio of abaxial epidermal cells 1.278; depth of adaxial epidermal cells 0 115 mm; depth of abaxial epidermal cells 0.069 mm; reticulate cuticle sculpturing.

Stomatal apparatus

Hypostomatic; superficial stomata; length of abaxial stomata 0.065 mm; width of abaxial stomata 0.064 mm; length to width ratio of abaxial stomata 1.016.

Vascular bundles

Primary vascular bundle with parenchymatous bundle sheath; adaxial and abaxial schlerenchyma caps present at poles of primary vascular bundle; 4 secondary vascular bundles with parenchymatous bundle sheaths; abaxial schlerenchyma caps at pole of secondary vascular bundle; 32 tertiary vascular bundles with parenchymatous bundle sheaths.

Leaf articulation mechanism

Expansion cells present at midrib.

Photosynthetic tissue

Homogeneous chlorenchyma; rounded cells in mesophyll; length of longest axis of mesophyll cells 0.058 mm.

Appendix 4

Pollen Descriptions.

Subtribe Coryciinae

Disperis lindleyana.

Massulae rounded, tetrads isodiametric, exine scuplture reticulate, exine structure semi-tectate.

Disperis villosa.

Massulae rounded, tetrads isodiametric, exine sculpture reticulate, exine structure semi-tectate.

Disperis cuculata.

Massulae rounded, tetrads isodiametric, exine sculpture reticulate, exine structure semi-tectate.

Disperis thorncroftii.

Massulae rounded, tetrads isodiametric, exine sculpture reticulate with reduced muri, exine structure semi-tectate to partly intectate

Disperis circumflexa.

Massulae fasciculate, tetrads elongated, exine granulate, exine structure tectate.

Ceratandra atrata.

Massulae fasciculate, tetrads elongated, exine sculpture rugulate with fine punctae, exine structure tectate.

Ceratandra grandiflora.

Massulae fasciculate, tetrads elongated, exine sculpture rugulate with fine punctae, exine structure tectate.

Evota bicolor.

Massulae fasciculate, tetrads elongated, exine sculpture strongly rugulate with fine punctae, exine structure tectate.

Evota venosa.

Massulae fasciculate, tetrads elongated, exine finely striate with a slight granular appearance and fine punctae, exine structure tectate.

Anochilus hallii.

Massulae fasciculate (fan-shaped), tetrads elongated, exine psilate with fine punctae. Exine structure tectate

Corycium nigrescens.

Massulae rounded, tetrads isodiametric, exine sculpture verrucose, exine structure uncertain.

Corycium dracomontanum.

Massulae rounded, tetrads more or less isodiametric, exine sculpture verrucose and granulate, exine structure uncertain.

Corycium orobanchoides.

Massulae fasciculate, tetrads elongated, exine finely striate with fine puntae, exine structure tectate.

Corycium magnum.

Massulae fasciculate, tetrads elongated, exine finely striate with foveolae, exine structure tectate.

Corycium excisum.

Massulae fasciculate, tetrads elongated, exine finely striate,

foveolate, exine structure tectate.

Corycium bifidum.

Massulae fasciculate, tetrads elongated, exine finely striate, foveolate, exine structure tectate.

Corycium deflexum.

Massulae fasciculate, tetrads elongated, exine finely striate, foveolate, exine structure tectate.

Pterygodium catholicum.

Massulae fasciculate, tetrads elongated, exine finely striate, foveolate, exine structure tectate.

Pterygodium pantherianum.

Massulae fasciculate, tetrads elongated, exine finely striate, foveolae, exine structure tectate.

Pterygodium acutifolium.

Massulae fasciculate, tetrads elongated, exine finely striate, foveolate, exine structure tectate.

Pterygodium platypetalum.

Massulae fasciculate, tetrads elongated, exine finely striate, foveolate, exine structure tectate.

Subtribe Disinae

Monadenia physodes.

Massulae rounded, tetrads isodiametric, exine sculpture rugose with tetrad margins distinct, exine structure semi-tectate.

Monadenia atrorubens.

Massulae rounded, tetrads isodiametric, exine sculpture rugose with fine punctae on rugae, tetrad margins distinct, exine structure semi-tectate.

Monadenia sabulosa.

Massulae rounded, tetrads isodiametric, exine sculpture rugose tending to verrucose with foveolae, finely rugulate distinct margins, exine structure semi-tectate.

Monadenia densifolia.

Massulae rounded, isodiametric tetrads, exine sculpture hamulate with pilate lumina, exine structure semi-tectate.

Monadenia brevicornis

Massulae rounded, isodiametric tetrads, exine sculpture hamulate with pilate lumina, exine structure semi-tectate.

Brownleea galpinii ssp. major.

Massulae rounded, tetrads isodiametric, exine sculpture reticulate, exine structure semi-tectate.

Brownleea coerula.

Massulae rounded, tetrads isodiametric, exine sculpture reticulate, exine structure semi-tectate.

Schizodium bifidum.

Massulae rounded, tetrads isodiametric, exine sculpture ornate, or loosely reticulate with pilate lumina, exine structure semi-tectate.

Schizodium inflexum.

Massulae rounded, tetrads isodiametric, exine sculpture reticulate with pilate muri, exine structure semi-tectate.

Section Micranthae

Disa welwitschii ssp. welwitschii.

Massulae rounded, tetrads isodiametric, exine sculpture rugose, finely rugulate with supra-ornate baculae and pilae, distinct rugulate tetrad margin, exine structure semi-tectate.

Disa ukingensis.

Massulae rounded, tetrads isodiametric, exine sculpture rugose, with tectum pierced by foveolae, exine structure semi-tectate.

Disa englerana.

Massulae rounded, tetrads isodiametric, exine sculpture rugose with tectum incomplete leaving mostly free baculae (columella-homologues) covering surface of rugae, tetrad margins distinct, exine structure semi-tectate to intectate.

Disa ochrostachya.

Massulae rounded, tetrads isodiametric, exine sculpture rugose with tectum incomplete leaving mostly free baculae (columella homologues) covering surface of rugae, exine structure semi-tectate to intectate.

Disa ornithantha.

Massulae rounded, tetrads isodiametric, exine sculpture rugose with tectum incomplete leaving mostly free baculae (columella homologues) covering surface of rugae, exine structure semi-tectate to intectate.

Disa chrysostachya.

Massulae rounded, tetrads isodiametric, exine sculpture verrucose with pilae between verrucae, exine structure semi-tectate.

Disa fragrans.

Massulae rounded, tetrads isodiametric, exine sculpture verrucose with pilae between verrucae, exine structure semi-tectate.

Section Disa

Disa bivalvata.

Massulae rounded, tetrads isodiametric, exine sculpture rugose with baculae and pilae (columellae homologues), exine structure semi-tectate.

Disa atricapilla.

Massulae rounded, tetrads isodiametric, exine sculpture rugose, finely rugulate with foveolae, tetrad margin distinct, exine structure semi-tectate.

Disa richardiana.

Massulae rounded, tetrads isodiametric, exine sculpture rugose with tectal granules and foveolae, exine structure semi-tectate.

Disa uniflora.

Massulae rounded, tetrads elongate, exine sculpture rugose with pilae, tetrad margins distinct, exine structure semi-tectate.

Disa venosa.

Massulae rounded, tetrads isodiametric, exine sculpture rugose with pilae, exine structure semi-tectate.

Disa filicornis.

Massulae rounded, tetrads isodiametric, exine sculpture rugose with foveolae piercing the tectum, exine structure semi-tectate.

Section Phlebidia

Disa maculata.

Massulae rounded, tetrads isodiametric, exine sculpturing verrucose with distinct tetrad margin, exine structure semi-tectate.

Section Stenocarpa

Disa saxicola.

Massulae rounded, tetrads isodiametric, exine sculpture tightly rugose with foveolae piercing the tectum, exine structure semi-tectate.

Disa gladioliflora ssp. gladioliflora.

Massulae rounded, tetrads isodiametric, exine sculpture rugose with foveolae piercing the tectum, exine structure semi-tectate.

Section Coryphaea

Disa marlothii.

Massulae rounded, tetrads isodiametric, exine sculpture hamulate, with supra-tectal granules and lace-like foveolate margins, exine structure semi-tectate.

Disa triloba.

Massulae rounded, tetrads isodiametric, exine sculpture reticulate with ornate muri, exine structure semi-tectate.

Section Emarginatae

Disa patula.

Massulae rounded, tetrads isodiametric, exine sculpture rugose with distinct margins and foveolae piercing the tectum, exine structure semi-tectate.

Disa stachyoides.

Massulae rounded, tetrads isodiametric, exine sculpture rugose with distinct margins, exine structure semi-tectate.

Section Stoloniferae

Disa stairsii.

Massulae rounded, tetrads elongate, exine sculpturing verrucose with foveolae piercing the tectum, exine structure semi-tectate.

Section Ovalifoliae

Disa ovalifoliae.

Massulae rounded, tetrads isodiametric, exine sculpturing verrucose with foveolae piercing the tectum and supra-tectal granules, exine structure semi-tectate.

Section Disella

Disa tenuicornis.

Massulae rounded, tetrads isodiametric, exine sculpturing rugose with a finely rugulate tectum pierced by foveolae and punctae and supra-tectal granules, exine structure semi-tectate.

Disa obtusa ssp. picta.

Massulae rounded, tetrads isodiametric, exine sculpturing verrucose with supra-tectal granules and tectum pierced by foveolae and punctae. Exine structure semi-tectate.

Section Aconitoideae

Disa aconitoides.

Massulae rounded, tetrads isodiametric, exine sculpturing verrucose with foveolae piercing tectum, exine structure semi-tectate.

Herschelianthe

Herschelianthe lugens.

Massulae rounded, tetrads isodiametric, exine sculpture rugose with foveolae piercing tectum, exine structure semi-tectate.

Herschelianthe forficaria.

Massulae rounded, tetrads isodiametric, exine sculpture rugose (with verrucae in places) and foveolae piercing the tectum, exine structure semi-tectate.

Herschelianthe chimanimaniensis.

Massulae rounded, tetrads isodiametric, exine sculpture verrucose with foveolae piercing tectum and supra-tectal granules, exine structure semi-tectate.

Herschelianthe baurii.

Massulae rounded, tetrads isodiametric, exine sculpture verrucose with foveolae piercing tectum and supra-tectal granules, exine structure semi-tectate.

Herschelianthe graminifolia.

Massulae rounded, tetrads isodiametric, exine sculpture verrucose with foveolae supra-tectal granules, exine structure semi-tectate.

Herschelianthe hians.

Massulae rounded, tetrads isodiametric, exine sculpture verrucose with foveolae piercing tectum and supra-tectal granules, exine structure semi-tectate.